

# **Antisense Oligonucleotide-Mediated Therapeutic Strategies for Neurodegenerative Repeat Expansion Diseases**

*Craig Stewart McIntosh, BSc, MPhil*



**Murdoch**  
UNIVERSITY

This thesis is presented for the degree of Doctor of Philosophy at Murdoch University

School of Veterinary and Life Sciences

Molecular and Medical Sciences

2020



## THESIS DECLARATION

---

I, Craig Stewart McIntosh, declare that this thesis is my own account of my research and contains work that has not been previously submitted for a degree of any kind at any tertiary education institution.

This work does not contain any material previously published or written by another person, except where due reference has been made in the text. This document consists, in part, a thesis by publication, and all publications have been inserted as the journal formatted PDF, designated with a Chapter number. All publications adhere to Creative Commons licensing.

**PLEASE NOTE:** For Chapters consisting of publications, the Tables and Figures in these Chapters are numbered in accordance with the journal in which they were published and are not listed in the “List of Tables and Figures”. Additionally, the references in these Chapters are also numbered in accordance with the journal in which they were published and are not listed in the final “References”.

The work(s) are not in any way a violation or infringement of any copyright, trademark, patent, or other rights whatsoever of any person. All published papers abide by creative commons licence and are not in violation of any copyright.

The research involving human data reported in this thesis was assessed and approved by Murdoch University Human Research Ethics Committee, Approval #: 2013/156 and 2017/101.

The research in this thesis was funded by Sarepta Therapeutics and NHMRC grants APP1086311 and APP1144791. Scholarships supporting the candidate during the undertaking of this work were kindly provided by the Research Training Program (formerly Australian Postgraduate Award) and the Murdoch University Top-up Scholarship.

Technical assistance was kindly provided by AGRF who performed all RNA-sequencing described in **Chapter 3**, and Dr May Thandar Aung-Htut in preparation of the manuscripts presented in **Chapter 6**

and **Chapter 7**, for which we are both co-first authors. Thank you to Professor Merrilee Needham, who performed all the local human dermal biopsies used for preparation of fibroblast cultures.

Signature:

Date: 28 May 2020

## ABSTRACT

---

Over 40 diseases, primarily affecting the nervous system, are caused by expansion of simple repetitive sequences found throughout the human genome, termed repeat expansion diseases. Expansions can occur in coding and non-coding regions of the genome, leading to several proposed mechanisms of disease, accumulation of either toxic RNA or toxic protein, although gain-of-function mechanisms are suggested causes of pathogenesis.

Currently, there is no cure nor effective treatment strategy for any repeat expansion diseases. However, for many of these expansion diseases, splice-switching antisense oligonucleotides (AOs) may offer promise as a therapeutic strategy, as these compounds have already demonstrated efficacy in the treatment of other types of genetic disorders. Antisense oligonucleotides are short synthetic nucleic acid analogues, designed to target specific pre-mRNA sequences by reverse-complementary Watson-Crick binding, thereby modifying processing and/or abundance of the transcript and the sequence of the encoded protein. While there are a number of applications for AOs, this study focuses on their utility for preventing translation of toxic protein isoforms, either by altering the target transcript to encode a truncated protein isoform, or by disrupting the reading frame to downregulate endogenous protein production.

The first part of this study focused on ameliorating the toxic polyglutamine tract found in the ataxin-3 protein that causes spinocerebellar ataxia type 3 (SCA3). One of nine known polyglutamine disorders, SCA3 is a clinically heterogeneous disease, primarily exemplified by progressive ataxia impairing the speech, balance and gait of affected individuals. SCA3 is caused by expansion of a glutamine-encoding tract located at the 5' end of the penultimate exon (exon 10) of the *ATXN3* gene transcript, resulting in conformational changes in ataxin-3 and a toxic gain-of-function. Here, we describe highly efficient removal of the toxic polyglutamine tract of ataxin-3 *in vitro* by phosphorodiamidate morpholino oligomers (PMOs). Additionally, these PMOs induced a potentially beneficial downregulation of both the expanded

and non-expanded protein isoforms. As SCA3 has a typical age of onset in the fourth decade, the observed downregulation could delay age of onset by reducing the amounts of the toxic aggregates. Although we induce downregulation of both isoforms, we believe that the proportion of the truncated protein may be sufficient for overall function of ataxin-3, as some studies have shown ataxin-3 protein to be partially dispensable.

Recently, several *in vitro* and *in vivo* studies have found that targeted knockdown of transcription elongation factors *SUPT4H1*, and to a lesser extent *SUPT5H*, can reduce aggregation of expanded transcripts and protein, and alleviate the disease phenotype in animal models of various expansion diseases. We therefore sought to investigate *in vitro*, the potential of AO-mediated *SUPT4H1* downregulation as a therapeutic strategy. We found that our AOs were able to significantly downregulate *SUPT4H1*, with minimal changes to the rest of the transcriptome. We then assessed whether this downregulation of *SUPT4H1* lead to a reduction in expanded *ATXN3* mRNA and/or *ATXN3* protein expression, however, unfortunately in the models available and under the current study, no modification to the *ATXN3* transcript or protein was observed. This lack of effect may be due to the relatively short, expanded repeat lengths in SCA3 cell lines, and we therefore recommend that future studies assess genes with larger expansions, such as the 100-1000s repeat tracts frequently observed in myotonic dystrophy type 1 (*DMPK*).

In order to create an efficient screening process for finding clinic-ready AOs, it is important to have a detailed understanding of the principles of AO design. We therefore present a comprehensive rationale for efficiently design and *in vitro* delivery of splice modulating AOs. These approaches and recommendations provide a streamlined methodology for any researcher developing AO therapeutics.

The results presented in this thesis indicate that morpholino oligomers will provide superior benefit for the treatment of spinocerebellar ataxia type 3, without the toxic effects that result from other antisense oligomer chemistries. Additionally, AO-induced *SUPT4H1* knockdown may yet demonstrate therapeutic

application for a multitude of expansion diseases, pending further investigation into the whole transcriptome effects and *in vivo* efficacy of this strategy. Lastly, our guidelines for therapeutic AO developments should aid other researchers in creating the most efficacious and safe AOs for clinical trials. The work presented in this thesis contributes to the greater body of knowledge about the applications of AOs, as well as the need for reliable and systematic protocols in AO research and interpretation. With ongoing collaboration from our industry partners, Sarepta Therapeutics, there is hope that the work presented here will provide a solid foundation for further research into AO therapeutics for the treatment of neurodegenerative expansion diseases.

# TABLE OF CONTENTS

---

<b>THESIS DECLARATION.....</b>	<b><i>i</i></b>
<b>ABSTRACT.....</b>	<b><i>iii</i></b>
<b>TABLE OF CONTENTS.....</b>	<b><i>vi</i></b>
<b>LIST OF TABLES AND FIGURES.....</b>	<b><i>xi</i></b>
<b>ACKNOWLEDGEMENTS .....</b>	<b><i>xiv</i></b>
<b>AUTHOR DECLARATIONS – (THESIS BY PUBLICATION – CHAPTERS 4 – 7).....</b>	<b><i>xvi</i></b>
<b>LIST OF ABBREVIATIONS.....</b>	<b><i>xix</i></b>
<b>Chapter 1 –Introduction and Literature Review .....</b>	<b><i>1</i></b>
<b>1.1 Transcription.....</b>	<b><i>3</i></b>
1.1.1 Initiation.....	<i>4</i>
1.1.1.1 Transcription, promoters, and enhancers.....	<i>4</i>
1.1.1.2 Transcription factors.....	<i>5</i>
1.1.1.3 Assembly of preinitiation complex.....	<i>5</i>
1.1.1.4 Open complex formation.....	<i>6</i>
1.1.1.5 Promoter escape.....	<i>6</i>
1.1.2 Elongation.....	<i>7</i>
1.1.2.1 Elongation factors.....	<i>7</i>
1.1.2.2 Transcription fidelity.....	<i>8</i>
1.1.3 Termination.....	<i>9</i>
1.1.3.1 Factor-dependent termination.....	<i>9</i>
1.1.3.2 RNA Pol II disassociation.....	<i>10</i>
<b>1.2 Splicing.....</b>	<b><i>11</i></b>
1.2.1 Process of pre-mRNA Splicing.....	<i>11</i>



1.2.2	The Spliceosome.....	12
1.2.3	Splicing Factors.....	14
1.2.4	Alternative Splicing.....	15
1.2.5	Splicing and Disease.....	17
<b>1.3</b>	<b>Antisense Oligonucleotides .....</b>	<b>19</b>
1.3.1	Chemistries and Modifications.....	19
1.3.2	Modes of Action and Clinical Applications.....	22
1.3.2.1	RNaseH-mediated degradation.....	24
1.3.2.2	Splice-switching.....	25
1.3.2.3	Alternative steric hindrance mechanisms.....	26
1.3.2.4	Small interfering RNA (siRNA).....	28
1.3.3	Benefits and Drawbacks of Antisense Oligonucleotides.....	28
1.3.3.1	Therapeutic benefits.....	29
1.3.3.2	Current drawbacks.....	29
<b>1.4</b>	<b>Aims of this Thesis.....</b>	<b>31</b>
1.4.1	Spinocerebellar Ataxia Type 3.....	31
1.4.2	SUPT4H1 and SUPT5H.....	32
1.4.3	<i>In vitro</i> Validation of Antisense Oligonucleotides.....	32
<b>Chapter 2</b>	<b>– Materials and Methods .....</b>	<b>34</b>
<b>2.1</b>	<b>Materials.....</b>	<b>35</b>
2.1.1	Chemicals and Reagents.....	35
2.1.2	Stock Buffers - Made in House.....	37
<b>2.2</b>	<b>Methods .....</b>	<b>38</b>
2.2.1	Antisense Oligonucleotide Design and Synthesis.....	38
2.2.2	Cell Culture and Seeding.....	39
2.2.2.1	Proliferation conditions and cell lines.....	39
2.2.2.2	Passage and seeding cells into plates and flasks.....	40

2.2.3	Transfection and Nucleofection.....	41
2.2.3.1	2'-O-methyl AOs transfection of cells in 24 well plates (for RNA analysis) .....	41
2.2.3.2	2'-O-methyl AO transfection of cells in T25 cm <sup>2</sup> flasks (for protein analysis) .....	41
2.2.3.3	Nucleofection.....	42
2.2.3.4	PMO transfection using Endo-Porter as a delivery agent.....	42
2.2.3.5	Transfection with PPMOs.....	43
2.2.4	Harvesting of Cells for Analysis.....	43
2.2.4.1	Harvesting cells for RNA isolation using TRIzol reagents.....	43
2.2.4.2	Harvesting of cells for RNA isolation using MagMAX kit.....	44
2.2.4.3	Harvesting cells for protein analysis by western blot.....	45
2.2.5	Reverse-transcriptase Polymerase Chain Reaction and Agarose Gel Electrophoresis.....	45
2.2.6	Band Stab and Sequencing.....	46
2.2.7	Western Blot Analysis.....	47
2.2.7.1	Sample preparation .....	47
2.2.7.2	Protein loading gel and bicinchoninic acid assay .....	47
2.2.7.3	Western blot .....	48
<b>Chapter 3 – SUPT Downregulation .....</b>		<b>51</b>
<b>3.1</b>	<b>Background &amp; Introduction .....</b>	<b>52</b>
<b>3.2</b>	<b>Materials and Methods.....</b>	<b>56</b>
3.2.1	AO Design and Synthesis.....	56
3.2.2	Cell Culture.....	58
3.2.3	Transfection.....	58
3.2.4	RNA Extraction and RT-PCR assays.....	58
3.2.5	Western Blotting.....	59
3.2.6	Transcriptome Analysis.....	60
3.2.7	Densitometric and Statistical Analysis.....	61
<b>3.3</b>	<b>Results.....</b>	<b>62</b>

3.3.1	<i>SUPT4H1</i> & <i>SUPT5H</i> Target Identification and Therapeutic Strategy.....	62
3.3.1.1	<i>SUPT4H1</i> gene and protein.....	62
3.3.1.2	<i>SUPT5H</i> gene and protein.....	63
3.3.2	Initial 2'-Me PS AO Screen.....	64
3.3.2.1	<i>SUPT4H1</i> 2'-Me PS screen.....	65
3.3.2.2	<i>SUPT5H</i> 2'-Me PS screen.....	67
3.3.3	Initial PPMO AO Screen and <i>SUPT4H1</i> Protein Analysis.....	69
3.3.3.1	<i>SUPT4H1</i> PPMO screen.....	69
3.3.3.2	<i>SUPT5H</i> PPMO screen.....	71
3.3.3.3	<i>SUPT4H1</i> exon 2 protein analysis.....	73
3.3.4	<i>SUPT4H1</i> and <i>SUPT5H</i> Transcriptome Analysis.....	74
3.3.4.1	Multidimensional scaling plot analysis.....	75
3.3.4.2	Analysis of differentially expressed genes in treated samples compared to GTC.....	76
3.3.4.3	Analysis of differentially expressed genes in PPMO 103 treated samples compared to GTC	
	79	
3.3.5	Assessment of the effect of <i>SUPT4H1</i> Downregulation on Expanded Ataxin-3 Protein.....	82
<b>3.4</b>	<b>Discussion.....</b>	<b>84</b>
<b>Chapter 4 – Published Review Article.....</b>		<b>90</b>
<b>Chapter 5 – Published Research Article 1.....</b>		<b>108</b>
<b>Chapter 6 – Published Research Article 2.....</b>		<b>124</b>
<b>Chapter 7 – Published Research Article 3.....</b>		<b>137</b>
<b>Chapter 8 – Final Discussion and Conclusion.....</b>		<b>149</b>
<b>8.1</b>	<b>The Current Therapeutic Landscape for Expansion Diseases.....</b>	<b>150</b>
8.1.1	Modulation of Cognitive Aging Pathways.....	151
8.1.2	Increasing Mutant Protein Clearance.....	152
8.1.3	Genetic Therapies to treat repeat expansion disorders.....	154

8.1.3.1	Gene silencing in repeat expansion disorders.....	155
8.1.3.2	Single stranded oligonucleotide therapies.....	156
<b>8.2</b>	<b>AO Strategies to Treat Expansion Diseases and the Major Findings .....</b>	<b>157</b>
8.2.1	Antisense Oligonucleotide-mediated removal of the polyglutamine repeat in ATXN3 .....	158
8.2.2	AO-Mediated Knockdown of SUPT4H1 as a Modifier to Ameliorate Repeat Expansion Diseases 159	
8.2.3	Systematic Development of 2'-Me PS AO and Delivery Optimisation of PMOs.....	161
<b>8.3</b>	<b>Final Thoughts and Conclusion.....</b>	<b>162</b>
<b>Chapter 9 – Appendices.....</b>		<b>164</b>
9.1	Appendix 1: Supplementary Figures .....	165
9.2	Appendix 2: List of Awards and Achievements Received during PhD Candidature .....	168
<b>REFERENCES.....</b>		<b>169</b>

## LIST OF TABLES AND FIGURES

---

### CHAPTER 1 – INTRODUCTION and LITERATURE REVIEW

Page #

#### Tables:

<b>Table 1.1:</b> Transcription initiation factors and their individual functions	5
<b>Table 1.2:</b> List and function of common transcription elongation factors	7
<b>Table 1.3:</b> List of typical RNA Pol II termination factors and their functions	10

#### Figures:

<b>Figure 1.1:</b> Diagrammatic representation of the pre-initiation complex	6
<b>Figure 1.2:</b> Positive and negative transcription elongation	8
<b>Figure 1.3:</b> Schematic of the splicing process and major spliceosome assembly	14
<b>Figure 1.4:</b> Various mechanisms of transcript modification	16
<b>Figure 1.5:</b> Common chemical modifications used in antisense oligonucleotide synthesis	21
<b>Figure 1.6:</b> Mechanisms of antisense oligonucleotide mediated modulation of gene expression	23

### CHAPTER 2 – MATERIALS and METHODS

#### Tables:

<b>Table 2.1:</b> List of reagents used in this study and their respective manufacturer	35-36
<b>Table 2.2:</b> Stock buffers prepared in-house	37
<b>Table 2.3:</b> List of control AOs used in this study, with sequences shown 5'-3'	38
<b>Table 2.4:</b> Proliferation media used to maintain cell lines	40
<b>Table 2.5:</b> Cell density for seeding various cell types for 2'-Me transfections	40
<b>Table 2.6:</b> List of Primers used in this study	45-46
<b>Table 2.7:</b> List of antibodies used for Western blot in this study	49

## CHAPTER 3 – SUPT DOWNREGULATION

Page #

### Tables:

<b>Table 3.1:</b> List of SUPT4H1 2'-Me PS AOs and their corresponding PPMO homologues	<b>56</b>
<b>Table 3.2:</b> List of SUPT5H 2'-Me PS AOs and their corresponding PPMO homologues	<b>57</b>
<b>Table 3.3:</b> List of SUPT cocktails used	<b>57</b>
<b>Table 3.4:</b> Table displaying primer information used in this Chapter	<b>59</b>
<b>Table 3.5:</b> List of antibodies used with corresponding dilutions and manufacturer information	<b>60</b>
<b>Table 3.6:</b> : List of PPMOs analysed for potential off-target effects on the transcriptome	<b>74</b>
<b>Table 3.7:</b> Number of differentially expressed genes $\geq \log_2$ in PPMO 1083 treated SH-SY5Y cells	<b>79</b>

### Figures:

<b>Figure 3.1:</b> Representation of the SUPT4H1 reading frame and protein structure	<b>63</b>
<b>Figure 3.2:</b> Representation of the SUPT5H reading frame and protein structure	<b>64</b>
<b>Figure 3.3:</b> Evaluation of AOs designed to alter SUPT4H1 transcript structure in normal human fibroblasts	<b>66</b>
<b>Figure 3.4:</b> Evaluation of AOs designed to alter SUPT5H transcript structure in normal human fibroblasts	<b>68</b>
<b>Figure 3.5:</b> Evaluation of AOs designed to alter SUPT4H1 transcript structure in undifferentiated SH-SY5Y cells	<b>70</b>
<b>Figure 3.6:</b> Evaluation of AOs designed to alter SUPT5H transcript structure in undifferentiated SH-SY5Y cells	<b>72</b>
<b>Figure 3.7:</b> Evaluation of SUPT4H1 exon 2 skipping in SH-SY5Y cells, transfected with PPMOs	<b>73</b>
<b>Figure 3.8:</b> RNA sequencing analysis of PPMO treated SH-SY5Y cells showing MDS plots	<b>76</b>
<b>Figure 3.9:</b> RNA sequencing analysis of PPMO treated SH-SY5Y cells showing parallel coordinates graph and heatmap of differentially expressed transcripts	<b>78</b>
<b>Figure 3.10:</b> RNA sequencing analysis of SH-SY5Y cells showing a heat map and MA plot	<b>80</b>

**Figure 3.11:** Gene ontology enrichment analysis of differentially expressed genes in PPMO 1083 treated SH-SY5Y cells **81**

**Figure 3.12:** Evaluation of SUPT4H1 exon 2 skipping in SCA3 fibroblasts transfected with PPMOs at a concentration of 5  $\mu$ M **83**

## **CHAPTER 9 – APPENDICES**

Page #

**Supplementary Figure S3.1:** RT-PCR analysis of PCR primers conducted in normal human fibroblasts at three various annealing temperatures 55, 60 and 62°C **166**

**Supplementary Figure S3.2:** Evaluation of SUPT5H exon skipping in SH-SY5Y cells, transfected with PPMOs **167**

**Supplementary Figure S3.3:** RT-PCR analysis of free uptake of PPMOs in SH-SY5Y cells at a concentration of 5  $\mu$ M for 72 hours **168**

## ACKNOWLEDGEMENTS

---

This thesis, although attributed to me, would not have been possible without the support, kindness, and love of so many people.

Firstly, I would like to say a huge, huge thank you to my three supervisors, Steve, Sue, and May. Steve and Sue, you took a chance on me, when I came to you with no tissue culture or AO experience and the faith you two have shown in me means more than you will ever know, so thank you. Steve and Sue, the commitment you both show to your work, students and staff is inspiring, your door is always open and have been the most supporting supervisors I know. Steve, I hope to enjoy a lot of whisky with you in the future and Sue all the treats you bring in have given me so much joy, once again from the bottom of my heart THANK YOU. To May, I cannot say thank you enough for all your help and technical assistance you have given me over the past 3.5 years. At times I must have infuriated you with all my questions and troubleshooting, yet you never got frustrated and always had time for me. This thesis is as much yours as it is mine. You were my mentor in the lab and gave me so much support that I can never repay, thank you.

To everyone at MTL thank you for your help over the years, especially Russell for Westerns and Abbie for the countless hours of management and lab organisation. To Jodie and Bri thank you for all you do for the centre and your tireless hours of administration to keep everyone ticking over you guys are the best. To the crew, May, Loren, Kristin, Kane, lanthe, Kelly, and Niall, not only have you always helped me and calmed me down, you listened to my heavy breathing and heavy metal. We have become more than colleagues and I see you all as my close friends. It is truly an honour and privilege to work in such a fantastic lab. To many more wine and cheese nights.

To my Mom and Dad, I wrote one of these for my Master's thesis and I said I would finally get a job (a lie!), well it has come true and I cannot wait. Thank you for your 30-year support, you both are truly an



inspiration and if I can be half as successful as you two then I have done myself proud. Sherri and Ashley, my two sisters, thank you for always bringing me down to earth and reminding me of the fun times. We argued a lot and sometimes I was not the best brother but thank you for always sticking up for me and believing in me.

Lastly, to the most important person in my life, my little human, my soulmate, my wife, Mariska, words cannot begin to describe how much I love you and how much I appreciate everything you have done. We met just before this journey began and ever since day one you have been nothing but supportive, you have put up with my mood swings and down times, but you were always there to pick me up. Thanks for being a great Mom to our fur baby Walter, who I have to thank as well. Walter you have brought me so much joy the past year and your Bully-runs and zoomies keep me entertained for hours. Mariska FROM THE BOTTOM OF MY HEART, **THANK YOU, THANK YOU, THANK YOU**. It is time to make a difference in the lives of those less fortunate than us. Here is to our future together. I LOVE YOU.

## AUTHOR DECLARATIONS – (THESIS BY PUBLICATION – CHAPTERS 4 – 7)

---

Please note: Hard copy signatures (written) can be provided on request

**Chapter 4** – McIntosh, C. S., Aung-Htut, M. T., Fletcher, S., & Wilton, S. D. (2017). Polyglutamine ataxias: From Clinical and Molecular Features to Current Therapeutic Strategies. *J Genetic Syndromes Gene Therapies*, 8(319), 2.

	C McIntosh	M Aung-Htut	S Fletcher	S Wilton
Conceptualisation	•			
Methodology	•			
Formal Analysis	•			
Investigation	•			
Writing	•	•	•	•
Editing	•	•	•	•
Supervision		•	•	•
<b>Signature (Digital)</b>	CSM	MTAH	SF	SDW

**Chapter 5** – McIntosh, C. S., Aung-Htut, M. T., Fletcher, S., & Wilton, S. D. (2019). Removal of the Polyglutamine Repeat of Ataxin-3 by Redirecting pre-mRNA Processing. *International Journal of Molecular Sciences*, 20(21), 5434.

	C McIntosh	M Aung-Htut	S Fletcher	S Wilton
Conceptualisation	•	•		
Methodology	•			
Formal Analysis	•			
Investigation	•			
Writing	•	•	•	•
Editing	•	•	•	•
Supervision		•	•	•
<b>Signature (Digital)</b>	CSM	MTAH	SF	SDW

**Chapter 6** – Aung-Htut, M. T.\* , McIntosh, C. S\*., Ham, K. A., Pitout, I. L., Flynn, L. L., Greer, K., ... & Wilton, S. D. (2019). Systematic approach to developing splice modulating antisense oligonucleotides. *International Journal of Molecular Sciences*, 20(20), 5030.

	<b>C McIntosh</b>	<b>M Aung-Htut</b>	<b>K Ham</b>	<b>I Pitout</b>	<b>L Flynn</b>	<b>K Greer</b>	<b>S Fletcher</b>	<b>S Wilton</b>
<b>Conceptualisation</b>	•	•						
<b>Methodology</b>	•	•						
<b>Formal Analysis</b>	•	•	•					
<b>Investigation</b>	•	•	•					
<b>Writing</b>	•	•	•				•	•
<b>Editing</b>	•	•	•	•	•	•	•	•
<b>Supervision</b>							•	•
<b>Signature (Digital)</b>	<i>CSM</i>	<i>MTAH</i>	<i>KAH</i>	<i>ILP</i>	<i>LLF</i>	<i>KLK</i>	<i>SF</i>	<i>SDW</i>

**Chapter 7** – Aung-Htut, M. T.\*, McIntosh, C. S.\*, West, K. A., Fletcher, S., & Wilton, S. D. (2019). In vitro validation of phosphorodiamidate morpholino oligomers. *Molecules*, 24(16), 2922.

	<b>C McIntosh</b>	<b>M Aung-Htut</b>	<b>K Ham</b>	<b>S Fletcher</b>	<b>S Wilton</b>
<b>Conceptualisation</b>	•	•			
<b>Methodology</b>	•	•			
<b>Formal Analysis</b>	•	•	•		
<b>Investigation</b>	•	•	•		
<b>Writing</b>	•	•	•	•	•
<b>Editing</b>	•	•	•	•	•
<b>Supervision</b>				•	•
<b>Signature (Digital)</b>	<i>CSM</i>	<i>MTAH</i>	<i>KAH</i>	<i>SF</i>	<i>SDW</i>

## LIST OF ABBREVIATIONS

Abbreviation	Word(s) in Full
2'-Me	2'-O-methyl
2'-MOE	2'-O-methoxyethyl
3'ss	3' splice site
5'ss	5' splice site
aa	Amino acid
ALS	Amyotrophic lateral sclerosis
AO	Antisense oligonucleotide
BP	Branchpoint
CMV	Cytomegalovirus retinitis
CPSF	Cleavage and polyadenylation specificity factor
CstF	Cleavage stimulation factor
DE	Differentially expressed
DMD	Duchenne muscular dystrophy
DNA	Deoxyribonucleic acid
DPR	Dipeptide repeat
DSIF	DRB-sensitive inducing complex
ESE	Exonic splicing enhancer
ESS	Exonic splicing silencer
Ex	Exon
FBN1	Fibrillin 1
FBS	Fetal bovine serum
FDA	Food and Drug Administration
FDR	False detection rate
FL	Full Length
GO	Gene Ontology
GTC	Gene Tools Control
HD	Huntington's disease
hnRNPs	Heterogenous ribonucleoproteins
HS	Horse serum
iPSC	Induced pluripotent stem cell
ISE	Intronic splicing enhancer
ISS	Intronic splicing silencer
kDa	Kilo Dalton
LNA	Locked nucleic acid
MDS	Multidimensional scaling
MND	Motor neuron disease
mRNA	messenger RNA
NELF	negative elongation factor
NES	Nuclear export signal

<b>Abbreviation</b>	<b>Word(s) in Full</b>
<b>NLS</b>	Nuclear localisation signal
<b>NMD</b>	Nonsense mediated decay
<b>NONO</b>	Non-POU domain containing, octamer-binding
<b>PCR</b>	Polymerase chain reaction
<b>PIC</b>	Pre-initiation complex
<b>PMO</b>	Phosphorodiamidate morpholino oligomer
<b>PNA</b>	Peptide nucleic acid
<b>PolyA</b>	Polyadenylation
<b>PolyQ</b>	Polyglutamine
<b>PPMO</b>	Peptide conjugated PMO
<b>Pre-mRNA</b>	Precursor messenger RNA
<b>PS</b>	Phosphorothioate
<b>RAN</b>	Repeat-associated non-ATG
<b>RISC</b>	RNA-induced silencing complex
<b>RNA</b>	Ribonucleic acid
<b>RNA Pol I</b>	RNA polymerase I
<b>RNA Pol II</b>	RNA polymerase II
<b>RNA Pol III</b>	RNA polymerase III
<b>RNA-seq</b>	RNA Sequencing
<b>RP</b>	Retinitis pigmentosa
<b>RT-PCR</b>	Reverse transcription PCR
<b>SCA</b>	Spinocerebellar ataxia
<b>SF1</b>	Splicing factor 1
<b>siRNA</b>	Short interfering RNA
<b>SMA</b>	Spinal muscular atrophy
<b>SNP</b>	Single nucleotide polymorphism
<b>snRNA</b>	small nuclear RNA
<b>snRNP</b>	small nuclear ribonucleoproteins
<b>SR</b>	Serine/arginine rich RNA binding protein
<b>TBP</b>	TATA box binding protein
<b>TSS</b>	Transcription start site
<b>UIM</b>	Ubiquitin interacting motif
<b>UT</b>	Untreated
<b>Δ</b>	Missing/Removed (Delta)

# **Chapter 1 – Introduction and Literature Review**

Gene expression can be defined as the process by which genetic information stored in DNA is converted into gene products. These products may be functional proteins encoded by genomic regions that are transcribed, processed and translated into polypeptides, but may also arise from outside the classically defined “coding regions” – in fact, it is now known almost all of the genome is transcribed into RNA [1]. Intergenic and intragenic non-coding regions contribute to the control of gene expression, and evidence of pervasive transcription throughout the genome from both sense and antisense strands implicates a functional role for nearly all regions of the genome [2]. Much of the human genome was once classified as “junk DNA”, however we now know that many such regions are transcribed into a staggering 100 distinct types of RNA, all of which are integral facets of the control of gene expression [3].

Our understanding of gene expression has significantly improved over the past few decades. In the 1960s, it was proposed that each gene was responsible for the expression of a single protein [4], but now it is known that through pre-mRNA processing and translational mechanisms such as alternative splicing, phosphorylation, and acetylation, one gene can give rise to many different protein isoforms, some with diametrically opposed roles and functions [5]. Advances in molecular research techniques have also shown that genomic elements outside of protein-coding regions can greatly influence gene expression [3,6].

While the genomes of different individuals of the same species differ, these differences are most frequently small alterations such as single nucleotide changes, but other types of genetic variation are prevalent and can have unique and characteristic effects. All known species carry ‘microsatellites’, stretches of 1-6 nucleotide repeating sequences, throughout their genomes. Although microsatellites are not inherently disease causing, they can affect genome function and gene expression, and may change in number over the lifespan of an individual, or across successive generations [7].

Repeat expansion disorders are a group of approximately 40 diseases caused by both coding and non-coding microsatellite repeats that become unstable and expand beyond a threshold length, and includes



the spinocerebellar ataxias, spinal and bulbar muscular atrophy, fragile X syndrome, myotonic dystrophy, and Huntington's disease [8]. The root cause of these diseases is the instability of their repeat tracts, as this instability can lead to 'anticipation', the expansion of the repeat with each successive generation that manifests as a more severe phenotype and earlier age of onset [9]. Repeat expansions can interfere with nuclear function, gene regulation, transcript structure or function and/or protein coding sequence. In some cases, the mechanism of disease is a loss of function of the encoded protein, while in others, either the mRNA or the protein evokes toxic gain-of-function [10].

This introduction examines two fundamental steps in gene expression that occur prior to translation: transcription and pre-mRNA splicing. For the purpose of this review, protein-coding gene expression will be addressed rather than the non-coding regulatory regions.

## 1.1 Transcription

Transcription is the first of a series of events in protein coding gene expression. Simplistically, one DNA strand of a gene acts as the template to direct the synthesis of an antiparallel, complementary RNA strand by an RNA polymerase through precise, complex and tightly regulated steps [11]. Typically, in protein coding genes only one strand of DNA, the antisense strand, is transcribed and is read 3' end to the 5' end (3' – 5'). The corresponding (non-template) strand of DNA is known as the sense strand as it is the same sequence as the newly created RNA, bar the substitution of uracil for thymine. For the purpose of this review the process of transcription will be broken down into three major steps:

1. Initiation
2. Elongation
3. Termination

Eukaryotic genome transcription is performed by either nuclear RNA polymerase I (RNA Pol I), RNA Pol II or RNA Pol III. RNA Pol I is responsible for the transcription of rRNA precursors, RNA Pol III transcribes

small non-coding RNAs (e.g. tRNA) [12] and RNA Pol II, the focus of this review, is responsible for transcribing long non-coding RNAs and protein coding gene transcription that ultimately produces the mRNAs that are processed, exported and translated into polypeptides. RNA Pol II is a 12-subunit enzyme, the regulation of which is crucial to cell identity, cell maintenance and differentiation [12]. Understanding the regulatory basis of RNA Pol II therefore requires a firm comprehension of the RNA Pol II initiation complex and molecular mechanisms of transcript initiation, as well as elongation of the transcript, RNA Pol II pausing and eventual termination and dissociation from the transcript.

## **1.1.1 Initiation**

### *1.1.1.1 Transcription, promoters, and enhancers*

Transcription initiation commences with RNA Pol II gaining access to the promoter region at the 5' end of the sense strand of the gene. Chromatin opening and accessibility are differentially regulated by two classes of promoters [13], one containing CpG islands and the other consisting of TATA regulatory promoters. The CpG promoters facilitate polymerase access through impairment of the assembly of inhibitory nucleosomes [14], and are often found in genes encoding ubiquitously expressed proteins. TATA regulatory promoters contain TATA elements located upstream of the transcription start site (TSS) [15], and are often found in genes that show tissue-specific expression [16].

Transcription factors are able to bind to promoters and facilitate transcription initiation. Some also bind to transcriptional enhancers, distinct *cis*-acting elements that positively regulate transcription and may be found up to a million or more base pairs away from the TSS [17]. Transcription enhancers often contain multiple transcription factor binding sites that function synergistically [18], and are located within genome regions known as topologically associated domains [19]. In addition to enhancers, negative regulatory elements also exist, such as transcription silencers and insulators. Like enhancers, negative elements may be located great distances from the core promoter region.

### 1.1.1.2 Transcription factors

RNA Pol II and the general class II transcription factors bind to the promoter region of a given gene and form an enormous 2000 kDa pre-initiation complex (PIC) [12]. Class II transcription factors include the TATA-box binding protein, TBP that binds upstream DNA; as well as the general transcription factors [15,20]. The general initiation factors include TFIIA, TFIIIB, TFIID, TFIIIE, TFIIIF, TFIIH [21], and as their names suggest aid RNA Pol II in transcription initiation. The main function assigned to each transcription factor can be found in **Table 1.1**.

**Table 1.1:** Transcription initiation factors and their individual functions [12,22-26]

Transcription Initiation Factor	Function
TFIIA	Aids in binding of TBP to TATA-box-containing promoter DNA
TFIIIB	Acts as a bridge between RNA Pol II and DNA
TFIID	Helps with promoter DNA recognition and includes TBP
TFIIIE	Stabilises the open promoter complex and activates TFIIH
TFIIIF	Stabilises the PIC and TFIIIB
TFIIH	Catalyses DNA opening and incites promoter escape

### 1.1.1.3 Assembly of preinitiation complex

A representation of eukaryotic RNA Pol II can be seen in **Figure 1.1**. For promoters that contain a TATA-box near the TSS, initial assembly of the PIC occurs when the TATA-box is recognised by the TBP subunit of TFIID [27,28]. Subsequently, TFIIA and TFIIIB enter the PIC that stabilises the DNA-TFIID complex and recruits RNA Pol II in conjunction with TFIIIF, while TFIIIB plays a vital role in the bridge between RNA Pol II and DNA [25,26]. One of the last factors to be recruited into the PIC is TFIIH that catalyses opening of the DNA and thus allows the next stage of transcription initiation to begin [26,29].

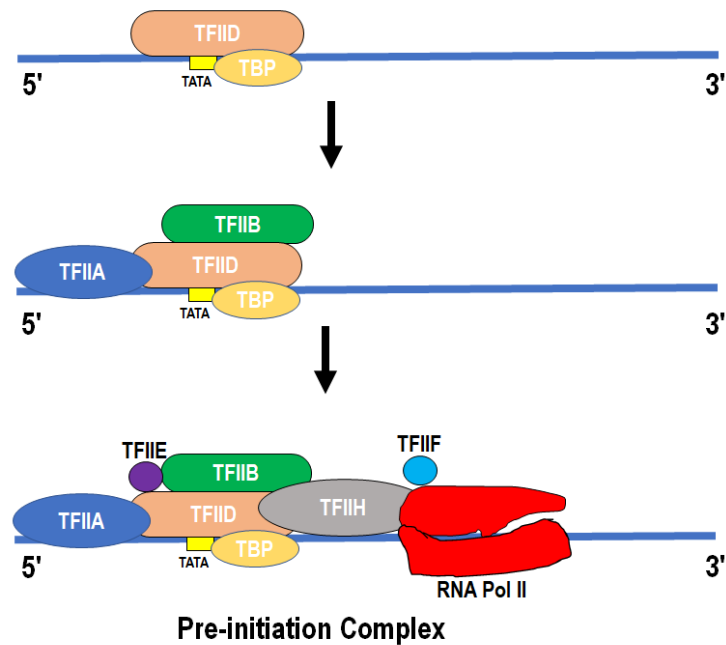


**Figure 1.1:** Diagrammatic representation of the pre-initiation complex, including the general transcription factors. Adapted from Cramer et al. (2019) [11].

#### 1.1.1.4 Open complex formation

The transition from a closed complex to an open state results in the separation of the two DNA strands, and subsequently positions the template strand close to the active site of RNA Pol II [30]. TFIIH plays a critical role in the separation of the two DNA strands, while TFIIID holds the upstream promoter DNA in a fixed position [30]. Downstream, double-stranded DNA is pulled into the cleft of RNA Pol II by TFIIH, that drives the separation of the DNA strands and transitions the complex into an open state. In addition to DNA strand separation, TFIIH also plays a vital role in promoter escape [22].

#### 1.1.1.5 Promoter escape

Once a nascent RNA transcript has reached a threshold length of 10 nucleotides, the transcript enters the RNA exit channel of the initiation complex and RNA Pol II and subsequently disassociates interactions between the promoter elements and the rest of the complex [24]. In eukaryotes, promoter escape requires

the hydrolysis of ATP, meanwhile the transcription bubble collapses and provides the required energy for promoter escape [24]. After promoter escape, transcription enters the elongation stage.

## 1.1.2 Elongation

Once RNA Pol II has escaped from the promoter and shed most of the initiation factors, the next phase of transcript elongation commences with the recruitment of new transcription elongation factors. Unlike initiation, transcription elongation is processive, with progress occurring in consecutive enzymatic reactions without substrate release. A list of the frequent factors involved in transcription elongation can be seen in **Table 1.2**.

**Table 1.2:** List and function of common transcription elongation factors [31-34]

Transcription Elongation Factor	Function
<b>DSIF</b>	Assists in RNA Pol II pausing and active elongation
<b>NELF</b>	Promotes and stabilises RNA Pol II promoter proximal pausing
<b>TFIIS</b>	Aids in stimulating RNA cleavage and improves RNA proofreading fidelity
<b>P-TEFb</b>	Initiates activation of promoter-proximal pausing of RNA Pol II by phosphorylating RNA Pol II. Also phosphorylates DSIF
<b>ELL</b>	Accelerates elongation by limiting RNA Pol II pausing
<b>5'-capping enzymes</b>	Catalyse 5' RNA cap formation and inhibits pre-mRNA degradation - includes RNA triphosphatase, guanylyltransferase and methyltransferase

### 1.1.2.1 Elongation factors

Unlike initiation, transcription elongation factors are of various classes, with some stimulating the overall rate of transcript elongation while others slow the rate or assist in transcriptional pausing [31-33]. Of particular importance is P-TEFb, a factor that phosphorylates the Ser-2 of the carboxyl terminal domain of the RPB1 subunit of RNA Pol II, and phosphorylates and activates the protein SUPT5H. Together,

SUPT5H and SUPT4H1 form the DRB-sensitivity inducing complex (DSIF), which in conjunction with negative elongation factor (NELF) can influence elongation in either a negative or positive manner [35,36].

Transcriptional pausing is facilitated by non-phosphorylated DSIF in conjunction with NELF [34]. Transcriptional promoter-proximal pausing is a typical mechanism to regulate genes that are rapidly expressed or need to be expressed in a coordinated fashion. Conversely, elongation is promoted when NELF releases from RNA Pol II and DSIF is phosphorylated [31]. The mechanism of action of DSIF is illustrated in **Figure 1.2**. Transcriptional blockade can be overcome once the RNA Pol II receives an activation signal, such as the phosphorylation of Ser-2 of the C-terminal domain. Other elongation factors such as TFIIIS and ELL stimulate the rate of elongation by limiting the duration of RNA Pol II pausing [37].

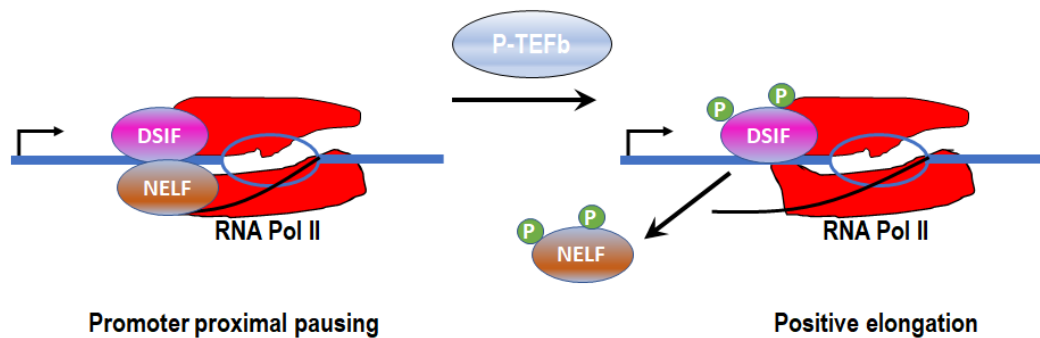


**Figure 1.2:** Positive and negative transcription elongation mediated by elongation factors DSIF and NELF. Adapted from Cramer et al. (2019) [11]. Green circle with P represents a phosphoryl group. DSIF = DRB Sensitivity Inducing Factor. NELF = Negative Elongation Factor.

### 1.1.2.2 Transcription fidelity

In order to minimise errors during transcription, RNA Pol II only recruits a nucleoside triphosphate into the active centre if it correctly base-pairs with the DNA [38]. RNA Pol II has two known proof-reading functions for detecting and removing mis-incorporated bases from the nascent transcript: hydrolytic

editing and pyrophosphorylytic editing [39]. Hydrolytic editing is the process whereby RNA Pol II backtracks and cleaves the segment of the transcript that contains the error, while pyrophosphorylytic editing entails simply removing the mis-incorporated ribonucleotide via reversal of the polymerisation reaction, i.e. 3' - 5' nuclease degradation [39]. It should be noted that all reactions performed by RNA Pol II involve the use of a single active centre [38].

### 1.1.3 Termination

The final stage of transcription is termination, wherein RNA Pol II releases the completed RNA transcript and dissociates from the template DNA strand. This process occurs in a factor-dependent manner, unlike RNA pol III, which is factor-independent [40]. Termination is the least understood process in transcription and some mechanistic processes at this time are only theorised. Although poorly understood, transcription termination is essential to many downstream cellular functions, including the prevention of RNA Pol II from interfering with potential downstream DNA elements, such as promoters, while also promoting RNA Pol II recycling [41].

#### 1.1.3.1 *Factor-dependent termination*

As RNA Pol II reaches the end of a transcribable gene, two protein complexes; cleavage and polyadenylation specificity factor (CPSF) and cleavage stimulation factor (CstF), recognise the polyadenylation (poly-A) signal in the transcribed RNA [42]. Subsequently, after RNA cleavage 15-20 bases downstream from the polyadenylation signal, poly-A polymerase adds approximately 200 adenines to the hydroxyl moiety generated at the 3' end of the RNA, without the use of a template [43,44]. Interestingly, the addition of a poly-A tail is unique to RNA transcripts synthesised by RNA Pol II [45]. Although disassociation of RNA Pol II from DNA might appear rather straight forward, it is a very complex and challenging task to stall and remove the RNA Pol II juggernaut. A list of typical termination factors is shown in **Table 1.3**.

**Table 1.3:** List of typical RNA Pol II termination factors and their functions [42,43,45]

<b>Transcription Termination Factor</b>	<b>Function</b>
<b>CPSF</b>	Recognises Poly-A sequence and cleaves pre-mRNA
<b>CstF</b>	Binds Pol II CTD and contributes to RNA binding
<b>XRN2 Complex</b>	'Torpedo' nuclease complex that degrades the emerging RNA from the 5' end and subsequently terminates RNA Pol II transcription

### 1.1.3.2 RNA Pol II disassociation

Two theories have been proposed as to how termination and disassociation are achieved. The allosteric model suggests that, when transcription proceeds through the termination sequence, this causes a disassembly of elongation factors and/or assembly of termination factors that directly leads to conformational changes in the elongation complex [46], ultimately leading to the dissociation of RNA Pol II. Conversely, the torpedo model proposes that a 5' – 3' exonuclease degrades the RNA strand as it emerges from the elongation complex after cleavage, and RNA Pol II is subsequently released when overtaken by the highly processive exonuclease [46].



## 1.2 Splicing

Unlike bacterial RNA, most protein coding transcripts in higher eukaryotes require an additional stage of processing prior to nuclear export and cytoplasmic translation, known as pre-mRNA splicing. Splicing typically occurs during or immediately after transcription and entails the precise joining together of the transcript's protein coding sequences - exons - and removal of the intervening non-coding introns.

### 1.2.1 Process of pre-mRNA Splicing

All spliced pre-mRNA transcripts contain exons, defined regions destined for inclusion in the mature mRNA. Exons are separated by introns, sequence tracts that are ultimately excluded from the mature mRNA [47]. During mRNA maturation, the introns are excised from the transcript, while the exons are consecutively ligated together to form the mature mRNA, which is then ready for export and potential protein translation or regulatory function. Accurate splicing requires highly complex coordination of numerous noncoding RNAs and proteins that interact with splicing motifs on the pre-mRNA to generate a large multi-protein complex called the spliceosome, to coordinate these molecular gymnastics [48]. At its most fundamental, a single splice event consists of two sequential transesterification reactions that ligate neighbouring exons together. However, this process is far from simple and requires hundreds of interacting proteins, small nuclear RNAs (snRNAs) and small nuclear ribonucleoproteins (snRNPs). Unfortunately, the delicate balance of this process renders it vulnerable to disruption by mutation, and errors in splicing are thought to account for up to a third of all human diseases [49].

In order to efficiently and precisely remove an intron, while leaving the flanking exons intact, exact intron/exon boundaries must be defined. These boundaries are termed the 5' splice site (5'ss) and 3' splice site (3'ss), or exon donor and exon acceptor, respectively. Exon definition is achieved via several *cis*-acting motifs that include the 5'ss and 3'ss, the branchpoint sequence, the polypyrimidine tract and competing positive and negative splicing factor binding sites [50]. The canonical 5'ss is defined by a

conserved AGGURAGU motif, while the 3'ss is defined by a (Yn)-YAG| motif (where; | = exon boundary; underlined sequence identifies invariant nucleotides; R = purine; Y = pyrimidine;) [51]. The branchpoint motif, typically located up to 40 nucleotides (nt) upstream from the 3'ss, is required for U2 snRNA binding during spliceosome formation. This motif is defined as YNCUR**A**Y (underlined sequence denotes branch formation region; bold nucleotides are highly conserved; N = any nucleotide) [51]. The polypyrimidine tract, as the name suggests, is a C/U rich region located between the 3'ss and branchpoint. The polypyrimidine tract, as well as the 3'ss, are required for assembly of complex A of the spliceosome, with the polypyrimidine tract specifically binding the U2AF protein [52].

## 1.2.2 The Spliceosome

The catalysis of splicing cannot occur without the involvement of a multi-megadalton ribonucleoprotein (RNP) complex, termed the spliceosome. The spliceosome is highly dynamic, with a constantly changing composition and conformation, allowing for flexibility and accuracy during splicing [50]. Two types of spliceosome are currently recognised: the U2-dependent spliceosome (major spliceosome) and the U12-dependent spliceosome (minor spliceosome). The major spliceosome catalyses the removal of U2-type introns, while U12 type introns (~0.5% of all introns) are spliced out by the minor spliceosome [53].

The major spliceosome is composed of 5 snRNPs; U1, U2, U5 and U4/U6 as well as numerous non-snRNP proteins, while the minor spliceosome is composed of U11, U12, U5, and U4atac/U6atac snRNPs [54]. The minor spliceosome is able to recognise the boundaries of introns with non-canonical terminal dinucleotides, such as AU-AG and AU-AC [55]. Interestingly, the divergent characteristics of U12-type and U2-type donor and acceptor splice sites has been theorised to produce unique alternative splicing patterns in higher eukaryotes [54].

The dynamic nature of the major spliceosome means that different subunits are required at various stages during splicing, as illustrated in **Figure 1.3**. The process of splicing is highly ordered, involving the

snRNPs mentioned above as well as several splicing factors, and is characterised by distinct temporal complexes. Initial assembly into Complex E involves binding of the U1 snRNP (U1) to the 5'ss, while non-snRNP splicing factor 1 (SF1) and U2AF bind to the branchpoint sequence and polypyrimidine tract respectively [56]. Subsequently, U2 snRNP is recruited by SF1 and U2AF, replaces SF1 at the branchpoint, and initiates the formation of Complex A. The recruitment of U2 then facilitates enlistment of the pre-assembled U4/U6-U5 tri-snRNP to form the pre-catalytic Complex B. Next, destabilisation of U4 and U1 leads to the dissociation of U4, while U6 replaces U1 at the 5'ss and gives rise to the activated spliceosome. This catalytically-activated Complex B initiates the first step of splicing, giving rise to Complex C. Complex C then cleaves the 5'ss, releasing the first exon and allowing the 5'ss to join to the branchpoint, thus forming a lariat within the intron. Next, the intron is cleaved at its 3'ss, releasing the lariat, and the two neighbouring exons are ligated. Finally, the spliceosome dissociates and splicing of any subsequent introns occurs. This is repeated until all the introns are removed from the pre-mRNA and a mature transcript is generated [50,57].

The minor spliceosome is assembled in a fashion broadly similar to that of the major spliceosome, but shares only a single common snRNP, U5. In the minor spliceosome, U11 and U12 replace U1 and U2, respectively, while U12 recruits U4atac, U6atac and U5 [53].

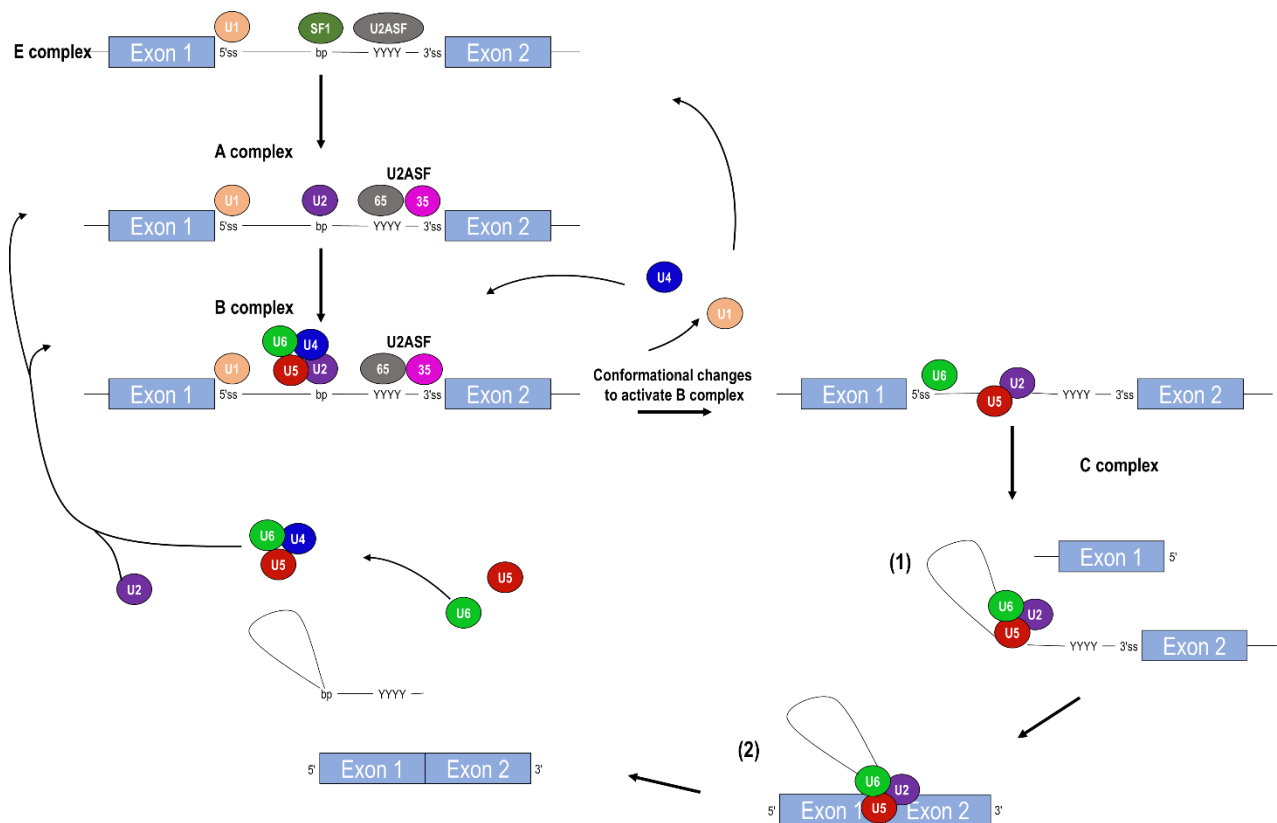


**Figure 1.3:** Schematic of the splicing process and major spliceosome assembly, including formation of the E, A, B and C complexes, and the two pre-mRNA splicing transesterification reactions. Following intron excision and ligation of the exons, the UsnRNPs are recycled. 5'ss, 3'ss, branchpoint and polypyrimidine tracts are shown in the line representing the intron. Exons are shown as light blue boxes. Adapted from Pitout (2019).

### 1.2.3 Splicing Factors

Precise and efficient splicing of exons is orchestrated by a delicate balance between positive and negative splicing factors. These factors contribute to the definition of a nucleotide sequence as an exon or an intron, bind to splicing motifs in the pre-mRNA transcript and direct the spliceosome to either exclude or include that sequence in the mature mRNA transcript. Splice enhancer motifs may be located in either the intron (intronic splicing enhancers – ISE) or the exon (exonic splicing enhancer – ESE) and these recruit the positive splicing factors that promote exon recognition by the spliceosome. Of these factors, the serine/arginine (SR) family of proteins is by far the most important and well-studied, and are believed to play a crucial role in 3'ss recognition and spliceosome direction [58,59]. Conversely, splice silencer motifs - exonic (ESS) and/or intronic splicing silencer (ISS) motifs - recruit negative splicing

factors to inhibit exon recognition by the spliceosome. The heterogeneous ribonucleoproteins (hnRNPs) are the most well-characterised class of negative splicing factors [58,60]. It has been proposed that hnRNPs function by physically blocking spliceosome assembly, thereby leading to exon exclusion [60].

The delicate balance and interplay of positive and negative splicing factors is thought to be foundational to the phenomenon known as alternative splicing.

## 1.2.4 Alternative Splicing

Alternative splicing is a process whereby multiple different isoforms arise from a single protein coding gene, and is an essential element in spatial and temporal regulation of gene expression in higher eukaryotes [5]. Alternative splicing contributes, to a large degree, the major discrepancy between the ~23 000 protein coding genes in the human genome that give rise to the ~ 100 000 proteins that are generated [5], with over 95% of all human genes undergoing some form of alternative splicing or post-translational modification (e.g. acetylation, phosphorylation and glycosylation) [5]. Alternative splicing is typically achieved by the exclusion or inclusion of one or more exons; or the use of alternative splice sites to give rise to partial exons or the retention of an intronic sequence, or part thereof to form a coding region [61]. Furthermore, these differences in splicing and ultimately mRNA sequence may have an effect on mRNA stability, localisation and translation [62] that result in various protein isoforms with distinct biological functions. The mechanisms of alternative splicing are illustrated in **Figure 1.4**.

Several *cis*-acting elements that regulate splicing are described in **Chapter 1.1.3**, and it is these elements that may cause subtle differences in recognition of the exon by the spliceosome, giving rise to alternatively spliced transcripts [63]. Alternative exons or sequences share similar 3' and 5' splice sites, however, they typically have a weaker binding affinity to the spliceosome than consensus exons, resulting in reduced recognition [64]. Next to splice site recognition, splicing factors play a major role in alternative exon recognition; SR proteins typically enhance the recognition of alternative exons while hnRNPs

conversely aid in exclusion of the exon from the mature mRNA transcript. However, there are exceptions to these rules [65,66], where two SR proteins, SF2/ASF and hTra2-beta, cause skipping of several ceramide regulated exons [65].

Alternative splicing is an integral component of the network regulating differentiation, tissue homeostasis and organ development [62]. This is most clearly exemplified by the phenomenon of tissue-specific alternative splicing, whereby specific mRNA isoforms from the same gene are selectively expressed and translated in different tissue or cell types or during specific stages of development. However, with great complexity comes an increase in opportunity for error, and errors in both alternative and constitutive splicing play a major role in many human diseases [47,67-69].

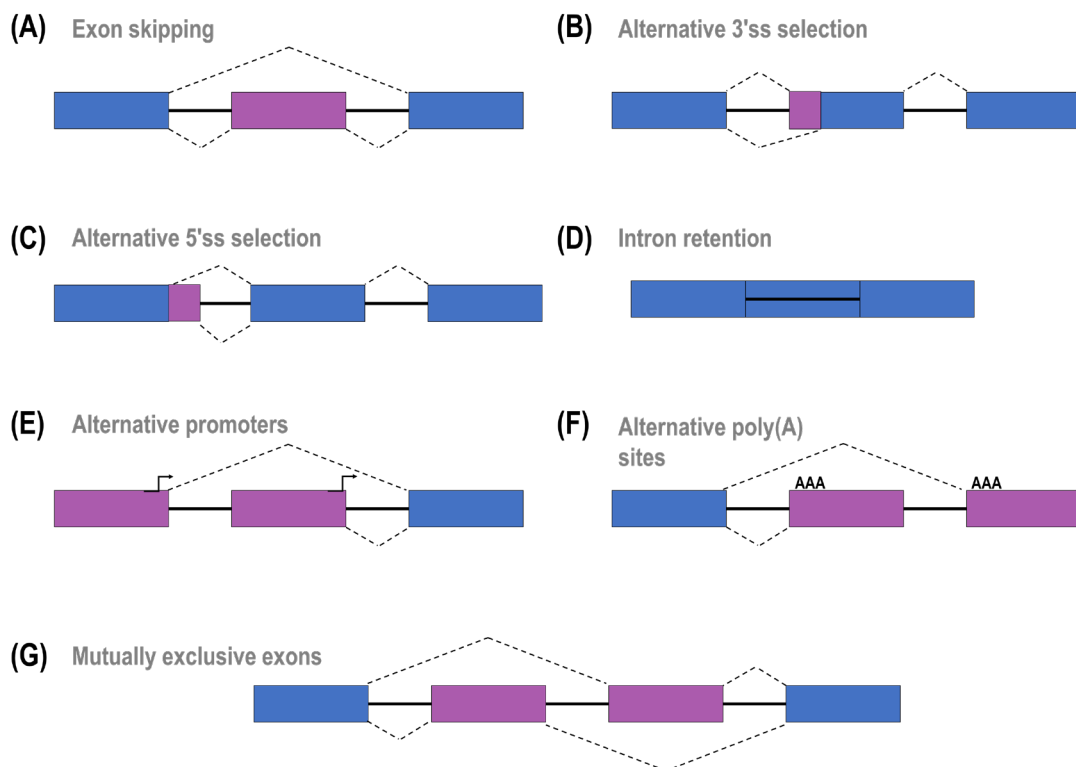


**Figure 1.4:** Various mechanisms of transcript modification. (A) Exon skipping (B) Alternative 3' splice site selection (C) Alternative 5' splice site selection (D) Intron retention (E) Alternative promoters, allowing gene expression at different times and in different tissues (F) Alternative polyadenylation site, shifting the polyadenylation site for the respective protein (G) Mutually exclusive (also known as cassette) exons. Blue boxes denote segments included in the final message, while purple boxes denote segments missed in the mature mRNA transcript. Dotted lines show the splicing pattern. Note: mechanisms are not mutually exclusive, and combinations can often occur.

## 1.2.5 Splicing and Disease

The division of eukaryote genes into exons and introns has several evolutionary benefits, such as genetic plasticity, an extended repertoire of proteins and fine control of gene expression and cellular function. However, the split construction arrangement of protein coding genes requires immense accuracy and precision in processing to efficiently and correctly splice gene transcripts, since a single base insertion or deletion will have catastrophic consequences. The most common mutations that affect splicing disrupt *cis* elements found in the regulatory elements (ESE, ESS, ISE and ISS) or canonical 5'ss (GT) and 3'ss (AG) sequences, and to a much lesser extent the branchpoint [69]. One of the most well studied disease-causing splice mutations is the single base change (C to T transition) in exon 7 of the *SMN2* transcript [70,71]. This base change, in conjunction with the homozygous deletion of *SMN1* is the cause of spinal muscular atrophy (SMA). The single base change in the duplicate gene *SMN2*, leads to an ESE motif changing to an ESS motif, leading to significant exon 7 exclusion from the mature *SMN2* transcript so that the low levels of functional *SMN2* protein are inadequate in supporting motor neuron survival [71]. Interestingly, the single base change (C to T transition) in exon 7 is both the cause and the potential treatment for SMA, without it the homozygous mutation and lack of *SMN* would be incompatible with life.

Next to *cis* elements, mutations in core constituents of the spliceosome lead to a number of discrete genetic diseases, including cancer and retinitis pigmentosa (RP) [69]. In regard to RP, it is the leading cause of hereditary blindness and arises from mutations in over 70 different genes [72]. Of these, six forms of autosomal dominant RP are caused by mutations in the *PRPF* family of genes that encode associated factors of the U4/U5.U6 tri-snRNP; namely, *PRPF4*, *PRPF6*, *PRPF8*, *PRPF31* and *SNRNP200* [73]. Although these are ubiquitously expressed splicing factors that can influence global gene expression in most cells and tissues, the retina has a disproportionately high demand for these splicing factors and thus mutations affecting these protein manifest in the retina [73].

As previously stated, splicing relies on a precise and delicate balance of factors, motifs, and splice sites, therefore any small disturbance to this balance can have catastrophic effects. Since splicing errors are involved in a substantial proportion of genetic diseases, interventions targeting pre-mRNA processing to potentially correct or compensate for these errors could be an attractive therapeutic approach for many conditions. Therapeutics could target the error at either the DNA (gene editing) or RNA processing levels, and one therapy that has achieved great momentum in the recent years is the use of antisense oligonucleotides (AO) to mediate specific modulation of the splicing process.



## 1.3 Antisense Oligonucleotides

Antisense oligonucleotides (AOs) are synthetic nucleic acid analogues that may be used to manipulate gene expression through specific sequence hybridization to a particular complementary transcript or DNA strand. Most AOs are designed to be 15 – 30 bases in length and may bind to either the target DNA or RNA strands of interest via Watson-Crick bases pairing. The first report of AO-mediated gene suppression was in 1978, when Stephenson and Zamecnik showed inhibition of viral replication through what they believed to be translational arrest [74]. However, it was later determined that the repression was due to the AO-mediated cleavage and degradation of the mRNA through RNaseH [75]. Since then, great advances have been made in AO chemistries, design and synthesis, giving rise to new mechanistic actions of these compounds. Antisense oligonucleotides now have been shown to have the ability to sterically block transcription factors, suppress translation of an mRNA via redirection of the ribosome (translational blockade), alter pre-mRNA splicing or redirect polyadenylation. This study will focus on the use of AOs to modify pre-mRNA processing by targeting sequences crucial to normal splicing of the primary gene transcript. The activity of an AO is largely determined by the specific target site as well as the respective chemistry or modification of the AO. Many of these nucleic acid modifications were designed to improve efficiency and consistency of oligonucleotide synthesis, increase resistance to nuclease degradation, increase binding affinity or reduce toxicity [76-78]. Over time and continual experimentation and refinement, AOs have moved beyond a simple laboratory tool and have progressed into the clinic as therapeutics for serious diseases previously considered untreatable [79].

### 1.3.1 Chemistries and Modifications

The chemical structures of commonly available AO chemistries are illustrated in **Figure 1.5**; however, this list is not comprehensive, as new chemistries are continually being developed. This review will consider only those AO chemistries currently pertinent.

The AOs used by Stephenson and Zamecnik were chemically synthesised DNA strands (**Figure 1.5**) on a natural phosphodiester backbone [80]. Nucleic acid synthesisers have only been readily available for the last few decades, but today DNA and RNA oligonucleotide synthesis are somewhat taken for granted. However, early experiments requiring such compounds were much more challenging, as even synthesising an AO could require months of work by expertly-trained nucleic acid chemists. The identification of the RNaseH DNA:RNA degradation mechanism [75] was an important step, but these early DNA AOs had several limitations, the greatest being their high susceptibility to nuclease degradation [81]. To overcome this issue, backbone modifications were explored and one of the most significant modifications was substitution of the non-bridging oxygen residue of the natural phosphodiester backbone with a sulphur residue to generate a phosphorothioate (PS) backbone [82]. The PS modification substantially improved DNA-AO biological stability and increased resistance to nucleases. Since DNA-PS-AOs are negatively charged and able to induce RNaseH, these compounds became a popular choice for transcript downregulation due to ease and efficiency of synthesis and relatively low cost of production [83]. However, the drawbacks of DNA-PS-AOs are their tendencies to induce sequence-independent off-target effects associated with the PS backbone, and to activate sequence-dependant innate immune response through Toll-like receptors (e.g. Toll-like receptor 7 and 9) [84-87].

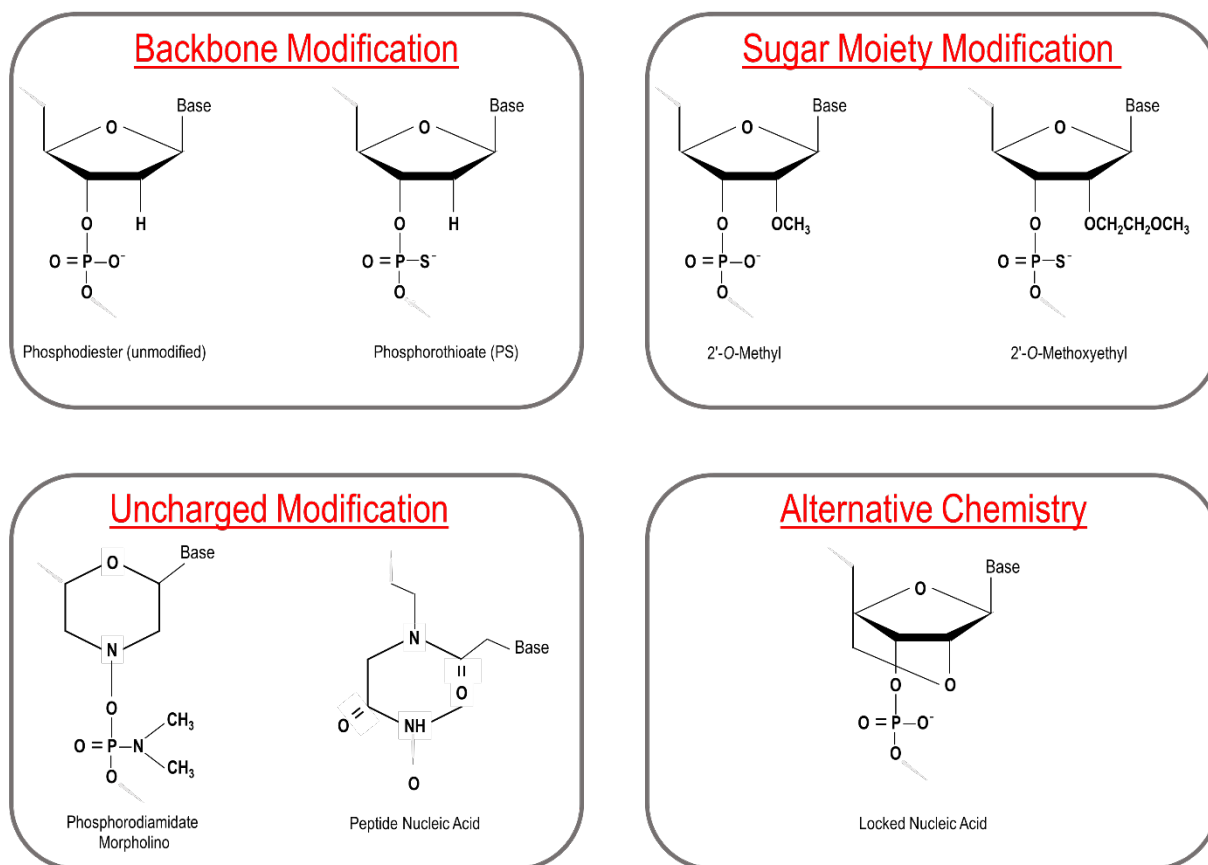


**Figure 1.5:** Common chemical modifications used in antisense oligonucleotide synthesis. Upper left panel shows the natural phosphodiester backbone and the phosphorothioate modification. Upper right panel shows the 2' modification to the sugar moieties, conferring “RNA-like” properties. Lower left panel shows structural changes imparting neutral charge to the backbone. Lower right panel shows an alternative chemistry the ‘locked nucleic acid’.

Subsequent modifications were added to the sugar moieties, while maintaining the backbone PS modification. The most common modification is a change at the 2' position of the sugar moiety; 2'-O-Methyl (2'-Me) and 2'-O-methoxyethyl (2'-MOE), with addition of a methyl or a methoxyethyl group to the 2' oxygen atom of the sugar, respectively [88,89]. These modifications result in the AOs having a higher target binding affinity, allowing for steric blocking applications, such as splice-switching. In addition to these 2' position modifications, the locked nucleic acid (LNA) offers an alternative modification to the sugar moiety [90]. The LNA is formed by creating a methylene bridge between the 2' oxygen and 4' carbon atoms, creating a ‘locked’ structure [90,91]. This modification increases the melting temperature of the AO-target hybrid, thereby increasing the binding affinity and increasing nuclease resistance [92]. The LNA can be used in two contexts, firstly oligomers composed of only LNA bases have been used in

splice-switching applications [93]. Secondly, LNA gapmers (hybrid AOs with a central core of unmodified nucleotides that are flanked by regions with LNA nucleotides) has shown improved RNaseH activity [94]. These AOs have increased stability and target specificity to the addition of an LNA backbone at several bases within the oligonucleotide.

Peptide nucleic acids (PNAs) and phosphorodiamidate morpholino oligomers (PMOs) are oligomers that are “unnatural”, and these uncharged molecules offer a new set of advantages and limitations to the use of AOs. When synthesising PNAs, the entire sugar-phosphate backbone is replaced by polyamide linkages [95,96]. PMOs possess a morpholine ring instead of a ribose moiety and have phosphorodiamidate inter-nucleoside linkages rather than phosphodiester bonds [97,98]. One significant feature of these AOs is the fact that they are neutrally charged, and this somewhat unnatural backbone arrangement is highly resistant to nucleases and proteases, greatly increasing the stability and biological half-life of the oligomers. These AOs are able to prevent the electrostatic repulsion from the negatively charged RNA or DNA due to their neutral backbone [97,99], enabling higher binding specificity and affinity when compared to the charged AOs. Furthermore, PMOs and PNAs demonstrate little to no off-target effects or non-specific binding *in vivo* [97], and this may be attributed to their neutral charge, although poor cellular uptake could also contribute to this outcome [99]. Although uncharged AOs show the best on-target binding affinity and lowest toxicity there are several limitations that constrain AOs *in vivo* application; due to their uncharged nature these AOs cannot readily move through cellular membranes and are rapidly cleared by the renal system [100].

### **1.3.2 Modes of Action and Clinical Applications**

Depending on the chemistry and nature and location of the target, AOs can be used to modulate gene expression through a variety of distinct mechanisms, as shown in **Figure 1.6**.

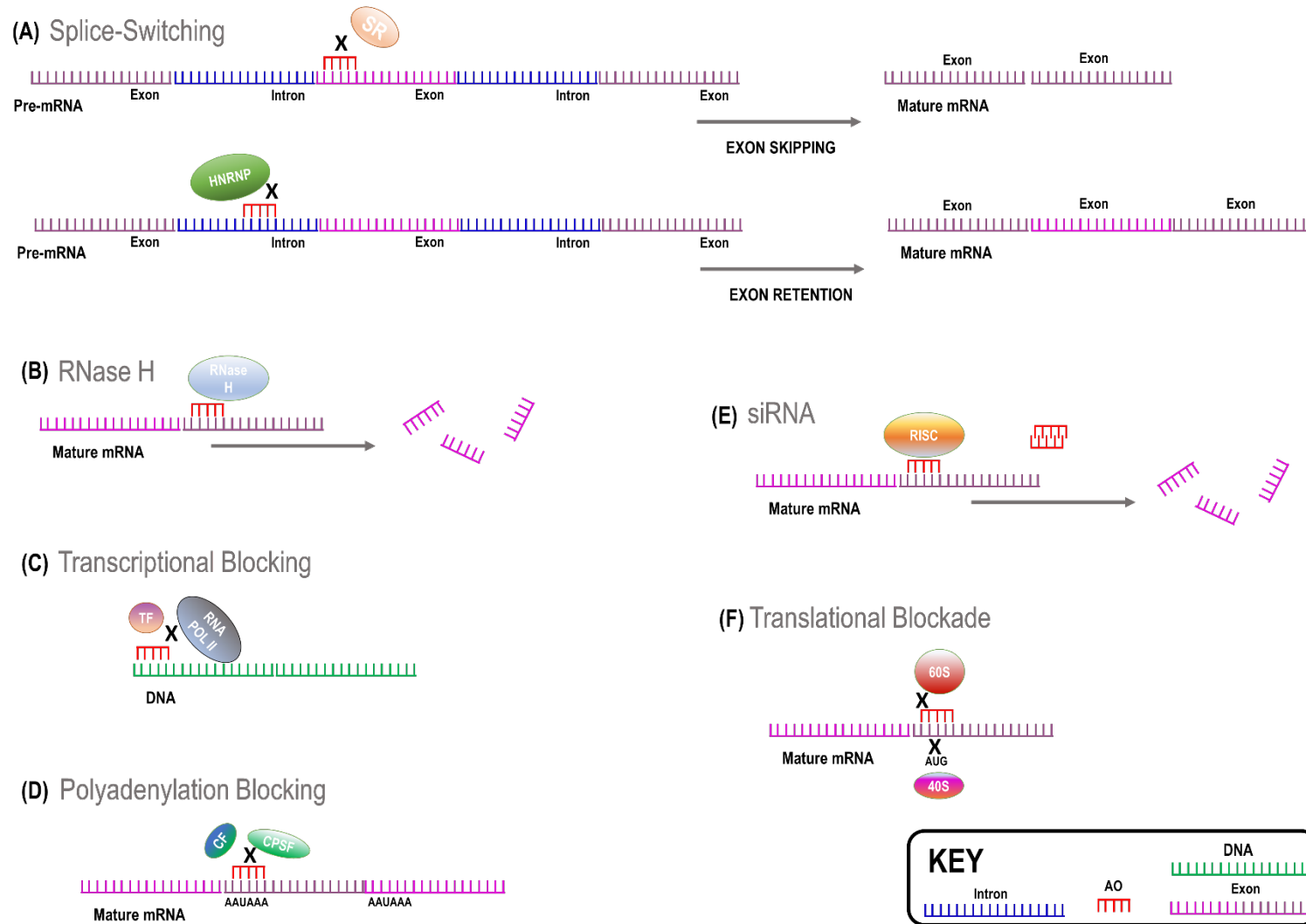


**Figure 1.6:** Mechanisms of antisense oligonucleotide mediated modulation of gene expression. (A) Splice-switching (B) RNaseH-mediated degradation (C) Transcriptional blocking (D) Polyadenylation blocking (E) siRNA-mediated degradation (F) Translational blockade

### 1.3.2.1 RNaseH-mediated degradation

RNaseH-mediated degradation of mRNA has been the most widely exploited of the AO-mediated mechanisms to alter gene expression. RNaseH enzymes cleave phosphodiester bonds of RNA in a double-stranded RNA:DNA duplex, subsequently leaving a 5' phosphate and 3' hydroxyl group on either end of the cleavage site [101]. There are two types of RNaseH, RNaseH1 and RNaseH2 that have distinct substrate preferences. RNaseH1 specifically degrades the RNA of RNA-DNA hybrids and plays a role in RNA Pol II transcription termination by degrading the R-loop RNA-DNA hybrid formation [101], while RNaseH2 is the major source of ribonuclease H activity in mammalian cells and endonucleolytically cleaves ribonucleotides. It is predicted to remove Okazaki fragment RNA primers during lagging strand DNA synthesis and to excise single ribonucleotides from DNA-DNA duplexes.

The first approved antisense drug, *Fomivirsen*, was a 21mer DNA AO on a PS backbone that degraded viral mRNA for the treatment of cytomegalovirus retinitis (CMV) in AIDS and immunocompromised patients [102,103]. *Fomivirsen* inhibits protein production from the CMV viral mRNA by binding to the sequence of a key CMV gene *UL123* that encodes the protein IE2 [103]. The *Fomivirsen* nucleotide sequence is complementary to human CMV *IE2* encoding several proteins responsible for regulation of viral gene expression essential for viral replication. Although approved in 1998, *Fomivirsen* was withdrawn from the market in 2006 due to advances in AIDS-related treatment and medications. *Fomivirsen* application was also compromised by numerous off-target effects such as, but not limited to, inflammation and retinal detachment [102,104].

*Mipomersen*, a 2'-MOE PS AO was granted US FDA approval in 2013 as a treatment for familial hypercholesterolemia [105] through lowering levels of low-density lipoproteins, but rejected by the European Medicine Agency due to concerns regarding liver and cardiac toxicity. Currently *Mipomersen* cannot be freely prescribed in the USA, with individuals wishing to use *Mipomersen* required to enrol in a Risk Evaluation and Mitigation Strategies program. Off-target effects of *Mipomersen* were evident in

clinical trials with almost 20% of all participants withdrawing due to severe injection site reactions and/or severe liver damage [104,105].

### 1.3.2.2 *Splice-switching*

As their name suggests splice-switching AOs modulate processing of the pre-mRNA target during mRNA maturation, achieved through selective targeting of motifs involved in splicing. Targeting positive exon splicing motifs (SR) inhibits targeted exon selection/recognition to induce exon skipping [106], while conversely, AOs targeting silencer motifs that typically mediate sequence exclusion from the mature mRNA can enhance or promote retention of selected sequences in the processed transcript [107].

Splice-switching AOs used to date include PNAs, 2'-Me PS AOs, 2'-MOE-PS AOs and PMOs, among others. The PMOs have an excellent safety profile to date and have not shown the off-target/non-antisense effects associated with PS AOs, supporting clinical application of PMOs, including for long-term treatment [108-110]. Interestingly, PMOs were initially designed for translational blockade due to their particularly high binding affinity and were being developed as a new class of anti-viral agents by an Oregon based company, AVI BioPharma (Portland, Or). Although in operation for more than 30 years, not a single PMO based anti-viral has been approved for sale, but when our laboratory first recognised the potential of these oligomers as splice-switching agents in the mid-2000s [111-114], a collaboration was established to explore PMOs to treat Duchenne muscular dystrophy (DMD). Our laboratory has since evaluated PMOs for translation blockade, exon skipping and exon inclusion, altering polyadenylation and selection of transcription start sites. The first of our splice-switching applications to gain commercial approval is the PMO *Exondys 51* targeting exon 51 of the *DMD* transcript. To date, only three commercial splice-switching AOs have been approved for therapeutic use, *Spinraza*, *Exondys 51* and most recently, *Vyondys 53* [110,115-120]. In addition, *Sepofarsen* (QR-110) used for the treatment of Leber's congenital amaurosis 10, has received orphan drug designation from the U.S. Food and Drug Administration (FDA)

and European Medicines Agency [121]. *Sepofarsen* was also awarded fast-track designation by the FDA as well as entry to PRIME program by the European Medicines Agency.

*Spinraza*, a 18mer 2'-MOE AO with a PS backbone, was approved by the FDA in December 2016 for the treatment of SMA, a rare genetic disorder that is the leading genetic cause of infant mortality [122]. SMA is caused by homozygous loss of *SMN1* expression leading to degeneration of  $\alpha$ -motor neurons in the spinal cord and progressive muscle weakness, followed by respiratory failure and ultimately death [123,124]. Identified in 2004 by the Singh laboratory, ISS-N1 is the target sequence/motif for a splice modulating AO designed to promote recognition and retention of *SMN2* exon 7 into the mature transcript to increase the levels of functional SMN2 protein [124]. The drug was then licenced by IONIS Pharmaceuticals as *Nusinersen* and translated by Biogen, who market the drug as *Spinraza* [125].

In September 2016, the FDA approved *Exondys 51*, a 30mer PMO, the first dystrophin restoring drug to treat a subset of patients with DMD, licensed through The University of Western Australia to Sarepta Therapeutics, (Cambridge, MA) [108,109]. This drug, developed in our laboratory [126], targets exon 51 in the *DMD* transcript in order to skip the exon and restore the reading frame in amenable *DMD* deletion mutations, thereby producing an internally truncated, yet partly functional dystrophin protein. The drug restored modest dystrophin expression in patient muscle where previously no, or only traces of dystrophin were evident [117]. The PMO chemistry has shown excellent biological stability, and found to be safe and well tolerated with no serious adverse effects reported in the *Exondys 51* treated children and young men to date [117]. In December 2019, *Vyondys 53*, also licensed to Sarepta Therapeutics was approved for the treatment of DMD, and with the addition of this drug, approximately 18% of all DMD mutations are now amenable to treatment by antisense-mediated exon skipping.

### 1.3.2.3 *Alternative steric hindrance mechanisms*

Several additional steric hinderance mechanisms may be elicited by AO action, including transcriptional or translational blockade and interference of polyA signals. PMOs were initially designed to induce



translational blockade and are widely used for AO-mediated gene inactivation in zebrafish. Typically injected into the yolks of 1-8-cell-stage zebrafish embryos [127], it has been hypothesised that PMOs diffuse into the dividing cells, allowing ubiquitous cytosolic delivery through cytosolic bridges [127,128]. Administration of PMOs to adult zebrafish has been used to inhibit thrombocyte function, with PMOs targeting the *Integrin- $\alpha$ IIb* transcript showing knockdown of  $\alpha$ IIb, leading to increased gill bleeding [128].

PNAs are known not to induce RNaseH, however, their steric hinderance properties are extensive. PNAs are able to bind double stranded DNA (strand invasion) in a sequence dependent manner, inhibiting transcriptional initiation and elongation by RNA Pol II [129] and hence blocking transcription. Additionally, PNAs have the ability to inhibit the binding and action of various transcription factors, such as nuclear factor  $\kappa$ B and indirectly downregulate transcription of NF $\kappa$ B regulated genes [130,131].

Inhibition of translation is also achieved by physically blocking the assembly of ribosomal components needed for initiation and elongation. PMOs are often seen as the best chemistry for translational blockade due to their superior binding affinity and low toxicity, and for this purpose are typically designed to target upstream of the translation start site in an effort to down-regulate protein production. One such case is a PMO designed to regulate the protein produced by the proto-oncogene *c-myc*. *Resten-RG* was developed by AVI BioPharma (now Sarepta Therapeutics) and inhibited ribosomal assembly, thereby preventing mRNA translation [132]. In 2012, the PMO was shown to be effective in the reduction of the *c-myc* protein in a Phase II trial for the treatment of cardiovascular restenosis, with little to no adverse findings [133,134]. However, this drug was not further developed due to commercial issues [132].

In an effort to prevent polyadenylation or direct the usage of alternative polyadenylation site, AOs may be designed to mask the native sequences critical for polyadenylation and thus initiate the cleavage and polyadenylation at an alternative site. A study by Vickers *et al.* (2001), reported AO-mediated alteration of the polyA tail using a 2'-MOE AO to redirect polyadenylation to one of two upstream cryptic polyA sites of the E-selectin mRNA by targeting the 3'most polyadenylation signal [135]. At that time, the study was

the first of its kind to show AO-mediated upregulation of a message, rather than downregulation. Another example of modifying polyadenylation is shifting the isoform expression of the long non-coding RNA *NEAT-1* in an effort to modulate paraspeckle formation [136]. *NEAT-1\_1* can be transcribed into two main isoforms: the shorter 3 kb, polyadenylated form and the longer 20 kb *NEAT1\_2*. Although *NEAT1\_1* is the more abundant isoform, it does not provide the scaffold necessary for paraspeckle formation, while only the longer *NEAT1\_2* forms the essential RNA scaffold for paraspeckle formation [136]. The group then showed that AOs were able to block the *NEAT1\_1* polyA signal and cleavage, favouring expression of the longer isoform and subsequently create better conditions for paraspeckle formation.

#### 1.3.2.4 *Small interfering RNA (siRNA)*

Small interfering RNAs (siRNAs) are a separate class of double-stranded oligonucleotides and may still be regarded as a subset of antisense oligonucleotides. One strand of the siRNA duplex is designed to anneal to a specific target and activate the RNA-induced silencing complex (RISC), resulting in targeted gene silencing [99]. Mechanistically, one of the strands of the siRNA will link with RISC proteins prior to the annealing of the RNA target, thus activating the Argonaut 2 enzyme that cleaves the transcript and prevents any subsequent protein production. Although siRNAs have been shown to induce many off-target effects and immune cell responses [137], *Patisiran* became the first siRNA to be approved by the FDA in August 2018 [138,139]. The drug is used to reduce levels of the transthyretin protein to treat the polyneuropathy observed in individuals with hereditary transthyretin-mediated amyloidosis [138,139].

### 1.3.3 **Benefits and Drawbacks of Antisense Oligonucleotides**

As with all emerging and in some cases still experimental therapies, especially when applied to conditions where no other treatment options are available, there are clear benefits and several draw backs that should be addressed.

### 1.3.3.1 *Therapeutic benefits*

Antisense oligonucleotides can be designed to modify gene expression through a variety of mechanisms, thereby offering unique therapeutic strategies for diseases where no effective treatment is available. Of particular interest to this thesis is the development of splice-switching therapeutics. These treatments aim to change splicing to by-pass a mutation/correct abnormal gene expression and can be applicable to a plethora of genetic diseases [77,79,92,95,97,106,140-143]. Antisense therapies can be highly specific and even customised to suit selected patients, evidenced by the personalised FDA-approved drug *Milasen* that was specifically designed to treat the disease causing mutation in one patient with Batten's disease [144]. Additionally, AOs offer the ability to treat patients with orphan diseases that may be viewed as commercially unviable drug targets.

As successive antisense therapeutics are approved, it is thought that the developmental period and costs may be reduced due to enhanced consistency and scales of synthesis, possible class approval and reduced safety concerns for established chemistries shown to be non-toxic, such as PMOs [97,100]. Lastly, AOs may offer hope to those who will not respond to gene therapy due to seroconversion in response to the viral capsid, and for those cases where the transgene exceeds the cargo capacity of the viral vector, neither of which are factors in AO therapeutics.

### 1.3.3.2 *Current drawbacks*

While antisense therapies have many potential benefits, there are still a number of limitations. One of the major issues is the toxicity of the PS backbone chemistries [85,141,145]. All PS backbone chemistries elicit some form of adverse event, such as site injection reactions, thrombocytopenia and in selected cases, extreme liver toxicity [79,84]. There is a high degree of difficulty in targeting some AO chemistries to specific tissues, such as the heart and bone marrow, as well as impediments to crossing the blood-brain barrier. In saying that, these are the subject of extensive research to increase cellular uptake [79]. For example, since the PMOs are uncharged and do not efficiently enter cells or tissues, intensive

research is being undertaken to identify effective and safe cell-penetrating peptides that may be conjugated to the PMOs for enhanced delivery [97].

However, perhaps the greatest current drawback would have to be the exorbitant cost of the current AO therapeutics, although this is set by what the companies feel can be charged for treating a particular condition[146]. Although industry needs to recoup the value of translational research and development, including the cost of failed drugs, there must be some models to reduce cost of drug development, validation, synthesis and re-imburement so that affordable and effective therapies may be offered to those who need treatment, rather than the few covered by insurance or government subsidies.

## 1.4 Aims of this Thesis

### 1.4.1 Spinocerebellar Ataxia Type 3

This thesis reports a new molecular therapy for a class of neurodegenerative diseases known as “expansion diseases”. These diseases are caused by unstable microsatellite expansions in several different genes (as reviewed in **Chapter 3** and **Chapter 4**). This thesis focuses initially on one of the polyglutamine (polyQ) expansion diseases [147], which are caused by expansions of CAG or CAA repeats in the affected coding genes (**reviewed in Chapter 4**). In particular, we examined spinocerebellar ataxia type 3 (SCA3), a devastating neurodegenerative disease that is one of nine polyglutamine disorders. SCA3 is caused by an expansion of a polyglutamine tract in ataxin-3, resulting in conformational changes in the protein leading to toxic gain of function [148]. This expanded glutamine tract is encoded by the 5' end of the penultimate exon (exon 10) of *ATXN3*. Although SCA3 is pathogenically heterogeneous, its main feature is progressive ataxia, which in turn affects the patient's speech, balance and gait [10,149,150]. There is currently no cure and no effective treatment strategy for affected individuals.

In evaluating potential therapeutic strategies for SCA3, my overall aim is to induce an internally truncated ataxin-3 protein missing the toxic polyQ tract. To achieve this, I will:

1. Design AOs targeting exon 10 of the *ATXN3* transcript that contains the CAG expansion.
2. Assess if skipping of exon 10 alone is a viable treatment.
3. Assay treated cells to assess the functionality of the induced isoform.

## 1.4.2 SUPT4H1 and SUPT5H

For some repeat expansion diseases, possibly including SCA3, the pathogenic expansion may lie in a region not amenable to AO-mediated splice intervention, for example, the first exon so that an alternative approach is required. One possible strategy is to inhibit transcription across the expansion, and thereby suppress transcript levels of the affected *ATXN3* allele. Recent studies have elucidated the role of the transcription elongation factors SUPT4H1 and SUPT5H in assisting RNA polymerase II transcription through repeat expansions [151-153]. It is therefore possible that, without SUPT4H1 and/or SUPT5H, RNA polymerase II may not effectively transcribe through the repeat expansions (see **Chapter 3**).

My aims are as follows:

1. Design AOs targeting out-of-frame exons of *SUPT4H1* and *SUPT5H* to downregulate levels of the respective proteins.
2. Determine the global consequences of AO-mediated knockdown of SUPT4H1 and/or SUPT5H on the transcriptome.
3. Determine whether AO-mediated knockdown of SUPT4H1 and/or SUPT5H alters aberrant *ATXN3* expression *in vitro*.

## 1.4.3 *In vitro* Validation of Antisense Oligonucleotides

In the past, our laboratory has focused on AO-mediated interventions to treat DMD, but with recent advances in AO chemistries and knowledge of genetic diseases, this narrow focus has vastly broadened. To date, we have screened over 5 000 unique AOs targeting over 40 genes linked to dozens of genetic diseases. This rapid expansion of research focus often highlights challenges relating to workflow for AO optimisation and assay designs. Furthermore, despite more than 20 years having elapsed since the design of the first exon skipping AO in our laboratory, there is still no reliable algorithm for splice-switching

oligonucleotide design. In order to address these challenges, a proportion of this thesis is devoted to developing systems and workflows for designing and validating both 2'-Me PS AO and PMOs.

The topics of this section are:

1. *In vitro* validation of PMOs, whereby we aim to optimise and categorise methods for the delivery of PMOs into cultured cells.
2. The creation of a systematic approach for designing and developing splice-switching 2'-Me PS AOs *in vitro*, as well as assessing several critical factors in their validation, such as the selection of target splicing motifs, choice of cells, and various delivery reagents.

In summary, this thesis aims to develop systematic and efficient practices for the development of AOs *in vitro*, and to create molecular therapies for the treatment of SCA3 and other repeat expansion diseases.

# **Chapter 2 – Materials and Methods**



## 2.1 Materials

### 2.1.1 Chemicals and Reagents

*Table 2.1: List of reagents used in this study and their respective manufacturer or supplier*

Reagents	Supplier/Manufacturer
100bp molecular size marker (Mid)	Geneworks (Adelaide, Australia)
Acetic acid, glacial	BDH Laboratories (Radnor, PA)
Agarose powder	Scientifix (Cheltenham, Australia)
AmpliTaq Gold DNA polymerase and reaction buffer	Applied Biosystems (Melbourne, Australia)
Anti-ATXN3 mouse monoclonal antibody	Merck (Melbourne, Australia)
Baxter sterile water	Baxter Healthcare (Toongabbie, Australia)
Anti-Beta Tubulin mouse monoclonal antibody	Thermo Fisher Scientific (Melbourne, Australia)
Bromophenol blue	Sigma-Aldrich (Sydney, Australia)
Chick embryo extract	Jomar Diagnostics (Scoresby, Australia)
Chloroform	Sigma-Aldrich (Sydney, Australia)
Coomassie blue R250	Bio-Rad Laboratories (Gladesville, Australia)
Deoxynucleotide triphosphates (dNTPs)	Life Technologies (Melbourne, Australia)
Diffinity Rapid tips	Sigma-Aldrich (Sydney, Australia)
Dimethyl sulfoxide (DMSO)	Sigma-Aldrich (Sydney, Australia)
Dithiothreitol (DTT)	Roche Diagnostics (Perth, Australia)
Dulbecco's modified Eagle's Medium (DMEM)	Life Technologies (Melbourne, Australia)
Ethanol, Absolute	Sigma-Aldrich (Sydney, Australia)
Ethylenediaminetetraacetic acid (EDTA)	Sigma-Aldrich (Sydney, Australia)
Foetal bovine serum (FBS)	Scientifix (Cheltenham, Australia)
Glycerol	Sigma-Aldrich (Sydney, Australia)
Glycine	Sigma-Aldrich (Sydney, Australia)
Ham's-F10 medium	Life Technologies (Melbourne, Australia)
Ham's-F12 medium	Life Technologies (Melbourne, Australia)
Hoechst 33342	Sigma-Aldrich (Sydney, Australia)
Horse serum (HS)	Life Technologies (Melbourne, Australia)
IgG Alexa Fluor 488 goat anti-mouse	Thermo Fisher Scientific (Melbourne, Australia)
IgG Alexa Fluor 568 goat anti-rabbit	Thermo Fisher Scientific (Melbourne, Australia)
Isopropanol	Sigma-Aldrich (Sydney, Australia)
Lipofectamine 3000 (L3K)	Life Technologies (Melbourne, Australia)
Lipofectin	Life Technologies (Melbourne, Australia)
MagicMark XP Western protein standard	Life Technologies (Melbourne, Australia)
Matrigel	Becton Dickinson (Sydney, Australia)
Minimal essential medium (EMEM)	Life Technologies (Melbourne, Australia)
MOPS buffer	Life Technologies (Melbourne, Australia)
Anti-NONO mouse monoclonal antibody	Prof. Archa Fox (UWA, Perth, Australia)

Reagents	Supplier/Manufacturer
Novex NuPAGE 4-12% Bis/Tris precast gels	Life Technologies (Melbourne, Australia)
OptiMEM reduced serum media	Life Technologies (Melbourne, Australia)
P3 nucleofection kit	Lonza (Melbourne, Australia)
Phenylmethylsulphonyl fluoride (PMSF)	Sigma-Aldrich (Sydney, Australia)
Anti PolyQ mouse monoclonal antibody	Merck (Melbourne, Australia)
Polyvinylidene fluoride transfer membrane (PVDF)	Pall (Port Washington, NY)
Precision Plus Protein Kaleidoscope Standards	Bio-Rad Laboratories (Gladesville, Australia)
Prolong Gold Antifade Mountant	Thermo Fisher Scientific (Melbourne, Australia)
Protease inhibitor cocktail (P8340)	Sigma-Aldrich (Sydney, Australia)
Red Safe nucleic acid stain	iNtRON Biotechnology (South Korea)
Roswell Park Memorial Institute medium (RPMI)	Life Technologies (Melbourne, Australia)
Sodium dodecyl sulphate (SDS)	Sigma-Aldrich (Sydney, Australia)
Anti-SPT4 rabbit polyclonal antibody	Cell Signalling (Beverly, MA)
Anti-SPT5 rabbit polyclonal antibody	Santa Cruz (Dallas, TX)
Superscript III one-step RT-PCR kit	Life Technologies (Melbourne, Australia)
Triton X-100	Sigma-Aldrich (Sydney, Australia)
Trizma base	Sigma-Aldrich (Sydney, Australia)
TRIzol reagent	Life Technologies (Melbourne, Australia)
Trypan Blue	Sigma-Aldrich (Sydney, Australia)
Trypsin (x1) (used at 0.25% in PBS)	Life Technologies (Melbourne, Australia)
TURBO DNase	Ambion (Austin, TX)
Tween 20	Sigma-Aldrich (Sydney, Australia)
Western Breeze chemiluminescent immunodetection kit	Life Technologies (Melbourne, Australia)
Polyvinylidene fluoride transfer membrane - iBlot	Life Technologies (Melbourne, Australia)
Bicinchoninic acid assay (BCA)	Thermo Fisher Scientific (Melbourne, Australia)

## 2.1.2 Stock Buffers - Made in House

**Table 2.2:** Stock buffers prepared in-house

Stock Buffer Name	pH	Reagents
<b>Gel loading dye</b>	N/A	0.25 g Bromophenol blue
		0.125 g Xylene cyanol
		7.5 g Ficoll 400
		0.5 g SDS
		made to 50 ml with H <sub>2</sub> O
<b>1x PBS</b>	7.4	137 mM NaCl
		2.7 mM KCl
		10 mM Sodium Phosphate dibasic
		2 mM Potassium Phosphate monobasic
		Autoclaved and filter sterilised
<b>1x TBST</b>	8.0	10 mM Tris/HCl, pH 8.0
		150 mM NaCl
		0.05% Tween-20 (v/v)
<b>1x TAE</b>	8.2	20 mM Trizma base
		40 mM Acetic acid
		1 mM EDTA
<b>1x Western transfer buffer</b>	8.4	50 mM Trizma base
		400 mM Glycine
		0.01% SDS (w/v)

## 2.2 Methods

### 2.2.1 Antisense Oligonucleotide Design and Synthesis

Splice-switching antisense oligonucleotides (AOs) were designed to anneal to specific splice factor motifs, as predicted by the web-based applications *Human Splicing Finder 3.1* [154] and *SpliceAid 2.0* [155]. AOs were also targeted to the canonical exonic acceptor and donor sites, and oligonucleotide nomenclature was based on that described by Aung-Htut, McIntosh *et al.* (2019) [156], modified from that originally reported by Mann *et al.* (2002) [112].

ATXN3 H n A/D ( $\pm xx \pm yy$ ) = e.g. ATXN3 H10A(+35+59)

Briefly, gene transcript (e.g. ATXN3), the species (H), exon number (n), acceptor or donor splice site (A/D) and the AO binding co-ordinates (x/y) are indicated. Numbers prefixed with a '+' indicate bases within the exon, while those labelled '-' bind to intronic regions. Hence (-x+y) would span an acceptor splice site, (+x+y) is entirely intra-exonic and (+x-y) would indicate a donor splice site (with the x indicating the number of bases from the end of that exon). Control AOs are used as sham controls in all experiments; two AOs were selected as transfection controls, a 2'-Me PS AO that does not anneal to any sequences in human genome after Blast search, named 'Control AO', and a commercially available sequence 'Gene Tools Control' used as PMO and peptide-conjugated PMOs (PPMOs) controls (**Table 2.3**). The Gene Tools Control sequences has no binding target except for in reticulocytes from thalassemic humans having a splice mutation in the *beta-globin* transcript.

**Table 2.3:** List of control AOs used in this study, with sequences shown 5'-3'.

AO name	Sequence (5' - 3')
Control AO	GGA UGU CCU GAG UCU AGA CCC UCC G
Gene Tools Control (GTC)	CCT CTT ACC TCA GTT ACA ATT TAT A

Note: PMO and PPMO oligomers are synthesised with Thymine (T) rather than Uracil (U).

Initial AO screening was conducted using 2'-Me PS AOs, due to their lower cost, ease of in-house synthesis on an Expedite 8909 nucleic acid synthesiser using the 1  $\mu$ M thioate synthesis protocol [156] and efficient transfection as cationic liposome preparations. During periods when large numbers of AOs were required, some 2'-Me PS AOs were purchased from TriLink (San Diego, CA). Following identification of optimal 2'-Me PS AO sequences as determined by exon skipping titration experiments, these sequences were resynthesised using the phosphorodiamidate morpholino chemistry. Phosphorodiamidate morpholino oligomers were either purchased through GeneTools LLC (Philomath, OR, USA), or provided by Sarepta Therapeutics (Cambridge, MA, USA) through an ongoing collaboration. Individual AO sequences and nomenclature can be found in each respective results chapter.

## 2.2.2 Cell Culture and Seeding

### 2.2.2.1 Proliferation conditions and cell lines

Primary normal human fibroblasts were obtained from healthy human skin biopsy samples performed at the Murdoch University Health Futures Institute Clinic after informed consent [156]. The use of human cells for this research was approved by the Murdoch University Human Ethics Committee, approval number 2013\_156 and 2017\_101. Patient fibroblasts were obtained from skin biopsies, taken after informed consent, or were purchased from the Coriell Cell Repository (Camden, NJ). The human bone marrow neuroblastoma cell line, SH-SY5Y, was purchased from ATCC (In Vitro Technologies Pty. Ltd., Noble Park North, VIC, Australia). Cells were resurrected from long term liquid nitrogen storage by thawing the 1 ml aliquot and adding it to 9 ml of 10% HS-DMEM, followed by centrifugation for 4 mins at 1 000 x g, before the supernatant was discarded and the cell pellet was resuspended in the relevant proliferation media (**Table 2.4**). Media was changed 2-3 times per week, depending on growth rate

**Table 2.4:** Proliferation media used to maintain cell lines

Cell Type	Proliferation Media
Primary normal human fibroblasts	10-15% FBS in Dulbecco's Modified Eagle Medium (DMEM)
Patient primary fibroblasts	15% FBS in Minimal Essential Medium (EMEM), with 1% G-Max
SH-SY5Y cells	10% FBS in EMEM/HAMSF12 (1:1)

### 2.2.2.2 Passage and seeding cells into plates and flasks

Once cells were approximately 80% confluent, they were either passaged or plated for transfection. For splitting cells, proliferation media was aspirated, and cells were washed with 4-10 ml of PBS, depending on size of the flask. For a T75 cm<sup>2</sup> flask, 3 ml of 1x Trypsin in PBS was added and incubated at 37°C until all cells detached. The trypsin was then neutralised by addition of 5 ml of 10% HS-DMEM, which was then transferred into a 10 ml falcon tube and centrifuged at 1 000 x g for 4 minutes. The supernatant was then removed, and 1 ml of the appropriate proliferation media was added. If the cells were not destined for transfection, the 1 ml cell suspension was added to 19 ml of proliferation media (T175 cm<sup>2</sup> flask) and returned to the 37°C, 5% CO<sub>2</sub> incubator.

For transfection experiments, cells were counted using a haemocytometer (counting chamber) and seeded into 24 well plates for RNA analysis or T25 cm<sup>2</sup> flasks for protein analysis. Please refer to **Table 2.5** for required density of various cell types when seeding for 2'-Me PS AO transfections. The concentrations of cells per 1 ml was determined from the following equation:

$$\frac{\text{Sum of cells in 8 large chamber squares}}{8} \times (1 \times 10^4) \times \text{dilution factor} = \text{cells/ml}$$

**Table 2.5:** Cell density for seeding various cell types for 2'-Me transfections

Cell Type	Cell density (24 well plate)	Growth volume	Cells density (T25 flasks)	Growth volume
Fibroblasts	1.5 x 10 <sup>4</sup> per well	0.5 ml per well	2.5 x 10 <sup>5</sup> per flask	5 ml per flask
SH-SY5Y	7 x 10 <sup>4</sup> per well	0.5 ml per well	7 x 10 <sup>5</sup> per flask	5 ml per flask

## 2.2.3 Transfection and Nucleofection

### 2.2.3.1 2'-O-methyl AOs transfection of cells in 24 well plates (for RNA analysis)

The calculated individual molecular weight (g/mol) and concentration (ng/ $\mu$ l) of each AO was used to determine the volume required for a 2 ml master mix of 400 nM for each AO or AO cocktail. As 2'-Me PS AOs are charged molecules, a cationic transfection reagent can be used to facilitate AO entry into the cell. Lipofectamine 3000 was used to prepare the 400 nM lipoplex master mix. The delivery complexes were prepared in a 15 ml falcon tube, where 3  $\mu$ l of Lipofectamine 3000 per 1 ml was added to a fixed volume (2 ml) of *Opti-MEM*, a predetermined volume of AO or AO cocktail was then added, mixed gently and incubated at room temperature for 5 minutes to allow lipocomplex formation. Immediately following incubation, additional *Opti-MEM* was added to make a final stock solution of 2 ml with a concentration of 400 nM. This stock solution was then serially diluted into fresh tubes to concentrations of 200 nM, 100 nM, and 50 nM.

Cells seeded 24 hours prior were removed from the incubator and proliferation media was then aspirated from the wells before 500  $\mu$ l of the designated AO complex was then added to two well to allow duplicate transfections. Transfected cells were then incubated at 37°C for 24 or 48 hours as indicated and depending on the transfection protocol specific to the experiment.

### 2.2.3.2 2'-O-methyl AO transfection of cells in T25 cm<sup>2</sup> flasks (for protein analysis)

Transfection with 2'-Me PS AOs for protein analysis was conducted as described above, however volumes were increased to account for the larger vessel surface area and thus increased volume of AO required for each transfection. Master mix volumes of 4ml at 400 nM were prepared, with 3 ml of the designated AO mix added to each T25 cm<sup>2</sup> flask. Flasks were then incubated at 37°C for a minimum of 48 hours, depending on the transfection protocol specific to the experiment.

### 2.2.3.3 *Nucleofection*

Transfections of cells by nucleofection requires cells to be in the nucleofection solution prior to seeding and incubation. The cells were split and counted as previously described. The working transfection solution was prepared using reagents supplied in the P3 nucleofection kit (Lonza) as per the manufacturer's guidelines, with 82% comprising the primary solution and 18% comprising the supplement. Prior to transfection, the solution and PMOs were warmed to 37°C to ensure any precipitate or AO aggregates formed at 4°C were solubilised.

Transfection of fibroblasts in a 6 well plate required 300 000 – 450 000 cells per well, depending on the experimental protocol and allow for approximately 10% cell death. The required number of cells was suspended in 19 µl of the P3 supplemented solution and then placed into a 20 µl cuvette. Following this, 1 µl of a pre-diluted concentration of PMO (varied depending on experimental parameters) was added to the cell suspension and the appropriate nucleofection program was performed (e.g. program CA-137 was used for fibroblasts). Following confirmation from the nucleofector that the nucleofection was successful, the cuvette was removed and 80 µl of pre-warmed RPMI was immediately added to aid recovery of the cells. The cuvette was then placed in a 37°C incubator for 10 minutes prior to the cell suspension being transferred into the 6 well plates with 1.9 ml of 2% FBS-DMEM. The cells were then incubated for 2-4 days prior to harvesting

### 2.2.3.4 *PMO transfection using Endo-Porter as a delivery agent*

PMOs that showed reduced transfection efficiency after nucleofection were re-evaluated by transfection using Endo-Porter (Gene Tools, Philomath, OR) as the delivery reagent. Endo-Porter is a novel peptide capable of delivering PMOs into the cytoplasm and nucleus of cells via a endocytosis-mediated mechanism without damaging the cell membrane [157]. Cells were plated appropriately into multi-well plates 24 hours prior to transfection. Prior to transfection, the solution and PMOs were warmed to 37°C to ensure any precipitate or AO aggregates formed at 4°C were solubilised. Media was removed, and



the cells were washed with an appropriate volume of PBS before fresh media containing 10% FBS was added to each well and followed by the equivalent volume of 6  $\mu$ M Endo-Porter. Lastly between 5 – 20  $\mu$ M of PMO was added directly to the media/Endo-Porter and gently swirled to ensure complete mixing of the solution. Transfected cells were then incubated at 37°C for 24 to 48 hours, depending on the specific experimental transfection protocol.

#### *2.2.3.5 Transfection with PPMOs*

Selected AO sequences were synthesised as peptide-conjugated PMOs (PPMOs) as these compounds, supplied by our industry partner Sarepta Therapeutics, are readily taken up in cell culture. Cells were seeded in multi-well plates, 24 hours prior to transfection. The solution and PPMOs were warmed to 37°C, prior to transfection, to ensure any precipitate or AO aggregates formed at 4°C were solubilised. Fresh Opti-MEM was then added to each well, and subsequently 0.5 – 5  $\mu$ M of PPMO was added directly to the media and gently mixed. Transfected cells were then incubated at 37°C for 24 hours to 7 days, depending on the experimental protocol.

## **2.2.4 Harvesting of Cells for Analysis**

#### *2.2.4.1 Harvesting cells for RNA isolation using TRIzol reagents*

Once the incubation period (1 - 6 days as indicated) had elapsed, the transfection media was removed and 200  $\mu$ l of TRIzol (Zymo Research) was added to each well (for adherent cells in a 24 well plate) and incubated at room temperature for 5 minutes. Duplicate wells were combined into a single 1.5 ml micro-centrifuge tubes, for a total volume of 400  $\mu$ l.

An equal amount of 100% ethanol was added to the 400  $\mu$ l and vigorously vortexed before transferring into a Direct-zol RNA purification column (Zymo Research). The mixture was then centrifuged for 1 minute at 12 000 x g, the flow through was discarded and the column placed in a new collection micro-centrifuge

tube. Following this, 800 µl of Pre-Wash Buffer (Zymo Research) was added to the column and centrifuged for 1.5 minutes at 12 000 x g. The flow through was discarded and 700 µl of Wash Buffer (Zymo Research) was added to the column and centrifuged for 2 minutes at 12 000 x g. The flow through was then discarded and the columns placed in a final collection tube (1.5 ml micro-centrifuge tube). RNase/DNase free water (30 µl) was added into the column and centrifuged for 1 minute at 12 000 x g. The column was then discarded, and the RNA quality and concentration were determined using a NanoDrop-100 Spectrophotometer (NanoDrop Technologies). The RNA was then stored at -20°C until required for cDNA synthesis and PCR analysis.

#### *2.2.4.2 Harvesting of cells for RNA isolation using MagMAX kit*

Once the treatment period (1 - 4 days) had elapsed, the transfection media was removed from the transfected cells and 70 µl of Lysis Buffer (Life Technologies) was added to each well (for adherent cells in a 24 well plate) and incubated at room temperature for 10 minutes. Duplicate wells were combined for a single RNA extraction in one well of a 96 well collection plate (total 140 µl). Once a complete 96 well collection plate was full, RNA isolation was performed as per the manufacturer's instructions using the Kingfisher™ Purification system (Thermo Fisher Scientific).

Briefly, magnetic extraction beads were added to the 140 µl lysed samples and mixed thoroughly. The sample plate and the other components (wash buffers, DNase and elution buffer) were placed in the Kingfisher™ Purification system (Thermo Fisher Scientific) before RNA extraction was performed using the protocol KW-DW1830. Samples were homogenised and washed three times, with two different wash buffers provided by the manufacturer. Samples were then DNase treated and finally eluted in 25 – 40 µl of manufacturer supplied elution buffer. The RNA quality and concentration were determined using a NanoDrop-100 Spectrophotometer (Nanodrop Technologies). The RNA was then stored at -20°C until required for cDNA synthesis and PCR analysis.

### 2.2.4.3 Harvesting cells for protein analysis by western blot

Transfection media was removed from cells (in a T25 cm<sup>2</sup> flask) that were then washed with 5 ml of PBS, followed by addition of 1 ml of 1 x trypsin and incubation at 37°C for 2-3 minutes or until all cells detached, before 3 ml of 10% HS-DMEM was immediately added. Cells were placed in a 15 ml centrifuge tube (Falcon) and centrifuged at 3 000 x g for 2.5 minutes. The supernatant was then removed, and 1 ml of cold PBS was added to resuspend the cell pellet. This cell preparation was then separated into two 1.5 ml microcentrifuge tubes, one for RNA analysis (200 µl) and the other for protein analysis (800 µl). Both tubes were then centrifuged at 3 000 x g for 5 minutes. The supernatant was then aspirated, and the tubes were either placed directly on to dry ice, or appropriate lysis buffer was added for protein or RNA analysis. The lysed cells and cell pellets were then placed at -80°C until required.

## 2.2.5 Reverse-transcriptase Polymerase Chain Reaction and Agarose Gel Electrophoresis

The reverse-transcriptase polymerase chain reaction (RT-PCR) and reagents were all individually optimised for each gene transcript of interest. RT-PCRs were performed using the one-step Superscript III RT-PCR kit with Platinum Taq polymerase (Life Technologies) according to the manufacturer's instructions. Each PCR reaction included 50 ng of total RNA and 25 ng of each forward and reverse primer. Primers used to amplify human gene transcripts in this study are listed in **Table 2.6**.

**Table 2.6:** List of Primers used in this study

Primer Name (Inc. Gene Name)	Sequence (5' – 3')	Annealing Temp (°C)	Cycle Number
ATXN3_ Ex7-F	GTC CAA CAG ATG CAT CGA CCA A	55	28
ATXN3_ Ex11-R	AGC TGC CTG AAG CAT GTC TTC TT		
FBN1_ Ex13-F	GGA TAT CAG AGC ACA CTC AC	55	20
FBN1_ Ex20-R	GTA GAT AAA TCC CTT GGG GC		
SPT4_ Ex1-F	TTA CTT CCT GCG GGT GCA CA	60	25
SPT4_ Ex5-R	CTG GAT TTG TAG GCC ACT CC		
SUPT5H_ Ex1-F	CGA GGA CAG CAA CTT TTC CG	60	27
SUPT5H_ Ex12-R	TCA GGG AGA TGG TGT TCT GG		

Primer Name (Inc. Gene Name)	Sequence (5' – 3')	Annealing Temp (°C)	Cycle Number
SUPT5H_Ex11-F	AAG CGG GGC ATC TAC AAG GA	60	26
SUPT5H_Ex19-R	TTC TGC TCT GAG TCC AAG GC		
SUPT5H_Ex18-F	GAC TAG AAC GGG AGA CCT TC	60	28
SUPT5H_Ex26-R	GCG TCT GCG GGT TGT ATT GT		
SUPT5H_Ex24-F	ATG ACC TCG ACC TAT GGG AG	60	28
SUPT5H_Ex30-R	ATC CTC GCC CAG GAT CAC TT		

Following RT-PCR, resultant amplicons were fractionated on a 2% agarose gel in TAE buffer at 111 V for 1.5 hours or when the low molecular weight dye (BPB) reached the end of the gel. Prior to loading, samples were mixed with loading buffer (4:1, v:v). Size standards, 4 µl of 100 bp ladder (Geneworks) were loaded either side of the experimental samples. Gels were stained for 5-10 minutes in TAE containing 1x RedSafe (iNtRON Biotechnology, South Korea), then de-stained for 60 minutes in ddH<sub>2</sub>O, prior to image capture on a Vilber Lourmat Fusion FX system, using Fusion software for image acquisition. Image analysis and preparation were conducted with ImageJ (Version 1.8.0\_112) and Photoshop (Version CC 2020), respectively.

## 2.2.6 Band Stab and Sequencing

To confirm product sequences, agarose gel fractionation was undertaken as described above, stained in RedSafe, and the amplicons were visualised on a UV lightbox. Each band of interest was “stabbed” with a 200 µl pipette tip and then dispersed into pre-prepared PCR mix containing AmpliTaq Gold DNA Polymerase. Products were amplified according to the following conditions: 94°C for 4 minutes (35 cycles: 94°C for 40 seconds, 55°C for 1 minute and 72°C for 1.5 minutes).

Upon confirmation of amplification of a single transcript, the PCR reaction was then purified using Diffinity Rapid Tips (Diffinity Genomics, PA, USA) as per the manufacturer’s instructions. Purified DNA products along with the necessary primer were referred to the Australian Genome Research Facility (AGRF, Perth Australia) for Sanger sequencing and then analysed using Chromas 2.6.6 (Technelysium Pty Ltd).

## 2.2.7 Western Blot Analysis

### 2.2.7.1 *Sample preparation*

Cells were harvested 2 - 7 days after transfection (depending on the target gene) for protein analysis. Cells were pelleted at 2 000 x g, resuspended in 1 mL PBS to remove excess media, and then re-pelleted, with 80% of the volume allocated for protein analysis and 20% for RNA assays. Cell pellets for protein analysis were placed immediately on dry ice following removal of the supernatant. Lysis buffer was prepared as below, and 100 - 200 µl was added to each sample, depending on pellet size and estimation of cell number. Pellets were sonicated for six, 1 second pulses and samples heated to 94°C for 5 minutes before being snap frozen on dry ice. Samples were centrifuged at 14 000 x g for 2 minutes before loading onto SDS-polyacrylamide gels or used for BCA analysis to determine protein concentration. Following BCA analysis, the samples were resuspended in loading buffer before further analysis to allow equal loading and western blotting as described below.

- Lysis buffer: 125 mM Tris/HCl, pH 6.8, 15% SDS, 10% glycerol, 0.5 mM PMSF, protease inhibitor cocktail (3.12 mM AEBS; 0.0025 mM Aprotinin; 1.2 mM Bestatin; 0.42 mM E-64; 0.6 mM Leupeptin; 0.45 mM Pepstain A) – Final concentration
- Loading Buffer (107.66 µl of sample): 0.2% µl Bromophenol blue, 100 µl of lysed sample: 50 mM Dithiothreitol (DTT) – Final concentration

### 2.2.7.2 *Protein loading gel and bicinchoninic acid assay*

To estimate the amount of total protein within each sample, 4 µl of the sample was loaded on a NuPAGE Novex 4-12% BIS/Tris gel (Life Technologies) and fractionated at 200 V for 55 minutes in 1x MOPS buffer (Life Technologies). A Kaleidoscope molecular 45 weight marker (BioRad, Sydney, Australia) was loaded to allow molecular weight estimation. Gels were stained in Coomassie blue for 5 minutes and de-stained in 7% Acetic acid overnight. Images were captured using a Vilber Lourmat Fusion FX system with a white

light conversion screen. ImageJ imaging software was used to analyse the relative levels of major proteins in order to normalise sample loading to a known sample control.

A BCA assay was performed in conjunction with the protein loading gel in order to determine protein concentration and standardise the amount of protein loaded onto the gel. The BCA assay (Thermo Fisher Scientific) was performed according to the manufacturer's instructions. Samples were incubated at 37°C for 30 minutes to allow for the reaction to take place. Relative sample absorbance was analysed and total protein per  $\mu\text{l}$  was subsequently calculated.

### 2.2.7.3 *Western blot*

An estimated 20  $\mu\text{g}$  of total protein, as determined by BCA assay (protein dependent) and normalised by gel densitometry was loaded per sample on a NuPAGE Novex 4-12% BIS/Tris gel (Life Technologies) and run at 200 V for 45-55 min. The Kaleidoscope marker (7  $\mu\text{l}$ ) was loaded to visualise and monitor separation, and 5  $\mu\text{l}$  of Magic Mark molecular weight marker (Life Technologies) was used to allow size estimation of proteins. Proteins were transferred onto a Pall Fluorotrans polyvinylidene fluoride (PVDF) membrane (Merk ) at 350 mA for 2 hours in western transfer buffer or transferred via the iBlot system using the P0 setting, according to the manufacturer's instructions. The membranes were then blocked with 5% skim milk in TBST for 1 hour. Primary antibodies for specific proteins were diluted in 5% skim milk in TBST at various concentrations and incubated overnight at 4°C. All antibody details and dilutions are listed in **Table 2.7**. Proteins under investigation were detected using either a Western Breeze Chemiluminescent Immunodetection System (Life Technologies) or the Crescendo system (Merk). All reagents were supplied with the kit and immunodetection was performed according to manufacturer's instructions. The signals were detected using the respective chemiluminescent substrate and incubated in the dark for 5 minutes. Western blot images were captured on a Vilber Lourmat Fusion FX system using Fusion software and ImageJ software was used for image and densitometric analysis.

**Table 2.7:** List of antibodies used for Western blot in this study, along with their respective dilution and detections

Antibody	Supplier and Catalogue Number	Host Species and Clone	Dilution	Secondary antibody	Dilution
ATXN3	Merk (MAB5360)	Mouse monoclonal	1:500	Western Breeze AP	N/A
Beta-Tubulin	Thermo Fisher (TBN06)	Mouse monoclonal	1:1 000	Mouse HRP	1:10 000
POLY-Q	Merk (MAB1574)	Mouse monoclonal	1:500	Western Breeze AP	N/A
SPT4	Cell Signalling (64828)	Rabbit monoclonal	1:1 000	Rabbit HRP	1:10 000

**NOTE:** All other specific materials and methods used in this study are found in their respective results chapter.



# **Chapter 3 – SUPT**

## **Downregulation**

### 3.1 Background & Introduction

Expansion disorders are a class of disease caused by unstable, expanded microsatellites, and currently account for over 40 genetically distinct diseases, the majority of which present as neurological pathologies [7,10,150,158,159]. Expansion diseases include the hexanucleotide repeat *C9orf72*-related amyotrophic lateral sclerosis (ALS) and all the tri-nucleotide expansion diseases (namely Huntington's disease, myotonic dystrophy type 1 and Friedrich's ataxia [7,9], among others). These diseases are pathologically diverse but are most commonly found to affect the central and peripheral nervous system. With a few exceptions, such as Friedrich's ataxia, most disease phenotypes are thought to arise from a toxic gain of function, resulting in aggregation of aberrant proteins/RNA that lead to neurodegeneration; however, the exact mechanism of disease is not always well understood [9,160]. A prime example of this poor understanding is the expanded GGGGCC hexanucleotide repeat found in the first intron of *C9orf72*, leading to ALS [161,162]. It is hypothesised that there may be at least three potential pathogenic mechanisms:

- i. Reduced expression of functional C9ORF72 (also termed DENNL72) that indicates haploinsufficiency, as C9ORF72 is required for normal vesicle trafficking and lysosomal biogenesis in motor neurons [163]. This suggests that there may be a delicate balance between gain of function and loss of function, as has been observed in other diseases.
- ii. A toxic gain of function through nuclear RNA aggregation is the most widely held theory of pathogenicity for most expansion diseases [164]. The *C9ORF72* repeat expansion is transcribed in both directions, generating antisense transcripts in *C9ORF72* ALS neurons. Aggregation of the toxic RNA or protein is suggested to directly cause neuronal death as a result of sequestration of other non-disease related proteins, leading to cellular dysfunction and ultimately cell death.

- iii. The accumulation of dipeptide repeat (DPR) proteins as a result of unconventional repeat-associated non-ATG (RAN) translation of the expanded repeat RNA. This mechanism is closely related to the above (ii) and not found in typical expansion repeat diseases.

The pathogenesis of *C9orf72*-related ALS and other expansion diseases is not yet fully characterised and to date, no effective treatment strategy exists for the treatment of expansion diseases. Thus, a therapeutic strategy that aims to target the direct cause of disease, that is the deleterious effects of the expansion, rather than the resulting pathogenic pathways appears highly attractive, rational, and logical.

Recently, the transcription elongation factor SUPT4H1 was reported to be selectively required to assist RNA polymerase II (RNA Pol II) in transcribing through these large expanded repeats [151-153]. Several studies, both *in vitro* and *in vivo*, found that targeted knockdown of SUPT4H1, and to a lesser extent SUPT5H, reduces aggregation of expanded transcripts and resulting aberrant proteins, and alleviated disease phenotype [151-153]. SUPT4H1 and SUPT5H are two subunits that form the DRB sensitivity-inducing factor (DSIF) complex that regulates transcription elongation and mRNA processing through RNA Pol II [31,36,165]. The DSIF complex induces the mRNA guanylyl transferase activity of RNGTT/CAP1A and is thus involved in regulating mRNA capping. Additionally, DSIF interacts with the negative elongation complex, allowing the enhancement of transcriptional pausing at proximal promoter sites [31]. Although the DSIF seems to play a pervasive role in transcription elongation, mutation of the SUPT4H1 yeast ortholog (Spt4) resulted in the selective reduction of transcription of long CAG trinucleotide repeats [153]. Reduction of murine Supt4a also decreased amounts of expanded polyglutamine (polyQ) aggregates in striatal neurons and most interestingly, knocking down of Supt4a did not appear to affect expression of proteins that contained short CAG repeats. Lastly, RNA-sequencing (RNA-seq) analysis showed Supt4a knockdown had a limited effect on overall gene expression throughout the genome [153]. These data suggest that knockdown of SUPT4H1 may be a viable therapeutic strategy for expansion diseases. Another study demonstrated that knocking down SUPT5H in conjunction with SUPT4H1, increased the efficacy in the amelioration of *C9orf72* related pathogenesis

*in vitro*, compared to SUPT4H1 knockdown alone [152]. However, SUPT5H is highly conserved across all domains of life and the implications of suppressing SUPT5H expression on the global transcriptome are currently unknown. Although most studies to date have used siRNA to knockdown the SUPT proteins, we hypothesise that splice-switching antisense oligonucleotides (AOs) offer a safer, more specific and clinically applicable strategy [99].

Splice-switching AOs are gaining traction as therapeutic agents to treat genetic diseases, with the U.S. Food and Drug Administration (FDA) having approved three drugs, *Exondys 51*, *Vyondys 53* and *Spinraza* in the last 3 years, and that number is only expected to rise [117,166]. *Exondys 51* and *Vyondys 53* are designed to excise exon 51 and exon 53, respectively, from amenable disease-causing *DMD* transcripts to restore the reading frame and rescue some functional dystrophin expression. These drugs have been designed to treat Duchenne muscular dystrophy (DMD) and are synthesised as phosphorodiamidate morpholino oligomers (PMOs), an antisense oligomer chemistry that has an excellent safety profile and is well suited to clinical application [167]. The accelerated approval of *Exondys 51* and *Vyondys 53* clearly demonstrate proof of concept that PMOs can be used as splice-switching agents to ameliorate genetic disease. However, delivery of these compounds to the muscle is inefficient and there is room for improvement to enhance potency, reduce frequency and amounts of PMO administered to treat DMD. Chemical modifications or conjugation of PMOs to peptides and other moieties can enhance cellular uptake, and clinical studies to evaluate cell penetrating peptide-conjugated PMOs (PPMOs) in DMD have begun in the USA (NCT03769116 and NCT03375255).

We propose to utilise our experience in developing splice-switching PMOs to disrupt the open reading frame and downregulate *SUPT4H1*, and to a lesser extent *SUPT5H*, to reduce the ability of RNA Pol II to read through and transcribe expansions in cells derived from patients with repeat expansion diseases. We hypothesise that reducing transcription across the disease-associated triplet expansions that directly lead to pathology could be a viable therapy for many different conditions. We designed AOs to target

exons that, when excluded, disrupt the reading frame of the *SUPT4H1* and *SUPT5H* transcripts to down-regulate expression of their respective proteins. Initial *in vitro* studies were conducted in a spinocerebellar ataxia type 3 (SCA3) expansion disease cell line, as well as the commercially available SH-SY5Y neuroblastoma cell line.

## 3.2 Materials and Methods

### 3.2.1 AO Design and Synthesis

Splice-switching AOs were designed to anneal to the acceptor and donor splice sites at the intron/exon boundaries of selected exons, as well as predicted exon splice enhancer motifs identified using the web-based application, *Human Splicing Finder 3.1* [154]. In addition, specificity of the AOs for the *SUPT4H1* and *SUPT5H* target motifs was assessed using BLAST analysis to identify potential off-target annealing. 2'-O-methyl AOs on a phosphorothioate backbone (2'-Me PS) were obtained from TriLink Biotechnologies (Maravai LifeSciences, San Diego, CA), while PPMOs were supplied by Sarepta Therapeutics (Cambridge, MA) (**Table 3.1 and 3.2**). Due to intellectual property constraints at this time, our standard nomenclature for describing the AOs in this Chapter cannot be provided. Instead, AOs are identified by a numbering system, as outlined below.

The nomenclature is as follows: S4/S5-AO-(Exon Number.AO number) – (where S4/S5 = *SUPT4H1/SUPT5H* gene). For example, *SUPT4H1* AO number 1, targeting exon 2 is named as **S4-AO.2.1**. The AO sequences found to induce robust levels of exon skipping and/or transcript knockdown were subsequently synthesised as the PPMO chemistry and assigned a unique catalogue number.

**Table 3.1:** List of *SUPT4H1* 2'-Me PS AOs and their corresponding PPMO homologues. N/A = not applicable.

2'-Me PS Name	PPMO Name
S4-AO-2.1	N/A
S4-AO-2.2	1074
S4-AO-2.3	1083
S4-AO-2.4	1087
S4-AO-2.5	N/A
S4-AO-3.1	1106
S4-AO-3.2	1107
S4-AO-3.3	1108

**Table 3.2:** List of SUPT5H 2'-Me PS AOs and their corresponding PPMO homologues. N/A = not applicable.

2'-Me PS Name	PPMO Name
S5-AO-3.1	N/A
S5-AO-3.2	N/A
S5-AO-3.3	1096
S5-AO-3.4	1101
S5-AO-3.5	1092
S5-AO-3.6	N/A
S5-AO-6.1	1109
S5-AO-6.2	N/A
S5-AO-6.3	N/A

In addition to single AO transfections, equimolar amounts of two AOs targeting the *SUPT* transcripts were combined into cocktails and evaluated. We have previously found that select combinations of AOs can enhance the efficiency of exon removal in a synergistic fashion [168,169] (Table 3.3). All cocktails reported contained equimolar amounts of each AO (1:1) ratios.

**Table 3.3:** List of *SUPT* cocktails used. AO cocktails contain two different, non-overlapping sequences.

Cocktail Name	2'-Me AOs used	PPMOs used
<b>SUPT4H1 cocktails</b>		
4-Cocktail 1	4-AO-2.2 & 4-AO2.3	N/A
4-Cocktail 2	4-AO-2.3 & 4-AO2.4	1083 & 1087
4-Cocktail 3	4-AO-2.4 & 4-AO2.5	N/A
4-Cocktail 4	4-AO-2.3 & 4-AO2.5	N/A
4-Cocktail 5	4-AO-2.2 & 4-AO2.4	1074 & 1087
4-Cocktail 6	4-AO-2.1 & 4-AO2.5	N/A
4-Cocktail 7	4-AO-3.2 & 4-AO-3.3	1107 & 1108
<b>SUPT5H cocktails</b>		
5-Cocktail 1	5-AO-3.2 & 5-AO-3.3	N/A
5-Cocktail 2	5-AO-3.3 & 5-AO-3.4	1096 & 1101
5-Cocktail 3	5-AO-3.3 & 5-AO-3.5	N/A
5-Cocktail 4	5-AO-3.4 & 5-AO-3.5	N/A
5-Cocktail 5	5-AO-3.3 & 5-AO-3.6	N/A
5-Cocktail 6	5-AO-3.3 & 5-AO-3.5	N/A
5-Cocktail 7	5-AO-3.1 & 5-AO-3.6	N/A

### **3.2.2 Cell Culture**

Primary dermal fibroblasts were cultured from a skin biopsy taken from a healthy volunteer, with informed consent, and the project received approval from the Human Research Ethics Committee at Murdoch University (approval number, 2013/156). Healthy human fibroblasts were cultured in Dulbecco's Modified Essential Medium (Gibco; Life Technologies, Melbourne, Australia), supplemented with 15% fetal bovine serum (FBS) (Scientifix, Cheltenham, Australia). The SCA3 fibroblast cell line (GM6153–71Q and 23Q) was obtained from Coriell Cell Repositories (Camden, NJ) and cultured in minimal essential medium (MEM), supplemented with 15% FBS (Scientifix), 1% Glutamax (Gibco) and 1x penicillin/streptomycin. The human bone marrow-derived neuroblastoma cell line, SH-SY5Y (un-differentiated), was purchased from ATCC (In Vitro Technologies Pty. Ltd., Noble Park North, Australia) and maintained in a 1:1 ratio of MEM and F-12 Medium supplemented with 10% FBS.

### **3.2.3 Transfection**

All cell strains were either transfected with 2'-Me PS AO, Lipofectamine 3000 (Life Technologies) lipoplexes in Opti-MEM (Gibco) according to manufacturer's instructions, or as uncomplexed PPMOs. PPMOs were incubated at 37°C for 10 minutes prior to transfection to ensure any precipitation that may have occurred at 4°C was solubilised. Fresh Opti-MEM was then added to each well, and subsequently 0.5 – 5 µM of PPMO was added directly to the media and gently mixed. Transfected cells were then incubated at 37°C for 24 hours to 6 days, depending on the experiment-specific transfection protocol.

### **3.2.4 RNA Extraction and RT-PCR assays**

Total RNA was extracted using the MagMax™ nucleic acid isolation kits (ThermoFisher Scientific, Melbourne Australia) in accordance with the manufacturer's instructions. Transcripts were amplified using the one-step SuperScript® III reverse transcriptase, with 50 ng of total RNA as the template. To amplify



the *SUPT4H1* and *SUPT5H* transcripts, various primer sets were used (**Table 3.4**) and the resultant amplicons were fractionated on 2% agarose gels in Tris-Acetate-EDTA buffer.

**Table 3.4:** Table displaying primer information used in this Chapter

Primer Name	Sequence (5' – 3')	Annealing Temp (°C)	Cycle Number
FBN1_ Ex13-F	GGA TAT CAG AGC ACA CTC AC	55	20-22
FBN1_ Ex20-R	GTA GAT AAA TCC CTT GGG GC		
SPT4_ Ex1-F	TTA CTT CCT GCG GGT GCA CA	60	24
SPT4_ Ex5-R	CTG GAT TTG TAG GCC ACT CC		
SUPT5H_ Ex1-F	CGA GGA CAG CAA CTT TTC CG	60	26
SUPT5H_ Ex12-R	TCA GGG AGA TGG TGT TCT GG		
SUPT5H_ Ex11-F	AAG CGG GGC ATC TAC AAG GA	60	26
SUPT5H_ Ex19-R	TTC TGC TCT GAG TCC AAG GC		
SUPT5H_ Ex18-F	GAC TAG AAC GGG AGA CCT TC	60	28
SUPT5H_ Ex26-R	GCG TCT GCG GGT TGT ATT GT		
SUPT5H_ Ex24-F	ATG ACC TCG ACC TAT GGG AG	60	28
SUPT5H_ Ex30-R	ATC CTC GCC CAG GAT CAC TT		

### 3.2.5 Western Blotting

Cell lysates were prepared in 50 - 200 µl of 125 mM Tris-HCl, pH 6.8, 15% SDS, 10% Glycerol, 1.25 µM PMSF (Sigma-Aldrich, Sydney, Australia) and 1x protease inhibitor cocktail (Sigma-Aldrich) and subsequently sonicated 6 times (1 second pulses on ice), prior to the addition of bromophenol blue (0.004%) and dithiothreitol (2.5mM). Samples were heated at 94°C for 5 minutes, cooled on ice and then centrifuged at 14 000 x g for 1 minute before loading onto the gel.

Total protein (20 µg), determined by a BCA assay (ThermoFisher Scientific), was loaded onto each lane of NuPAGE Novex 4-12% Bis/Tris gradient gels (ThermoFisher Scientific). Samples were subsequently fractionated at 200 volts for 1 hour. Proteins were then transferred onto a polyvinylidene fluoride membrane using the P0 program on the iBlot transfer system according to the manufacturer's instructions. Following blocking in 5% skim milk in TSBT for 1 hour, the membrane was incubated with various antibodies diluted in 5% skim milk in TSBT, overnight at 4°C (**Table 3.5**). For immunodetection, polyclonal goat anti-rabbit or anti-mouse HRP-labelled immunoglobulins (Dako, cat. no P0448 and D0447 respectively, Sydney,

Australia) at a dilution of 1:10 000 and Luminata Crescendo western HRP substrate (Merk, Sydney, Australia) were used. The blots were exposed for a serial scan of 20 seconds using the Fusion FX gel documentation system (Vilber Lourmat, Marne-la-Vallée, France).

**Table 3.5:** List of antibodies used with corresponding dilutions and manufacturer information.

Antibody	Supplier	Host Species & Clone	Dilution	Secondary antibody
<b>ATXN3</b>	Merk (MAB5360)	Mouse monoclonal	1:500	Goat anti-mouse AP
<b>Beta-Actin</b>	Sigma-Aldrich (A2228)	Mouse monoclonal	1:500 000	Goat anti-mouse HRP
<b>Beta-Tubulin</b>	Thermo Fisher (TBN06)	Mouse monoclonal	1:1 000	Goat anti-mouse HRP
<b>SPT4</b>	Cell Signalling (64828)	Rabbit monoclonal	1:1 000	Goat anti-rabbit HRP

### 3.2.6 Transcriptome Analysis

Total RNA samples, prepared as described in **Chapter 2** were sent to the Australian Genome Research Facility (AGRF, Perth and Melbourne, Australia) for whole transcriptome library preparation using the TruSeq Stranded Total RNA Library Prep Kit (Illumina, CA, USA) and ribosomal RNA depletion with the Ribo-Zero-Gold kit (Illumina, CA, USA). RNA quality was assessed using a Bioanalyser (Elmar, MA, USA) prior to RNA-seq and only those samples with an RNA integrity number (RIN) of  $\geq 8$  were analysed. RNA-sequencing was performed using an Illumina HiSeq 2500 (Illumina, CA, USA) to generate 150 bp paired end reads that yielded an average 122 million reads per sample. Raw sequencing files were quality checked using FastQC (0.11.7), with all files passing. No adapter contamination was detected, and reads were not trimmed.

Bioinformatics analysis was conducted using several web-based programs. Gene differential expression (DE), heat map, multidimensional scaling (MDS) plots and parallel coordinate analyses were conducted

using the *Degust: interactive RNA-seq analysis* (Version 4.1.1) [170]. All analyses conducted using *Degust: interactive RNA-seq analysis* used a false detection rate (FDR) cut-off of 0.1, with a minimum count per million of 1 in a minimum of 2 samples, using the edgeR method of analysis. Ontology of differentially expressed genes was performed using the web-based application *GOnet Enrichment Analysis* (Ontology version 2019-07-01) [171], with  $p < 0.05$ ,  $FDR < 0.1$  and  $edge > 0.3$  cut-offs. Gene ontology networks were generated through *GOnet Enrichment Analysis*, while applying the interactive graph feature and assessing the biological processes network.

### **3.2.7 Densitometric and Statistical Analysis**

Densitometric analysis was performed using the ImageJ (version 1.8.0\_112) imaging software [172]. The One-way ANOVA with Bonferroni correction was performed to determine significance ( $p < 0.05$ ). P value refers to unpaired two tailed student's t test. A p value  $< 0.05$  was considered statistically significant.

## 3.3 Results

### 3.3.1 *SUPT4H1* & *SUPT5H* Target Identification and Therapeutic Strategy

Studies by other researchers have shown that *SUPT4H1*, and to a lesser degree *SUPT5H*, are selectively required to facilitate RNA Pol II transcription through disease expansions. Others have shown that knockdown of these transcription factors ameliorates disease characteristics in both *in vitro* and *in vivo* models of different expansion diseases [151-153,173]. Consequently, we examined the gene transcripts for both *SUPT4H1* and *SUPT5H* and designed AOs to target out-of-frame exons for exclusion to downregulate expression of the respective proteins.

#### 3.3.1.1 *SUPT4H1* gene and protein

The major human *SUPT4H1* human transcript (ENST00000225504.8) contains 5 exons, with the ATG initiation codon located in exon 1 and the TAG termination signal in exon 5 (**Figure 3.1A**). The *SUPT4H1* gene encodes a 117 aa, 14 kDa protein, *SUPT4H1*. This protein is a conserved eukaryotic transcription elongation factor that contains a zinc finger domain, essential to its biochemical activity (**Figure 3.1B**). In addition, *SUPT4H1* has a *SUPT5H* interaction domain that allows *SUPT4H1* to directly bind to *SUPT5H* and form the transcription elongation factor complex DSIF (**reviewed in Chapter 1.1**). Initially, we designed AOs to anneal to exon 2 of the *SUPT4H1* transcript, as this contained the *SUPT5H* interaction domain and the Zinc finger domain, and importantly, the loss of this exon would disrupt the normal mRNA reading frame. In addition, we also designed AOs to anneal to exon 3 as we have observed that some exons are more readily excised than others during splicing. As with exon 2, the omission of exon 3 from the mature mRNA of *SUPT4H1* would also disrupt the reading frame, lead to a premature termination codon and possibly induction of nonsense mediated decay.

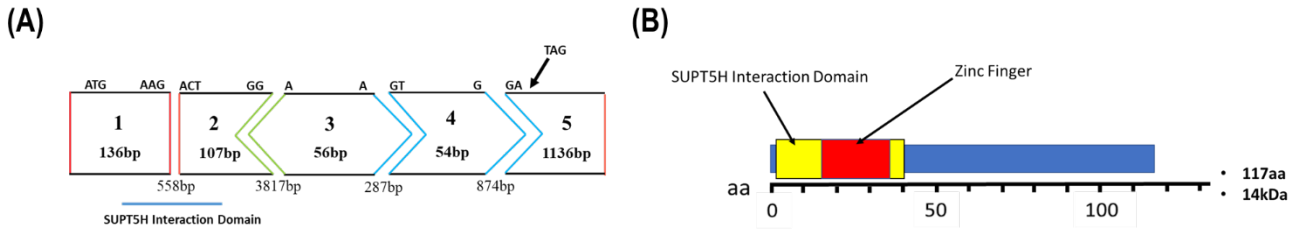


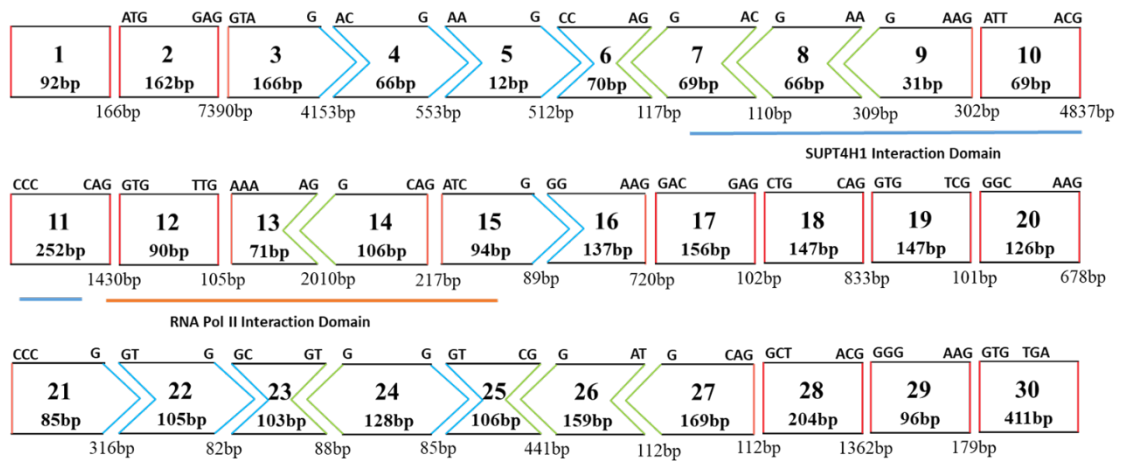
**Figure 3.1:** Representation of (A) the *SUPT4H1* reading frame (ENST00000225504.8) (B) the *SUPT4H1* protein structure, indicating functional domains. Each box in (A) represents an exon and the exon number and size are shown within the box. The *SUPT5H* interaction domain encoding exons are indicated below the exon map. In-frame exons are represented as rectangles, whereas those bounded by partial codons are represented with chevron sides.

### 3.3.1.2 *SUPT5H* gene and protein

The major *SUPT5H* transcript (ENST00000225504.8) contains 30 exons (**Figure 3.2A**) and encodes a 1087 aa, 150 kDa protein, *SUPT5H* (**Figure 3.2B**). *SUPT5H* is a large, highly conserved transcription elongation factor with multiple recurring KOW domains as well as a larger RNA Pol II interaction domain, among others. Unlike *SUPT4H1*, *SUPT5H* directly interacts with RNA Pol II.

Both exons 3 and 6 were targeted for exon skipping, since excluding either exon would induce an in-frame premature termination codon and potentially induce some level of nonsense mediated decay.

(A)



(B)

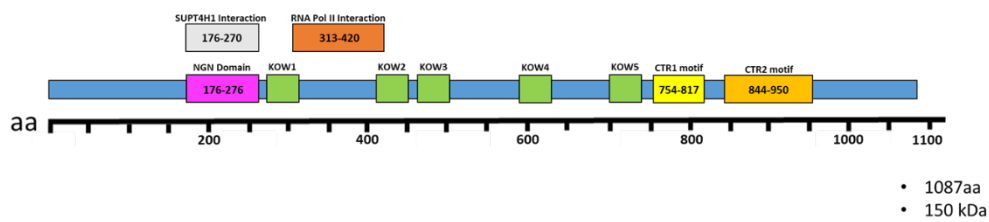


**Figure 3.2:** Representation of (A) the *SUPT5H* reading frame (ENST00000225504.8) (B) the *SUPT5H* protein structure showing functional domains. Each box in (A) represents an exon and the exon number and size are shown within the box. The *SUPT4H1* and *RNA pol III* interaction domain encoding exons are indicated. In-frame exons are represented as rectangles, whereas those bounded by partial codons are represented with chevron sides.

### 3.3.2 Initial 2'-Me PS AO Screen

Following PCR optimisation (**Supplementary Figure S3.1**) and AO design, AOs targeting the two *SUPT* transcripts were evaluated for their ability to skip the target exons. All first-round 2'-Me PS AO screening *in vitro* was conducted in healthy primary dermal fibroblasts. Where any potential cell death or loss of transcript occurred, a house-keeping gene, Fibrillin 1 (*FBN1*) was included in the RT-PCR assay to determine and quantify any global loss of RNA.

### 3.3.2.1 *SUPT4H1* 2'-Me PS screen

Several 2'-Me PS AOs were designed to target exon 2 and exon 3 of the *SUPT4H1* transcript in an effort to disrupt the reading frame. In addition, an unrelated control AO [22] that does not anneal to any known transcript was included as a negative experimental control in all transfections. Single 2'-Me PS AOs and two-AO cocktails were transfected into normal dermal fibroblasts at concentrations of 400 and 100 nM, incubated for 24 hrs prior to RNA extraction and subsequent RT-PCR to assess exon skipping efficiency. Gel fractionation of the RT-PCR amplicons revealed shorter products arising from exclusion of either exon 2 ( $\Delta$ 107 bp) (**Figure 3.3A**) or exon 3 ( $\Delta$ 56 bp) (**Figure 3.3B**). The identity of the amplicons was confirmed by Sanger sequencing (**Figure 3.3**) and (**Figure 3.3**), respectively. Efficient exon 2 skipping after single AO transfections was induced by S4-AO-2.3 and S4-AO-2.4, as well as with cocktails 1, 2 and 5.

The six lead sequences revealed by the AO screening pipeline were synthesised as the PPMO chemistry (**Table 3.1**). The PPMOs are comprised of a PMO sequence, conjugated to a proprietary cell penetrating peptide that facilitates cellular uptake of the AO.

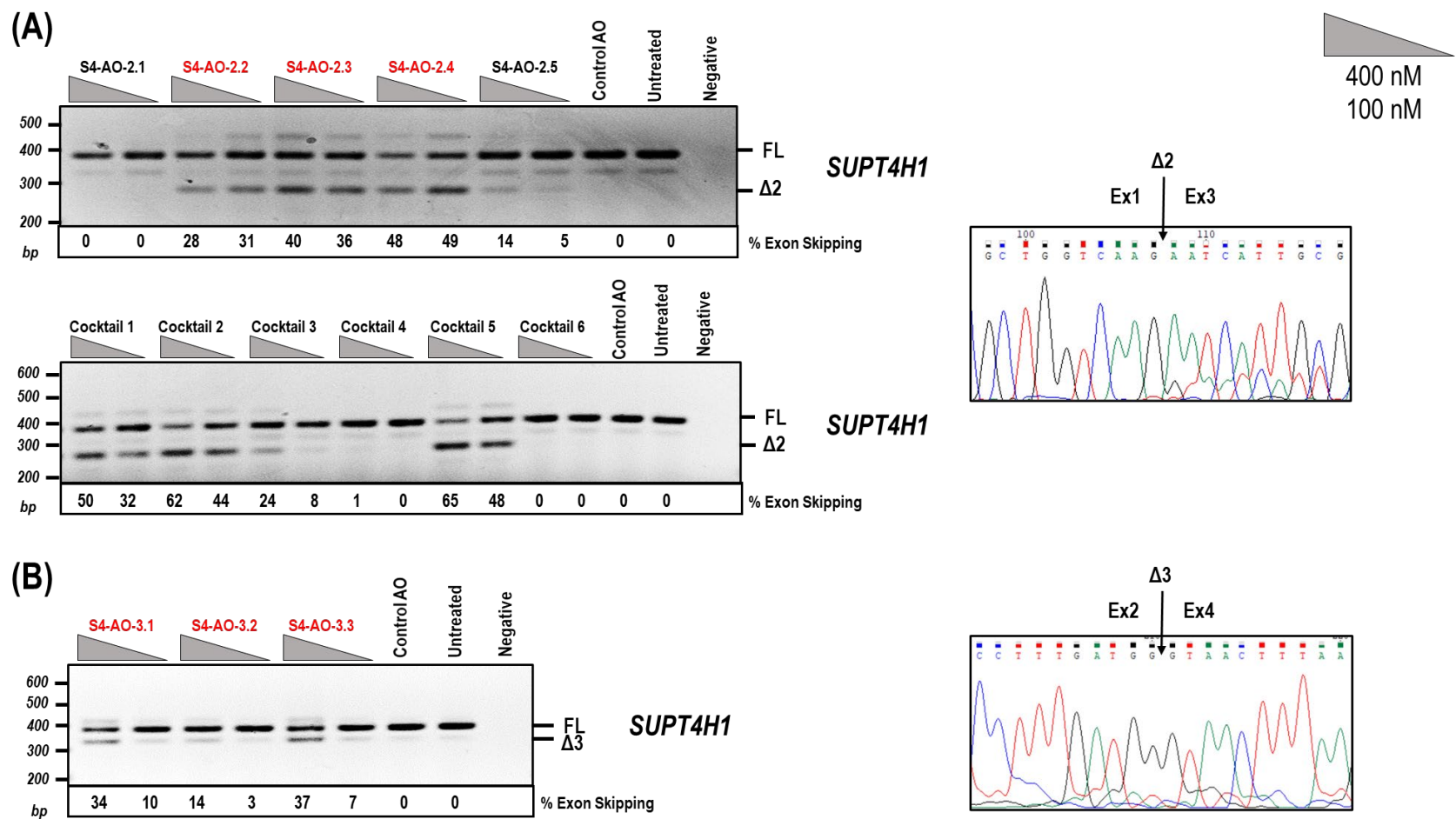


**Figure 3.3:** Evaluation of antisense oligonucleotides (AOs) designed to alter SUPT4H1 transcript levels in normal human fibroblasts. Screening of 2'-Me phosphorothioate (PS) AOs targeting (A) exon 2 and (B) exon 3 for removal. AOs were transfected as lipoplexes at two concentrations, 400, 100 nM for 24 hours. After RT-PCR amplification of SUPT4H1 transcript and gel fractionation, products representing the full-length (FL) and exon-skipped ( $\Delta 2/\Delta 3$ ) transcripts were identified. Sanger sequencing (right) of the RT-PCR products generated by skipping of exon 2 or 3 confirm the corresponding exon junctions. Exon skipping efficiencies quantitated using ImageJ are shown below gel images. AOs represented as red text were synthesised as PPMOs.



### 3.3.2.2 *SUPT5H* 2'-Me PS screen

Initially, several 2'-Me PS AOs were designed to target early exons in the *SUPT5H* transcript to disrupt the reading frame and reduce synthesis of the functional protein. Single 2'-Me PS AOs and two AO cocktails were transfected into healthy dermal fibroblasts at concentrations of 400 and 100 nM for 24 hrs prior to RNA extraction and subsequent RT-PCR to assess exon skipping and down-regulation efficiency (**Figure 3.4**). Interestingly, gel fractionation showed only modest skipping of exon 3 induced by 5-AO-3.3, with most treatments inducing skipping of multiple exons (exons 3, 4 and 5) simultaneously (**Figure 3.4A**). Multi-exon skipping or induction of several mRNA isoforms after treatment with a single AO has been previously observed in our laboratory [174]. Loss of transcript was also evident as a result of some AO treatments, most notably with cocktails 4 and 6. Amplification of the transcript further downstream shows only modest reduction of the transcript levels after transfection at 400 nM, which suggested the apparent downregulation may have been a limitation of the RT-PCR assay due to the intron or part thereof being retained (**Figure 3.4A**). However, attempts to amplify this region were unsuccessful (data not shown), this reduction in *SUPT5H* transcripts could be due to efficient exon skipping with nonsense mediated decay reducing the induced exon 2-skipped isoform. Yet another explanation could be one or more off-target effects of 2'-Me PS AOs [175]. To explore this possibility, it was shown that *FBN1* expression, an unrelated and non-targeted gene transcript, was also reduced suggesting some toxicity associated with that particular AO sequence.

Fibroblasts treated with AOs directed to *SUPT5H* exon 6 showed no detectable exon 6 skipping, however, at 400 nM, 5-AO-6.1 showed approximately 80% transcript knockdown (**Figure 3.4B**). There was no detectable intron retention and other knockdown analyses were accounted for by the loading control transcript fibrillin 1 (*FBN1*) and normalisation to the Control AO sample [169].

The four lead sequences revealed by this AO screen were synthesised as PPMOs (**Table 3.2**).

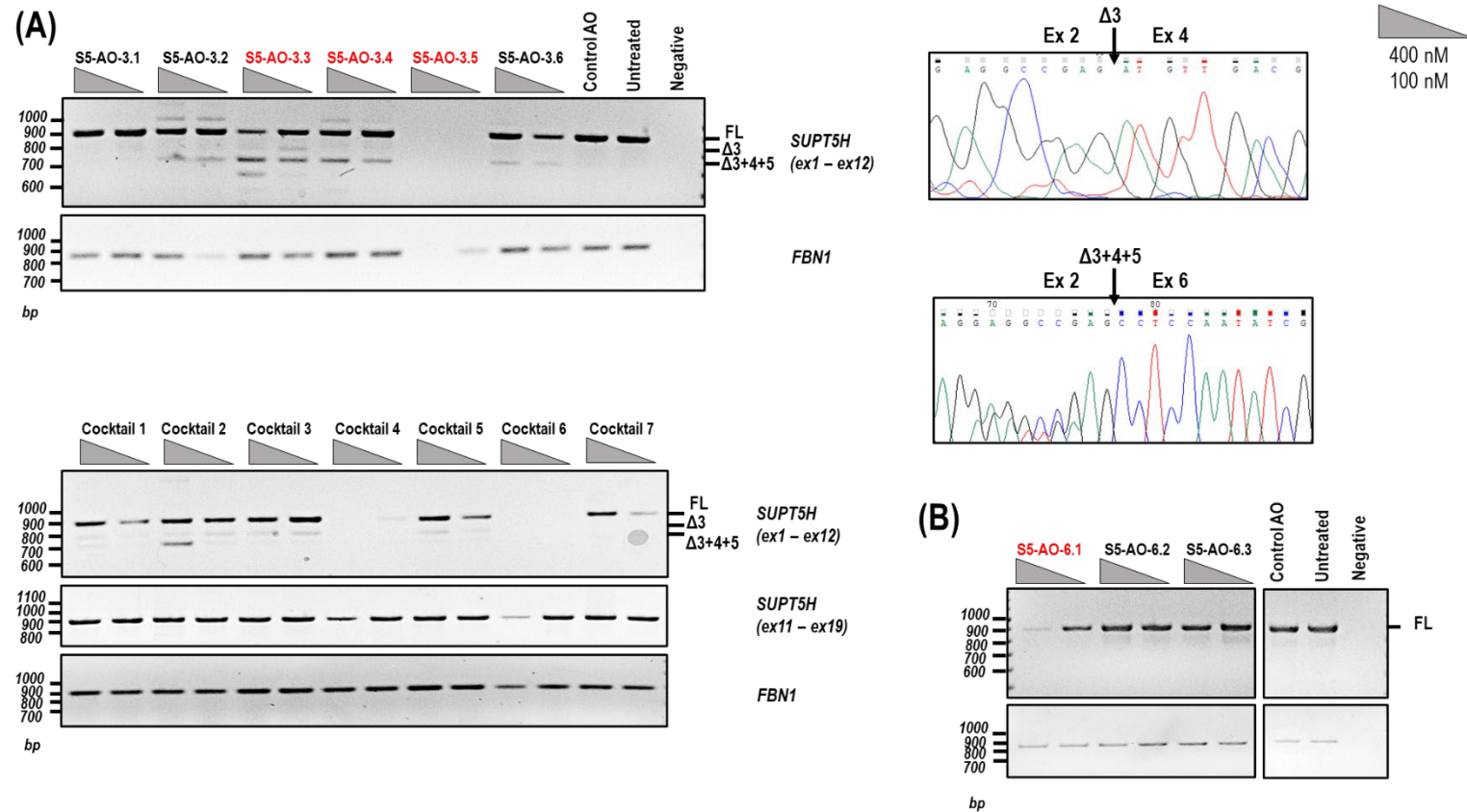


**Figure 3.4:** Evaluation of antisense oligonucleotides (AOs) designed to alter SUPT5H transcript structure in normal human fibroblasts. (A) Screening of 2'-Me phosphorothioate (PS) AOs targeting exon 3 for removal. AOs were transfected as lipoplexes, at two concentrations, 400, 100 nM for 24 hours, and after RT-PCR and gel fractionation, products representing the full-length (FL), exon 3-skipped ( $\Delta 3$ ) and exons 3, 4 and 5-skipped simultaneously ( $\Delta 3+4+5$ ) transcripts were identified. Sanger sequencing of the RT-PCR products (right) generated by skipping of exon 3 and exon 3, 4 and 5 simultaneously, shows the junction between exon 2 and 4 and the junction between exon 2 and 6, respectively. (B) Screening of 2'-Me PS AOs targeting exon 6 for removal. AOs were transfected as lipoplexes at two concentrations, 400, 100 nM, and after RT-PCR and gel fractionation, products representing the full-length (FL) was identified. Loading control transcript Fibrillin 1 (FBN1) was used where apparent loss of SUPT5H transcript occurs. AOs represented as red text were resynthesised as PPMOs

### 3.3.3 Initial PPMO AO Screen and SUPT4H1 Protein Analysis

Following the 2'-Me PS AO screen in normal dermal fibroblasts, four sequences targeting the two *SUPT* transcripts were selected for synthesis as PPMOs and evaluated for their ability to skip the target exons. Our experience is such that PMOs generally show improved splice-switching efficiency when compared to 2'-Me PS AOs of the same sequence [169,174,176,177]. Further *in vitro* screening studies were conducted in the bone marrow-derived neuroblastoma cell line, SH-SY5Y, to gain insights as to how the *SUPT*-targeting PPMOs may perform in cells within the neuronal lineage. While patient-derived neuronal cells, carrying expanded repeats would have been preferable for this part of the study, iPSCs and therefore *in vitro* differentiated neuronal cells from patients were unavailable at the time.

#### 3.3.3.1 *SUPT4H1* PPMO screen

Single and cocktail *SUPT4H1* targeting PPMOs were transfected at various concentrations into undifferentiated SH-SY5Y cells (5, 2.5, 1, 0.5  $\mu$ M), incubated for 72 hrs prior to RNA extraction and RT-PCR to assess exon skipping efficiencies. The 72-hr time point was chosen to allow sufficient time for the PPMO to penetrate the cell. Gel fractionation of the RT-PCR amplicons revealed shorter products arising from exclusion of either exon 2 ( $\Delta$ 107 bp) (**Figure 3.5A**) or exon 3 ( $\Delta$ 56 bp) (**Figure 3.5B**), with Sanger sequencing confirming amplicon identity (**Figure 3.5A** and **Figure 3.5B**), respectively. Of the single PPMO treatments, PPMO 1083 induced efficient exon 2 skipping (84% exon 2 skipping at 5 $\mu$ M), however, both cocktail treatments showed nearly 100% exon 2 skipping after transfection at 5  $\mu$ M. Treatments targeting exon 3 showed varying levels of exon skipping; PPMO 1106 induced a high degree of cell death at concentrations out or above 2.5  $\mu$ M (**Figure 3.5B**); PPMO 1108 induced 100% exon 3 skipping at 5  $\mu$ M, while PPMO 1107 was less than 50% efficient at the highest concentration tested. All PPMOs, with the exception of PPMO 1106, had little effect on cell viability when compared to the GTC transfection and untreated cells.

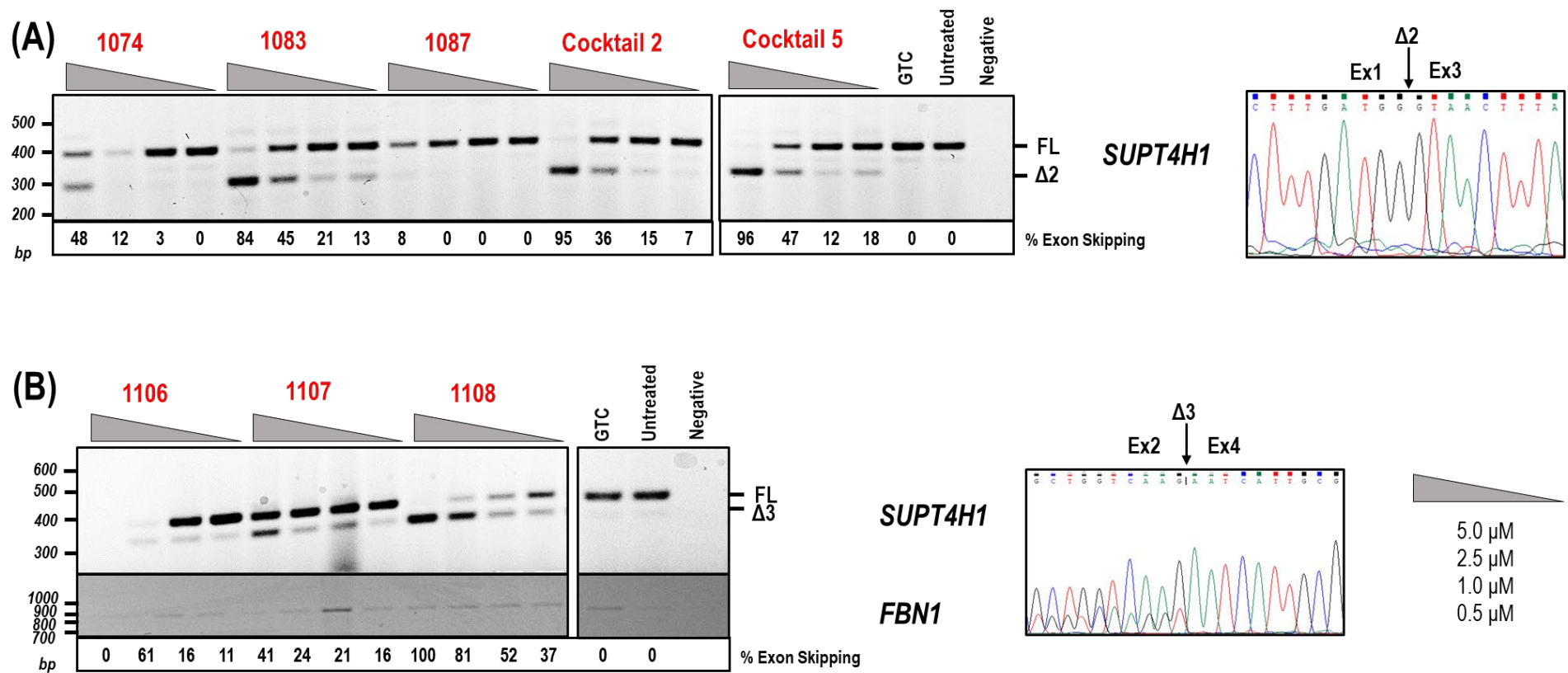


**Figure 3.5:** Evaluation of antisense oligonucleotides (AOs) designed to alter *SUPT4H1* transcript structure in undifferentiated SH-SY5Y cells. Screening of peptide conjugated-PMOs (PPMOs) targeting (A) exon 2 and (B) exon 3 for removal. PPMOs were added to the SH-SY5Y cells and allowed free uptake at four concentrations, 5, 2.5, 1, 0.5 μM for 72 hours, and after RT-PCR and gel fractionation, products representing the full-length (FL) and exon 2/3-skipped (Δ2/3) transcripts were identified. Sanger sequencing (right) of the RT-PCR products generated by skipping of exon 2 or 3 confirmed target exon skipping. Loading control transcript Fibrillin 1 (*FBN1*) used where apparent loss of *SUPT4H1* transcript occurs. Exon skipping efficiencies quantitated using Image J are shown below gel images. Refer to Table 3.3 for cocktails.

### 3.3.3.2 *SUPT5H* PPMO screen

Single oligomers and PPMO cocktails targeting *SUPT5H* were transfected into SH-SY5Y cells at various concentrations (5, 2.5, 1, 0.5  $\mu$ M) for 72hr prior to RNA extraction and RT-PCR to assess induced exon skipping and/or *SUPT5H* transcript knockdown. Gel fractionation of the RT-PCR amplicons revealed shorter products arising from exclusion of either exon 3 ( $\Delta$ 166 bp) (**Figure 3.6A**) or exon 6 ( $\Delta$ 70 bp) (**Figure 3.6B**). Amplicon identity was confirmed by Sanger sequencing (**Figure 3.6A** and **Figure 3.6B**), respectively. PPMO 1101 was the only single oligomer to induce robust skipping of exon 3, without evidence of conspicuous cell toxicity (**Figure 3.6A**). Remarkably, PPMO 1092 appeared highly toxic to the cells and induced 100% cell death within 24 hrs at concentrations above 0.5  $\mu$ M (**Figure 3.6A**). Cocktail of PPMOs targeting exon 3 showed high levels of exon skipping, however cocktail 5 was toxic at the highest concentration. Interestingly, the multi-exon skipping induced by the 2'-Me PS AO treatments was not observed when the cells were transfected with PPMO combinations of the same sequences. This is potentially due to the higher binding affinity of PPMOs and reduced off-target effects when compared to 2'-Me PS AOs. PPMO 1109 targeting exon 6 of the *SUPT5H* transcript induced 65% skipping of exon 6 at 5  $\mu$ M, however, lower concentrations induced no detectable exon 6 skipping (**Figure 3.6B**).

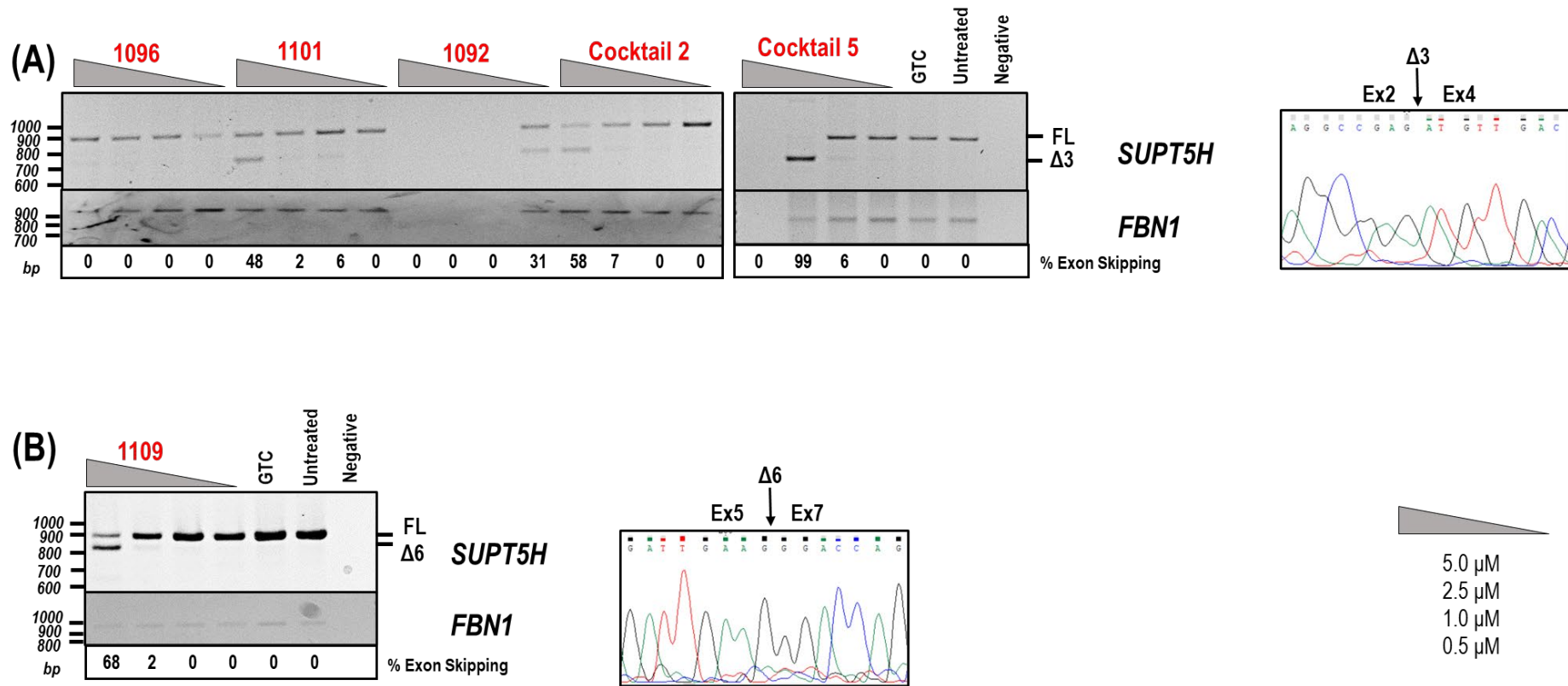


**Figure 3.6:** Evaluation of antisense oligonucleotides designed to alter *SUPT5H* transcript structure in undifferentiated SH-SY5Y cells. (A) Screening of peptide conjugated-PMOs (PPMOs) targeting (A) exon 3 and (B) exon 6 for removal. PPMOs were added to the SH-SY5Y cells and allowed free uptake at four concentrations, 5, 2.5, 1, 0.5  $\mu\text{M}$  for 72 hours, and after RT-PCR and gel fractionation, products representing the full-length (FL) and exon 3/6-skipped ( $\Delta 3/6$ ) transcripts were identified. Sanger sequencings (right) of the RT-PCR products generated by skipping of exon 3 or 6 confirmed target exon skipping. Loading control transcript *Fibrillin 1* (*FBN1*) used where apparent loss of *SUPT5H* transcript occurs. Exon skipping efficiencies quantitated using Image J are shown below gel images. Refer to Table 3.3 for cocktails.

### 3.3.3.3 SUPT4H1 exon 2 protein analysis

To investigate the effects of exon 2 skipping and consequent modification and/or knockdown of SUPT4H1 protein, SH-SY5Y cells were transfected with the lead candidate single and exon 2-targeting cocktail PPMOs at a concentration of 5  $\mu$ M, and RNA and protein were isolated 4 days following transfection. Gel electrophoresis of the RT-PCR amplicons revealed that PPMO 1083, as well as cocktails 2 and 5 induced nearly 100% skipping of exon 2 (**Figure 3.7A**). PPMO 1083 and cocktail 2 induced high levels of SUPT4H1 knockdown, with cocktail 2 reducing the protein by 75% when compared to the protein level from the GTC treated sample (**Figure 3.7B**). Although cocktail 5 induced robust exon 2 skipping, this was not associated with any detectable protein knockdown, and we are currently uncertain as to why no protein knockdown occurred, as there was no change in cell viability nor any knockdown associated with the loading control gene, *FBN1*.

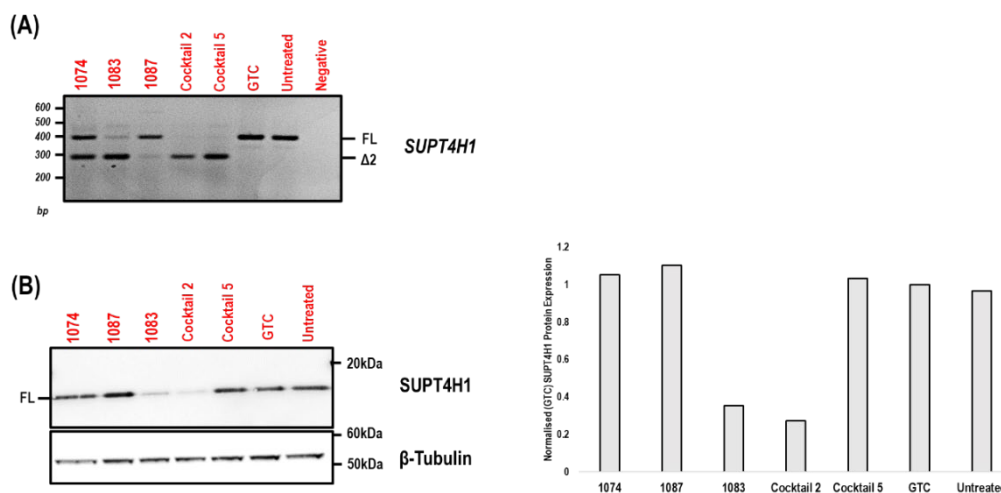


**Figure 3.7:** Evaluation of SUPT4H1 exon 2 skipping in SH-SY5Y cells, transfected with peptide conjugated-PMOs (PPMOs). Cells were harvested 4 days following transfection for protein and RNA analysis. (A) Agarose gel fractionation of SUPT4H1 amplicons, following transfection at a concentration of 5  $\mu$ M, shows full-length (FL) and exon 2 ( $\Delta$ 2) skipped transcript products. (B) SUPT4H1 protein was analysed by Western blotting following transfection at a concentration of 5  $\mu$ M and it shows full-length (FL) SUPT4H1 at approximately 14 kDa. Beta-Tubulin was used as a loading control. The bar graph of densitometric analysis performed on the Western blots (SUPT4H1 expression normalised to beta-tubulin) is shown on the right. Relative expression of SUPT4H1 protein normalised to that expressed in the GeneTools Control (GTC) treated cells is shown.

In addition to assessing SUPT4H1 protein knockdown, we analysed the effects of PPMO-mediated *SUPT5H* exon skipping on protein expression from this gene. Interestingly, we did not see any downregulation of the SUPT5H protein, rather all of the PPMO treated cells showed clear upregulation (**Supplementary Figure S3.2**). This result leads us believe that there may be as yet uncharacterised underlying regulatory mechanism(s) for SUPT5H, and this target may not be suitable for PPMO-mediated downregulation.

### 3.3.4 SUPT4H1 and SUPT5H Transcriptome Analysis

As the DSIF complex plays an important role in transcription elongation and pausing, it is essential to determine if any negative consequences occur through AO-mediated downregulation of *SUPT4H1* and/or *SUPT5H*. RNA samples, prepared from cells treated with three of the PPMOs targeting *SUPT4H1*, two targeting *SUPT5H* and one co-transfected with *SUPT4H1* and *SUPT5H* targeting PPMOs, along with two controls, were chosen for RNA-seq analysis (**Table 3.6**).

**Table 3.6:** List of PPMOs analysed for potential off-target effects on the transcriptome.

PPMO Name	Target	Rational
1083	<i>SUPT4H1</i> – Exon 2	PPMO 1083 shows high levels of SUPT4H1 protein reduction at 5 $\mu$ M in SH-S5Y cells.
1087	<i>SUPT4H1</i> – Exon 2	PPMO 1087 shows no obvious reduction in SUPT4H1 protein. Therefore, used as a target-specific control.
1108	<i>SUPT4H1</i> – Exon 3	PPMO 1108 target a different exon of <i>SUPT4H1</i> transcript to PPMO 1083, however, still induces modest SUPT4H1 protein reduction.
1109	<i>SUPT5H</i> – Exon 6	PPMO 1109 shows high levels of <i>SUPT5H</i> exon 6 skipping with no apparent toxicity at 5 $\mu$ M.
Cocktail 2	<i>SUPT5H</i> – Exon 3	Cocktail shows high levels of <i>SUPT5H</i> exon 3 skipping, however, show no apparent toxicity at 5 $\mu$ M.
Co-Transfected (1083 & 1109)	<i>SUPT4H1</i> – Exon 2 & <i>SUPT5H</i> – Exon 6	PPMO 1083 and PPMO 1096 were chosen as they both show little to no toxicity and induce efficient exon 2 and exon 3 skipping of the <i>SUPT4H1</i> and <i>SUPT5H</i> transcripts, respectively.
GTC	N/A	Control to account for effects of transfection with PPMO.
Untreated	N/A	Untreated control.



SH-SY5Y cells were transfected with the PPMOs at a concentration of 5  $\mu$ M, and RNA and protein isolated 4 days following transfection; treatments were conducted in replicate (n=4), however, only 3 replicates per sample were analysed by RNA-seq due to cost constraints. RNA-sequencing was performed on an Illumina HiSeq 2500 (Illumina, CA, USA) to generate 150 bp paired end reads that yielded an average 122 million reads per sample. Gel fractionation of the RT-PCR amplicons revealed highly reproducible exon skipping and/or downregulation of the target transcript for all PPMO treated SH-SY5Y samples (**Supplementary Figure S3.3**).

#### 3.3.4.1 *Multidimensional scaling plot analysis*

Count files generated after sequence alignment was analysed using the *Degust: interactive RNA-seq analysis* (Version 4.1.1) [170] for multidimensional scaling (MDS) plot analysis (**Figure 3.8A and 3.8B**). The MDS Two-dimension plot shows replicates of individual PPMO treated SH-SY5Y cells clustered together, suggesting that treatments are reproducible, with both of the controls showing little deviation in dimension one and two (**Figure 3.8A**). However, the MDS three-dimension plot for treatments with 1083, 1108 and Co-transfected (CO\_T) show a replicate for each treatment that is not as tightly clustered, albeit a modest deviation (**Figure 3.8B**). Clustering of the GTC, UT, 1083, 1109 treated samples in both MDS plots, suggests that 1083 and 1109 treated SH-SY5Y cells are most similar to control samples, while CO\_T, 1108 and 1087 treated cells show the highest levels of deviation from the control samples. Interestingly, the transcriptome of PPMO 1087 transfected cells shows the greatest deviation from controls, despite the PPMO having little effect on the level of SUPT4H1 protein (**Figure 3.7, Figure 3.8A and 3.8B**).

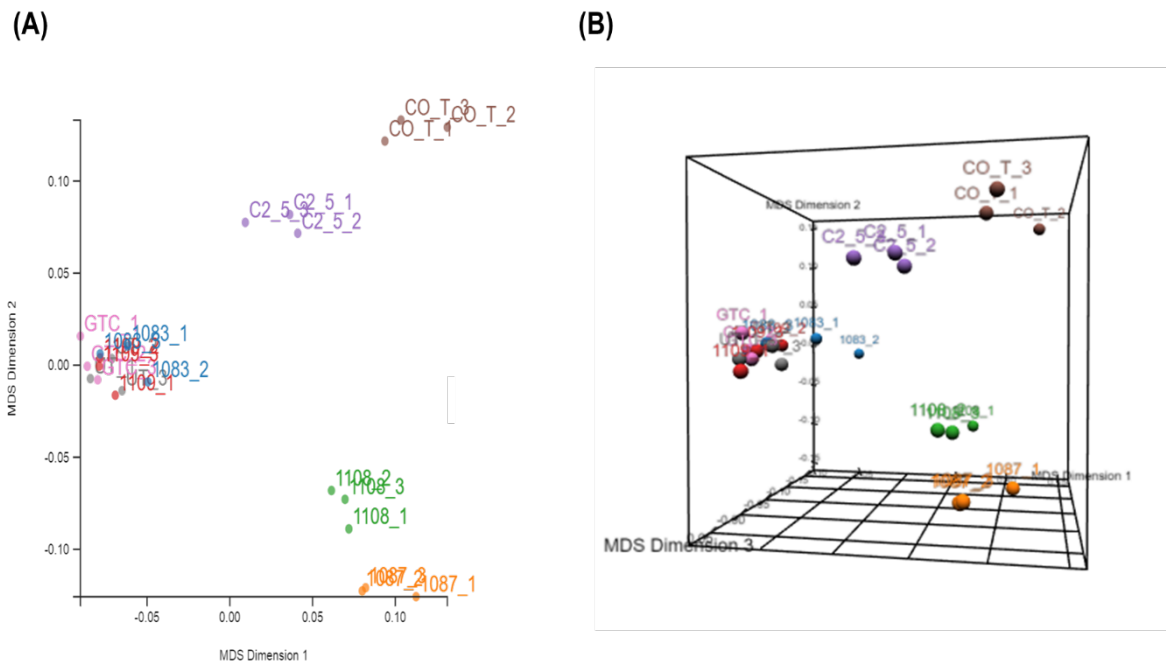


**Figure 3.8:** RNA sequencing analysis of PPMO treated SH-SY5Y cells showing (A) two-dimensional and (B) three-dimensional MDS plots of all PPMO treated SH-SY5Y samples. Samples are labelled with PPMO name followed by replicate number. CO\_T; co-transfection of SUPT4H1 and SUPT5H PPMOs.

### 3.3.4.2 Analysis of differentially expressed genes in treated samples compared to GTC

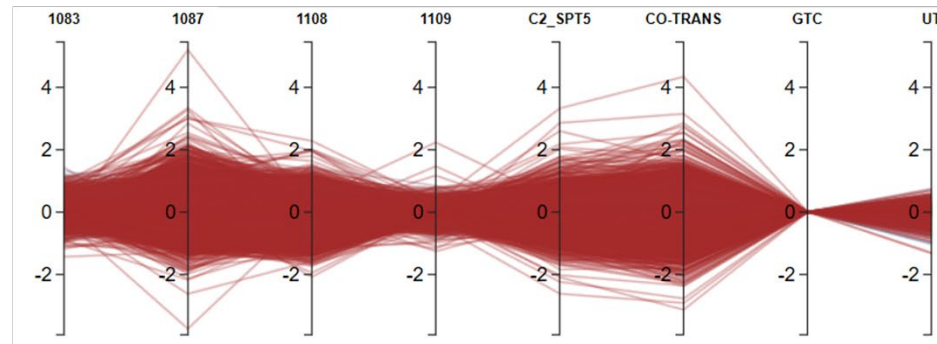
We next evaluated the PPMO treatments for their effect on total gene expression using the *Degust: interactive RNA-seq analysis* (Version 4.1.1) [170]. Initially, we compared the GTC treated SH-SY5Y cells to the untreated samples to determine any effects of the transfection on the transcriptome, and showed no significant changes in differentially expressed (DE) genes in the GTC-treated cells, relative to untreated cells when using the Limma function in *Degust: interactive RNA-seq analysis* (Version 4.1.1) [170].

An RNA-seq heatmap comparing the average expression of transcripts in PPMO transfected SH-SY5Y cells to that of the GTC and a parallel coordinates graph showed modest differences in expression between the groups (**Figures 3.9A and 3.9B**). Transcripts that are overexpressed in PPMO transfected cells compared to GTC are indicated in red, while those that are under-expressed are shown in blue. The most significant changes observed were in PPMO 1087, cocktail 2 (*SUPT5H*) and the co-transfected

treated SH-SY5Y cells. This data complements that shown in **Figure 3.8**, with PPMO 1083 and PPMO 1109 having the least effect on differential gene expression.

Although the PPMO 1109 treated cells showed little deviation from the GTC PPMO treated cells, we considered that SUPT5H may not be a suitable target for downregulation as a therapy for expansion diseases. The resulting decision was made from a holistic review of the literature, protein data (data not shown) and transcriptome analysis.

(A)



(B)

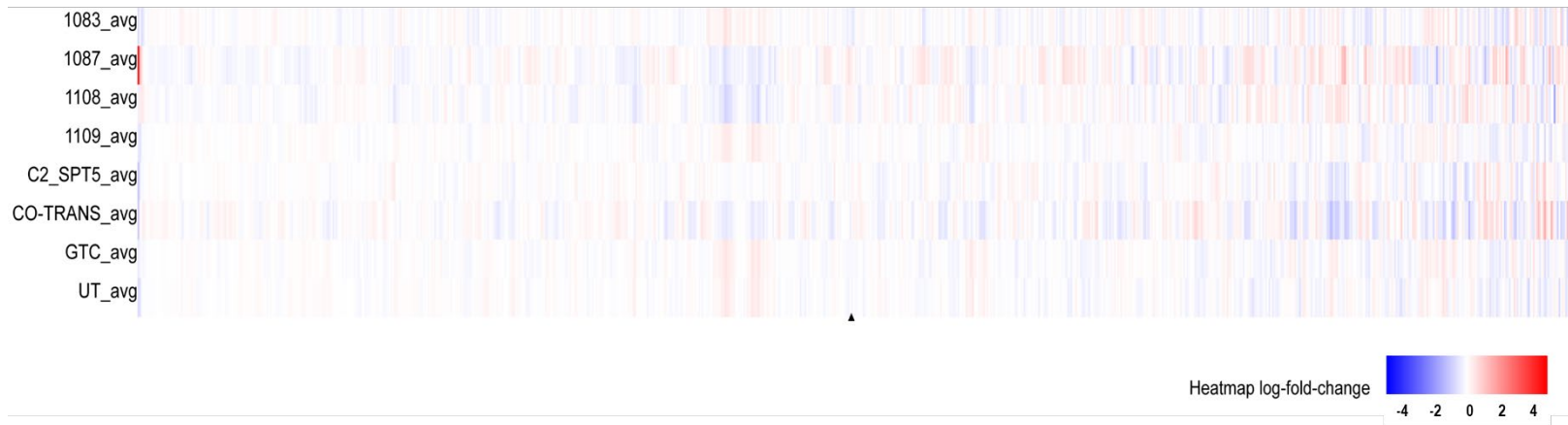


**Figure 3.9:** RNA sequencing analysis of PPMO treated SH-SY5Y cells showing (A) parallel coordinates graph of all averaged treated SH-SY5Y samples relative to the GeneTools Control treated sample (B) heatmap of differentially expressed transcripts of all averaged PPMO treated SH-SY5Y samples relative to GeneTools Control treated sample, whereby red represents over-expressed transcripts, and blue indicate under-expressed transcripts.

### 3.3.4.3 Analysis of differentially expressed genes in PPMO 1083 treated samples compared to GTC

Compiling all data thus far shows that PPMO 1083 stands as the most promising sequence for downregulation of SUPT4H1, as a potential modifier to treat repeat expansion disorders. Thus, we performed a detailed analysis of PPMO 1083 transfected samples, relative to the GTC treated samples. Analyses were performed after averaging triplicates. A total of 7514 genes for all replicates were differentially expressed, relative to the averaged GTC transfected sample (**Figure 3.10**), however, only a limited number of these genes were either up or downregulated  $\geq \log_2 2$  (**Table 3.7**) (**Figure 3.10A**, **Figure 3.10B** and **Figure 3.10C**). We selected the top 100 DE genes (ranked by P value), both up and down regulated after PPMO 1083 treatment, relative to samples from the GTC treated cells. The DE genes were calculated using Degust, FDR = 0.1. The 100 genes were subsequently analysed using the gene ontology (GO) web-based application GOnet Enrichment Analysis (Ontology version 2019-07-01) [171] and assessed for enriched biological processes, with a cut off of  $p \leq 0.05$  (**Figure 3.11**).

**Table 3.7:** Number of differentially expressed genes  $\geq \log_2 2$  in PPMO 1083 treated SH-SY5Y cells

PPMO 1083 Replicate	Number of Genes upregulated $\geq \log_2 2$	Number of Genes downregulated $\geq \log_2 2$
1083_1	0	0
1083_2	6	3
1083_3	0	0

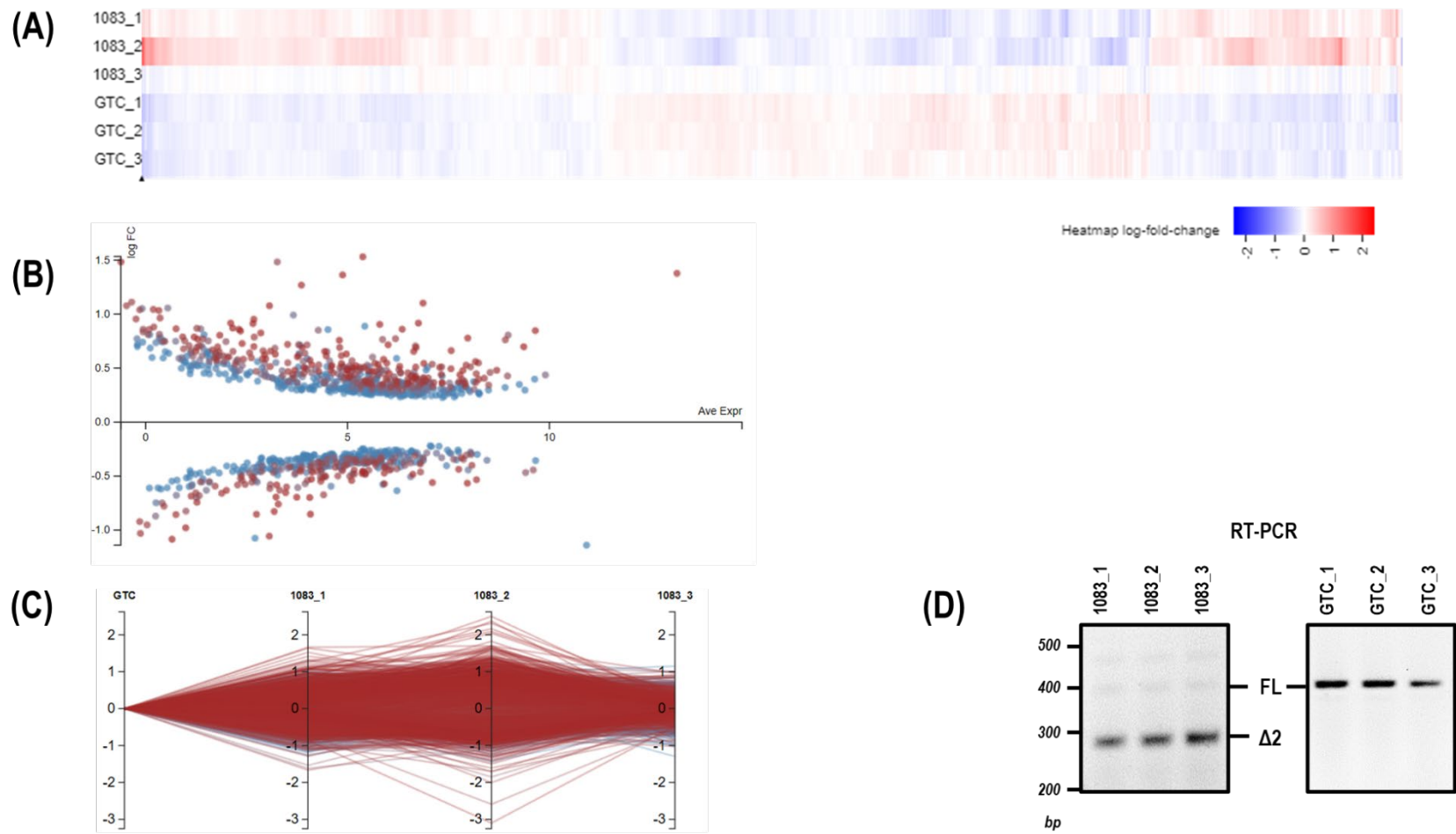


**Figure 3.10:** RNA sequencing analysis of SH-SY5Y cells showing (A) Heat map (B) MA plot (C) parallel coordinates plot of differentially expressed transcripts in 1083 PMMO treated cells relative to the GeneTools Control (GTC) treated samples. Red represents overexpressed transcripts, and blue represents underexpressed transcripts. (D) Agarose gel fractionation of amplified SUPT4H1 transcript from PMMO treated SH-SY5Y cells transfected for 4 days at a concentration of 5  $\mu$ M.

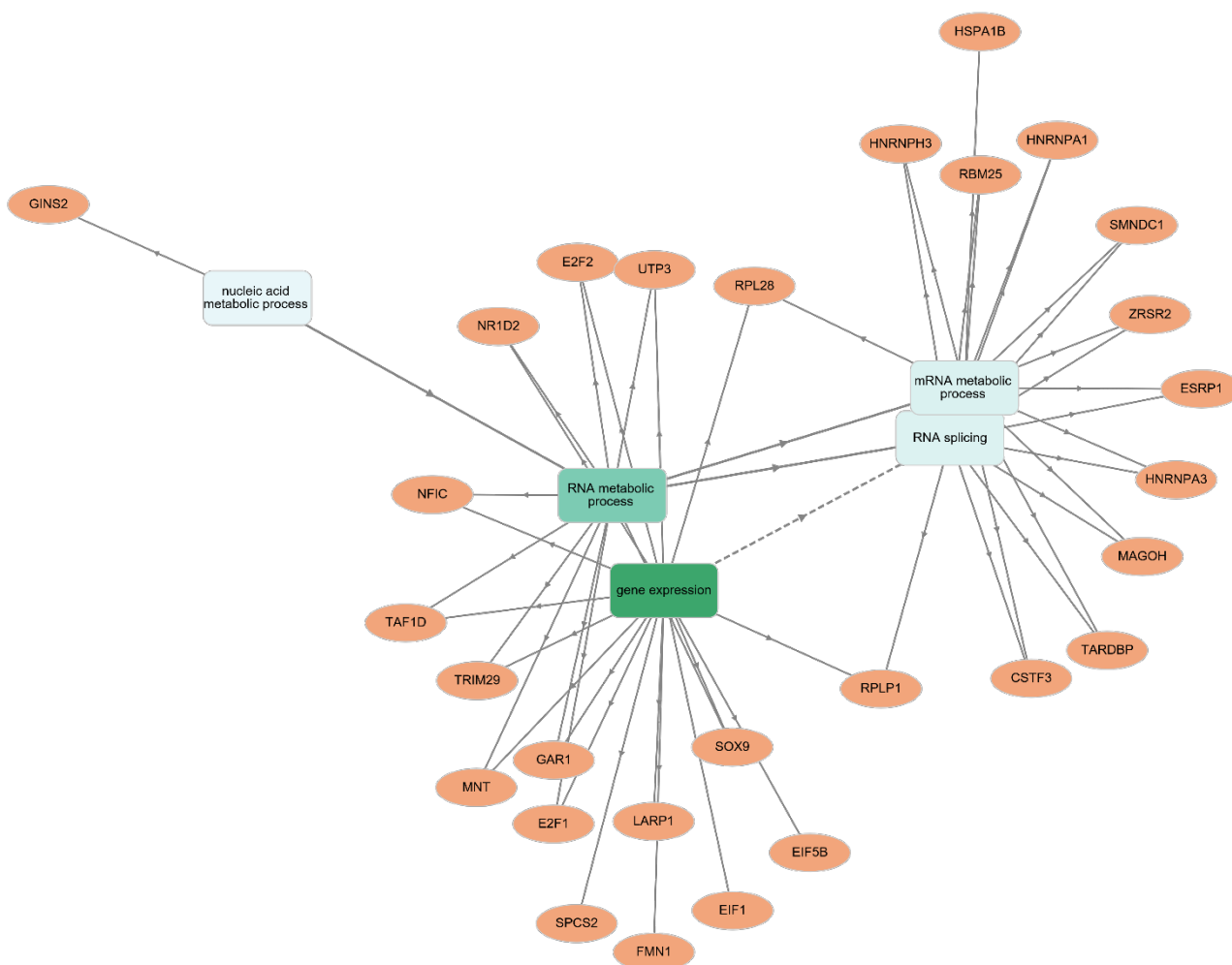


**Figure 3.11:** Gene ontology enrichment analysis of differentially expressed genes in PPMO 1083 treated SH-SY5Y cells, relative to the Gene Tool Control-treated SH-SY5Y cells, using the web-based application GOnet Enrichment Analysis (Ontology version 2019-07-01) [171]  $p \leq 0.05$ . Compound spring embedder layout is presented here. Colour intensity of the green node indicates enrichment value for the given node.

The GO network revealed cellular processes and pathways that are significantly enriched ( $p$  value  $< 0.05$ ) and included regulation of gene expression, mRNA processivity, RNA splicing, RNA metabolic process and nucleic acid metabolic process (**Figure 3.11**). Overall, these data suggest that there may be moderate effects on gene expression and RNA processivity in SH-SY5Y cells treated with PPMO 1083.

### 3.3.5 Assessment of the effect of SUPT4H1 Downregulation on Expanded Ataxin-3 Protein

As our intention is to develop SUPT4H1 downregulation as a therapeutic option for repeat expansion diseases, we examined the effect of PPMO 1083, the lead candidate, on fibroblasts derived from a patient diagnosed with SCA3. A SCA3 fibroblast cell line (GM6153) reported to carry a CAG expansion coding for 71Q repeats on the mutant allele and 23Q repeats on the non-pathogenic allele was obtained from the Coriell Cell Repository. The SCA3-derived fibroblasts were transfected with PPMO 1083 at a concentration of 5  $\mu$ M, and RNA and protein were isolated 6 days following transfection (n=3) to allow time for the knockdown of SUPT4H1 to have exert an effect on mutant ATXN3. In a the study conducted on a similar cell line (**Chapter 5**), ATXN3 protein was reduced 48 hours following transfection with PMOs that targeted exon carrying the repeat expansion[169].

Gel electrophoresis revealed that an average of 86% ( $\pm$  2.08%) of the *SUPT4H1* transcripts were missing exon 2 after transfection with PPMO 1083 (**Figure 3.12A**), and the protein was reduced by a significant 71% ( $\pm$  4.53%) relative to the GTC transfected sample (p value = 0.0014) (**Figure 3.12B**). This sustained exon 2 skipping and SUPT4H1 protein knockdown at six days is comparable to that seen after four days in SH-SY5Y treated cells (**Figure 3.7**). We also attempted to analyse ATXN3 protein expression to determine if SUPT4H1 knockdown has any effect on the mutant ATXN3, but unfortunately no changes were evident for either protein isoform (expanded and non-expanded). We believe that iPSC-derived neurons generated from SCA3 patients with confirmed expansions may be more suitable than dermal fibroblasts to conclude our study, as fibroblast do not show the hallmark pathogenic feature of nuclear aggregation. Furthermore, SCA3 pathogenesis by all accounts is localised to neuronal cells, thus differentiated patient-derived iPSCs would provide a more phenotypically relevant cell type.



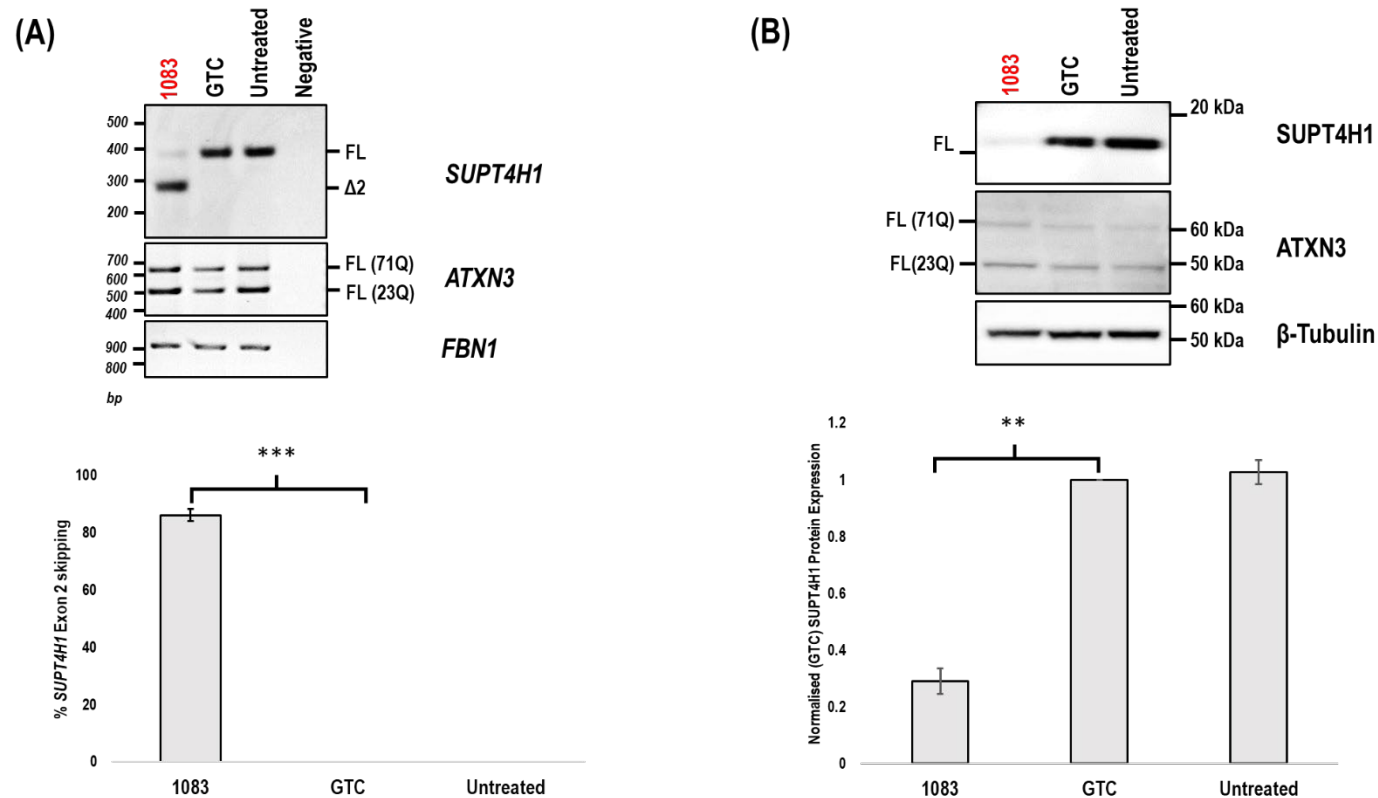


**Figure 3.12:** Evaluation of SUPT4H1 exon 2 skipping in SCA3 fibroblasts transfected with peptide conjugated-PMOs (PPMOs) at a concentration of 5  $\mu$ M. Cells were harvested 6 days following transfection for protein and RNA analysis. (A) Agarose gel fractionation of SUPT4H1 amplicons, following transfection, shows full-length (FL) and induced transcript products after skipping of exon 2 ( $\Delta$ 2). ATXN3 amplicons shows full-length (FL 71Q; FL 23Q). FBN1 amplicons was used to assess transcript quality (B) SUPT4H1 protein analysed by Western blotting following transfection shows full-length (FL) SUPT4H1 at approximately 14 kDa. ATXN3 disease-causing 71Q protein is approximately 60 kDa and the protein encoded by the healthy allele is approximately 48 kDa, Beta-Tubulin was used as a loading control. Densitometric analysis performed on the gel and Western blot are shown below the gel/blot. Sample values are normalised to those obtained after transfection with the GeneTools Control (GTC).

### 3.4 Discussion

The pathogenesis of repeat expansion diseases is generally, but not always attributed to the expanded repeat tract that typically confers a toxic gain of function to a given protein [7,8]. Directly targeting the cause of disease, the expanded repeat transcript/protein, may provide a logical therapeutic strategy to delay onset or reduce severity of expansion diseases. Recently, the transcript elongation factor SUPT4H1 has been found to be selectively required to transcribe through these large expansions, thus targeted knockdown of SUPT4H1, and to a lesser degree, its binding partner SUPT5H could present a logical therapeutic strategy.

With the increase in number of FDA approvals of AO therapeutics, AO-mediated pre-mRNA splice modulation to downregulate expression of a disease-causing toxic gain of function protein has therapeutic potential. Some expansion diseases may be amenable to direct exon skipping methodologies, whereby the expansion tract is found in a removable and dispensable exon. However, the majority are located in vital exons or introns and may not be amenable to exon skipping [9]. For example, the *Huntingtin (HTT)* expansion occurs within the coding sequence in exon 1, and is thus not amenable to exon skipping, since this would remove the start codon and completely compromise the transcript. A therapy that could be a “one-size-fits-all” for expansion diseases, especially those expansions that show dramatic anticipation and ‘explode’ to thousands of repeats (e.g. repeat expansions that cause myotonic dystrophy type 1, Friedrich’s ataxia, C9orf72 ALS) could eliminate the need for an individual approach to each specific disease and potentially render development of the therapeutic commercially viable.

The transcription elongation factors SUPT4H1 and SUPT5H form the DSIF complex and assist RNA polymerase II in transcription elongation [31,36,165]. We analysed knockdown of both transcripts and proteins, individually and together, and after more detailed evaluation, considered that SUPT5H may not be an appropriate target for suppression since this is a protein conserved through all domains of life

[32,36]. The RNA-seq data generated in this study supported the notion that exon skipping to knockdown *SUPT5H* will be detrimental due to pervasive and substantial changes in the transcriptome. The GO enrichment analysis after knockdown of *SUPT5H* expression showed disruption of numerous processes, including neuronal development and neurogenesis that in any situation could be expected to be extremely damaging in to the central nervous system [178]. Additionally, studies have shown that the yeast homolog Spt5 globally regulates transcription by RNA Pol II *in vivo* and controls the level and rate of RNA Pol II transcription elongation [32,179]. Analysis of SUPT5H binding to RNA Pol II reveals SUPT5H directly binds to RNA Pol II through its KOW domain located towards the middle of the protein, while SUPT4H1 has no direct interaction with RNA Pol II [180]. Instead, SUPT4H1 scaffolds onto SUPT5H and binds to its NGN domain located towards the N-terminus of the SUPT5H protein [31]. As SUPT4H1 does not directly interact with RNA Pol II, we believe SUPT4H1 to be a much more attractive target for AO-mediated downregulation to modulate repeat expansion expression.

Here, we describe significant and reproducible AO-mediated knockdown of SUPT4H1 *in vitro*, across two different cell lines. Several studies have reported that knockdown of SUPT4H1 (Spt4) has a positive effect on expanded protein aggregates and RNA foci *in vitro*, as well as causing *in vivo* rescue of the phenotype. Liu *et al.* (2012) were the first group to report altered repeat expansion expression from Spt4 knockdown in *S. cerevisiae* and *in vitro* cell cultures expressing expanded trinucleotide repeats [153]. They showed that while mutations in Spt4 lead to a decrease in expanded polyQ tracts (87Q – 111Q repeats), non-expanded polyQ (< 30Q repeats) stretches were not significantly reduced [153]. This data was replicated in various cell lines expressing either non-expanded (7Q repeats) or expanded polyQ repeats (111Q repeats). Taken together, the authors implied that SUPT4H1 may not be responsible for transcribing through non-expanded CAG repeats throughout genome but is functionally active when an expanded trinucleotide repeat is transcribed. This is attributed to the expanded CAG repeats forming an impediment that requires the presence of Spt4 for efficient transcription elongation [153]. The precise threshold of CAG repeat size that this hypothesis applies to is yet to be determined. Various studies by others all

report the potential therapeutic and phenotypic benefits of SUP4H1 knockdown both *in vitro* and *in vivo* [151,152,173]. All three subsequent studies report a selective requirement for SUPT4H1 for transcription of expanded repeats, while having a limited effect on the overall transcriptome. However, one recent study has provided opposing data to suggest that SUPT4H1 depletion leads to global RNA reduction *in vitro* [181], although this observation remains to be confirmed.

Although other reports suggest a selective requirement of SUPT4H1 to transcribe repeat-containing DNA, in 2019, Dowdle and colleagues demonstrated through siRNA mediated knockdown that SUPT4H1 is required for the homeostatic maintenance of total RNA levels in human cells [181]. To analyse reduction of RNA, the group included exogenous spike-in controls in the experimental design, stating that internal normalisation strategies may obscure RNA reduction [182]. Here, we used such internal normalisation strategies; however, we find these results consistent with other RNA-seq analyses that report DE genes and GO networks, and therefore are confident that RNA reduction is not obscured. In fact, SH-SY5Y cells transfected with our lead candidate PPMO 1083 showed most DE genes were upregulated and that normalisation of the RNA output showed a slight increase in RNA output as opposed to a decrease. With the 2019 study using siRNA, it is plausible that some of these results could be attributed to the common and known off-target effects elicited by siRNA, albeit the study control samples showed no statistical reduction in RNA output [137,183,184].

Short interfering RNAs are widely known for their numerous off-target effects [39-42], with the most striking being non-specific gene silencing [185]. Several studies have shown that mRNA transcripts that have less than 100% complementarity with a given siRNA may be targeted for gene silencing through the RNAi pathway [186-188]. These off-target effects were found to be concentration-dependent and can induce up to threefold suppression of dozens of non-targeted genes that are mediated by either the sense or antisense strand of the siRNA [184]. Moreover, a study conducted by Fedorov *et al.* (2006) demonstrated that siRNA off-target effects are sequence dependent, target independent and rely on the

siRNA's ability to enter the intact RNAi pathway [184]. This group showed that these off-target effects were substantial enough to induce quantifiable phenotypes *in vitro* and can be reduced with non-toxic chemical modifications. In light of these data, it is not impossible that siRNA suppression may lead to off-target effects that could appear to lower overall transcript output in studies examining siRNA-mediated knockdown. However, the exact extent of the relevance to the SUPT4H1 knockdown study requires further validation. Although certain AO chemistries are not without their toxicity and off-target effects, the PMO chemistry appears to have little to no off-target effects and has an excellent safety profile to date. The long term safety of PMOs is evident from clinical trials on boys and young men who have now been receiving *Eteplirsen* for close to a decade without any known off-target effects or serious drug-related adverse events [108,117,189]. The same cannot be said for outcomes of studies on the experimental DMD therapeutic 2'-Me PS AO, *Drisapersen* [190]. Participants who received *Drisapersen* in a series of clinical trials reported severe injection site reactions, thrombocytopenia, and apparent liver toxicity. The trials were discontinued in the presence of these unacceptable adverse effects and failure to meet primary and secondary endpoints [79,110]. In fact, all PS backbone AOs to date elicit some off-target effects associated with the backbone, while the same consequences do not result from treatment with PMO drugs [79,104,191,192]. Although the long-term safety of PPMOs has yet to be established, and several cell penetrating peptides studied to date show toxic effects, the RNA-seq data generated here suggests that the proprietary peptide does not induce *in vitro* toxicity in terms of gene expression profiling, as the GeneTools Control oligonucleotide transfected samples used as a transfection control show a statistically similar RNA-seq profile to that generated from the untreated samples. However, a few PPMO sequences reported here did induce high levels of cell death, attributed to the high G/C content of the sequences rather than the cell penetrating peptide.

The lead candidate PPMO 1083 demonstrated mild to moderate transcriptome changes in transfected SH-SY5Y cells, relative to the GeneTools Control transfected samples. The GO network of DE genes was closely related to gene expression, mRNA processivity and mRNA splicing, which is not surprising

based on the high degree of knockdown of SUPT4H1 [32,36]. Although the changes relate to gene expression processes, the DE genes were mainly below  $\log_2 2$  fold difference, suggesting the disruptions may not be extreme, but nevertheless warrant further investigation and validation *in vivo*.

Whilst *in vitro* data provides an underlying understanding of how a therapeutic compound may operate and be tolerated in a single cell-type system, these models are very limited and do not indicate or reflect the responses likely *in vivo* [137]. This will almost certainly be the case with regards to the SCA3 fibroblast experiment in this study. Although we observed an average of 70% SUPT4H1 protein knockdown in SCA3 fibroblasts transfected with the lead candidate PPMO, we did not observe a significant reduction in mutant ATXN3 protein levels. Our levels of knockdown of SUPT4H1 protein exceed the reported 50% knockdown suggested as necessary for therapeutic benefit [153]. All other studies demonstrate that if SUPT4H1 is knocked down, expansion protein/RNA is reduced, however none of these experiments followed ATXN3 levels in fibroblasts. Since mutant protein aggregation does not readily occur in fibroblasts [193], this cell type is unlikely to be an ideal *in vitro* model to assess potential therapeutic benefit.

The greatest limitation associated with this study is that the threshold repeat length at which SUPT4H1 is theorised to be activated remains unknown. Our SCA3 cell model has an expansion of 71Q repeats, considerably smaller than the 87Q or 111Q repeats used in the Liu *et al.* (2012) study. It may be that in order to confer therapeutic benefit a given threshold of repeated nucleotides has to be reached prior to recruitment of SUPT4H1. The other studies all implemented models of a larger, hexanucleotide expansion or a 111Q repeat length, suggesting that transcription intervention may be more applicable to much larger expansions [152,173]. Such expansions seen in *C9orf72*-related ALS or myotonic dystrophy type 1, where expansions can reach 1000s of repeats could potentially be better targets than some of the polyQ diseases caused by expanded repeat lengths as little as 27Q repeats (SCA6) [164,194,195].

Studies by others assessed aggregation clearance in models where an expanded repeat was expressed by a plasmid, providing a better platform to accurately assess aggregation reduction [151-153]. Besides exogenous protein expression, *in vivo* expansion models were used to determine the therapeutic benefit of SUPT4H1 knockdown and thus may be the focus of future studies. Although no mutant SCA3 knockdown was observed in *SUPT4H1* PPMO transfected patient fibroblasts the current study, there are several areas of future focus and refinement we believe may overcome the current limitations. The use of a disease-appropriate cell type carrying a larger expansion, such as the commercially available striatal neurons derived from a homozygous knock-in (111Q repeats) Huntington's disease mouse model [196,197] could be a more suitable model than dermal fibroblasts. In the light of the need to study larger expansions, *C9orf72* or myotonic dystrophy type 1 expansion neuronal lines, differentiated from patient derived iPSCs may provide clearer proof of concept, as opposed to targeting all repeat expansion diseases. Additionally, the use of an inducible fluorophore-tagged expanded repeat protein would provide a potential visual measurement of aggregation prone repeats, potentially providing data on how aggregated protein clearance could occur *in vivo* [153,198].

With several *in vitro* avenues to address as well as the obvious *in vivo* transgenic models, there are still exciting outlooks for PPMO mediated reduction of SUPT4H1 as a therapeutic for expansion diseases. This study shows proof of concept that our lead candidate PPMO is able to knockdown SUPT4H1, while inducing only moderate changes to the transcriptome, with no global disturbance in RNA levels. This provides optimism that SUPT4H1 protein knockdown may offer a suitable therapeutic strategy for diseases caused by large repeat expansions.

# Chapter 4 – Published

## Review Article

McIntosh, C. S., Aung-Htut, M. T., Fletcher, S., & Wilton, S. D. (2017). **Polyglutamine ataxias: From Clinical and Molecular Features to Current Therapeutic Strategies.** *J Genetic Syndromes Gene Therapies*, 8(319), 2.

### First Authored

**Author Contributions:** Conceptualisation, C.S.M.; Methodology, C.S.M.; Formal Analysis: C.S.M.; Investigation, C.S.M.; Writing, C.S.M., M.T.A-H., S.F. and S.D.W.; Supervision, M.T.A-H., S.F. and S.D.W.; Resources, S.F. and S.D.W.; Funding Acquisition, S.F. and S.D.W.



# Polyglutamine ataxias: From Clinical and Molecular Features to Current Therapeutic Strategies

Craig S McIntosh<sup>1,2</sup>, May Thandar Aung-Htut<sup>1,2</sup>, Sue Fletcher<sup>1,2</sup> and Steve D Wilton<sup>1,2\*</sup>

<sup>1</sup>Molecular Therapy Laboratory, Centre for Comparative Genomics, Murdoch University, Health Research Building, Discovery Way, Western Australia

<sup>2</sup>Perron Institute for Neurological and Translational Science, Sarich Neuroscience Institute, University of Western Australia, Verdun Street, Nedlands, Australia

## Abstract

Spinocerebellar ataxias are a large group of heterogeneous diseases that all involve selective neuronal degeneration and accompanied cerebellar ataxia. These diseases can be further broken down into discrete groups according to their underlying molecular genetic cause. The most common are the polyglutamine ataxias, of which there are six: Spinocerebellar ataxia type 1, 2, 3, 6, 7 and 17. These diseases are characterised by a pathological expanded cytosine–adenine–guanine (CAG) repeat sequence, in the protein coding region of a given gene. Common clinical features include lack of coordination and gait ataxia, speech and swallowing difficulties, as well as impaired hand and motor functions. The polyglutamine spinocerebellar ataxias are typically late onset diseases that are progressive in nature and often lead to premature death, for which there is currently no known cure or effective treatment strategy. Although caused by the same molecular mechanism, the causative gene and associated protein differ for each disease. The exact mechanism by which disease pathogenesis is caused remains elusive. However, the variable (CAG)<sub>n</sub> repeats are codons that may be translated to an expanded glutamine tract, leading to conformational changes in the protein, giving it a toxic gain of function. Several pathogenic pathways have been implicated in polyglutamine spinocerebellar ataxia diseases, such as the hallmark feature of neuronal nuclear inclusions, protein misfolding and aggregation, as well as transcriptional dysregulation. These pathways are attractive avenues for potential therapeutic interventions, as the potential to treat more than one disease exists. Research is ongoing, and several promising therapies are currently underway in an attempt to provide relief for this devastating class of diseases.

**Keywords:** Spinocerebellar ataxia; Triplet repeat expansion; Polyglutamine diseases; Genetic therapies

## Introduction

The spinocerebellar ataxias (SCAs) are a large group of typically late onset, progressive disorders characterised by neurodegeneration and other pathologically heterogeneous clinical features [1,2]. These diseases are often grouped into categories based on their causative mutation, of which there are three:

1. Non-coding repeat ataxias, where the repeat expansion is located outside the protein coding region for the gene of interest.
2. Ataxias where disease is caused by an 'orthodox' mutation, such as missense or splice site mutation.
3. Polyglutamine (polyQ) ataxias where the disease is characterized by an expanded cytosine–adenine–guanine (CAG) repeat located in the coding region of the respective gene [3].

As the triplet CAG encodes for the amino acid glutamine, this leads to an elongated glutamine tract in the translated protein resulting in conformational changes that are thought to cause several pathogenic mechanisms. Although the presence of an expansion does not necessarily correlate to phenotypic modifications, once a threshold for a specific gene is met, this tends to lead to disease and pathogenesis. Due to the nature of these mutations, the pathogenic severity and penetrance is typically determined by the size of the expansion, where there is a common trend: the larger the expansion, the more severe the pathogenesis and/or the earlier the onset [4]. These diseases tend to follow what is known as 'genetic anticipation', whereby the expansion size increases with each successive generation [5,6]. It should be noted that the genetic anticipation in most SCA diseases is typically more likely to be passed down from the paternal gene rather than the maternal. Rare cases have been reported where individuals possess two mutant alleles, leading to more severe symptoms than individuals with just one mutant allele.

However, mutations can arise *de novo*, through errors in DNA replication such that two genetically healthy parents can give rise to an affected child.

There are currently six characterised polyQ SCAs (1, 2, 3, 6, 7 and 17) (Table 1), and together with three other diseases, namely Huntington's disease, spinal and bulbar muscular atrophy and dentatorubropallidoluysian atrophy (DRPLA), form a larger category of polyQ diseases [7-10]. There is little relief for individuals suffering from polyQ SCA disorders, with symptomatic treatments the only available option. Long term pharmacological treatment, although admirable, tends to fall short in an effective management strategy, as unwanted complications and low drug efficacy still exist. In addition, none of these diseases have any treatments that slow the progression of the disease; leaving affected individuals with the daunting reality that time may be a severe limiting factor. Several experimental approaches are currently being assessed to overcome these difficulties. This review will focus on the clinical and molecular features of polyQ SCA diseases (which will be referred to as SCA diseases), as well as highlight several promising and emerging therapeutic strategies. We will begin by describing the molecular events leading to a CAG expansion, followed by the SCA diseases in general, before delving into greater depth of all six diseases. The review will then focus on potential therapeutic strategies that target common molecular and pathological features of these diseases.

**\*Corresponding author:** Steve D Wilton, Perron Institute for Neurological and Translational Science, Sarich Neuroscience Institute, Verdun Street, Nedlands WA 6009, Australia, Tel: 61 417 982 365; E-mail: [swilton@ccg.murdoch.edu.au](mailto:swilton@ccg.murdoch.edu.au)

Received July 25, 2017; Accepted August 04, 2017; Published August 11, 2017

**Citation:** McIntosh CS, Aung-Htut MT, Fletcher S, Wilton SD (2017) Polyglutamine ataxias: From Clinical and Molecular Features to Current Therapeutic Strategies. J Genet Syndr Gene Ther 8: 319. doi: [10.4172/2157-7412.1000319](https://doi.org/10.4172/2157-7412.1000319)

**Copyright:** © 2017 McIntosh CS, et al. This is an open-access article distributed under the terms of the Creative Commons Attribution License, which permits unrestricted use, distribution, and reproduction in any medium, provided the original author and source are credited.

Disease Name*	ADCA classification**	Age of onset	Age range (years)	Additional characteristic features, other than cerebellar ataxia
SCA1	Type I	3 <sup>rd</sup> -4 <sup>th</sup> decade	Childhood to 60+	Purkinje cell loss, faster progression of disease
SCA2	Type I	3 <sup>rd</sup> -4 <sup>th</sup> decade	Childhood to 60+	Slow saccadic ocular movements, peripheral neuropathy
SCA3	Type I	4 <sup>th</sup> decade	10 to 70+	Pyramidal and extra pyramidal signs, ocular movement abnormalities
SCA6	Type III	5 <sup>th</sup> -6 <sup>th</sup> decade	18 to 70+	Slower progression of the disease, ocular abnormalities
SCA7	Type II	3 <sup>rd</sup> -4 <sup>th</sup> decade	Infancy to 60	Visual loss with accompanying retinal pathology
SCA17	Type I	4 <sup>th</sup> decade	Infancy to 55	Psychiatric abnormalities, dementia, chorea

\*SCA: Spinocerebellar Ataxia

\*\*ADCA: Autosomal Dominant Cerebellar Ataxia

**Table 1:** Clinical and age related features of the six polyQ spinocerebellar ataxias.

## Molecular Genetics behind CAG Expansion

Microsatellites are commonly found repetitive arrangements of DNA, typically consisting of 1-6 nucleotide repeated sequences. These repetitive sequences along with short interspaced nuclear elements and long interspaced nuclear elements constitute approximately 30% of the 2.91 billion base-pair human genome [11,12]. Although the repeated sequence may vary in nucleotide length, trinucleotide repeats (TNRs) are the most common microsatellite found in coding regions [13]. Variations in the copy number of these TNRs will not affect the reading frame, but simply allow for variation in the translated protein. In most species, both plant and mammalian, the variation in these repeating sequences is what creates and drives evolutionary diversity between and in species subsets [14-16]. However, in some instances, these normal variations lead to disease through a larger than normal expansion of the copy number. All SCA diseases are caused by mutations from conception, whether it is from a pre-mutation or mutant parent allele or arises *de novo* from an error in gamete production. Additionally, somatic mosaicism has been reported for several SCA diseases, where several studies have found cases of considerable genetic homogeneity within regions of the brain [17,18]. SCA1 and SCA3 patients were found to have a varying pathogenic CAG length in all but 1 of the 20 regions of the brain examined [17]. Due to their repetitive nature, the CAG repeats are unstable and often prone to mutations that are typically attributed to either slip-strand mispairing during DNA replication and/or errors in mismatch repair [19-21]. These two processes are often thought to be inter-linked, with slip-strand mispairing occurring concurrently, where mismatch repair does not effectively correct the hairpin instability. SCA expansions are typically relatively small and less than 400 TNRs, while the expansion noted in myotonic dystrophy type 1 can be measured in the thousands [22].

### Slip-strand mispairing

TNR and other repetitive sequences are prone to the formation of DNA secondary structures. Slip-strand mispairing is an error that occurs when DNA is incorrectly replicated, in particular where the template strand and the synthesised strand become temporarily mis-aligned and result in the mispairing of the complementary pairs [23,24]. As the DNA polymerase  $\beta$  encounters the CAG repeating sequence (or any repeating sequencing for that matter), it momentarily pauses, however the helicase is left unaffected. In an attempt to avoid uncoupling of the helicase and polymerase, a misalignment is caused on the newly synthesised strand. During this separation, single strand loops of CAG repeats are created and the repetitive characteristics of the sequences allow the strands to displace (or slip) by a variable number of TNR (Figure 1) [25,26]. Insertions/expansion are caused when the loop is formed on the synthesised strand, also termed backward slippage, while deletions/concretion of the repeat sequence is caused when the loop forms on the template strand, also termed forward slippage.

In non-dividing cells such as spermatogonia, slip-strand mispairing is typically responsible for small expansions of a few TNRs that are often too small to fall within disease range. It is theoretically possible for numerous slippage events to occur, leading to a larger expansion. It is therefore more likely that large expansions are the result of repair dependant mechanisms in non-dividing cells, such that loop formation may arise during the base and/or nucleotide excision repair of single strand breaks [11].

### Mutagenic mismatch repair

DNA mismatch repair is a conserved system that recognises and repairs erroneous DNA replication such as insertions, deletions and the mis-incorporation of nucleotides (nt) [27]. Ironically this system is solely in place as an anti-mutagenic pathway; however, the mutagenic action of mismatch repair has been implicated in TNR expansions. Mismatch repair and error leading to mutagenesis is a complex mechanism involving several factors. As this mechanism is not the main focus of this review, we will only discuss a summarised version, since a current review describes the following paragraph in greater detail [28].

To be effective, the MMR system needs to not only identify the mismatch, but distinguish the difference between the newly synthesised and template strands. This process has been well studied and is highly conserved, even between prokaryotes and eukaryotes [29]. Studies in *Escherichia coli* discovered a gene, that when silenced lead to highly mutable strains, leading researchers to term the proteins encoded for by these genes 'Mut' proteins. In particular, three proteins are vital in directing and facilitating post-replicative MMR; MutS, MutL and MutH, all with eukaryotic homologs (MSHs) [30]. These proteins generate a single strand break that serves as a gateway for exonuclease and DNA helicase II activity that leads to degradation of the newly synthesised strand, until the mismatch is removed [28]. Error occurs through two proposed models; 1) the MutS $\beta$  (MSH2 and MSH3 complex) entrapment/hairpin escape model 2) the dysregulated strand directionality model. Both provide attractive arguments for a role of mismatch repair in TNR expansion, as both models propose impaired or dysregulated function of MutS, with the second also accounting for the MutL function [31-33]. Taken together, it can be seen why the presence of both slip-strand mispairing and mismatch repair creates a 'perfect genetic storm', where an error in transcription is introduced and the exact mechanism supposedly responsible for correcting the mutation unwittingly aids in its formation.

### Spinocerebellar Ataxia

Autosomal dominant cerebellar ataxias (ADCAs) account for 34 unique disease types [34]. Although not all the causative genes/proteins for this large category of diseases have been identified, all have been unequivocally localised to different subchromosomal loci. With the genes/proteins of the six SCAs being identified no less than 20 years

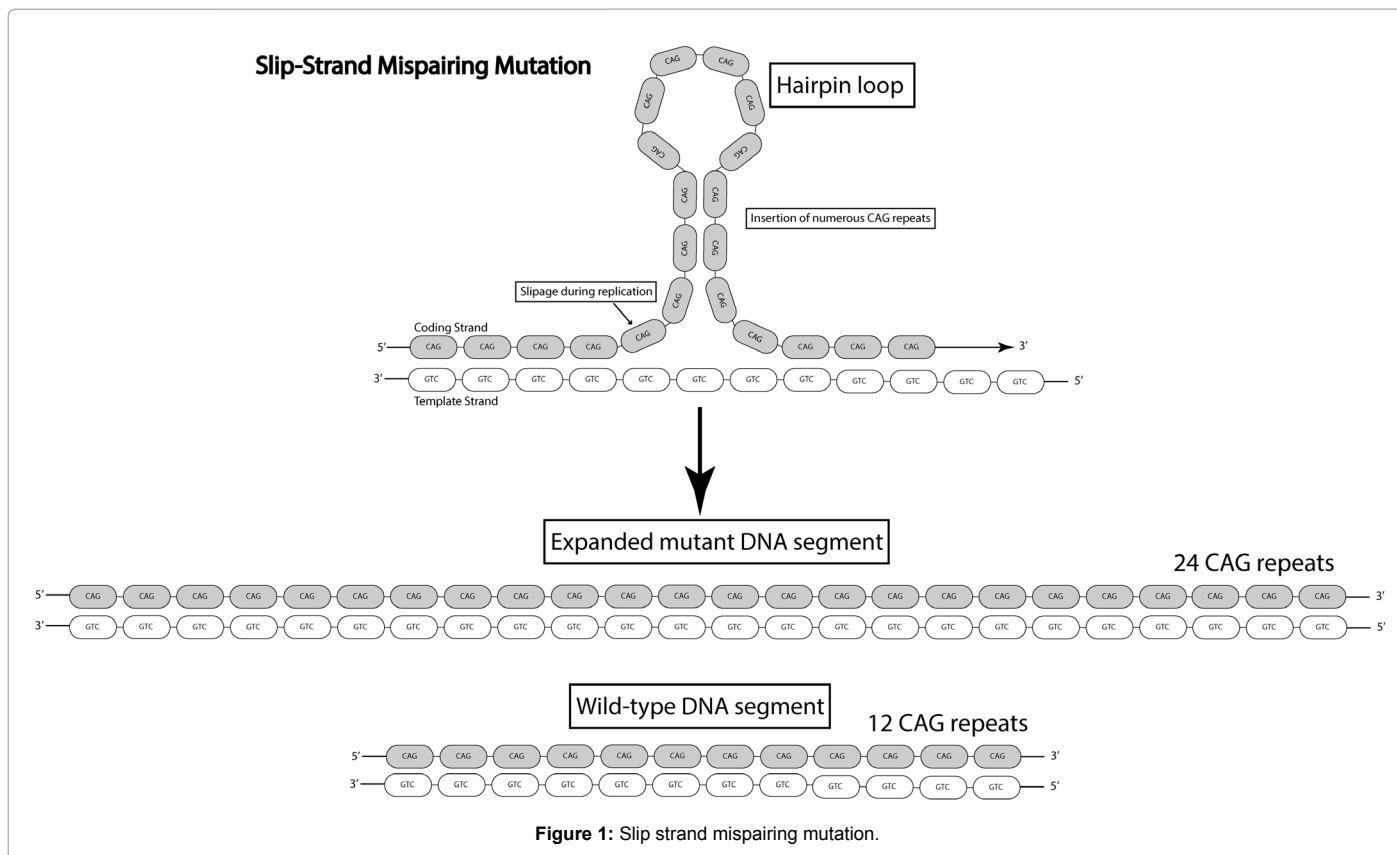


Figure 1: Slip strand mispairing mutation.

ago, with the exception of SCA17, characterised in 1999 (Table 1) [35-41]. Interestingly, the current numbering system of the various SCA diseases has been done in such a manner that follows the chronological order of gene locus discovery [34].

### Autosomal dominant cerebellar ataxia (ADCA) type classification

ADCA may refer to any type of spinocerebellar ataxia that is inherited in an autosomal dominant manner. This classification system was introduced by AE Harding in 1982 to account for the varying degree of heterogeneity between the dominantly inherited ataxias [42]. Although, the classification is somewhat out-dated due to the genetically classified SCA system used in the present day, it is of some benefit to mention, as the system broadly classifies all ADCA into three discrete categories [43,44]. These categories were created on the basis of separating dominant ataxias by their complex phenotypes of ataxic and non-ataxic clinical manifestations; termed ADCA type I, II and III (Table 1) [42,45].

**ADCA-I:** This subtype is the most common form of ADCA and manifests as typical cerebellar ataxia with the addition of extrapyramidal signs, dementia, ophthalmoplegia, optic atrophy and amyotrophy. This classification includes SCA 1, 2, 3 and 17.

**ADCA-II:** The most highly specific of the subtypes as it is classified as cerebellar ataxia with associated retinal degeneration. SCA7 is the only SCA disease to be classified into this type.

**ADCA-III:** The classification that is defined as “pure” cerebellar ataxia, with secondary pathology not as prominent in this classification. SCA6 is the only disease to fall into this category.

### Common clinical features

As previously stated, the six diseases are pathogenically heterogeneous; however, there are some features that are common to all types of SCA diseases. These diseases are typically late onset, with the mean age being in the third and fourth decade [46]. The age of onset may vary and is greatly, but not solely, dependent on the size of the expansion in the corresponding gene, with generally no significant difference in the age of onset between the sexes [47]. The average life span is approximately 10-20 years following diagnosis/symptomatic onset [48,49]. These diseases have selective neurodegeneration of areas such as the cerebellum, globus pallidus, pons and substantia nigra [2], along with progressive ataxia (incoordination and imbalance) leading to impairment of gait, speech and movement. In two thirds of SCA 1, 2, 3 and 6 cases, disorders of the individual’s gait are the first pathogenic symptoms. Typically, individuals will need walking assistance within the first decade of onset and not long after become wheelchair bound [50]. Other common features include dysarthria, oculomotor disturbances and tremors, leading to impaired motor function of the hand. In addition to the physical aspects, several psychological disorders have been reported, most commonly depression, irritability and impaired sleep [51,52].

### Protein aggregation: A hallmark feature

A hallmark molecular feature of SCA diseases, and all polyQ diseases for that matter, is the presence of protein aggregation and neuronal nuclear inclusions. An early example of this was reported by Paulson et al. [53] who provided patient-derived observations that mutant ataxin-3 results in significant nuclear inclusions in the neurons. These inclusions were mainly focused in the ventral pons of the brain,

however, these were also observed less frequently in the dorsal medulla, globus pallidus and the substantia nigra. The same group also showed that intracellular aggregates only occurred when ataxin-3 contained an expanded polyQ repeat, thus providing compelling evidence to the notion that mutant polyQ expansion directly leads to aggregation in the brain [53]. This research taken on its own does not provide definitive backing for the role of the polyQ tract in ataxin-3 aggregation, however, several subsequent studies both in animal and cell models have supported this concept over several different polyQ diseases [54-59]. Along with the presence of an expanded polyQ region, the length of the expansion itself is said to play a major role in aggregation. As studies have shown that the repeat length and the flanking sequences of most proteins implicated in polyQ diseases have an impact on severity of aggregation [60].

The ubiquitin-proteasome system and macroautophagy (autophagy) are two vital biological processes involving self-degradation of proteins and organelles [61]. These pathways are responsible for the clearance and degradation of misfolded and/or superfluous proteins. It stands to reason that these systems are somewhat compromised in SCA patients, and numerous studies have now shown that these systems do in fact exhibit impairment in SCA diseases [61-65]. The dysregulation is believed to play a role in protein aggregation, as the misfolded polyQ proteins are unable to be effectively degraded, which leads to an increased proportion of aggregates. These pathways are currently an obvious and attractive therapeutic avenue for SCA diseases [65,66].

### Genetic testing

Each SCA disease has its own defined healthy and disease size ranges (Table 2). The healthy range represents a CAG repeat variation where anticipation and potential transmission does not occur unless a *de novo* mutation arises during embryonic development [67]. Several of the SCAs have a well-documented pre-mutation range, known as incomplete penetrance. These individuals are typically asymptomatic, however due to their dynamic nature, the expansions have the ability to pass on the disease or pass on an increased CAG repeat range [68,69]. Paternally transmitted alleles are typically more unstable and prone to expansion than a maternal allele, so that diseased individuals are those who have met the pathogenic threshold for the given gene, are symptomatic and are likely to pass on a larger expansion [69,70].

The advancement in genetic technology and testing has given rise to readily available commercial tests for all six SCA diseases [1,71,72]. Genetic testing may be conducted for five distinct clinical reasons: predictive testing, diagnostic testing, carrier testing, parental testing and risk factor assessment [67]. Thus, the primary benefit of genetic testing is to provide an accurate and specific diagnosis. These tests are often better done as early as possible, as this gives families precious time to come to terms with the potential disease, while giving affected individuals insight and the ability to make fundamental and necessary lifestyle changes and reproductive decisions. For those individuals where a *de novo* mutation has occurred, genetic testing would most

likely provide relief and a psychological benefit in identifying a previously unknown disease and an end to the diagnostic saga.

### Prevalence and incidence

Current data shows that SCA3 is the most common of the diseases [46,73-75], with an overall SCA prevalence of approximately 1-2 per 100 000. The epidemiological data available about the prevalence of SCA diseases is limited, and most likely does not represent an accurate occurrence, due to the high degree of variation between different populations and ethnic backgrounds. Founder effects are seen in Cuba (particularly those of Spanish descent), Portugal and South Africa in SCA2, SCA3 and SCA7, respectively [47,76-78]. Several geographically localised studies have been conducted on the prevalence of ADCAs, with the focus on the six SCA diseases. With regards to SCA3, the prevalence is at its highest in Brazil (69% of SCA cases), Portugal (58%) and China (49%) and relatively low in USA (21%), India (3%) and Italy (1%) [77,79-83]. An interesting case is the founder effect of SCA7 in South Africa, where this disease represents 26.6% of SCA diseases [84], a figure that is significantly higher than the 2% occurrence worldwide [78]. This figure increases again when considering the native African population, in whom SCA7 represents 59% of all SCA diseases, while SCA3 only represents 1% [84]. In fact, distribution of SCAs in South Africa as a whole, drastically differs from that elsewhere [78,84].

### SCA1

#### Clinical features

SCA1 is classified by a “cerebellar plus” syndrome with varying degrees of the commonly described SCA clinical characteristics [34,85]. Disease onset is usually in the third decade and progresses at a faster rate than seen in SCAs 2, 3, 6 and 17. SCA1 is known to have a main pathogenic feature of loss and atrophy of the cerebellar Purkinje cells, the major integrative neuron of the region [86] (Table 1). These cells are some of the largest cells in the brain and are responsible for the output of all motor coordination in the cerebellar cortex [87]. Death of these cells and cerebellar atrophy has a devastating effect on coordination and motor skills, contributing to the rapid decline and increased progression of ataxia [86,88].

#### Molecular genetics

SCA1 is caused by a CAG expansion in *ATXN1* that is localised to 6p22.3. *ATXN1* was first cloned by Zoghbi and colleagues in 1993, and then identified in 1994 by the same group [36,37]. The gene contains 9 exons with the potentially mutagenic CAG repeat region in exon 8. Although this gene contains 9 exons, only the last two (exons 8 and 9) are protein-coding, with exon 8 containing most of the coding sequence (1,950 nt). Healthy individuals are found to contain 6-39 CAG repeats, while the pathogenic range is from 40-82 [9,37]. Interestingly, repeats greater than 21 may be interrupted by 1-3 repeats of a CAT trinucleotide, which effectively rescues some individuals from disease [37] (Table 2).

Disease Name	Gene	Encoded protein	Locus	Exons in gene	PolyQ location	Healthy repeat range	Pathogenic repeat range
SCA1	<i>ATXN1</i>	Ataxin-1	6p22.3	9	Exon 8	6-39	40-82
SCA2	<i>ATXN2</i>	Ataxin-2	12q24.1	25	Exon 1	17-29	37+
SCA3	<i>ATXN3</i>	Ataxin-3	14q24.3	11	Exon 10	7-44	55-86
SCA6	<i>CACNA1</i>	$\alpha$ 1A subunit of the P/Q calcium-dependent voltage channel	19p13	47	Exon 47	4-18	21-30
SCA7	<i>AXTN7</i>	Ataxin-7	3p14.1	13	Exon 3	7-19	36 to >400
SCA17	<i>TBP</i>	TATA box binding protein	6q27	8	Exon 3	25-42	47-66

**Table 2:** Molecular genetics of the six polyQ spinocerebellar ataxias.

### Wild-type and mutant protein

*ATXN1* is expressed as the ~90 kDa, ataxin-1 protein, although it should be noted that this is an approximation, as the protein length will vary depending on the size of the expansion, a feature holding true across all variable repeat-containing genes and proteins further described. This review will discuss the 815 amino acid (aa) protein with a healthy polyQ region of 29 repeats (ENST00000244769.8). Normal ataxin-1 has the polyglutamine tract located towards the N-terminus, with three known functional regions; a conserved AXH domain, a nuclear localisation signal (NLS) and a Ser<sup>775</sup> located at the C-terminus of the NLS (Figure 2). The protein is ubiquitously expressed, rather than being localised to the brain [89].

The evolutionary conserved 120 aa AXH domain that spans exon 8 and 9 is highly homologous to the large region of the high mobility group box transcription factor-binding protein 1 (HBP1) [90,91]. The AXH domain is known as a dimerization domain and is the only globular dimer forming region identified in the protein [92]. Additionally, the AXH folds independently into an oligonucleotide-binding fold, able to recognise RNA with a similar nucleotide preference, to that of full length ataxin-1 [91,93]. Second to RNA binding, the AXH domain contains a cluster of charged surface residues that allows for another secondary binding surface. This leads to the several protein-protein interactions through the ataxin-1 AXH domain, namely a paralog of ataxin-1, brother of ataxin-1 (BOAT), which also contains a AXH domain, the SMRT/SMRTER and Capicua proteins [94]. These interactions, along with interactions between several transcriptional factors, give ataxin-1 its transcriptional repression activity [90,91,93].

In terms of mutant ataxin-1, as with all SCA diseases, the addition of glutamines outside the healthy range leads to conformational changes in the affected protein, conferring a toxic gain of function [75,89,95-97]. The increased polyQ stretch not only increases the tendency to aggregate, but also leads to conformational changes of other regions and domains of the SCA proteins. In the case of SCA1, conformational changes to the AXH domain, along with its ability to fold leads to the potential contribution of misfolded protein aggregation [92,98,99].







his was shown by de Chiara et al. [100], where ataxin-1 aggregations were significantly mitigated by the removal of the AXH domain or by replacement of the HBP1 sequence, which is not known to aggregate [100]. Additionally, the self-association of ataxin-1 through its AXH domain leads to multimerisations that have the ability to aggregate polyQ stretches [98,101]. In conclusion, the AXH domain is crucial for both normal and aberrant functions of ataxin-1. Its ability to independently fold and in the presence of an elongated polyQ stretch, allow for rapid aggregation, may be a factor in the increased rate of progression when compared to other SCA diseases.

### SCA 2

SCA2 is thought to be among the most prevalent of the SCAs, and demonstrates a founder effect in Cuba, in particular the north-eastern province of Holguin [50]. This region has a 40% prevalence rate of SCA2, well above the national average of approximately 6% [47]. The age of onset can range from as young as 3 years to age 80, with the typical mean age of onset in the third decade [47] (Table 1).

### Clinical features

SCA2 demonstrates an atrophy pattern that resembles sporadic multi-system-atrophy, including some associated clinical features. These include early and marked saccadic slowing, initial hyperreflexia that is followed by hyporeflexia, Parkinson rigidity and myoclonus or fasciculation like movements [102,103]. With the slowing of saccadic jumps for horizontal gaze being the noticeable oculomotor abnormality (Table 1) [104-106]. This is attributed to the early, and sometimes rapid degeneration of the pontine brainstem. A study by Velazquez-Perez *et al.* (2004) was conducted to assess the effect on expansion size and maximal saccade velocity of 82 SCA2 patients and 80 healthy controls. It was found that 60-degree maximal saccade velocity was influenced by polyQ size rather than disease duration, suggesting that the saccade velocity of SCA2 patients is sensitive and specific to polyQ length, more so than disease stage or duration [107]. The same group conducted a follow up study in 2016 and found that patients with larger expansions deteriorated at a faster rate when compared to

Protein	Protein Size (amino acids)	Implicated Protein Functions
Ataxin-1 (SCA1)	815 aa 	transcriptional repression, RNA metabolism
Ataxin-2 (SCA2)	1313 aa 	transcriptional regulation, RNA metabolism, cytoskeletal reorganisation, calcium homeostasis
Ataxin-3 (SCA3)	361 aa 	de-ubiquitination, proteasomal protein degradation, regulation of misfolded proteins
CACNA1* (SCA6)	2506 aa 	pore formation, neurotransmitter release from presynaptic terminals, gives rise to P/Q type calcium currents
Ataxin-7 (SCA7)	892 aa 	transcriptional regulation, mediates interaction of STAGA complex with the CRX, retinal functions
TATA box binding protein (SCA17)	339 aa 	general transcription factor, initiation of transcription through TFIID binding to TATA box, interacts with all three RNA polymerases

\* α1A subunit of the P/Q calcium-dependent voltage channel

Figure 2: Protein mutation.

those with smaller expansions. It was concluded that rate of decline in maximal saccade velocity is directly influenced by expansion size, thus providing clinicians with a sensitive biomarker and a potential measure of therapeutic success during clinical trials [108].

Other associated secondary characteristics such as insomnia (20% of cases) and sexual dysfunction (10%) are not uncommon for SCA2 patients [109]. Interestingly, individuals with relatively large expansions (>200) are reported to have retinitis pigmentosa/macular degeneration and myoclonus-epilepsy, which are two features commonly found in SCA7 and DRPLA, respectively [110,111]. As with SCA1, the early and significant loss of Purkinje cells is seen in this disease, with analysis indicating that the cerebellar flocculus is also affected to varying degrees [86,112].

### Molecular genetics

The causative gene of SCA2 is *ATXN2* that was first localised to 12q24.1 in 1993 by Gispert et al. [113]. It was not until 1996 when three groups independently identified the CAG repeat expansion in *ATXN2* [40,114,115]. *ATXN2* encompasses approximately 130 kb of genomic DNA and consists of 25 exons, with the triplet repeat region located in the first exon (Table 2). The CAG repeat region in healthy individuals was found to have 1-3 interruptions of interspaced CAAs, the most common being two CAA interruptions, with a structure (CAG)<sub>8</sub> CAA (CAG)<sub>4</sub> CAA (CAG)<sub>8</sub> [40,115]. Healthy individuals have 17-29 repeats, while those individuals with incomplete penetrance (pre-mutation) have between 30-36 repeats. Severe pathogenesis is seen in individuals who have an uninterrupted CAG repeating range of 37 and above [40,114,115]. Interestingly, a moderate expansion size has also been implicated in another common motor neuron disease, amyotrophic lateral sclerosis (ALS) [116].

### Wild-type and mutant protein

*ATXN2* encodes for a highly basic protein (1,313 aa) with a molecular weight of approximately 140 kDa and in this specific isoform of ataxin-2, 23 glutamines are at the polyQ domain (ENST00000377617.7) (Figure 2). Ataxin-2, is the largest of the 'ataxin proteins' and the second largest protein after the CACA1A protein of the SCAs. The polyQ repeat region is located at the N-terminus of the protein. There are four other known functional domains in ataxin-2; two globular domains, spanning exons 2-7 named the Like Sm domain (Lsm; aa 255-346) and the Lsm associated domain (LsmAD; aa 354-476); towards to the C-terminus there is a PAM2 motif, aa 909-926, encoded by exon 16 that facilitates the association of polyA-binding protein (PABP); lastly the C-terminus contains a A2D region, that associates with Mp1 [117,118]. Ataxin-2 is ubiquitously expressed in adult tissues, with common, highly expressed regions such as the brain, gut, liver, heart muscle thyroid and lung. The most prominent expression of the protein is in the brain, with its major localisation being in Purkinje cells [119].

Normal ataxin-2 has been shown to be involved in numerous cellular processes, including transcriptional regulation, RNA metabolism, cytoskeletal reorganisation and calcium homeostasis [120-123]. Ataxin-2 is considered a cytoplasmic protein that is localised at the rough endoplasmic reticulum (rER) [124]. The globular domains (Lsm and LsmAD) are two regions that are highly conserved in proteins thought to be involved the process of RNA metabolism, such as splicing and modification [125,126]. The Lastres-Becker et al. study, found that when starved, mouse and human ataxin-2, was able to modulate translational control at the pre-initiation complex via PI3K/mTOR pathways [125]. This study highlights another possible major function

of ataxin-2, its ability to regulate some metabolic activity with a study in *C. elegans* showing that down regulation of the ataxin-2 homolog leads to fat storage and an increase in growth. However, even when a dietary intervention was implemented, the *C. elegans* phenotype was unable to be reverted [127]. Several studies in the past several years have implicated ataxin-2 in body weight regulation and fat distribution, with a recent review Carmo-Silva et al. [123] describing the processes in greater detail [127-129].

Interestingly, neuronal nuclear inclusions are not as prominent in SCA2 patients when compared to other SCAs [130,131]. However, Purkinje cell death and selective neuronal degeneration is still apparent [130,131]. The conformational changes in ataxin-2, can be seen in the changes to the Lsm, LsmAD and PAM2 domains. A 2016 study used I-TASSER for 3D structure for protein structure prediction, and found several changes when the pathogenic polyQ repeat number was assessed. These changes are thought to contribute to the pathogenesis of SCA2 [132].

### SCA3

SCA3/ Machado-Joseph disease was first described in 1972, in Portuguese immigrants living in Massachusetts, who were known to be decedents of William Machado [133]. SCA3 is the most common of the SCA disorders, and is at its highest prevalence in the Azores Islands, Portugal (~1:3472) [134]. SCA3 is widely known to be the most common of the SCA diseases, however, this does fluctuate between populations [67,69,80,84,85,135].

### Clinical features

SCA3 typically onsets in the fourth decade and the average life span after onset is 10 years, with a range of 1-20 years. Along with the common clinical characteristics, SCA3 is often distinguished by the evident pyramidal and extrapyramidal signs [136]. The selective neuronal loss seen in SCA3 is found in the cerebellar dentate neurons, basal ganglia and brainstem [9,34,137]. SCA3 is also known for its higher frequency of lid retraction and infrequent blinking, commonly known as "staring eyes" (Table 1) [67]. The degree of peripheral involvement in pathogenesis is the greatest variable feature of SCA3, some patients have minor disease features, while others develop marked distal amyotrophic characteristics with sensory disturbances and areflexia [67].

### Molecular genetics

SCA3 is caused by an expanded tract of CAG repeats in the coding region of the penultimate exon (exon 10) of the *ATXN3* gene (14q32.1), encoding the ataxin-3 protein [35,75]. The *ATXN3* gene, spanning a genomic region of approximately 48 kb (ENST00000558190.5) consists of 11 exons, with the start codon in exon 1 and the CAG repeat sequence located at the 5' end of exon 10 (Table 2) [138]. Healthy individuals have up to 44 CAG repeats, whereas affected individuals possess 55-86 repeats, and the intermediate range of 45-54 repeats is generally associated with incomplete penetrance [75]. However, there is much conjecture as to exactly number of repeats that may be associated with disease, since as few as 51 repeats have been reported to be pathogenic in some cases.

### Wild-type and mutant protein

To date, 56 splice variants of *ATXN3* have been identified in blood, and 20 of these have the potential to be translated into a functional ataxin-3 protein [139]. Ataxin-3 has a molecular weight of approximately

42kDa and is 361aa in length with 8 glutamines [53] (Figure 2). Ataxin-3 is believed to have several roles within the cell, acting as an isopeptidase and is also thought to be involved in de-ubiquitination, proteasomal protein degradation, the chaperone system and regulation of misfolded proteins [98]. Although there are several isoforms of the Ataxin-3 protein, this review will refer to the isoform most commonly expressed in brain tissue, a 361aa protein with 8 glutamines at the polyQ region [75]. Located at the N-terminal of ataxin-3 is a Josephin domain, containing the amino acids (cysteine 14 (C) histidine 119 (H) and asparagine 134 (N)) that are crucial for the isopeptidase activity and two nuclear export signals (NES). The C-terminal contains three ubiquitin interacting motifs, a nuclear localisation signal and the polyQ tract [140-142].

Ataxin-3 is not only found in all cells, but is also dispersed throughout the cell. The protein has the ability to translocate from the cytoplasm to the nucleus and vice versa [143,144]. Todi et al. [145] conducted an *in vitro* study, where they catalytically inactivated ataxin-3 by a mutation to the active site cytosine at position 14 (C14A) and found that enzymatically active ataxin-3 preferentially localises to the nucleus, compared to the inactive form [145]. Additionally, the inactive form was degraded at a slower rate by the proteasome, an event found to be independent of ubiquitination. These two findings suggest that the catalytic activity of ataxin-3 regulates a number of its cellular properties and may in turn play a role in the disease pathogenesis of SCA3 [145]. Other studies suggest that there are several regions and factors that affect the localisation of ataxin-3, most of which are believed to be due to the NLS and NES [117,146].

The Josephine domain along with the three ubiquitin interacting motifs can either save proteins from degradation or stimulate the catalytic deubiquitination of proteins, thus resulting in protein degradation and clearance [140,147]. Poly-ubiquitin chains of four units or more are known to be recognised by ataxin-3 and the ubiquitin interacting motifs mediate selective binding to these ubiquitin chains and therefore restrict the types of chains that are cleaved [148]. Ataxin-3 is also implicated in the regulation of misfolded endoplasmic reticulum protein degradation as it binds to the valosin-containing protein (VCP/p97) involved in ER-associated degradation [149,150].

Two important impaired functions of mutant ataxin-3 have been recognised, impaired protein degradation and transcriptional deregulation [65,151]. As ataxin-3 is thought to play a role in transcriptional regulation due to its interaction with transcriptional regulators, deregulation of this process is thought to be a factor when considering SCA3 pathogenesis. Due to the sequestration of ataxin-3 and other factors into nuclear aggregates, a secondary effect of transcriptional deregulation is thought to occur [152,153]. Additionally, Evert et al. showed that mutant ataxin-3 had impaired transcriptional repression through its ability to inhibit histone acetylase activity [154].

Interestingly, ataxin-3 has been found to bind more efficiently to VCP/p97 compared to normal ataxin-3, but by mechanisms unknown, and it interferes with protein degradation and misfolded protein clearance [155]. Although the exact mechanism by which interference occurs is poorly understood, several theories have been proposed. One such theory postulates that due to the increased binding affinity of mutant ataxin-3, it is unable to release itself after the misfolded proteins are extracted from the endoplasmic reticulum, thus affecting the subsequent round of protein extraction and degradation [156].

It has previously been unclear whether the protein aggregates observed in patients with SCA3 are full-length protein, shorter

cleaved fragments or a combination of the two. However, more recently it appears that fragmented mutant ataxin-3 initially forms the intracellular aggregates and then acts a seed or a catalyst for recruitment of the full-length protein [53,157]. A study showed that L-glutamine-induced excitation of neurons lead to  $Ca^{2+}$  dependent proteolysis of ataxin-3, creating SDS-insoluble aggregates [57]: suggesting that initial microaggregates catalyse and precede large inclusion bodies that ultimately lead to neural death and rapid disease progression. It was also found that aggregation of the ataxin-3 fragments was calpain dependent and that the phenotypic changes could be abolished by calpain inhibition. The same study also showed that aggregation was neuron specific, which is in keeping with disease pathogenesis as aggregation is almost always observed in neural tissue of SCA3 patients.

Another line of thinking is that although mutant ataxin-3 is able to undergo ubiquitination at similar rates to wild type ataxin-3, mutant ataxin-3 was found to exist longer in the cell compared to wild type ataxin-3, thus facilitating aggregation through the lower rate of protein degradation [158]. There is ever growing evidence that both the truncated and full-length proteins are implicated in the aggregation of ataxin-3 in neurons. It is clear that neural aggregation of ataxin-3 directly leads to disease pathogenesis, however, the exact mechanism by which this is caused remains elusive.

## SCA6

### Clinical features

Unlike other SCA diseases, SCA6 typically presents as a milder form of disease, and is associated with “pure” cerebellar ataxia. However, ocular-movement abnormalities are often reported, with nystagmus being the most common form [112]. The disease onset tends to be later when compared to other SCA diseases (fifth or sixth decade) and is often less aggressive with average life duration being >25 years (Table 1) [136]. A comprehensive study on the frequency of nonataxic symptoms was conducted in 2008 by Klockgether and colleagues who found that SCA6 had a lower frequency in all but one (rigidity) of the 16 nonataxic symptoms when compared to SCA1, 2 and 3. These features included a number of very common symptoms such as; brainstem oculomotor signs, hyperreflexia, extensor planter and muscular atrophy [159]. It was also found that disease severity is largely age-dependent rather than linked to expansion size. This is not surprising due to the relatively small expansion size range.

### Molecular genetics

SCA6 is one of only two SCA diseases to be caused by expansion in a protein other than an ataxin, the other being SCA17. The CAG expansion is seen in the  $\alpha_1A$  voltage-dependant calcium channel gene (*CACNA1*), localised to 19p13 [39]. The expansion in *CACNA1* is located in the last exon of the gene (exon 47) and is relatively small compared to those in other SCA diseases, with a healthy range of 4-18 repeats and a disease range of 21-30 repeats, with most cases being reported as 22-23 repeats (Table 2) [159,160].

Interestingly, several dominant mutations in *CACNA1* are associated with three different, independent diseases; SCA6, episodic ataxia type 2 and familial hemiplegic migraine-1. Although these mutations arise in the same gene, the disease phenotypes are highly variable, with episodic ataxia type 2 being the most common form of episodic ataxia that typically presents during childhood or early adolescence. Familial hemiplegic migraine-1 is a debilitating variant of migraines, accompanied by aura that is characterised by severe attacks of motor deficits [161]. Traditionally, SCA6 is the only disease

to be associated with the polyQ expansion, as episodic ataxia type 2 is associated with a loss of function mutation, while familial hemiplegic migraine-1 is a gain of function mutation. However, familial studies in recent times have suggested that SCA6 phenotypes may also arise from missense mutations rather than expansion of the CAG repeating unit (more detail on these mutations can be found [162,163]).

### Wild-type and mutant protein

*CACNA1A* encodes for the  $\alpha 1A$  subunit of the P/Q calcium-dependent voltage channel ( $Ca_v2.1$ ). With the P/Q denoting the cell types in which the currents were initially isolated; P refers to Purkinje cells, while Q refers to granule cells in the cerebellum [164]. Unlike the ataxin proteins, *Cav2.1* is brain specific, with no expression found in the heart, liver or muscle.  $Ca_v2.1$  is the largest (by a significant manner) of the SCA proteins and its main isoform, of which there are seven, is a 2506 aa, 275 kDa protein with a polyQ region of 13 repeats (ENST00000360228.10) (Figure 2).  $Ca_v2.1$  is a subunit responsible for pore-formation and plays a crucial role in neurotransmitter release from presynaptic terminals, and to a lesser extent, intrinsic firing patterns in Purkinje cells [164].

SCA6 has attracted attention due to its apparent 'deviation' from other SCA diseases. The expansions in the other five diseases are between 35-300 repeats, whereas SCA6 is typically 22 [165]. The apparent mechanism of toxic gain of function might not be as applicable to SCA6 as it is to the other SCAs. The belief is that the polyQ expansion in SCA6 somehow affects the normal wild-type function of the protein, altering functions of the P/Q channel, leading to Purkinje cell degeneration. However, this view is contentious and conflicting reports are presented, with conflicting reports on the alterations of the P/Q calcium-dependent voltage channel properties as a direct result of the expanded polyQ region [165-167]. Most recently, a 2015 study on SCA6 knock-in mice was conducted [165] and showed that polyQ length does not directly affect function of the  $Ca_v2.1$ , as mice with varying CAG lengths (84Q; 30Q and 14Q) had similar changes in current density [165]. This study concluded that like other polyQ diseases, SCA6 is most likely the result of toxic gain of function. These conflicting reports highlight the complexity of SCA diseases and present prime examples of why additional research is required to identify the exact pathogenic mechanisms behind these diseases.

## SCA7

### Clinical features

SCA7 is almost always distinguished from other SCA disease by virtue of severe cone-rod dystrophy retinal degeneration, and is sometimes referred to as olivopontocerebellar atrophy III [168]. SCA7 is typically the only SCA where affected individuals go completely blind (Table 1) [111]. SCA7 retinal pathology initially affects the cones, with progression to the rod photoreceptors, although cones are found to be more severely affected [78]. The initial sign of retinal degeneration is dyschromatopia in the blue-yellow axis [169]. Due to the large range of expansions in SCA7, infantile onset has devastatingly widespread pathogenesis that extends outside the typical CNS pathology. Magnetic resonance imaging of SCA7 patients show that the cerebellum and the pons are the most affected regions of the brain, however other regions of SCA brains are also effected [170]. SCA7 patients may also present with an increased amount of pontine atrophy when compared to other SCA patients. Hernandez-Castillo et al. conducted a study using 24 confirmed SCA7 patients and assessed the effect of selective degradation and its relationship to ataxic symptoms. It was found that

ataxic severity was associated with a decrease in grey matter volume of distinct regions of the cerebellum, as well as degeneration of specific cortical areas [171].

Disease onset is typically in the third or fourth decade, however, SCA7 may present as early as the first year, the earliest onset of all SCA diseases [136]. Interestingly, in early onset patients, visual impairment can be apparent up to almost a decade before ataxic symptoms [73]. Conversely, late onset patients can experience ataxic symptoms decades before first visual pathology is observed [73].

### Molecular genetics

The causative gene for SCA7, *ATXN7* was mapped to 3p14.1 and first cloned in 1997 [38]. The gene has 13 exons with the polyQ repeat region in exon 3, the first coding exon of the gene. The healthy repeat range in SCA7 is 7-19, with an incomplete penetrance of 19-35, while a wide disease range of 36 to >400 repeats has been reported (Table 2) [172]. Although all SCA diseases have a tendency for genetic anticipation, *ATXN7* is particularly known to be highly unstable, resulting in extreme anticipation and expansion during paternal transmission [38]. Expansions as large as 60 or more are associated with infantile SCA7 and disease progression is rapid and premature death is almost a certainty [173]. Such is the nature of the disease that pathogenesis may be apparent well before the first year of life in extreme cases [136,174].

### Wild-type and mutant protein

*ATXN7* encodes for ataxin-7, a ubiquitously expressed protein thought to be involved in transcriptional regulation and ...other secondary functions. Ataxin-7 is an 892 aa, 98 kDa protein that has a polyQ repeat region of 10 (ENST00000295900.10) (Figure 2). The N-terminus of ataxin-7 contains the polyQ region, while nearer to the middle, a Block I domain is located with a zinc binding domain and a NLS located toward the C-terminus [175], with the nuclear localisation of ataxin-7 being vital for its transcriptional function. Preferential nuclear localisation occurs in many regions of the brain, such as the cerebellum, pons and inferior olive [176]. Along with these areas of the brain, nuclear localisation is also preferentially seen in the photoreceptor cell nuclei of the retina [177]. This is not surprising, considering the visual pathology seen in SCA7 that may be due to the increased presence of ataxin-7 in the retina. Ataxin-7 is also highly homologous to Sgf73, a protein found in yeast that acts as a subunit of the SAGA complex, which has its own mammalian homologs, namely SPT3/TAF9/GCN5 acetyl-transferase complex (STAGA) [178,179]. Ataxin-7 is thought to play an integral role in the interaction between the STAGA complex and rod-cone homeobox (CRX) [180]. The nuclear localisation of ataxin-7 has been long viewed as vital to its primary physiological function. However, a 2011 study by Okazawa and colleagues provided a novel role for cytoplasmic ataxin-7. The group found that cytosolic ataxin-7 associates with microtubules, and the expression of ataxin-7 aids in the stabilisation of microtubules against nocodazole treatment. This was further supported by the observation of increased microtubule degradation when ataxin-7 was knocked-down. These findings implicate ataxin-7 in the stabilisation of the cytoskeletal network, providing a novel function for cytosolic ataxin-7 [181].

As the role of ataxin-7 is well established in transcriptional regulation, as well as several biological functions in the retina, it stands to reason that mutant ataxin-7 may impair these functions. La Spada et al. found that an expanded polyQ region in ataxin-7 severely impaired its wild-type function and antagonised CRX function that lead to cone-rod dystrophy in mice [176]. This finding is of interest as typically,



polyQ diseases are attributed to toxic gain of function, while this study seems to suggest that one of the main pathogenesis may be due to loss of normal function. However, ataxin-7 is still thought to undergo protein misfolding and proteolytic cleavage that leads to selective retinal and neuronal toxicity as well as the hallmark neuronal nuclear inclusions.

A 2013 study conducted by Strom and colleagues revealed a novel pathogenic mechanism of ataxin-7 in autophagic dysregulation. The group found that the inhibition of autophagy was through the co-aggregation of p53-FIP200 proteins and ataxin-7 aggregates that resulted in destabilisation of ULK1, due to decreased soluble FIP200. It was further shown that inhibition of P53 is able to restore soluble FIP200 and ULK1, which increases autophagic activity and subsequently reduces mutant ataxin-7 toxicity [62]. Therapeutic strategies targeting the pathogenic autophagic dysregulation would benefit from the understanding of the exact mechanisms by which pathogenesis is caused.

### SCA17

SCA17 is an interesting SCA disorder for three reasons; 1) like SCA6, the causative gene is not an *ATXN* but rather the complex and vital *TBP* (*TATA-Box binding protein*) [41,182,183]. The biological functions of most ataxin proteins remain somewhat elusive; however, the TBP is a well-described protein. 2) Although *TBP* function has been described since 1991 and numerous protein studies have been conducted, SCA17 was only designated in 2001, a considerable time after all other SCAs [184,185]. 3) The glutamine tract seen in the TBP is due to a polymorphic repeat region of CAGs interrupted by CAA rather than the typical contiguous CAG repeats seen in the other SCA diseases [183].

### Clinical features

SCA17 shows typical ataxic symptoms much like other SCA diseases, with degeneration of the cerebellum, particularly the Purkinje cells. The characteristic feature of SCA17 is the occurrence of frequent seizures and the high prevalence of psychiatric abnormalities (Table 1). Interestingly, immunoreactivity of neuronal nuclear inclusions of SCA17 patients appear to be more widely distributed through the grey matter when compared to other SCA diseases [182]. Age of onset in SCA17 is typically in the fourth decade, however symptoms can be seen in juvenile patients in extreme cases [85]. The disease progression of SCA17 is fairly rapid, with an average life span after diagnosis being 10-20 years [136].

Other common clinical features of SCA17 are progressive dementia and subsequent and concurrent chorea. These clinical features are highly similar to another polyQ disease, Huntington's disease [186], and SCA17 is often initially mis-diagnosed as Huntington's disease prior to genetic testing. Due to this, SCA17 is also known as Huntington's disease-like 4, and seems to be most prevalent in Asia, particularly Japan, China and Korea. It has also been suggested that the polyQ expansion may affect the function of TBP and embryonic development to such an extent that many do not survive the initial stages of development [187].

### Molecular genetics

*TBP* is a well-studied gene localised to 6q27 that has 8 exons. The gene is known to contain a polymorphic CAA/CAG tract in exon 3 that when expanded causes SCA17 [41]. The *TBP* repeat region has been divided into five domains that include two variable domains (II and IV) and three fixed domains (I, III and V) [186]. The variability of domains II and IV gives rise to SCA17 with repeat ranges of 7-11 and

9-21, respectively. Healthy individuals have a total repeat range of 25-42, incomplete penetrance is caused by 43-46 repeats and the disease range varies between 47-66 (Table 2) [186,187].

### Mutant and wild-type protein

The TBP is a vital protein that plays a crucial role in the initiation of transcription. The protein consists of 339 aa, is 37 kDa in size, with a polymorphic glutamine tract of 38 repeats and is the smallest of the SCA disease causing proteins (ENST00000230354.10) (Figure 2). TBP is one of many general transcription factors and interacts with all three eukaryotic RNA polymerases [185]. Of these factors, transcription factor IID (TFIID) is the first transcription factor that binds to the TATA box, a highly conserved sequence approximately 25-30 nt upstream of the transcription start site. TBP, along with numerous (approximately 13) TBP-associated factors make up the TFIID, which in turn is a component of the RNA polymerase II pre-initiation complex [185]. The polyQ tract is at the N-terminal of the protein and is thought regulate the DNA binding capability of the C-terminal. The variation of TBP binding to DNA affects the rate of transcription complex formation, and in turn the initiation of transcription [188]. The N-terminus varies in length due to the polyQ region, while the C-terminal is highly conserved [184]. The C-terminal contains two repeats of 88 aa that produce an inverted "U" or "saddle-shape" structure that effectively mounts the DNA and binds to the TATA box [184]. Such is the importance of TBP to cell survival that a 2002 study demonstrated that embryos with homozygous knockout for TBP did not survive past the blastocyst stage [189]. Although there are many other intricate functions and biological aspects of TBP, these are outside the scope of this review. More detail of the functions of TBP and transcription in general can be found at [185,190,191].

Transcriptional dysregulation has been widely implicated in a number of the SCA and polyQ diseases [153,154,192,193]. It stands to reason that a SCA disease in which the causative protein is a well-known transcription factor would have associated transcriptional dysregulation. This theory however is weakened by conflicting reports. One study demonstrated, via mobility shift electrophoresis, that mutant TBP binds less efficiently to DNA contain a TATA box when compared to normal TBP, and the polyQ expansion caused aberrant interactions between TBP and TFIIB [194]. When a similar study was conducted, however using a luciferase assay instead of mobility shift electrophoresis, the expanded polyQ TBP actually stimulated TATA box transcriptional activity [195].

These results suggest that rather than a global model for transcription dysregulation in SCA17 patients, a more specific and localised impairment of transcription occurs. This has been confirmed by numerous studies that implicate mutant TBP in both gain and loss of function pathogenesis [187]. Transcription factors such as Su(H), Sp1, TFIIB and NFY are all associated with toxic gain of function, while XBP1 and MyoD are associated with loss of function [187]. Many cellular processes are thought to be involved with these transcription factors, such as the chaperone system, TrkA and notch signalling as well as ER stress response [196-200], illustrating the complexity of SCA diseases and the need for a clear understanding of pathogenic mechanisms.

### Potential Therapeutic Strategies

Although SCA diseases and their mechanisms of pathogenesis have been extensively studied for decades, there is still no effective treatment or prevention strategy. Some therapeutic strategies are in place that

attempt to alleviate symptomatic pathogenesis; however, these are often ineffective and rarely prolong life. For example, in SCA3, some respite is found in pharmaceutical strategies that aim to reduce the severity and progression of the Parkinsonian-like phenotype and other associated symptoms, such as depression [201-203]. Takei and colleagues have shown that Tansospirone, an antidepressant used in Asia, may provide some benefit to patients with SCA3, as significant improvement was observed in several self-rated physical and emotional scales [201]. While these results may support some improvement, the treatment is nonspecific to SCA3 and only symptomatic relief was observed.

It is clear that strategies aimed at alleviating progression and/or delay in onset in SCA diseases are of great interest to the patients and health researchers. In order to achieve such strategies, the events leading to neural aggregation and selective degeneration need to be identified. Although pathogenically heterogeneous, there is strong evidence to suggest a role for a number of potential universal pathogenic pathways. These include; aggregation-autophagy, protein misfolding, the ubiquitin-proteasome system and chaperone system, as well as transcriptional dysregulation. For the benefit of this review, only therapeutic strategies that have the potential to be applied to multiple SCA diseases will be addressed.

### Suppression/modification of mutant gene expression and protein assembly

The current consensus is that the expanded CAG region in SCA proteins leads to toxic gain of function. Therefore, a strategy that aims to suppress or modify the mutant genes and their translated proteins is both logical and highly attractive. The strategies currently being trialled include antisense oligonucleotides (AOs) and RNA interference (RNAi).

Antisense oligonucleotides are single stranded oligomers typically 20-25 bp long and are able to anneal to RNA or DNA via Watson-Crick base pairing to a target (sense) strand. This allows the antisense compound to modify gene expression in a very specific manner and is dependent on the type of base and backbone chemistry [204]. For a long period of time, these oligomers offered significant promise but failed to deliver, as first generation oligonucleotides were plagued by issues of inconsistent synthesis, delivery and sensitivity to nuclease-induced degradation. The synthetic single stranded molecules were often able to modulate gene expression *in vitro*, but were unable to survive degradation and effectively enter the cell. However, in recent times, chemical modifications were developed and introduced that not only allowed the AOs to survive nuclease degradation, but also provided additional mechanisms to manipulate gene expression.

Currently, AOs are being used to treat various muscular and neurodegenerative diseases at varying stages of clinical trials, as well as a variety of other disease such as cancer [205]. A recent review showed that over 25 genes have been targeted using splice-switching AOs. These AOs are used as therapeutics to redirect pre-mRNA splicing, in which sequences vital to pre-mRNA processing are targeted, effectively blocking binding of the splicing factors to the region [205,206]. These types of AOs can be used to restore gene function, correct aberrant splicing, produce a novel transcript or even down regulate gene expression [205]. Most notably are *Exondys 51* and *Nusinersen*, which are treatments for Duchenne muscular dystrophy and spinal muscular atrophy, respectively [207,208]. *Exondys 51* gained FDA accelerated approval in September 2016, and is designed to skip *DMD* exon 51 during pre-mRNA processing in order to restore the open reading frame. *Exondys 51* will treat a subset of Duchenne muscular dystrophy

patients who have deletions flanking exon 51 [208,209]. *Nusinersen* gained full FDA approval in December 2016 and provides the only approved treatment for patients with spinal muscular atrophy [207].

In terms of SCA diseases, van Roon-Mom et al. [210] have conducted several studies using AOs as a therapeutic strategy [95,211]. In 2011, the group used a single 2'-O-methyl (2'-O-Me) AO on a phosphorothioate backbone that effectively reduced several polyQ disease protein levels, which included ataxin-1 and ataxin-3 [211]. The group used the AOs to reduce transcript levels via selective repeat-length dependent reduction of the various CAG encoding transcripts. The *in vitro* study assessed the efficacy of various 2'-O-Me (CUG)<sub>n</sub> triplet repeat AOs and found that (CUG)<sub>n</sub> not only reduced the main target protein, Huntingtin, but also reduced the mutant mRNA levels of ataxin-1 and ataxin-3. Another benefit observed was that reduction in mRNA levels was mutant specific, with the wild-type allele remaining constant or only reduced by a nominal amount. This has major benefits for some of the SCA disease proteins, such as TBP that are essential for normal biological and cellular function. Therefore, a treatment that spares wild-type protein is viewed as the most beneficial strategy.

A subsequent 2013 study on SCA3 and its associated protein, ataxin-3 used AO mediated exon skipping *in vitro* to remove the CAG repeat region in exon 10 and still maintain normal biological function of the ataxin-3 protein [95]. Although results in patient cells were not as convincing as in healthy cells, the study still showed that exon skipping is an attractive potential therapy for SCA diseases. Furthermore, the FDA approval of *Exondys 51* shows that if an effective means of exon skipping *in vivo* is achieved, and modifications to the SCA proteins do not have any negative downstream effects, additional therapies using AO technology are not unrealistic. Most recently, a 2017 study showed that it was possible to suppress mutant ataxin-3 protein levels in a YAC MJD-84.2Q mouse (84 polyQ) transgenic mouse model. Methoxyethyl (MOE) modified gapmers, AOs with modified bases at the ends on a phosphorothioate backbone with a DNA core were injected intracerebroventricularly into the transgenic mice and resulted in widespread delivery of the AOs into several key regions of the brain. AOs were designed to reduce mutant and wildtype ataxin-3 levels by inducing RNase-H degradation of target mRNA at the AO:RNA duplex. Three of the 5 AOs tests showed a >50% reduction in the disease protein levels in the cerebellum, diencephalon and cervical spinal cord [212]. Although both mutant and wild-type mRNAs are suppressed in this study, it has been found that ataxin-3 knockout mice appear to be normal, which suggests that ataxin-3 may not be essential for viability [213]. This avenue therefore provides another strategy for targeting reduction or suppression of mutant ataxin-3.

Synthetic RNA analogues have the potential to bind to RNA target sequences and in turn regulate gene expression. Regulation of gene expression may be achieved in several ways, such as suppression of translation, promotion of specific transcript degradation, redirection of pre-mRNA processing or influencing mRNA stability. These molecules have long been thought of as attractive candidates for therapeutics [214]. Lentiviral encoded short-hairpin RNAs (shRNA) induced allele-specific RNA silencing in a rat model for mutant ataxin-3. This specificity was achieved through lentiviral vectors encoding siRNAs that selectively target a SNP that occurs in over 70% of SCA3 patients. This allele specific mechanism decreased the severity of neurological pathogenesis associated with SCA3 [215]. Furthermore, independent studies used a similar mechanism, adeno-associated viral (AAV) vector based delivery of shRNA and small interfering RNA (siRNA) to rescue phenotypes in SCA1 [216] and SCA7 in affected mouse models,

respectively. In the SCA7 mouse, treatment had a positive effect on Purkinje neuron molecular layer thickness and appeared to reduce the neuronal nuclear inclusions [217].

In 2012 Lima and colleagues noted that 2'-O-methyl (2'-O-Me) and 2'-fluoro (2'-F) modified bases on a phosphorothioate backbone yielded RNA-like single strands with the ability to overcome potential issues observed with vector based unmodified shRNA and siRNA technologies, such as susceptibility to degradation. These modifications, termed single-stranded siRNAs (ss-siRNA), allowed the molecules to effectively silence gene expression, however, the exact mechanisms by which this silencing occurred was not identified. It was hypothesised that the ss-siRNAs were able to enter the protein machinery and induce an RNAi like effect [218]. The same group went on to use these ss-siRNAs to silence expression in the two most common polyQ diseases, HD and SCA3 [219,220]. The ss-siRNA molecules are complementary to the CAG repeat regions found in these genes, thus, inhibiting expression of both ataxin-3 and Huntington via the same mechanisms for both diseases. A more recent 2017 study, using similar a chemistry supported these findings, with selective and efficient downregulation of mutant ataxin-3 observed in cultured fibroblasts [221]. Holistically, the positive results described show that both non-selective and selective modification of *ATXN3* and *HTT* is achievable, and further testing into the safety and efficacy of these treatments is needed. These tests will allow the treatment strategies to progress from preclinical to phase I and II trials, hopefully providing the first viable therapeutic strategies for the treatment of SCA diseases.

### Prevention of misfolding and protein aggregation

There is much debate as to the exact role neuronal nuclear inclusions plays in pathogenesis, as researchers are still unable to determine whether the aggregates directly induce neurodegeneration or if the presence of misfolded proteins and oligomeric intermediates are to blame [7,8,222-224]. However, the prevention or reversal of neuronal nuclear inclusions still remains one of the most attractive avenues for therapeutic treatment [225].

Of note, the prevention of mutant SCA proteins or the removal of the CAG repeat should have a positive downstream effect on protein aggregation. Prevention of mutant SCA proteins or removal of the toxic CAG expansion will inhibit protein aggregation before it has a chance to be produced. These strategies therefore, have a twofold benefit and are believed to be the most promising of therapeutic possibilities in the opinion of many clinical researchers. In terms of direct inhibition, two main approaches exist; the inhibition of protein misfolding and aggregation; and the upregulation of protein/neuronal nuclear inclusions clearance.

Molecular chaperones are a large group of proteins that aid in covalent folding/unfolding of macromolecular structures, with a primary focus on protein folding. Heat shock proteins (HSP) are one such class of chaperones that are believed to play a key protective role in the aggregation of many SCA disease misfolded proteins [226-228]. Several studies over the past few decades have found therapeutic promise in upregulating the expression of various HSPs due to their potential to refold proteins and increase degradation [225]. Specifically, HSP40 and HSP70 have been shown to repress polyQ-induced neurodegeneration, as well as protect from cell death [227,229].

Of the HSP, the HSPB subfamily that comprises 10 individual protein members has anti-aggregation properties *in vitro* [228]. Vos et al. [228] conducted an *in vitro* study and studies in a *Drosophila* model, to assess the individual polyQ anti-aggregation properties of

the HSPB. Although a significant proportion of the work reported was conducted in *Htt* expressing cells, many inferences can be drawn due to the similarities of pathogenic mechanism. HSPB7 and HSPB9 were the only two proteins shown to reduce aggregates in cells expressing a repeat region of 74, while HSPB7 was the only effective protein in cells expressing a 119 polyQ region. This work was replicated *in vivo* and showed that HSPB7 requires a functional autophagosomal machine in order to function [228]. These results suggest that increasing the expression of HSPB7 could be a potential therapeutic strategy. This may be easily achieved with a simple supplement of calcium pantothenate (a supplemental form of vitamin B5), as it has been reported to modulate gene expression of HSPB7 [230]. However, this is by no means a robust therapy and further studies would need to be conducted on the effects of upregulation and the effectiveness of calcium pantothenate to modulate HSPB expression to levels required for therapeutic benefit. Other drugs such as epigallocatechin and tetracycline have been linked to altered aggregation in SCA diseases, most notably SCA3 [231,232]. The two drugs have been shown to positively alter aggregation and toxicity of mutant ataxin-3 via two distinct mechanisms. Epigallocatechin is believed to inhibit the formation of the amyloidogenic  $\beta$ -sheet-rich structures that are known components in protein aggregation, and steer formation towards non-toxic forms. While tetracycline did not appear to create any structural alterations, it significantly increased the solubility of the previously insoluble aggregates [231].

The ubiquitin proteasome system and autophagy are believed to be the main avenues to improve protein clearance in SCA diseases and would be most beneficial when targeting the removal of short misfolded proteins, while autophagy is preferentially tailored to clear larger toxic fragments that potentially form oligomeric complexes. Autophagy is well known to be negatively regulated by mTOR, therefore therapies targeted at increasing autophagy may increase the biological clearance of aggregated protein. Rapamycin is one of the most widely known mTOR inhibitors and has been found to induce a higher rate of autophagy in several polyQ diseases [63,233]. Temsirolimus (a rapamycin analogue) was administered to mice via intraperitoneal injection and found to decrease SCA3 aggregates as well as ameliorate motor function and coordination [234]. More recently, a derivative of triazole, OC-13 showed promise in increasing autophagic clearance of insoluble aggregates and demonstrates another plausible therapy in increasing autophagy [66].

### Transcriptional dysregulation

Transcriptional dysregulation and repression have been implicated in several of the SCA diseases and none more so than SCA17, with SCA1, 3 and 7 also reported to involve some form of transcriptional dysregulation. Altered histone deacetylase activity has been reported in numerous SCA diseases, with a SCA3 mouse model providing evidence that HDAC overactivity may be apparent [153,235]. Histone deacetylases are a group of evolutionary conserved enzymes that are responsible for the removal of acetyl groups from lysine residues on proteins [236]. The group consists of four classes (I, II, III, IV), that are separated on the basis of biological mechanism [237].

Evidence suggests that SCA3 mouse models show transcriptional repression through the hypoacetylation of H3 and H4 histones [153,235]. A 2011 study by Wang and colleagues found that sodium butyrate, a known HDAC inhibitor, enhanced histone acetylation, which led to increased gene expression in genes that are typically suppressed in the cerebellum of SCA3 mice [235]. Additionally, sodium butyrate treatment delayed onset and improved ataxic symptoms in the mouse model, as well as improved survival and the neurological

phenotype. A subsequent study using a different HDAC inhibitor, valproic acid, supported these results. The study used *Drosophila* and SCA3 cell models in two independent studies. Studies in the fly model demonstrated that prolonged administration of valproic acid slowed neurodegeneration, reduced climbing disability and increased the average lifespan of the flies. In cultured cells, valproic acid suppressed apoptosis while increasing the H3 and H4 acetylation levels [238]. These studies show that it is possible to alleviate, to some degree the phenotypes associated with SCA3, and indicates potentially viable options for the treatment of SCA3.

Ataxin-7 has also been shown to interact with HDAC, with an increase in cerebellar (neurons and glia) HDAC3 protein levels observed in transgenic SCA7 mice. In fact, *in vitro* work conducted in transfected HEK293T cells, showed that ataxin-7 directly interacts with HDAC3, and that this interaction may be a possible route of pathogenesis through altered deacetylation [239]. In keeping with this concept, a study demonstrated altered decacetylase activity and lysine acetylation levels, in the brain of transgenic mice. Although the Wang et al.'s and the Yi et al. [238] study showed that HDAC inhibition is a potential therapeutic strategy, a more recent 2014 study reported a contradictory finding. Venkatraman et al. aimed to examine the role of HDAC3 in SCA1 and HDAC3s potential for therapeutic treatment, by testing the effects of a Purkinje-neuron specific, genetically depleted and null model of HDAC on transgenic SCA1 mice. Interestingly, knockout HDAC3 models showed a greater degree of motor impairment and neurodegeneration when compared to unmodified models. These results suggest that HDAC3 inhibition as a therapeutic strategy may pose potential risks, as it is likely HDAC3 function may play a crucial role in normal Purkinje neuron function [240]. It is clear that further research is required to accurately describe the role of HDAC in SCA pathogenesis, for it seems that targeting HDAC3 may not be a viable option.

## Final Remarks

Advances in diagnostics in the past few decades have revealed a similar pathogenic mechanism in six of the autosomal dominant spinocerebellar ataxias. These six diseases (SCA1, 2, 3, 6, 7, 17) are caused by an expansion of a CAG repeating sequencing in the coding region of six independent genes. All six diseases present with common ataxic symptoms, however, there is still a large degree of phenotypic variation, from the rapid and early progression of SCA7, to the more slowly progressive, milder form of SCA6. The high degree of phenotypic variation is attributed to the varying number of the CAG repeats as well as the toxic function of the mutant protein. Although significant resources have been utilised in an endeavour to discover the exact mechanisms of toxicity caused by polyQ SCA diseases, a definitive answer still remains elusive, however, there is consensus that disease is caused by a toxic gain of function rather than wild-type loss of function. Other secondary causes such as protein misfolding, aggregation, transcriptional dysregulation and RNA toxicity have also been proposed. These common modes of pathogenesis are logical and suggest potential avenues for therapeutic intervention, with several pre-clinical studies being conducted in an attempt to provide relief for patients, in areas such as protein clearance and modification of gene expression. It is clear that the current symptomatic alleviation treatments are severely limited in their benefit. Ongoing research into the pathogenic cause of these diseases is needed, since once the primary causative mechanism of disease is found, a more focused and directed therapeutic target for this class of devastating diseases may be possible.

## References

1. Dueñas AM, Goold R, Giunti P (2006) Molecular pathogenesis of spinocerebellar ataxias. *Brain* 129: 1357-1370.
2. Underwood BR, Rubinsztein DC (2008) Spinocerebellar ataxias caused by polyglutamine expansions: A review of therapeutic strategies. *Cerebellum* 7: 215-221.
3. Bettencourt C, Lima M (2011) Machado-Joseph Disease: From first descriptions to new perspectives. *Orphanet J Rare Dis* 6: 35.
4. Ashley CT Jr, Warren ST (1995) Trinucleotide repeat expansion and human disease. *Annu Rev Genet* 29: 703-728.
5. Warren ST (1996) The expanding world of trinucleotide repeats. *Science* 271: 1374-1375.
6. Tsilfidis C, MacKenzie AE, Mettler G, Barceló J, Korneluk RG (1992) Correlation between CTG trinucleotide repeat length and frequency of severe congenital myotonic dystrophy. *Nat Genet* 1: 192-195.
7. Fan HC, Ho LI, Chi CS, Chen SJ, Peng GS, et al. (2014) Polyglutamine (PolyQ) diseases: Genetics to treatments. *Cell Transplant* 23: 441-458.
8. Zoghbi HY, Orr HT (1999) Polyglutamine diseases: Protein cleavage and aggregation. *Curr Opin Neurobiol* 9: 566-570.
9. Matos CA, de Macedo-Ribeiro S, Carvalho AL (2011) Polyglutamine diseases: The special case of ataxin-3 and Machado-Joseph disease. *Prog Neurobiol* 95: 26-48.
10. Fiszer A, Krzyzosiak WJ (2013) RNA toxicity in polyglutamine disorders: Concepts, models and progress of research. *J Mol Med (Berl)* 91: 683-691.
11. McMurray CT (2010) Mechanisms of trinucleotide repeat instability during human development. *Nat Rev Genet* 11: 786-799.
12. Venter JC, Adams MD, Myers EW, Li PW, Mural RJ, et al. (2001) The sequence of the human genome. *Science* 291: 1304-1351.
13. Subramanian S, Mishra RK, Singh L (2003) Genome-wide analysis of microsatellite repeats in humans: Their abundance and density in specific genomic regions. *Genome Biol* 4: R13.
14. Slaterry JP, Murphy WJ, O'Brien SJ (2000) Patterns of diversity among SINE elements isolated from three Y-chromosome genes in carnivores. *Mol Biol Evol* 17: 825-829.
15. Kashi Y, King D, Soller M (1997) Simple sequence repeats as a source of quantitative genetic variation. *Trends Genet* 13: 74-78.
16. Pellerone F, Edwards K, Thomas M (2015) Grapevine microsatellite repeats: isolation, characterisation and use for genotyping of grape germplasm from Southern Italy. *VITIS-Journal of Grapevine Research* 40: 179.
17. Lopes-Cendes I, Maciel P, Kish S, Gaspar C, Robitaille Y, et al. (1996) Somatic mosaicism in the central nervous system in spinocerebellar ataxia type 1 and Machado-Joseph disease. *Ann Neurol* 40: 199-206.
18. Benton CS, de Silva R, Rutledge SL, Bohlega S, Ashizawa T, et al. (1998) Molecular and clinical studies in SCA-7 define a broad clinical spectrum and the infantile phenotype. *Neurology* 51: 1081-1086.
19. Levinson G, Gutman GA (1987) Slipped-strand mispairing: A major mechanism for DNA sequence evolution. *Mol Biol Evol* 4: 203-21.
20. Pearson CE, Wang YH, Griffith JD, Sinden RR (1998) Structural analysis of slipped-strand DNA (S-DNA) formed in (CTG)<sub>n</sub> (CAG)<sub>n</sub> repeats from the myotonic dystrophy locus. *Nucleic Acids Res* 26: 816-823.
21. Pearson CE, Edamura KN and Cleary JD (2005) Repeat instability: Mechanisms of dynamic mutations. *Nat Rev Genet* 6: 729-742.
22. Cho DH, Tapscott SJ (2007) Myotonic dystrophy: Emerging mechanisms for DM1 and DM2. *Biochim Biophys Acta* 1772: 195-204.
23. Petruska J, Hartenstine MJ, Goodman MF (1998) Analysis of strand slippage in DNA polymerase expansions of CAG/CTG triplet repeats associated with neurodegenerative disease. *J Biol Chem* 273: 5204-5210.
24. Ho TH, Savkur RS, Poulos MG, Mancini MA, Swanson MS, et al. (2005) Co-localization of muscle blind with RNA foci is separable from mis-regulation of alternative splicing in myotonic dystrophy. *J Cell Sci* 118: 2923-2933.
25. Wells RD (1996) Molecular basis of genetic instability of triplet repeats. *J Biol Chem* 271: 2875-2878.

26. Sinden RR, Wells RD (1992) DNA structure, mutations and human genetic disease. *Curr Opin Biotechnol* 3: 612-622.
27. Iyer RR, Pluciennik A, Burdett V, Modrich PL (2006) DNA mismatch repair: Functions and mechanisms. *Chem Rev* 106: 302-323.
28. Iyer RR, Pluciennik A, Napierala M, Wells RD (2015) DNA triplet repeat expansion and mismatch repair. *Annu Rev Biochem* 84: 199-226.
29. Groothuizen FS, Sixma TK (2016) The conserved molecular machinery in DNA mismatch repair enzyme structures. *DNA Repair (Amst)* 38: 14-23.
30. Acharya S, Foster PL, Brooks P, Fishel R (2003) The coordinated functions of the *E. coli* MutS and MutL proteins in mismatch repair. *Mol Cell* 12: 233-246.
31. Lang WH, Coats JE, Majka J, Hura GL, Lin Y, et al (2011) Conformational trapping of mismatch recognition complex MSH2/MSH3 on repair-resistant DNA loops. *Proc Natl Acad Sci* 108: E837-E44.
32. Owen BA, Yang Z, Lai M, Gajek M, Badger JD, et al (2005) (CAG) n-hairpin DNA binds to Msh2-Msh3 and changes properties of mismatch recognition. *Nat Struct Mol Biol* 12: 663-670.
33. Jakupciak JP, Wells RD (2000) Gene conversion (recombination) mediates expansions of CTG[middle dot]CAG repeats. *J Biol Chem* 275: 40003-40013.
34. Rüb U, Schöls L, Paulson H, Auburger G, Kerner P, et al. (2013) Clinical features, neurogenetics and neuropathology of the polyglutamine spinocerebellar ataxias type 1, 2, 3, 6 and 7. *Prog Neurobiol* 104: 38-66.
35. Kawaguchi Y, Okamoto T, Taniwaki M, Aizawa M, Inoue M, et al. (1994) CAG expansions in a novel gene for Machado-Joseph disease at chromosome 14q32.1. *Nat Genet* 8: 221-228.
36. Banfi S, Servadio A, Chung MY, Kwiatkowski TJ Jr, McCall AE, et al. (1994) Identification and characterization of the gene causing type 1 spinocerebellar ataxia. *Nat Genet* 7: 513-520.
37. Orr HT, Chung MY, Banfi S, Kwiatkowski TJ Jr, Servadio A, et al. (1993) Expansion of an unstable trinucleotide CAG repeat in spinocerebellar ataxia type 1. *Nat Genet* 4: 221-226.
38. David G, Abbas N, Stevanin G, Dürr A, Yvert G, et al. (1997) Cloning of the SCA7 gene reveals a highly unstable CAG repeat expansion. *Nat Genet* 17: 65-70.
39. Zhuchenko O, Bailey J, Bonnen P, Ashizawa T, Stockton DW, et al. (1997) Autosomal dominant cerebellar ataxia (SCA6) associated with small polyglutamine expansions in the alpha 1A-voltage-dependent calcium channel. *Nat Genet* 15: 62-69.
40. Imbert G, Saudou F, Yvert G, Devys D, Trottier Y, et al. (1996) Cloning of the gene for spinocerebellar ataxia 2 reveals a locus with high sensitivity to expanded CAG/glutamine repeats. *Nat Genet* 14: 285-291.
41. Nakamura K, Jeong SY, Uchihara T, Anno M, Nagashima K, et al. (2001) SCA17, a novel autosomal dominant cerebellar ataxia caused by an expanded polyglutamine in TATA-binding protein. *Hum Mol Genet* 10: 1441-1448.
42. Harding A (1982) The clinical features and classification of the late onset autosomal dominant cerebellar ataxias. A study of 11 families, including descendants of the Drew family of Walworth. *Brain*: 105: 1-28.
43. Sun YM, Lu C, Wu ZY (2016) Spinocerebellar ataxia: Relationship between phenotype and genotype - A review. *Clin Genet* 90: 305-314.
44. Whaley NR, Fujioka S, Wszolek ZK (2011) Autosomal dominant cerebellar ataxia type I: A review of the phenotypic and genotypic characteristics. *Orphanet J Rare Dis* 6: 33.
45. Harding AE (1984) The hereditary ataxias and related disorders. *Churchill Livingstone*.
46. Durr A1 (2010) Autosomal dominant cerebellar ataxias: Polyglutamine expansions and beyond. *Lancet Neurol* 9: 885-894.
47. Pérez LV, Cruz GS, Falcón NS, Mederos LEA, Batallan KE, et al (2009) Molecular epidemiology of spinocerebellar ataxias in Cuba: insights into SCA2 founder effect in Holguin. *Neurosci Lett* 454: 157-160.
48. Gusella JF, MacDonald ME (2000) Molecular genetics: Unmasking polyglutamine triggers in neurodegenerative disease. *Nat Rev Neurosci* 1: 109-115.
49. Seidel K, Siswanto S, Fredrich M, Bouzrou M, Brunt ER, et al. (2016) Polyglutamine aggregation in Huntington's disease and spinocerebellar ataxia type 3: Similar mechanisms in aggregate formation. *Neuropathol Appl Neurobiol* 42: 153-166.
50. Lastres-Becker I, Rüb U, Auburger G (2008) Spinocerebellar ataxia 2 (SCA2). *Cerebellum* 7: 115-124.
51. D'Abreu A, França MC, Paulson HL, Lopes-Cendes I (2010) Caring for Machado-Joseph disease: current understanding and how to help patients. *Parkinsonism Relat Disord* 16: 2-7.
52. Schmahmann JD (2004) Disorders of the cerebellum: Ataxia, dysmetria of thought and the cerebellar cognitive affective syndrome. *J Neuropsychiatry Clin Neurosci* 16: 367-378.
53. Paulson H, Perez M, Trottier Y, Trojanowski J, Subramony S, et al (1997) Intracellular inclusions of expanded polyglutamine protein in spinocerebellar ataxia type 3. *Neuron* 19: 333-344.
54. Evert BO, Vogt IR, Kindermann C, Ozimek L, de Vos RA, et al. (2001) Inflammatory genes are upregulated in expanded ataxin-3-expressing cell lines and spinocerebellar ataxia type 3 brains. *J Neurosci* 21: 5389-5396.
55. Schmidt T, Lindenberg KS, Krebs A, Schöls L, Laccone F, et al. (2002) Protein surveillance machinery in brains with spinocerebellar ataxia type 3: Redistribution and differential recruitment of 26S proteasome subunits and chaperones to neuronal intranuclear inclusions. *Ann Neurol* 51: 302-310.
56. Evert BO, Wüllner U, Schulz JB, Weller M, Groscurth P, et al. (1999) High level expression of expanded full-length ataxin-3 *in vitro* causes cell death and formation of intranuclear inclusions in neuronal cells. *Hum Mol Genet* 8: 1169-1176.
57. Koch P, Breuer P, Peitz M, Jungverdorben J, Kesavan J, et al. (2011) Excitation-induced ataxin-3 aggregation in neurons from patients with Machado-Joseph disease. *Nature* 480: 543-546.
58. Petrakis S, Schaefer MH, Wanker EE, Andrade-Navarro MA (2013) Aggregation of polyQ-extended proteins is promoted by interaction with their natural coiled-coil partners. *Bioessays* 35: 503-507.
59. Ross CA, Poirier MA (2004) Protein aggregation and neurodegenerative disease. *Nat Med* 10: S10-17.
60. Thakur AK, Jayaraman M, Mishra R, Thakur M, Chellgren VM, et al (2009) Polyglutamine disruption of the huntingtin exon 1 N terminus triggers a complex aggregation mechanism. *Nat Struct Mol Biol* 16: 380-389.
61. Jimenez-Sanchez M, Thomson F, Zavodszky E, Rubinsztein DC (2012) Autophagy and polyglutamine diseases. *Prog Neurobiol* 97: 67-82.
62. Yu X, Muñoz-Alarcón A, Ajayi A, Webling KE, Steinhof A, et al (2013) Inhibition of autophagy via p53-mediated disruption of ULK1 in a SCA7 polyglutamine disease model. *J Mol Neurosci* 50: 586-99.
63. Sarkar S, Ravikumar B, Floto R, Rubinsztein D (2009) Rapamycin and mTOR-independent autophagy inducers ameliorate toxicity of polyglutamine-expanded huntingtin and related proteinopathies. *Cell Death Differ* 16: 46-56.
64. Alves S, Cormier-Dequaire F, Marinello M, Marais T, Muriel MP, et al. (2014) The autophagy/lysosome pathway is impaired in SCA7 patients and SCA7 knock-in mice. *Acta Neuropathol* 128: 705-722.
65. Nath SR, Lieberman AP (2017) The ubiquitination, disaggregation and proteasomal degradation machineries in polyglutamine disease. *Front Mol Neurosci* 10: 78.
66. Hsieh CH, Lee LC, Leong WY, Yang TC, Yao CF, et al. (2016) A triazole derivative elicits autophagic clearance of polyglutamine aggregation in neuronal cells. *Drug Des Devel Ther* 10: 2947-2957.
67. Paulson HL (2009) The spinocerebellar ataxias. *J Neuroophthalmol* 29: 227-237.
68. Michalik A, Martin JJ, Van Broeckhoven C (2004) Spinocerebellar ataxia type 7 associated with pigmentary retinal dystrophy. *Eur J Hum Genet* 12: 2-15.
69. Martindale JE (2017) Diagnosis of spinocerebellar ataxias caused by trinucleotide repeat expansions. *Curr Protoc Hum Genet*.
70. Wagner JL, O'Connor DM, Donsante A, Boulis NM (2016) Gene, stem cell and alternative therapies for SCA 1. *Front Mol Neurosci* 9: 67.
71. Klockgether T (2008) The clinical diagnosis of autosomal dominant spinocerebellar ataxias. *Cerebellum* 7: 101-105.
72. Klockgether T, Paulson H (2011) Milestones in ataxia. *Mov Disord* 26: 1134-1141.

73. Schöls L, Bauer P, Schmidt T, Schulte T, Riess O (2004) Autosomal dominant cerebellar ataxias: Clinical features, genetics and pathogenesis. *Lancet Neurol* 3: 291-304.
74. van de Warrenburg BP, Sinke RJ, Verschuuren-Bemelmans CC, Scheffer H, Brunt ER, et al. (2002) Spinocerebellar ataxias in the Netherlands: Prevalence and age at onset variance analysis. *Neurology* 58: 702-708.
75. Evers MM, Toonen LJ, van Roon-Mom WM (2014) Ataxin-3 protein and RNA toxicity in spinocerebellar ataxia type 3: Current insights and emerging therapeutic strategies. *Mol Neurobiol* 49: 1513-1531.
76. Orozco G, Estrada R, Perry TL, Araña J, Fernandez R, et al. (1989) Dominantly inherited olivopontocerebellar atrophy from eastern Cuba. Clinical, neuropathological and biochemical findings. *J Neurol Sci* 93: 37-50.
77. Sequeiros J, Coutinho P (1993) Epidemiology and clinical aspects of Machado-Joseph disease. *Adv Neurol* 61: 139-153.
78. Watson L, Wood M, Smith D, Scholefield J, Ballo R, et al (2016) Spinocerebellar ataxia type 7 in South Africa: Epidemiology, pathogenesis and therapy. *S Afr Med J* 106: 107-109.
79. Teive HA, Munhoz RP, Raskin S, Werneck LC (2008) Spinocerebellar ataxia type 6 in Brazil. *Arq Neuropsiquiatr* 66: 691-694.
80. Tang B, Liu C, Shen L, Dai H, Pan Q, et al. (2000) Frequency of SCA1, SCA2, SCA3/MJD, SCA6, SCA7, and DRPLA CAG trinucleotide repeat expansion in patients with hereditary spinocerebellar ataxia from Chinese kindreds. *Arch Neurol* 57: 540-544.
81. Moseley ML, Benzow KA, Schut LJ, Bird TD, Gomez CM, et al. (1998) Incidence of dominant spinocerebellar and Friedreich triplet repeats among 361 ataxia families. *Neurology* 51: 1666-1671.
82. Faruq M, Scaria V, Singh I, Tyagi S, Srivastava AK, et al. (2009) SCA-LSVD: A repeat-oriented locus-specific variation database for genotype to phenotype correlations in spinocerebellar ataxias. *Hum Mutat* 30: 1037-1042.
83. Brusco A1, Gellera C, Cagnoli C, Saluto A, Castucci A, et al. (2004) Molecular genetics of hereditary spinocerebellar ataxia: Mutation analysis of spinocerebellar ataxia genes and CAG/CTG repeat expansion detection in 225 Italian families. *Arch Neurol* 61: 727-733.
84. Smith DC, Bryer A, Watson LM, Greenberg LJ (2012) Inherited polyglutamine spinocerebellar ataxias in South Africa. *S Afr Med J* 102: 683-686.
85. Manto MU (2005) The wide spectrum of spinocerebellar ataxias (SCAs). *Cerebellum* 4: 2-6.
86. Clark HB, Burchett EN, Yunis WS, Larson S, Wilcox C, et al. (1997) Purkinje cell expression of a mutant allele of SCA1 in transgenic mice leads to disparate effects on motor behaviors, followed by a progressive cerebellar dysfunction and histological alterations. *J Neurosci* 17: 7385-7395.
87. Ito M (2002) Historical review of the significance of the cerebellum and the role of Purkinje cells in motor learning. *Ann N Y Acad Sci* 978: 273-288.
88. Mullen RJ, Eicher EM, Sidman RL (1976) Purkinje cell degeneration, a new neurological mutation in the mouse. *Proc Natl Acad Sci USA* 73: 208-212.
89. Zoghbi HY, Orr HT (2009) Pathogenic mechanisms of a polyglutamine-mediated neurodegenerative disease, spinocerebellar ataxia type 1. *J Biol Chem* 284: 7425-7429.
90. de Chiara C, Giannini C, Adinolfi S, de Boer J, Guida S, et al. (2003) The AXH module: An independently folded domain common to ataxin-1 and HBP1. *FEBS Lett* 551: 107-112.
91. Deriu MA, Grasso G, Tuszyński JA, Massai D, Gallo D, et al (2016) Characterization of the AXH domain of ataxin-1 using enhanced sampling and functional mode analysis. *Proteins* 84: 666-673.
92. de Chiara C, Rees M, Menon RP, Pauwels K, Lawrence C, et al. (2013) Self-assembly and conformational heterogeneity of the AXH domain of ataxin-1: An unusual example of a chameleon fold. *Biophys J* 104: 1304-1313.
93. Grasso G, Deriu MA, Tuszyński JA, Gallo D, Morbiducci U, et al. (2016) Conformational fluctuations of the AXH monomer of Ataxin-1. *Proteins* 84: 52-59.
94. Mizutani A, Wang L, Rajan H, Vig PJ, Alaynick WA, et al. (2005) Boat, an AXH domain protein, suppresses the cytotoxicity of mutant ataxin-1. *EMBO J* 24: 3339-3351.
95. Evers MM, Tran HD, Zalachoras I, Pepers BA, Meijer OC, et al. (2013) Ataxin-3 protein modification as a treatment strategy for spinocerebellar ataxia type 3: Removal of the CAG containing exon. *Neurobiol Dis* 58: 49-56.
96. Taylor JP, Hardy J, Fischbeck KH (2002) Toxic proteins in neurodegenerative disease. *Science* 296: 1991-1995.
97. Orr HT, Zoghbi HY (2007) Trinucleotide repeat disorders. *Annu Rev Neurosci* 30: 575-621.
98. Kuiper EF, de Mattos EP, Jardim LB, Kampinga HH, Bergink S (2017) Chaperones in polyglutamine aggregation: Beyond the Q-stretch. *Front Neurosci* 11: 145.
99. de Chiara C, Menon RP, Kelly G, Pastore A (2013) Protein-protein interactions as a strategy towards protein-specific drug design: the example of ataxin-1. *PLoS ONE* 8: e76456.
100. de Chiara C, Menon RP, Dal Piaz F, Calder L, Pastore A (2005) Polyglutamine is not all: The functional role of the AXH domain in the ataxin-1 protein. *J Mol Biol* 354: 883-893.
101. Lasagna-Reeves CA, Rousseaux MW, Guerrero-Muñoz MJ, Park J, Jafar-Nejad P, et al (2015) A native interactor scaffolds and stabilizes toxic ATAXIN-1 oligomers in SCA1. *Elife* 4: e07558.
102. Furtado S, Payami H, Lockhart PJ, Hanson M, Nutt JG, et al (2004) Profile of families with parkinsonism-predominant spinocerebellar ataxia type 2 (SCA2). *Movement disorders* 19: 622-629.
103. Sasaki H, Fukazawa T, Wakisaka A, Hamada K, Hamada T, et al. (1996) Central phenotype and related varieties of spinocerebellar ataxia 2 (SCA2): A clinical and genetic study with a pedigree in the Japanese. *J Neurol Sci* 144: 176-181.
104. Termsarasab P, Thammongkolchai T, Rucker JC, Frucht SJ (2015) The diagnostic value of saccades in movement disorder patients: A practical guide and review. *J Clin Mov Disord* 2: 14.
105. Federighi P, Cevenini G, Dotti MT, Rosini F, Pretegianni E, et al. (2011) Differences in saccade dynamics between spinocerebellar ataxia 2 and late-onset cerebellar ataxias. *Brain* 134: 879-891.
106. Bürk K, Fetter M, Skalej M, Laccone F, Stevanin G, et al (1997) Saccade velocity in idiopathic and autosomal dominant cerebellar ataxia. *J Neurol Neurosurg Psychiatry* 62: 662-624.
107. Velázquez-Pérez L, Seifried C, Santos-Falcón N, Abele M, Ziemann U, et al. (2004) Saccade velocity is controlled by polyglutamine size in spinocerebellar ataxia 2. *Ann Neurol* 56: 444-447.
108. Rodríguez-Labrada R, Velázquez-Pérez L, Auburger G, Ziemann U, Canales-Ochoa N, et al. (2016) Spinocerebellar ataxia type 2: Measures of saccade changes improve power for clinical trials. *Mov Disord* 31: 570-578.
109. Reynaldo-Arminan R, Reynaldo-Hernandez R, Paneque-Herrera M, Prieto-Avila L, Perez-Ruiz E (2001) Mental disorders in patients with spinocerebellar ataxia type 2 in Cuba. *Revista de Neurologia* 35: 818-821.
110. Tan N, Zhou Y, Tan A, Chong S, Lee W (2004) Spinocerebellar ataxia type 2 with focal epilepsy-an unusual association. *Ann Acad Med Singapore* 33: 103-106.
111. Mao R, Aylsworth AS, Potter N, Wilson WG, Breningstall G, et al. (2002) Childhood-onset ataxia: Testing for large CAG-repeats in SCA2 and SCA7. *Am J Med Genet* 110: 338-345.
112. Ying SH, Choi SI, Lee M, Perlman SL, Baloh RW, et al. (2005) Relative atrophy of the flocculus and ocular motor dysfunction in SCA2 and SCA6. *Ann N Y Acad Sci* 1039: 430-435.
113. Gispert S, Twells R, Orozco G, Brice A, Weber J, et al. (1993) Chromosomal assignment of the second locus for autosomal dominant cerebellar ataxia (SCA2) to chromosome 12q23-24.1. *Nat Genet* 4: 295-299.
114. Sanpei K, Takano H, Igarashi S, Sato T, Oyake M, et al. (1996) Identification of the spinocerebellar ataxia type 2 gene using a direct identification of repeat expansion and cloning technique, DIRECT. *Nat Genet* 14: 277-284.
115. Pulst SM, Nechiporuk A, Nechiporuk T, Gispert S, Chen XN, et al. (1996) Moderate expansion of a normally biallelic trinucleotide repeat in spinocerebellar ataxia type 2. *Nat Genet* 14: 269-276.
116. Elden AC, Kim HJ, Hart MP, Chen-Plotkin AS, Johnson BS, et al. (2010) Ataxin-2 intermediate-length polyglutamine expansions are associated with increased risk for ALS. *Nature* 466: 1069-1075.

117. Albrecht M, Golatta M, Wüllner U, Lengauer T (2004) Structural and functional analysis of ataxin-2 and ataxin-3. *Eur J Biochem* 271: 3155-3170.
118. Meunier C, Bordereaux D, Porteu F, Gisselbrecht S, Chrétien S, et al. (2002) Cloning and characterization of a family of proteins associated with Mpl. *J Biol Chem* 277: 9139-9147.
119. Huynh DP, Del Bigio MR, Ho DH, Pulst SM (1999) Expression of ataxin-2 in brains from normal individuals and patients with Alzheimer's disease and spinocerebellar ataxia 2. *Ann Neurol* 45: 232-241.
120. Stubenvoll MD, Medley JC, Irwin M, Song MH (2016) ATX-2, the *C. elegans* ortholog of human Ataxin-2, regulates centrosome size and microtubule dynamics. *PLoS Genet* 12: e1006370.
121. Gnazzo MM, Uhlemann EE, Villarreal AR, Shirayama M, Dominguez EG, et al. (2016) The RNA-binding protein ATX-2 regulates cytokinesis through PAR-5 and ZEN-4. *Mol Biol Cell* 27: 3052-3064.
122. Magaña JJ, Velázquez-Pérez L, Cisneros B (2013) Spinocerebellar ataxia type 2: Clinical presentation, molecular mechanisms and therapeutic perspectives. *Mol Neurobiol* 47: 90-104.
123. Carmo-Silva S, Nobrega C, Pereira de Almeida L, Cavadas C (2017) Unraveling the role of Ataxin-2 in metabolism. *Trends Endocrinol Metab* 28: 309-318.
124. van de Loo S1, Eich F, Nonis D, Auburger G, Nowock J (2009) Ataxin-2 associates with rough endoplasmic reticulum. *Exp Neurol* 215: 110-118.
125. Lastres-Becker I, Nonis D, Eich F, Klinkenberg M, Gorospe M, et al (2016) Mammalian ataxin-2 modulates translation control at the pre-initiation complex via PI3K/mTOR and is induced by starvation. *Biochimica et Biophysica Acta (BBA)-Molecular Basis of Disease* 1862: 1558-1569.
126. Yokoshi M, Li Q, Yamamoto M, Okada H, Suzuki Y, et al. (2014) Direct binding of Ataxin-2 to distinct elements in 3' UTRs promotes mRNA stability and protein expression. *Mol Cell* 55: 186-198.
127. Bar DZ, Charar C, Dorfman J, Yadid T, Tafforeau L, et al (2016) Cell size and fat content of dietary-restricted *Caenorhabditis elegans* are regulated by ATX-2, an mTOR repressor. *Proc Natl Acad Sci* 113: E4620-E4629.
128. Mercader JM, González JR, Lozano JJ, Bak M, Kauppinen S, et al. (2012) Aberrant brain microRNA target and miRISC gene expression in the *anx/anx* anorexia mouse model. *Gene* 497: 181-190.
129. Dong L, Yan H, Huang X, Hu X, Yang Y, et al. (2015) A2BP1 gene polymorphisms association with olanzapine-induced weight gain. *Pharmacol Res* 99: 155-161.
130. Huynh DP, Yang HT, Vakharia H, Nguyen D, Pulst SM (2003) Expansion of the polyQ repeat in ataxin-2 alters its Golgi localization, disrupts the Golgi complex and causes cell death. *Hum Mol Genet* 12: 1485-1496.
131. Huynh DP, Figueroa K, Hoang N and Pulst S-M (2000) Nuclear localization or inclusion body formation of ataxin-2 are not necessary for SCA2 pathogenesis in mouse or human. *Nat Genet* 26: 44-50.
132. Wen J, Scoles DR, Facelli JC (2017) Effects of the enlargement of polyglutamine segments on the structure and folding of ataxin-2 and ataxin-3 proteins. *J Biomol Struct Dyn* 35: 504-519.
133. Nakano KK, Dawson DM, Spence A (1972) Machado disease. A hereditary ataxia in Portuguese emigrants to Massachusetts. *Neurology* 22: 49-55.
134. Bettencourt C, Santos C, Kay T, Vasconcelos J, Lima M (2008) Analysis of segregation patterns in Machado-Joseph disease pedigrees. *J Hum Genet* 53: 920-923.
135. Wang Y, Yang X, Ma W, Li J, Zhang Q, et al. (2016) Clinical features and genetic diagnosis of hereditary spinocerebellar ataxia 3. *Mol Med Rep* 14: 3731-3734.
136. Jayadev S, Bird TD (2013) Hereditary ataxias: Overview. *Genet Med* 15: 673-683.
137. Alves S, Régulier E, Nascimento-Ferreira I, Hassig R, Dufour N, et al (2008) Striatal and nigral pathology in a lentiviral rat model of Machado-Joseph disease. *Hum Mol Genet* 17: 2071-2083.
138. Ichikawa Y, Goto J, Hattori M, Toyoda A, Ishii K, et al. (2001) The genomic structure and expression of MJD, the Machado-Joseph disease gene. *J Hum Genet* 46: 413-422.
139. Bettencourt C, Santos C, Montiel R, do Carmo Costa M, Cruz-Morales P, et al (2010) Increased transcript diversity: Novel splicing variants of Machado-Joseph Disease gene (ATXN3). *Neurogenetics*. 11: 193-202.
140. Mao Y, Senic-Matuglia F, Di Fiore PP, Polo S, Hodsdon ME, et al. (2005) Deubiquitinating function of ataxin-3: Insights from the solution structure of the Josephin domain. *Proc Natl Acad Sci U S A* 102: 12700-12705.
141. Nicastro G, Menon RP, Masino L, Knowles PP, McDonald NQ, et al. (2005) The solution structure of the Josephin domain of ataxin-3: Structural determinants for molecular recognition. *Proc Natl Acad Sci U S A* 102: 10493-10498.
142. Nicastro G, Todi SV, Karaca E, Bonvin AM, Paulson HL, et al. (2010) Understanding the role of the Josephin domain in the PolyUb binding and cleavage properties of ataxin-3. *PLoS ONE* 5: e12430.
143. Tait D, Riccio M, Sittler A, Scherzinger E, Santi S, et al. (1998) Ataxin-3 is transported into the nucleus and associates with the nuclear matrix. *Hum Mol Genet* 7: 991-997.
144. Pozzi C, Valtorta M, Tedeschi G, Galbusera E, Pastori V, et al. (2008) Study of subcellular localization and proteolysis of ataxin-3. *Neurobiol Dis* 30: 190-200.
145. Todi SV, Laco MN, Winborn BJ, Travis SM, Wen HM, et al. (2007) Cellular turnover of the polyglutamine disease protein ataxin-3 is regulated by its catalytic activity. *J Biol Chem* 282: 29348-29358.
146. Antony PMA, Mantele S, Mollenkopf P, Boy J, Kehlenbach RH, et al (2009) Identification and functional dissection of localization signals within ataxin-3. *Neurobiology of disease* 36: 280-292.
147. Winborn BJ, Travis SM, Todi SV, Scaglione KM, Xu P, et al. (2008) The deubiquitinating enzyme ataxin-3, a polyglutamine disease protein, edits Lys63 linkages in mixed linkage ubiquitin chains. *J Biol Chem* 283: 26436-26443.
148. Berke SJS, Chai Y, Marrs GL, Wen H, Paulson HL (2005) Defining the role of ubiquitin-interacting motifs in the polyglutamine disease protein, ataxin-3. *J Biol Chem* 280: 32026-32034.
149. Zhong X, Pittman RN (2006) Ataxin-3 binds VCP/p97 and regulates retrotranslocation of ERAD substrates. *Hum Mol Genet* 15: 2409-2420.
150. Tsou WL, Ouyang M, Hosking RR, Sutton JR, Blount JR, et al. (2015) The deubiquitinase ataxin-3 requires Rad23 and DnaJ-1 for its neuroprotective role in *Drosophila melanogaster*. *Neurobiol Dis* 82: 12-21.
151. Kristensen LV, Oppermann FS, Rauen MJ, Hartmann-Petersen R, Thirstrup K (2017) Polyglutamine expansion of ataxin-3 alters its degree of ubiquitination and phosphorylation at specific sites. *Neurochem Int* 105: 42-50.
152. Perez MK, Paulson HL, Pendse SJ, Saionz SJ, Bonini NM, et al. (1998) Recruitment and the role of nuclear localization in polyglutamine-mediated aggregation. *J Cell Biol* 143: 1457-1470.
153. Chou AH, Yeh TH, Ouyang P, Chen YL, Chen SY, et al. (2008) Polyglutamine-expanded ataxin-3 causes cerebellar dysfunction of SCA3 transgenic mice by inducing transcriptional dysregulation. *Neurobiol Dis* 31: 89-101.
154. Evert BO, Araujo J, Vieira-Saecker AM, de Vos RA, Harendza S, et al. (2006) Ataxin-3 represses transcription via chromatin binding, interaction with histone deacetylase 3 and histone deacetylation. *J Neurosci* 26: 11474-11486.
155. Laço MN, Cortes L, Travis SM, Paulson HL, Rego AC (2012) Valosin-containing protein (VCP/p97) is an activator of wild-type ataxin-3. *PLoS ONE* 7: e43563.
156. Li X, Liu H, Fischhaber PL, Tang TS (2015) Toward therapeutic targets for SCA3: Insight into the role of Machado-Joseph disease protein ataxin-3 in misfolded proteins clearance. *Prog Neurobiol* 132: 34-58.
157. Haacke A, Broadley SA, Boteva R, Tzvetkov N, Hartl FU, et al. (2006) Proteolytic cleavage of polyglutamine-expanded ataxin-3 is critical for aggregation and sequestration of non-expanded ataxin-3. *Hum Mol Genet* 15: 555-568.
158. Matsumoto M, Yada M, Hatakeyama S, Ishimoto H, Tanimura T, et al. (2004) Molecular clearance of ataxin-3 is regulated by a mammalian E4. *EMBO J* 23: 659-669.
159. Schmitz-Hübsch T, Coudert M, Bauer P, Giunti P, Globas C, et al. (2008) Spinocerebellar ataxia types 1, 2, 3 and 6: Disease severity and nonataxia symptoms. *Neurology* 71: 982-989.
160. Sinke RJ, Ippel EF, Diepstraten CM, Beemer FA, Wokke JH, et al. (2001) Clinical and molecular correlations in spinocerebellar ataxia type 6: A study of 24 Dutch families. *Arch Neurol* 58: 1839-1844.

161. Rajakulendran S, Kaski D, Hanna MG (2012) Neuronal P/Q-type calcium channel dysfunction in inherited disorders of the CNS. *Nat Rev Neurol* 8: 86-96.
162. Bürk K, Kaiser FJ, Tennstedt S, Schöls L, Kreuz FR, et al. (2014) A novel missense mutation in CACNA1A evaluated by *in silico* protein modeling is associated with non-episodic spinocerebellar ataxia with slow progression. *Eur J Med Genet* 57: 207-211.
163. Pradotto L, Mencarelli M, Bigoni M, Milesi A, Di Blasio A, et al (2016) Episodic ataxia and SCA6 within the same family due to the D302N CACNA1A gene mutation. *J Neurol Sci* 371: 81-84.
164. Westenbroek RE, Sakurai T, Elliott EM, Hell JW, Starr TV, et al. (1995) Immunohistochemical identification and subcellular distribution of the alpha 1A subunits of brain calcium channels. *J Neurosci* 15: 6403-6418.
165. Watase K (2015) Spinocerebellar ataxia type 6: Lessons from faithful knock-in mouse models. *Neurol Clin Neurosci* 3: 14-17.
166. Matsuyama Z, Wakamori M, Mori Y, Kawakami H, Nakamura S, et al. (1999) Direct alteration of the P/Q-type Ca<sup>2+</sup> channel property by polyglutamine expansion in spinocerebellar ataxia 6. *J Neurosci* 19: RC14.
167. Toru S, Murakoshi T, Ishikawa K, Saegusa H, Fujigasaki H, et al. (2000) Spinocerebellar ataxia type 6 mutation alters P-type calcium channel function. *J Biol Chem* 275: 10893-10898.
168. Garden GA, La Spada AR (2008) Molecular pathogenesis and cellular pathology of spinocerebellar ataxia type 7 neurodegeneration. *Cerebellum* 7: 138-149.
169. McLaughlin ME, Dryja TP (2002) Ocular findings in spinocerebellar ataxia 7. *Arch Ophthalmol* 120: 655-659.
170. Bang OY, Huh K, Lee PH, Kim HJ (2003) Clinical and neuroradiological features of patients with spinocerebellar ataxias from Korean kindreds. *Arch Neurol* 60: 1566-1574.
171. Hernandez-Castillo CR, Galvez V, Diaz R, Fernandez-Ruiz J (2016) Specific cerebellar and cortical degeneration correlates with ataxia severity in spinocerebellar ataxia type 7. *Brain Imaging Behav* 10: 252-257.
172. Horton LC, Frosch MP, Vangel MG, Weigel-DiFranco C, Berson EL, et al. (2013) Spinocerebellar ataxia type 7: Clinical course, phenotype-genotype correlations and neuropathology. *Cerebellum* 12: 176-193.
173. David G, Dürr A, Stevanin G, Cancel G, Abbas N, et al. (1998) Molecular and clinical correlations in autosomal dominant cerebellar ataxia with progressive macular dystrophy (SCA7). *Hum Mol Genet* 7: 165-170.
174. Ansoorge O, Giunti P, Michalik A, Van Broeckhoven C, Harding B, et al. (2004) Ataxin-7 aggregation and ubiquitination in infantile SCA7 with 180 CAG repeats. *Ann Neurol* 56: 448-452.
175. Helmlinger D, Hardy S, Sasorith S, Klein F, Robert F, et al. (2004) Ataxin-7 is a subunit of GCN5 histone acetyl transferase-containing complexes. *Hum Mol Genet* 13: 1257-1265.
176. La Spada AR, Fu YH, Sopher BL, Libby RT, Wang X, et al. (2001) Polyglutamine-expanded ataxin-7 antagonizes CRX function and induces cone-rod dystrophy in a mouse model of SCA7. *Neuron* 31: 913-927.
177. Lindenberg KS, Yvert G, Müller K, Landwehrmeyer GB (2000) Expression analysis of ataxin-7 mRNA and protein in human brain: Evidence for a widespread distribution and focal protein accumulation. *Brain Pathol* 10: 385-394.
178. Mohan RD, Dialynas G, Weake VM, Liu J, Martin-Brown S, et al (2014) Loss of *Drosophila* Ataxin-7, a SAGA subunit, reduces H2B ubiquitination and leads to neural and retinal degeneration. *Genes Dev* 28: 259-272.
179. McMahon SJ, Pray-Grant MG, Schieltz D, Yates JR 3rd, Grant PA (2005) Polyglutamine-expanded spinocerebellar ataxin-7 protein disrupts normal SAGA and SLIK histone acetyltransferase activity. *Proc Natl Acad Sci U S A* 102: 8478-8482.
180. Palhan VB, Chen S, Peng GH, Tjernberg A, Gamper AM, et al. (2005) Polyglutamine-expanded ataxin-7 inhibits STAGA histone acetyltransferase activity to produce retinal degeneration. *Proc Natl Acad Sci U S A* 102: 8472-8477.
181. Nakamura Y, Tagawa K, Oka T, Sasabe T, Ito H, et al. (2012) Ataxin-7 associates with microtubules and stabilizes the cytoskeletal network. *Hum Mol Genet* 21: 1099-1110.
182. Rolfs A, Koeppen AH, Bauer I, Bauer P, Buhlmann S, et al. (2003) Clinical features and neuropathology of autosomal dominant spinocerebellar ataxia (SCA17). *Ann Neurol* 54: 367-375.
183. Koide R, Kobayashi S, Shimohata T, Ikeuchi T, Maruyama M, et al. (1999) A neurological disease caused by an expanded CAG trinucleotide repeat in the TATA-binding protein gene: A new polyglutamine disease? *Hum Mol Genet* 8: 2047-2053.
184. Nikolov DB, Hu SH, Lin J, Gasch A, Hoffmann A, et al. (1992) Crystal structure of TFIID TATA-box binding protein. *Nature* 360: 40-46.
185. Roeder RG (1991) The complexities of eukaryotic transcription initiation: Regulation of pre-initiation complex assembly. *Trends Biochem Sci* 16: 402-408.
186. Cui Y, Yang S, Li XJ, Li S (2017) Genetically modified rodent models of SCA17. *J Neurosci Res* 95: 1540-1547.
187. Yang S, Li XJ, Li S (2016) Molecular mechanisms underlying spinocerebellar ataxia 17 (SCA17) pathogenesis. *Rare Diseases*. 4: 349-365.
188. Lesclure A, Lutz Y, Eberhard D, Jacq X, Krol A, et al (1994) The N-terminal domain of the human TATA-binding protein plays a role in transcription from TATA-containing RNA polymerase II and III promoters. *EMBO J* 13: 1166.
189. Martianov I, Viville S, Davidson I (2002) RNA polymerase II transcription in murine cells lacking the TATA binding protein. *Science* 298: 1036-1039.
190. van Roon-Mom WM, Reid SJ, Faull RL, Snell RG (2005) TATA-binding protein in neurodegenerative disease. *Neuroscience* 133: 863-872.
191. White RJ, Jackson SP (1992) The TATA-binding protein: A central role in transcription by RNA polymerases I, II and III. *Trends Genet* 8: 284-288.
192. Mohan RD, Abmayr SM, Workman JL (2014) The expanding role for chromatin and transcription in polyglutamine disease. *Curr Opin Genet Dev* 26: 96-104.
193. Anglada-Huguet M, Vidal-Sancho L, Cabezas-Llobet N, Alberch J, Xifré X (2017) Pathogenesis of Huntington's disease: How to fight excitotoxicity and transcriptional dysregulation. *Huntington's Disease-Molecular Pathogenesis and Current Models*.
194. Friedman MJ, Shah AG, Fang ZH, Ward EG, Warren ST, et al. (2007) Polyglutamine domain modulates the TBP-TFIIB interaction: implications for its normal function and neurodegeneration. *Nat Neurosci* 10: 1519-1528.
195. Reid SJ, Rees MI, van Roon-Mom WM, Jones AL, MacDonald ME, et al. (2003) Molecular investigation of TBP allele length: A SCA17 cellular model and population study. *Neurobiol Dis* 13: 37-45.
196. Friedman MJ, Li S, Li XJ (2009) Activation of gene transcription by heat shock protein 27 may contribute to its neuronal protection. *J Biol Chem* 284: 27944-27951.
197. Huang S, Ling JJ, Yang S, Li XJ, Li S (2011) Neuronal expression of TATA box-binding protein containing expanded polyglutamine in knock-in mice reduces chaperone protein response by impairing the function of nuclear factor-Y transcription factor. *Brain* 134: 1943-1958.
198. Lee LC, Chen CM, Wang HC, Hsieh HH, Chiu IS, et al. (2012) Role of the CCAAT-binding protein NFY in SCA17 pathogenesis. *PLoS ONE* 7: e35302.
199. Ren J, Jegga AG, Zhang M, Deng J, Liu J, et al. (2011) A *Drosophila* model of the neurodegenerative disease SCA17 reveals a role of RBP-J/Su(H) in modulating the pathological outcome. *Hum Mol Genet* 20: 3424-3436.
200. Shah AG, Friedman MJ, Huang S, Roberts M, Li XJ, et al. (2009) Transcriptional dysregulation of TrkA associates with neurodegeneration in spinocerebellar ataxia type 17. *Hum Mol Genet* 18: 4141-4152.
201. Takei A, Hamada S, Homma S, Hamada K, Tashiro K, et al. (2010) Difference in the effects of tandospirone on ataxia in various types of spinocerebellar degeneration: An open-label study. *Cerebellum* 9: 567-570.
202. Takei A, Hamada T, Yabe I, Sasaki H (2005) Treatment of cerebellar ataxia with 5-HT1A agonist. *Cerebellum* 4: 211-215.
203. Buhlmann C, Bussopulos A, Oechsner M (2003) Dopaminergic response in Parkinsonian phenotype of Machado-Joseph disease. *Mov Disord* 18: 219-221.
204. Uhlmann E, Peyman A (1990) Antisense oligonucleotides: A new therapeutic principle. *Chem Rev* 90: 543-584.
205. Havens MA, Hastings ML (2016) Splice-switching antisense oligonucleotides as therapeutic drugs. *Nucleic Acids Res* 44: 6549-6563.



206. Bauman J, Jearawiriyapaisarn N, Kole R (2009) Therapeutic potential of splice-switching oligonucleotides. *Oligonucleotides* 19: 1-13.
207. Finkel RS, Chiriboga CA, Vajsar J, Day JW, Montes J, et al (2017) Treatment of infantile-onset spinal muscular atrophy with nusinersen: A phase 2, open-label, dose-escalation study. *Lancet* 388: 3017-3026.
208. Mendell JR, Rodino-Klapac LR, Sahenk Z, Roush K, Bird L, et al. (2013) Eteplirsen for the treatment of Duchenne muscular dystrophy. *Ann Neurol* 74: 637-647.
209. Charleston J, Schnell F, Dworzak J, Donoghue C, Lewis S, et al (2016) Long-term treatment with eteplirsen promotes exon 51 skipping and novel dystrophin protein production in Duchenne muscular dystrophy patients. *Neuromuscul Disord* 26: S153.
210. Toonen LJ, Schmidt I, Luijsterburg MS, van Attikum H, van Roon-Mom WM (2016) Antisense oligonucleotide-mediated exon skipping as a strategy to reduce proteolytic cleavage of ataxin-3. *Sci Rep* 6: 35200.
211. Evers MM, Pepers BA, van Deutekom JC, Mulders SA, den Dunnen JT, et al. (2011) Targeting several CAG expansion diseases by a single antisense oligonucleotide. *PLoS ONE* 6: e24308.
212. Moore LR, Rajpal G, Dillingham IT, Qutob M, Blumenstein KG, et al (2017) Evaluation of antisense oligonucleotides targeting ATXN3 in SCA3 mouse models. *Mol Ther Nucleic Acids* 7: 200-210.
213. Schmitt I, Linden M, Khazneh H, Evert BO, Breuer P, et al. (2007) Inactivation of the mouse Atxn3 (ataxin-3) gene increases protein ubiquitination. *Biochem Biophys Res Commun* 362: 734-739.
214. Watts JK, Corey DR (2012) Silencing disease genes in the laboratory and the clinic. *J Pathol* 226: 365-379.
215. Alves S, Nascimento-Ferreira I, Auregan G, Hassig R, Dufour N, et al. (2008) Allele-specific RNA silencing of mutant ataxin-3 mediates neuroprotection in a rat model of Machado-Joseph disease. *PLoS ONE* 3: e3341.
216. Xia H, Mao Q, Eliason SL, Harper SQ, Martins IH, et al (2004) RNAi suppresses polyglutamine-induced neurodegeneration in a model of spinocerebellar ataxia. *Nat Med* 10: 816-820.
217. Ramachandran PS, Boudreau RL, Schaefer KA, La Spada AR, Davidson BL (2014) Non-allele specific silencing of ataxin-7 improves disease phenotypes in a mouse model of SCA7. *Molecular Therapy* 22: 1635-1642.
218. Lima WF, Prakash TP, Murray HM, Kinberger GA, Li W, et al. (2012) Single-stranded siRNAs activate RNAi in animals. *Cell* 150: 883-894.
219. Liu J, Yu D, Aiba Y, Pendergraff H, Swayze EE, et al. (2013) ss-siRNAs allele selectively inhibit ataxin-3 expression: multiple mechanisms for an alternative gene silencing strategy. *Nucleic Acids Res* 41: 9570-9583.
220. Yu D, Pendergraff H, Liu J, Kordasiewicz HB, Cleveland DW, et al. (2012) Single-stranded RNAs use RNAi to potently and allele-selectively inhibit mutant Huntington expression. *Cell* 150: 895-908.
221. Fiszer A, Ellison-Klimontowicz ME, Krzyzosiak WJ (2017) Silencing of genes responsible for polyQ diseases using chemically modified single-stranded siRNAs. *Acta Biochimica Polonica* 63: 759-764.
222. Lipinski MM, Yuan J (2004) Mechanisms of cell death in polyglutamine expansion diseases. *Curr Opin Pharmacol* 4: 85-90.
223. Shao J, Diamond MI (2007) Polyglutamine diseases: Emerging concepts in pathogenesis and therapy. *Hum mol genet* 16: R115-R123.
224. Sengupta S, Bhattacharya S (2016) Polyglutamine diseases- understanding the mechanism of pathogenesis. *J Neurol Disord* 4: 2.
225. Escalona-Rayó O, Fuentes-Vázquez P, Leyva-Gómez G, Cisneros B, Villalobos R, et al (2017) Nanoparticulate strategies for the treatment of polyglutamine diseases by halting the protein aggregation process. *Drug Dev Ind Pharm* 43: 871-888.
226. Reina CP, Nabet BY, Young PD, Pittman RN (2012) Basal and stress-induced Hsp70 are modulated by ataxin-3. *Cell Stress Chaperones* 17: 729-742.
227. Muchowski PJ, Schaffar G, Sittler A, Wanker EE, Hayer-Hartl MK, et al. (2000) Hsp70 and hsp40 chaperones can inhibit self-assembly of polyglutamine proteins into amyloid-like fibrils. *Proc Natl Acad Sci* 97: 7841-7846.
228. Vos MJ, Zijlstra MP, Kanon B, van Waarde-Verhagen MA, Brunt ER, et al. (2010) HSPB7 is the most potent polyQ aggregation suppressor within the HSPB family of molecular chaperones. *Hum Mol Genet* 19: 4677-4693.
229. Jana NR, Tanaka M, Wang Gh, Nukina N (2000) Polyglutamine length-dependent interaction of Hsp40 and Hsp70 family chaperones with truncated N-terminal Huntingtin: Their role in suppression of aggregation and cellular toxicity. *Hum Mol Genet* 9: 2009-2018.
230. Wiederholt T, Heise R, Skazik C, Marquardt Y, Jousen S, et al. (2009) Calcium pantothenate modulates gene expression in proliferating human dermal fibroblasts. *Exp Dermatol* 18: 969-978.
231. Bonanomi M, Visentin C, Natalello A, et al. (2015) How Epigallocatechin-3-gallate and tetracycline interact with the Josephin domain of Ataxin-3 and alter its aggregation mode. *Chemistry* 21: 18383-18393.
232. Bonanomi M, Natalello A, Visentin C, Pastori V, Penco A, et al. (2014) Epigallocatechin-3-gallate and tetracycline differently affect ataxin-3 fibrillogenesis and reduce toxicity in spinocerebellar ataxia type 3 model. *Hum Mol Genet* 23: 6542-6552.
233. Ravikumar B, Vacher C, Berger Z, Davies JE, Luo S, et al. (2004) Inhibition of mTOR induces autophagy and reduces toxicity of polyglutamine expansions in fly and mouse models of Huntington disease. *Nat Genet* 36: 585-595.
234. Berger Z, Ravikumar B, Menzies FM, Oroz LG, Underwood BR, et al. (2006) Rapamycin alleviates toxicity of different aggregate-prone proteins. *Hum Mol Genet* 15: 433-442.
235. Wang HL, Chou AH, Chen SY, Yeh TH, Weng YH (2011) HDAC inhibitor sodium butyrate reverses transcriptional downregulation and ameliorates ataxic symptoms in a transgenic mouse model of SCA3. *Neurobiol Dis* 41: 481-488.
236. Dokmanovic M, Clarke C, Marks PA (2007) Histone deacetylase inhibitors: Overview and perspectives. *Mol Cancer Res* 5: 981-989.
237. Haberland M, Montgomery RL, Olson EN (2009) The many roles of histone deacetylases in development and physiology: Implications for disease and therapy. *Nat Rev Genet* 10: 32-42.
238. Yi J, Zhang L, Tang B, Han W, Zhou Y, et al. (2013) Sodium valproate alleviates neurodegeneration in SCA3/MJD via suppressing apoptosis and rescuing the hypoacetylation levels of histone H3 and H4. *PLoS ONE* 8: e54792.
239. Duncan CE, An MC, Papanikolaou T, Rugani C, Vitelli C, et al. (2013) Histone deacetylase-3 interacts with ataxin-7 and is altered in a spinocerebellar ataxia type 7 mouse model. *Mol Neurodegener* 8: 42.
240. Venkatraman A, Hu Y-S, Didonna A, Cvetanovic M, Krbanjevic A, et al. (2014) The histone deacetylase HDAC3 is essential for Purkinje cell function, potentially complicating the use of HDAC inhibitors in SCA1. *Hum Mol Genet* 23: 3733-3745.

### OMICS International: Open Access Publication Benefits & Features

#### Unique features:

- Increased global visibility of articles through worldwide distribution and indexing
- Showcasing recent research output in a timely and updated manner
- Special issues on the current trends of scientific research

#### Special features:

- 700+ Open Access Journals
- 50,000+ editorial team
- Rapid review process
- Quality and quick editorial, review and publication processing
- Indexing at major indexing services
- Sharing Option: Social Networking Enabled
- Authors, Reviewers and Editors rewarded with online Scientific Credits
- Better discount for your subsequent articles

Submit your manuscripts as E- mail: [www.omicsonline.org/submit](http://www.omicsonline.org/submit)

**Citation:** McIntosh CS, Aung-Htut MT, Fletcher S, Wilton SD (2017) Polyglutamine ataxias: From Clinical and Molecular Features to Current Therapeutic Strategies. *J Genet Syndr Gene Ther* 8: 319. doi: [10.4172/2157-7412.1000319](https://doi.org/10.4172/2157-7412.1000319)

# Chapter 5 – Published

## Research Article 1

McIntosh, C. S.\* , Aung-Htut, M. T., Fletcher, S., & Wilton, S. D. (2019). **Removal of the Polyglutamine Repeat of Ataxin-3 by Redirecting pre-mRNA Processing**. *International Journal of Molecular Sciences*, 20(21), 5434.

### First Authored

**Author Contributions:** Conceptualisation, C.S.M and M.T.A-H.; Methodology, C.S.M., M.T.A-H. and S.D.W.; Formal Analysis: C.S.M.; Investigation, C.S.M.; Writing, C.S.M., M.T.A-H., S.F. and S.D.W.; Supervision, M.T.A-H., S.F. and S.D.W.; Resources, S.F. and S.D.W.; Funding Acquisition, S.F. and S.D.W.



Article

# Removal of the Polyglutamine Repeat of Ataxin-3 by Redirecting pre-mRNA Processing

Craig S. McIntosh <sup>1,2</sup> , May Thandar Aung-Htut <sup>1,2</sup> , Sue Fletcher <sup>1,2</sup> and Steve D. Wilton <sup>1,2,\*</sup>

<sup>1</sup> Molecular Therapy Laboratory, Centre for Molecular Medicine and Innovative Therapeutics, Murdoch University, Health Research Building, Discovery Way, Murdoch WA 6150, Australia; C.McIntosh@murdoch.edu.au (C.S.M.); M.Aung-Htut@murdoch.edu.au (M.T.A.-H.); s.fletcher@murdoch.edu.au (S.F.)

<sup>2</sup> Perron Institute for Neurological and Translational Science, Centre for Neuromuscular and Neurological Disorders, The University of Western Australia, Nedlands WA 6009, Australia

\* Correspondence: s.wilton@murdoch.edu.au

Received: 10 October 2019; Accepted: 29 October 2019; Published: 31 October 2019



**Abstract:** Spinocerebellar ataxia type 3 (SCA3) is a devastating neurodegenerative disease for which there is currently no cure, nor effective treatment strategy. One of nine polyglutamine disorders known to date, SCA3 is clinically heterogeneous and the main feature is progressive ataxia, which in turn affects speech, balance and gait of the affected individual. SCA3 is caused by an expanded polyglutamine tract in the ataxin-3 protein, resulting in conformational changes that lead to toxic gain of function. The expanded glutamine tract is located at the 5' end of the penultimate exon (exon 10) of *ATXN3* gene transcript. Other studies reported removal of the expanded glutamine tract using splice switching antisense oligonucleotides. Here, we describe improved efficiency in the removal of the toxic polyglutamine tract of ataxin-3 in vitro using phosphorodiamidate morpholino oligomers, when compared to antisense oligonucleotides composed of 2'-O-methyl modified bases on a phosphorothioate backbone. Significant downregulation of both the expanded and non-expanded protein was induced by the morpholino antisense oligomer, with a greater proportion of ataxin-3 protein missing the polyglutamine tract. With growing concerns over toxicity associated with long-term administration of phosphorothioate oligonucleotides, the use of a phosphorodiamidate morpholino oligomer may be preferable for clinical application. These results suggest that morpholino oligomers may provide greater therapeutic benefit for the treatment of spinocerebellar ataxia type 3, without toxic effects.

**Keywords:** spinocerebellar ataxia type 3; antisense oligonucleotides; exon skipping; ataxin-3; polyglutamine; phosphorodiamidate morpholino oligomer

## 1. Introduction

Spinocerebellar ataxia type 3 (SCA3) is a progressive, typically late-onset autosomal dominant neurodegenerative disease [1]. SCA3 is one of a larger group of diseases, termed, the polyglutamine (polyQ) diseases [2,3]. These diseases all share a common pathogenic mechanism; an expanded CAG repeat in the coding sequence of nine genes, and in the case of SCA3, the CAG expansion is located in the penultimate exon (exon 10) of *ATXN3* (14q32.1) [4]. Healthy individuals have a stable repeat range of 7–44, while SCA3 patients usually have 54 or more repeats. SCA3 is known to have an unstable pre-mutation range of 45–53 repeats, and while these individuals are typically asymptomatic, they have the ability to pass on an expanded allele in what is known as ‘genetic anticipation’. As with other polyQ diseases, the pathogenic severity and age of onset is typically inversely correlated to the size of the expansion: the larger the expansion, the more severe the pathogenesis and the earlier the

age of onset [5]. The *ATXN3* encodes for a 361 amino acid (aa), 45 kDa protein (ENST00000558190.6), termed ataxin-3. The ataxin-3 protein is known to act as an isopeptidase and is well documented in cell ubiquitination, as well as proteasomal protein degradation [2,6].

The expanded CAG repeat located in exon 10 of *ATXN3* results in the addition of an extended glutamine tract in ataxin-3, directly leading to conformational changes that give the protein a toxic gain of function(s), as well as subjecting the protein to formation of neuronal nuclear inclusions [7]. Although SCA3 is clinically heterogeneous in presentation, the main feature is progressive ataxia, which in turn affects speech, balance and gait of the affected individual [3]. Despite arising from a single variant gene, the pathogenesis of SCA3 has been difficult to characterize, as several toxic pathways and mechanisms have been proposed to play a role in the disease.

Several studies that use antisense oligonucleotides (AOs) to modify the mRNA of *ATXN3* by attempting to remove the CAG containing exon have been conducted [8–10]. Until now, van Roon-Mom and colleagues have published two reports detailing the removal of the CAG containing exon in the *ATXN3* transcript [8,9]. These studies show removal of the CAG containing exon, and production of a functional truncated protein using a modified 2'-*O*-methoxy-ethyl nucleotide (2'-MOE) on a phosphorothioate (PS) backbone. Growing concerns regarding safety of PS oligonucleotides, such as hepatotoxicity, liver necrosis and altered regulation of protein and metabolic pathways [11–13] and thus, the consequences and safety of long-term exposure to AOs on a PS backbone [11–16] may limit applicability of these compounds. Phosphorothioate backbone AOs have resulted in severe injection site reactions, thrombocytopenia and renal toxicity in clinical studies [16,17]. An *in vitro* study by Flynn et al. (2018), demonstrated severe, sequence-independent backbone-specific effects of 2'-*O*-methyl modified bases on a phosphorothioate backbone (2'-Me PS) AOs, including altered distribution of nuclear proteins, the appearance of abnormal but highly structured nuclear inclusions and aggregates and global disturbance of the transcriptome [18].

An AO chemistry currently in clinical use is the phosphorodiamidate morpholino oligomer (PMO) [19]. This chemistry has a backbone of methylene morpholine rings, with phosphorodiamidate group linkages and an oligomer of this chemistry has been granted accelerated approval by the FDA. *Eteplirsen* (Sarepta Therapeutics, Ma) is designed to excise dystrophin exon 51 during pre-mRNA processing to restore functional protein expression in a subset of boys with Duchenne muscular dystrophy (DMD). The drug restored modest dystrophin expression in patient muscle where previously no, or only traces of dystrophin were evident [20]. The PMO chemistry is reported to have excellent biological stability, and to be safe and well tolerated, with no serious adverse effects reported in the *Eteplirsen* treated children and young men to date [21,22].

Here, we describe efficient removal of the CAG containing exon 10 to produce a truncated ataxin-3 protein, lacking the polyglutamine tract, an isoform reported by Toonen et al. (2017) to be functionally active [8]. Our study shows that by using the PMO chemistry, not only is exon 10 skipping enhanced at the RNA level, but also significant downregulation of the protein with higher number of glutamine repeats and an increase in production of the truncated protein is observed, when compared to the use of the 2'-Me PS AO chemistry. With robust splice switching efficiency and an established long-term safety profile, the PMO oligomers described here are presented as lead pre-clinical candidates to treat SCA3 patients.

## 2. Results

### 2.1. *ATXN3* Transcript and Strategic Removal of Exons

The predominant full-length *ATXN3* transcript (ENST00000558190.6) includes 11 exons and is approximately 7000 bases in length (Figure 1) and encodes the 361 aa ataxin-3 (Figure 1). The initial focus of this study was to utilise splice switching AOs to remove the polyQ containing exon from the mRNA transcript and thus create an internally truncated protein, missing the toxic polyQ tract. AOs were designed to remove exons 9 and 10 in order to keep the reading frame intact, with the

locations of the AO annealing sites illustrated in Figure 1. Removal of the polyQ tract as a therapeutic strategy is plausible, as the main functional domain (Josephin Domain) is located at the N-terminus of the protein, encoded by exons 1–7. Other vital functional domains include the ubiquitin interacting motifs (UIM1–3), as well as the nuclear localisation signal (Figure 1).

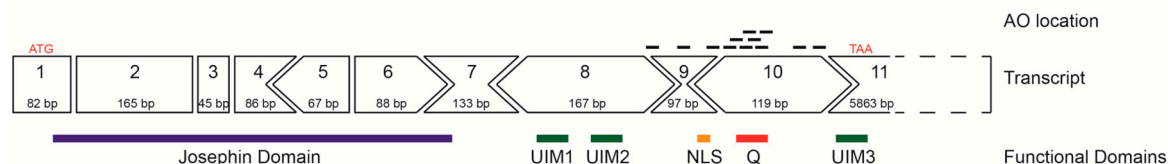


**Figure 1.** Schematic representation of the *ATXN3* gene transcript (ENST00000558190.6) and reading frame, showing location of encoded protein (361 amino acid) domains below the exon map. In-frame exons are represented as rectangles, whereas those bounded by partial codons are represented with chevron sides. Exonic/intronic locations of antisense oligonucleotides designed to redirect *ATXN3* pre-mRNA processing are represented as black bars above the transcript.

## 2.2. Evaluation of AOs to Induce Exon 9 and 10 Skipping from the *ATXN3* Transcript

Initially, several 2'-Me PS AOs were designed to target exon 9 and exon 10 simultaneously for removal from the *ATXN3* transcript (Table 1), in an effort to exclude the polyQ domain and maintain the open reading frame of the transcript and the entire 3'UTR. An unrelated control AO that does not anneal to any transcript was included in all transfections as a negative experimental control. All AOs were transfected into SCA3 patient-derived dermal fibroblasts (74Q; 24Q) at various concentrations (400, 200, 100 nM) for 24 h before RNA extraction and RT-PCR to assess exon skipping. Gel fractionation of the RT-PCR amplicons revealed shorter products arising from exclusion of either exon 9 ( $\Delta 97$  bp) or exon 10 ( $\Delta 119$  bp) (Figure 2A), confirmed by Sanger sequencing (Figure 2B). Efficient exon skipping was achieved with AOs targeting exon 9 at concentrations as low as 100 nM.

**Table 1.** Sequences and coordinates of AOs employed in this study.

Name	Sequence (5'–3')
ATXN3 H9A (– 22 + 03)	UACCUGAAAACAAAACACAACACAA
ATXN3 H9A (+ 38 + 62)	UUCUGAAGUAAGAUUUGUACCUGAU
ATXN3 H9D (+ 20 – 05)	UUUACUUUCAAAGUAGGCUUCUCG
ATXN3 H10A (– 17 + 08)	GCUGCUGUCUGAAACAUCAAAAGU
ATXN3 H10A (+ 10 + 34) *	CUGCUGCUGCUGCUGUUGCUGCUUU
ATXN3 H10A (+ 35 + 59) *	GUCCUGAUAGGUCCCCCUGCUGCUG
ATXN3 H10D (+ 24 – 01) *	CCUAGAUCACUCCCAAGUGCUCUG
ATXN3 H10A (+ 05 + 29)	GCUGCUGCUGUUGCUGCUUUUGCUG
ATXN3 H10A (+ 15 + 39) *	UGCUGCUGCUGCUGCUGCUGUUGCU
ATXN3 H10A (+ 30 + 54)	GAUAGGUCCCCCUGCUGCUGCUGCU
ATXN3 H10A (+ 40 + 64)	ACUCUGUCCUGAUAGGUCCCCCUGC
ATXN3 H10A (+ 66 + 90)	GUGGCUGGCCUUUCACAUGGAUGUG
ATXN3 H10A (+ 03 + 22) #/*	CUGUUGCUGCUUUUGCUGCU
Control AO @	GGAUGUCCUGAGUCUAGACCCUCCG
Gene Tools Control	CCTCTTACCTCAGTTACAATTTATA

\* These sequences were selected for synthesis as the phosphorodiamidate morpholino oligomer chemistry (PMO). PMO oligomers are synthesised with Thymine (T) rather than Uracil (U). # Sequence from Toonen et al. (2017) [8].

@ unrelated sham control sequence. GeneTools Control; commercially available from GeneTools.

Excising exon 10 alone removes the polyQ coding motif from the transcript and introduces a novel stop codon early in exon 11, resulting in the loss of 69 aa from the C-terminus of ataxin-3 (ENST00000558190.6). The consequence of excluding this block of amino acids leads to the loss of the UIM3 domain (Figure 2C,D). However, this exact isoform has been reported by Toonen et al. (2017) and from their data, it appeared that the loss of UIM3 does not adversely affect the ubiquitin binding capability of ataxin-3 [8]. The most efficient exon skipping was induced at a transfection concentration of 400 nM, with little cell death evident. At transfection concentrations of 600nM and greater, toxicity associated with 2'-Me PS AO cationic lipoplexes caused almost 100% cell death (data not shown).

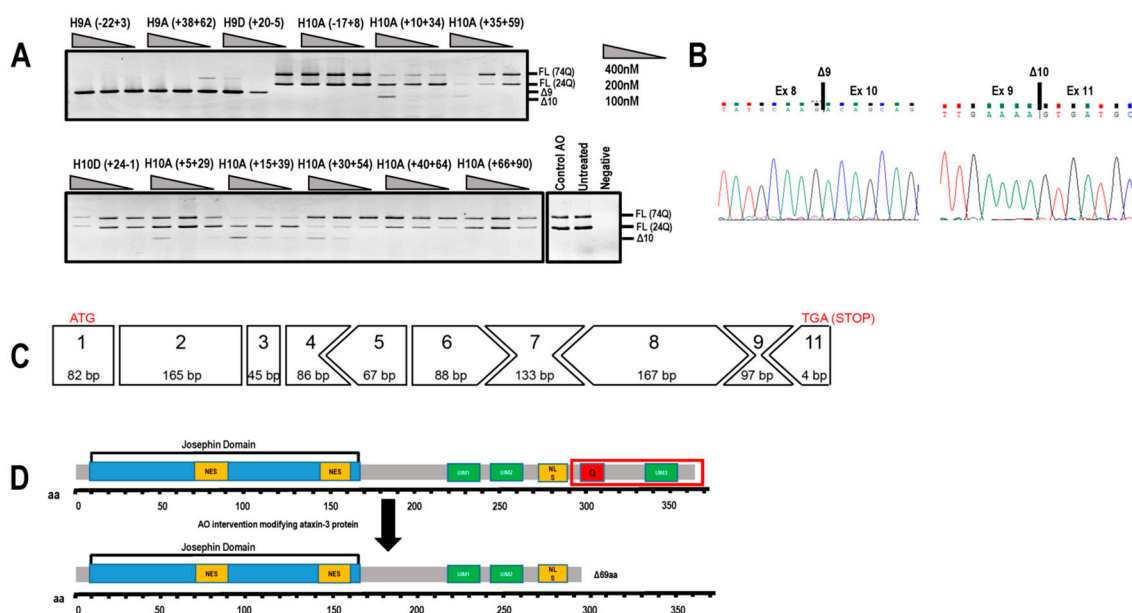


**Figure 2.** Evaluation of antisense oligonucleotides (AOs) designed to alter *ATXN3* transcript structure. (A) Screening of 2'-Me phosphorothioate (PS) AOs targeting exon 9 or exon 10 for removal. AOs were transfected as lipoplexes at three concentrations, 400, 200, 100 nM, and after RT-PCR and gel fractionation, products representing the full-length (FL 74Q; FL 24Q), exon 9-skipped ( $\Delta 9$ , 384 bp) and exon 10-skipped ( $\Delta 10$ , 362bp) transcripts were identified. (B) Sanger sequencing of the RT-PCR products generated by skipping of exon 9 or 10, shows the junction between exon 8 and 10, and exons 9 and 11, respectively. (C) Although removal of exon 10 alters the reading frame, the residue encoded by the exon 9 and 11 junction codon is synonymous (lysine). Immediately following this lysine is an in-frame termination codon (TGA). (D) Removal of exon 10 from the *ATXN3* coding sequence results in a truncated, 291 aa protein (missing the terminal 69 aa) of approximately 34 kDa that is reported to be functional. aa = amino acid; NES = nuclear export signal; NLS = nuclear localisation signal; UIM = ubiquitin interacting motif. Q = polyglutamine tract.

### 2.3. PMO Mediated Exon Skipping Reduces Full-Length Ataxin-3 Proteins and Induces a Truncated Ataxin-3 Isoform

Following initial screening of AOs to remove exon 10, this strategy was deemed most appropriate due to the need to only skip one exon to generate a functional ataxin-3 isoform. Equimolar amounts of two AOs targeting *ATXN3* exon 10 were combined into cocktails and evaluated, as we have found that the efficiency of exon removal can be greatly enhanced by such strategies (Table 2) [23,24]. All cocktails reported were co-transfected at equal molar AO (1:1) ratios. The transfection concentration of 400 nM (200 nM of each AO) was selected and as expected, some AO cocktails induced more efficient exon 10 skipping than single AO treatments (Figure 3A). The lead sequences revealed by the AO screening pipeline were synthesised as PMOs (Table 1), since this chemistry performs better both in vitro and in vivo when compared to 2'-Me PS AOs [20,23,25].

To investigate the effect of exon 10 skipping and consequent modification of ataxin-3 protein, SCA3 patient fibroblasts were transfected with the lead candidate cocktails, prepared as 2'-Me PS AOs or PMOs, and RNA and protein were isolated 48 h following transfection. The unrelated control AO and GeneTools control PMO were included. Gel electrophoresis showed that the 2'-Me PS AO transfection consistently produced lower levels of exon 10 skipping when compared to the PMO transfections, with the exception of cocktail 22 (Figure 3A,B). The 2'-Me PS AO cocktail 22 induced an approximate 25% higher percentage of exon 10 skipping, however, this did not translate to detectable changes in the modified ataxin-3 protein (Figure 3C). Consistent with our previous experience [26], 2'-Me PS AOs have a modest ability to generate the truncated ataxin-3 isoform in vitro, with cocktail 21 resulting in about 20% of the total ataxin-3 protein being truncated (Figure 3C). Most of the 2-Me PS AO transfections downregulated ataxin-3 protein production, which was evident when normalised to the sample from the control AO transfection (Figure 3C).

**Table 2.** AO cocktails containing two different, non-overlapping exon 10 sequences. Each cocktail comprises of a 1:1 molar ration of each AO.

Cocktail Number	AO Combination
Cocktail 19	ATXN3 H10A (+ 10 + 34)
	ATXN3 H10A (+ 35 + 59)
Cocktail 20	ATXN3 H10A (+ 10 + 34)
	ATXN3 H10D (+ 24 – 01)
Cocktail 21	ATXN3 H10A (+ 35 + 59)
	ATXN3 H10D (+ 24 – 01)
Cocktail 22	ATXN3 H10A (+ 15 + 39)
	ATXN3 H10D (+ 24 – 01)
Cocktail 23	ATXN3 H10A (+ 05 + 29)
	ATXN3 H10D (+ 24 – 01)
Cocktail 24	ATXN3 H10A (+ 30 + 54)
	ATXN3 H10D (+ 24 – 01)

In contrast, the PMOs induced downregulation of both expanded and non-expanded proteins when the data was normalised to the full-length isoforms from cells transfected with the Gene Tools control PMO ( $p$  value < 0.001) (Figure 3D). Downregulation of the full-length isoform was greatest after transfection with cocktail 21, with an average 5.49-fold reduction of full-length isoforms (Figure 3C,D). While full-length ataxin-3 downregulation was induced by all PMO cocktails, the truncated isoform was the predominant isoform when compared to the both full-length proteins (Figure 3C,D). Although an exact comparison may seem biased towards PMO treatments, due to the 50-fold discrepancy in transfection concentrations between the two chemistries, 2'-Me PS AO are negatively charged, and thus can be complexed with a lipid-based transfection agent (Lipofectamine 3000) for efficient cell uptake at much lower concentrations. The PMOs are uncharged and cannot be delivered into the cells under equivalent conditions.

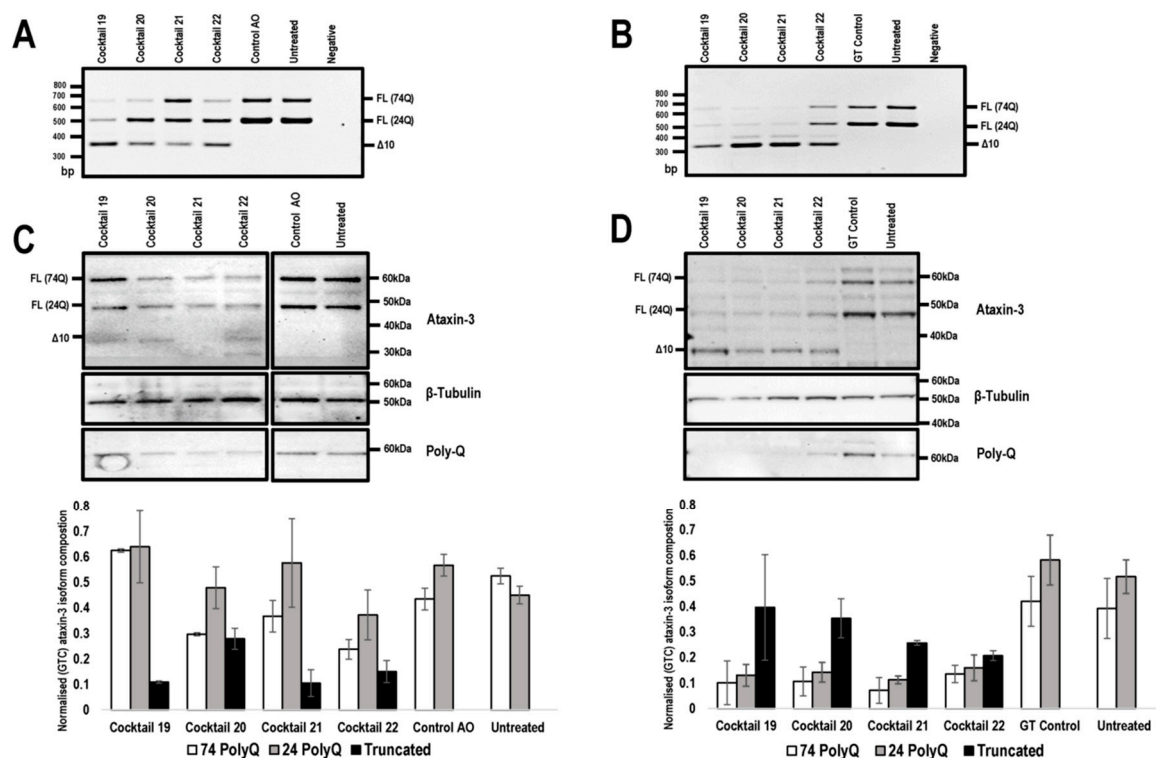


**Figure 3.** Comparison of *ATXN3* exon 10 skipping in patient cells, transfected with 2'-Me PS AOs and PMOs. Cells were harvested 48 hr following transfection for protein and RNA analysis. Agarose gel fractionation of *ATXN3* amplicons, following 2'-Me PS AO (A) and PMO (B) cocktail transfections at concentrations of 400 nM and 20  $\mu$ M, respectively shows full-length (FL 74Q; FL 24Q) and induced transcript products after skipping of exon 10 ( $\Delta 10$ ). Ataxin-3 protein was analysed by Western blotting following 2'-Me PS AO (C) and PMO (D) cocktail transfection at a concentration of 400 nM and 20  $\mu$ M, respectively. The disease-causing 74Q protein is approximately 60 kDa, the protein encoded by the healthy allele is approximately 48 kDa and the  $\Delta 10$  encoded protein, 34 kDa. Beta-Tubulin was used as a loading control. The samples were also probed with an anti-polyglutamine antibody to identify the pathogenic stretch of glutamines in the ataxin-3 protein. Densitometric analysis performed on the Western blots are shown below the blots (means plus error bars. Error bars = standard deviation,  $n = 3$ ). Samples are normalised to the GT control. (FL = full-length,  $\Delta 10$  = exon skipped product, GT = Gene Tools control PMO, Q = glutamine, PolyQ = polyglutamine).

#### 2.4. 2'-O-Methyl PS AOs Induce Sequence Independent Sequestration of Paraspeckle Protein NONO

Recently, a number of reports have described sequence-independent off-target effects associated with the phosphorothioate backbone, including non-specific interactions resulting in recruitment of paraspeckle and other nuclear proteins and formation of paraspeckle-like structures [12,15]. To establish if the 2'-Me PS ataxin-3 specific AOs can alter subcellular protein distribution, or induce nuclear inclusions, primary healthy human fibroblasts were transfected for 24 h and subsequently immunolabelled for the paraspeckle protein, NONO. Three *ATXN3* specific AOs, as well as the commercially available Gene Tools control AO, were tested as 2'-Me PS AOs and as PMOs to determine if any off-target effects are backbone specific and/or sequence dependent (Figure 4).

Immunofluorescent staining of NONO showed that all 2'-Me PS AOs sequestered NONO, at various subcellular locations (Figure 4A), while the identical sequences synthesised as PMOs had no such effects (Figure 4B). Consistent with the report by Flynn et al. (2018) [18], the Gene Tools control sequence seemed to induce the highest amount of NONO-containing nuclear inclusions when applied as a 2'-Me PS AO. All 2'-Me PS sequences tested in this study did induce NONO inclusions in most cells, some inclusions were located within the nucleus while others appear to be peri-nuclear or



distributed in the cytoplasm (Figure 4A). This suggests that the PS backbone is directly responsible for the sequestration of NONO, while such effects were not observed when the PMO chemistry was used at higher concentrations over the same time period.

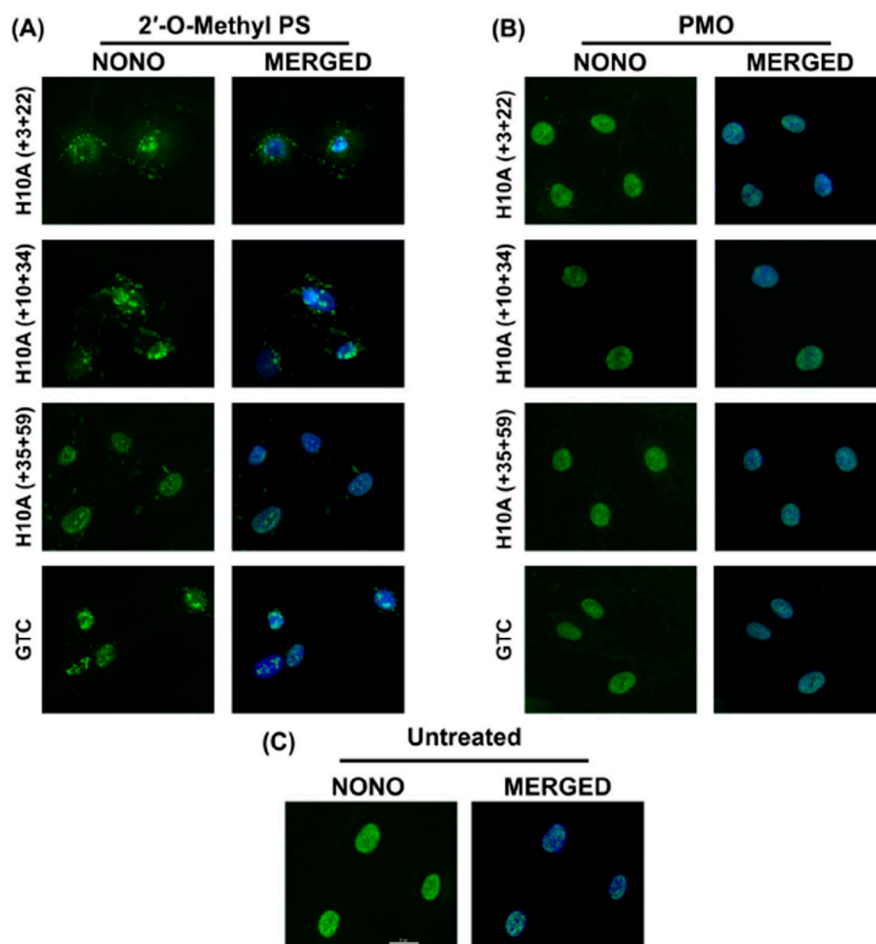


**Figure 4.** Immunofluorescent labelling of paraspeckle protein NONO in transfected healthy fibroblasts. (A) Immunolabelling of primary normal human fibroblasts following transfection with various 2'-Me PS AO lipoplexes at a concentration of 400 nM. Cells were fixed 24 hrs following transfection. Staining of the paraspeckle protein NONO shows sequestration and aggregation of NONO in various subcellular locations. (B) Immunofluorescent labelling of NONO following Endoportor transfection of primary normal human fibroblasts with various PMOs at concentrations of 10 or 5  $\mu$ M. Cells were fixed 24 hrs following transfection. (C) Untreated (control) showing endogenous subcellular distribution of NONO. GTC = Gene Tools Control sequence. Scale bar is 20  $\mu$ m.

In addition, we compared the efficiencies of exon 10 skipping mediated by the PMOs shown in Figure 4. The H10A (+ 03 + 22) AO that induced *ATXN3* exon 10 skipping was reported by Toonen et al. (2017) [8], while the other two PMOs were identified in this study (Figure 5). It can be seen that H10A (+ 10 + 34) out-performed H10A (+ 03 + 22) and H10A (+ 35 + 59) at both 10 and 5  $\mu$ M concentrations (Figure 5). Although H10A (+ 03 + 22) was synthesised as a PMO, the study conducted by Toonen et al. (2017) used the MOE chemistry and thus a direct comparison cannot be made to the published data.

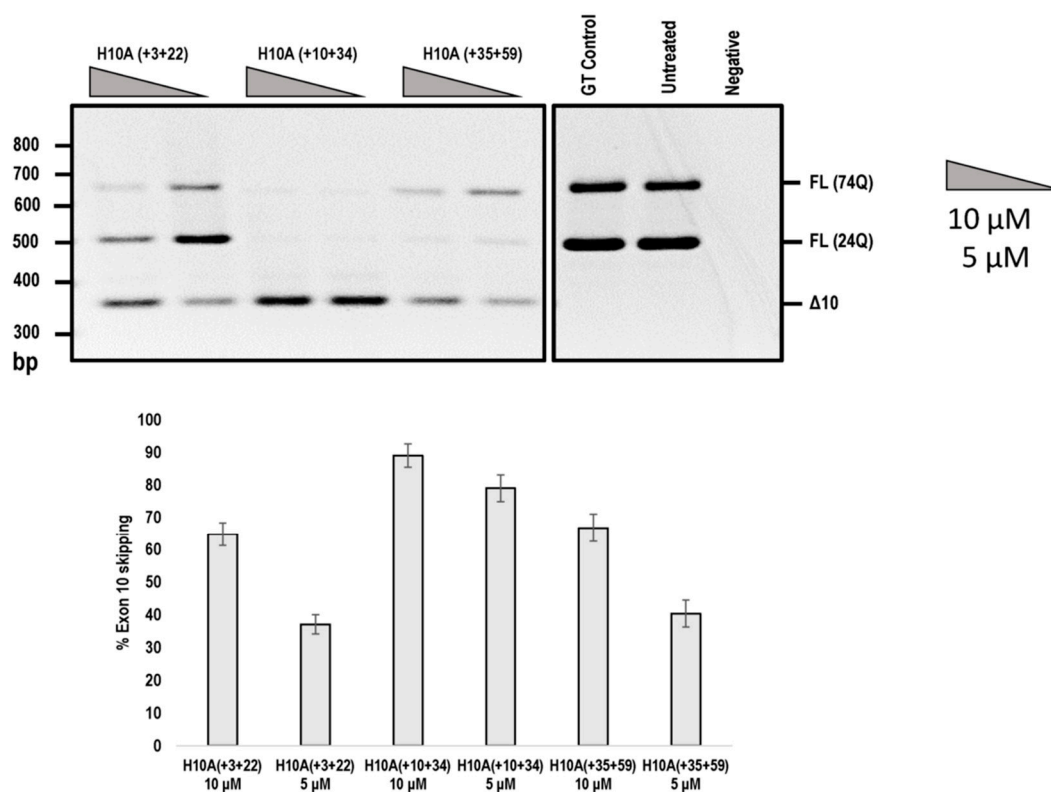


**Figure 5.** Agarose gel fractionation of *ATXN3* transcript products from SCA3 patient derived fibroblasts, following PMO transfection at concentrations of 10 and 5  $\mu\text{M}$ . Fractionation shows full-length products (FL 74Q; FL 24Q) and removal of exon 10 ( $\Delta 10$ ) (product size of 362 bp). Densitometric analysis of the gel image is shown below the gel (means plus error bars. Error bars = standard deviation,  $n = 3$ ). (FL= full-length,  $\Delta 10$  = exon skipped product, GT = Gene Tools control PMO, Q = glutamine).

### 3. Discussion

The pathogenesis of SCA3 is attributed to the expanded polyQ tract that confers a toxic gain of function to the protein [4,27,28]. Therefore, the removal of the polyQ tract may provide a therapeutic strategy to delay onset or reduce severity of SCA3. As a consequence of exon 10 removal, the induced ataxin-3 isoform is missing the UIM3 domain. As reported by van Roon-Mom and colleagues, the 291aa, 34kDa protein, although missing the UIM3 domain, still binds ubiquitin in a similar manner to the full-length ataxin-3 [8]. Additionally, two naturally occurring isoforms lacking UIM3 have been shown to actually have higher rates of deubiquitination, relative to the major isoform containing the UIM3 [29]. With recent FDA approvals of AO therapeutics to restore gene expression to treat spinal muscular atrophy and DMD, pre-mRNA splicing intervention could be applied to downregulate or modify expression of toxic-gain-of-function diseases. This proof of concept study may be relevant to other polyQ diseases where the polyQ tract is found in a removable and dispensable exon. However, this would need to be the subject of functional studies to determine the effect of removing regions of other polyQ proteins. For example, Huntington's disease is unlikely to be amenable to exon skipping, as the polyQ tract is located in the initial exon [3]. Here, we show removal of *ATXN3* exon 10, and consequently the polyQ repeat from the normal and expanded ataxin-3 protein, using two different AO chemistries. Additionally, these in vitro experiments demonstrate proof of concept and can provide pre-clinical candidate molecules for eventual in vivo administration. Dosage regimens, clearance rates and delivery methods will need to be optimised to assess the effects of PMOs compared to other chemistries.

We confirm apparent off-target effects of AOs on a PS backbone, transfected in vitro. The 2'-Me PS AO targeting *ATXN3* induced sequestration of the paraspeckle protein NONO, while no such

consequences were observed when cells were treated with the same sequences synthesised as PMOs, in keeping with our previously reported findings and those of the Crooke group [12,13,18]. While these studies were only conducted in vitro, van Roon-Mom and colleagues described activation of the innate immune system as the result of intracerebroventricular administration of 2'-Me AOs into mice [15]. Marked upregulation of *Oasl2* and *Bst2* proteins, both of which are involved in interferon signalling, particularly in response to viral infections [30–32], was a major finding [15]. Several other studies have described adverse effects of AOs on a PS backbone, including thrombocytopenia, severe injection site reaction, cytotoxicity and induction of double-stranded DNA breaks [33–35].

The safety of PMOs in the clinic is evident from long term treatment (240 weeks) of DMD patients with the PMO *Eteplirsen*. No evidence of serious adverse reactions were reported [33,36], while the same cannot be said for the 2'-Me PS AO drug *Drisapersen*. Every drug on a the PS backbone tested to date has been reported to elicit off-target effects [33,36,37]. This may be explained by the crucial difference that PMOs, unlike 2'-Me PS AOs, are uncharged and therefore do not readily interact with proteins [38–40]. We, and others have shown that PMOs generally outperform 2'-Me PS AOs for splice switching applications [37,41], possibly due to the superior stability, specificity and binding affinity of PMOs, compared to 2'-Me PS AOs [38,40]. Although PMO-treated cells were transfected at higher concentrations than the 2'-Me PS AOs that are transfected as lipoplexes, these high concentrations are required for gymnotic PMO uptake but were nevertheless well tolerated by cells. Although the delivery of 2'-Me PS AOs is greatly enhanced through the use of cationic liposome preparations, concentrations of 600 nM and above lead to widespread cell death in vitro.

Although PMOs outperformed 2'-Me PS AOs in vitro, the PMOs do have several limitations. When administered in vivo, PMOs are rapidly cleared by the renal system and must therefore be dosed at relatively high levels. This is compounded by poor uptake and delivery of PMOs into target tissues [42]; due to their uncharged nature PMOs cannot readily move through cellular membranes [43]. These limitations are currently subject to extensive research in developing technologies, such as conjugation to cell penetrating peptides and various physical and chemical methods to increase uptake and reduce the rapid clearance [42,44]. Despite these draw backs, from our in vitro data we believe PMOs to have greater therapeutic potential for SCA3 and other diseases, such as muscular disorders that are amenable to splice switching [45]. In saying that, it is important to note that in vitro studies and in vivo animal models do not always translate into successful treatments for patients. This is mainly due to sequence differences in the cases of in vivo models, with a prime example being a mouse model of Duchenne muscular dystrophy, whereby subtle changes in sequences can drastically affect AO efficiency [46].

We show significant knockdown of the full-length ataxin-3 isoforms encoded by both alleles, as well as modification of the ataxin-3 protein to produce a truncated protein, missing the polyQ tract. While the impact of global ataxin-3 knockdown is under debate [8,47,48], the role of ataxin-3 in the ubiquitin-proteasome machinery is well-established, and there are conflicting views as to whether ataxin-3 is essential in maintaining normal cellular function [3,49,50]. Figiel and colleagues (2011) created a functional *Atn3* knockout mouse that showed no obvious phenotype, with a life span comparable to that of the wildtype mouse [48]. Another group reported similar findings, with no adverse effects on *Atn3* knockout mouse life span or fertility and no apparent abnormalities, but they did report apparent increased anxiety and increased levels of ubiquitinated proteins in the *Atn3* knockout model [51]. Separately, AO treated transgenic SCA3 mice (expressing a human full-length, 84Q *ATXN3* gene), showed that knockdown of ataxin-3 was well tolerated with no signs of astrogliosis or microgliosis [52]. However, our data show a high proportion of the truncated protein as a consequence of *ATXN3* exon 10 skipping, and thus this may provide sufficient functional protein to support ubiquitination and protein degradation [53]. With that being said, the Paulson group conducted in vitro experiments to assess the effects of *ATXN3* knockout using *Atn3* null mouse embryonic stem cells. They found that the loss of *Atn3* caused dysregulation in signalling pathways that included depression of Wnt and BMP4 pathways, as well as elevated growth factor pathways [54].

In contrast, the same group showed that knockdown of an expanded *ATXN3* in a transgenic mouse model (MJD-Q84.2) using a 2'-MOE AO rescued the phenotype with no apparent adverse effects, thus suggesting *in vivo* treatment and knockdown of *ATXN3* may be feasible [55]. Moreover, in the current study it is believed that the removal of the CAG repeat alone without removal of key functional domains would result in limited downstream effects. Further studies investigating the long-term impact of ataxin-3 knockdown *in vivo* will be required to determine if skipping of exon 10 has potential as a treatment for SCA3.

In conclusion, while this study was a preliminary *in vitro* investigation, PMOs consistently produced a significantly higher proportion of the truncated protein, missing the toxic polyQ repeat, relative to 2'-Me PS AOs. With increasing numbers of AO therapeutics being approved for clinical use, our results suggest that the lead PMOs may be an attractive therapeutic option for the treatment of spinocerebellar ataxia type 3.

## 4. Materials and Methods

### 4.1. AO Design and Synthesis

Splice-switching AOs were designed to target and anneal to splicing motifs at the intron/exon boundaries as well as predicted exon splice enhancer sequences identified using the web-based application, *Human Splicing Finder 3.0* [56]. In addition, specificity of the AOs for the *ATXN3* target motifs was confirmed via BLAST analysis to identify potential off-target annealing. 2'-Me PS AOs were obtained from TriLink Biotechnologies (Maravai LifeSciences, San Diego, CA, USA), while PMOs were purchased from Gene Tools, LLC (Philomath, OR, USA). Nomenclature of AOs is according to Aung-Htut, McIntosh et al. (2019) and indicates gene, exonic target with annealing coordinates relative to the intron:exon:intron arrangement (Tables 1 and 2) [57].

### 4.2. Cell Culture

Primary dermal fibroblasts were cultured from a skin biopsy taken from a healthy volunteer, after informed consent, and the project received approval from the Human Research Ethics Committee at Murdoch University (approval number, 2013/156). Healthy human fibroblasts were cultured in Dulbecco's Modified Essential Medium (Gibco; Life Technologies, Melbourne, Australia), supplemented with 15% fetal bovine serum (FBS) (Scientifix, Cheltenham, Australia). The SCA3 fibroblast cell line (GM6151b) was obtained from Coriell Cell Repositories (Camden, NJ, USA) and cultured in minimal essential medium (MEM), supplemented with 15% FBS (Scientifix), 1% Glutamax (Gibco) and 1x penicillin/streptomycin.

### 4.3. Transfection

All cell strains were either transfected with 2'-Me PS AO, Lipofectamine 3000 (Life Technologies) lipoplexes in Opti-MEM (Gibco) according to manufacturer's instructions, or with PMOs, using Endo-Porter (Gene Tools, LLC) according to manufacturer's instructions in MEM (Gibco), supplemented with 7.5% FBS (Scientifix) [58]. Cells were harvested 24 h following transfection for transcript analysis or after 48 h for protein studies.

### 4.4. RNA Extraction and RT-PCR Assays

Total RNA was extracted using the MagMax™ nucleic acid isolation kits (ThermoFisher Scientific, Melbourne Australia) in accordance with the manufacturer's instructions. Transcripts were amplified using the one-step SuperScript® III reverse transcriptase, with 50 ng of total RNA as the template. To amplify the *ATXN3* transcript, exon 7-F (5'GTCCAACAGATGCATCGACCAA3') and exon 11-R (5'AGCTGCCTGAAGCATGTCTTCTT3') primers were used (Gene Works, Adelaide, Australia). The cycling reactions included 55 °C for 30 min, 94 °C for 2 min, with 28 cycles of 94 °C 30s, 55 °C 30s and 68 °C 1.5 min. The PCR products were fractionated on 2% agarose gels in Tris-Acetate-EDTA buffer.

#### 4.5. Western Blotting

Cell lysates (~800,000 cells) were prepared in 100  $\mu$ L of 125 mM Tris-HCl, pH 6.8, 15% SDS, 10% Glycerol, 1.25  $\mu$ M PMSF (Sigma-Aldrich, Sydney, Australia) and 1  $\times$  protease inhibitor cocktail (Sigma-Aldrich) and subsequently sonicated 6 times (1 s pulses) prior to the addition of bromophenol blue (0.004%) and dithiothreitol (2.5 mM). Samples were heated at 94  $^{\circ}$ C for 5 min, cooled on ice and centrifuged at 14,000 $\times$  g for 2 min before loading onto the gel.

Total protein (25  $\mu$ g), determined by a BCA assay (ThermoFisher Scientific), was loaded onto NuPAGE Novex 4–12% Bis/Tris gradient gels (ThermoFisher Scientific). Samples were subsequently fractionated at 200 volts for one hour. Proteins were then transferred onto a Pall Fluoro Trans<sup>®</sup> polyvinylidene fluoride membrane at 350 mA for one hour. Following blocking in 5% skim milk in TSBT for one hour, the membrane was incubated with either mouse monoclonal anti-ataxin-3 antibody (Millipore, cat. No. MAB5360, Billerica, USA) at 1:500 dilution or rabbit polyclonal anti- $\beta$ -tubulin antibody (ThermoFisher Scientific, cat. No. PA1-41331) at 1:1000 dilution in 5% skim milk in TSBT, overnight at 4  $^{\circ}$ C. For detection of pathogenic polyQ stretches, the membrane was probed with mouse monoclonal anti-polyQ antibody (Millipore, cat. no. MAB1574, Billerica, USA), at 1:1000 dilution in 5% skim milk in TSBT, overnight at 4  $^{\circ}$ C.

For immunodetection, polyclonal goat anti-rabbit or anti-mouse immunoglobulins/HRP (Dako, cat. no P0448 and D0447 respectively, Sydney, Australia) at a dilution of 1:10,000 and Luminata Crescendo Western HRP substrate (Merk Millipore, Sydney, Australia) were used. The blots were exposed for a serial scan of 20 s using the Fusion FX gel documentation system (Vilber Lourmat, Marne-la-Vallée, France).

#### 4.6. Immunofluorescence

Approximately 7500 patient fibroblasts were seeded into each well of an 8 well chamber slide (Ibidi, Martinsried, Germany) and incubated for 24 h, prior to transfection. Following transfection, with 2'-Me PS AOs or PMOs, cells were fixed in ice-cold acetone:methanol (1:1) for 5 min and then air dried.

Fixed cells were incubated in PBS containing 1% Triton X-100 for 10 min at room temperature to permeabilise the nuclear membrane, and then in PBS to remove excess Triton X-100. Mouse anti-NONO monoclonal antibody (a gift from Prof. Archa Fox, The University of Western Australia) was diluted in PBS containing 0.05% Tween20 and applied to cells for one hour at room temperature. NONO was detected using AlexaFluor488 anti-mouse IgG (ThermoFisher Scientific, cat no. A-11001) (1:400) after incubation for one hour at room temperature, and subsequently counterstained with Hoechst 33342 (Sigma-Aldrich) for nuclei detection (1 mg/mL diluted, 1:125).

#### 4.7. Densitometric and Statistical Analysis

Densitometric analysis was conducted using ImageJ (version 1.8.0\_112) imaging software (NIH, Bethesda, MD, USA) [59]. *p* value refers to unpaired two tailed student's *t* tests. A *p* value < 0.05 was considered statistically significant.

**Author Contributions:** Conceptualisation, C.S.M. and M.T.A.-H.; Methodology, C.S.M., M.T.A.-H. and S.D.W.; Formal Analysis: C.S.M.; Investigation, C.S.M.; Writing, C.S.M., M.T.A.-H., S.F. and S.D.W.; Supervision, M.T.A.-H., S.F. and S.D.W.; Resources, S.F. and S.D.W.; Funding Acquisition, S.F. and S.D.W.

**Funding:** This research was funded by NHMRC grants APP1086311 and APP1144791.

**Conflicts of Interest:** The authors declare no conflict of interest.

## Abbreviations

2'-Me	2'-O-methyl
2'-MOE	2'-O-methoxy-ethyl
AO	Antisense oligonucleotide
DMD	Duchenne muscular dystrophy
PMO	Phosphorodiamidate morpholino oligomer
PolyQ	Polyglutamine
PS	Phosphorothioate
SCA3	Spinocerebellar ataxia type 3
UIM	Ubiquitin interacting motif

## References

- Bettencourt, C.; Lima, M. Machado-joseph disease: From first descriptions to new perspectives. *Orphanet J. Rare Dis.* **2011**, *6*, 1. [[CrossRef](#)] [[PubMed](#)]
- Matos, C.A.; de Macedo-Ribeiro, S.; Carvalho, A.L. Polyglutamine diseases: The special case of ataxin-3 and Machado-Joseph disease. *Prog. Neurobiol.* **2011**, *95*, 26–48. [[CrossRef](#)] [[PubMed](#)]
- McIntosh, C.; Aung-Htut, M.; Fletcher, S.; Wilton, S. Polyglutamine ataxias: From clinical and molecular features to current therapeutic strategies. *J. Genet. Syndr. Gene Ther.* **2017**, *8*, 2. [[CrossRef](#)]
- Kawaguchi, Y.; Okamoto, T.; Taniwakiz, M.; Aizawa, M. CAG expansions in a novel gene for Machado-Joseph disease at chromosome 14q32.1. *Nat. Genet.* **1994**, *8*, 221. [[CrossRef](#)]
- Ashley, C.T.; Warren, S.T. Trinucleotide repeat expansion and human disease. *Annu. Rev. Genet.* **1995**, *29*, 703–728. [[CrossRef](#)]
- Tsou, W.-L.; Ouyang, M.; Hosking, R.R.; Sutton, J.R.; Blount, J.R.; Burr, A.A.; Todi, S.V. The deubiquitinase ataxin-3 requires rad23 and dnaj-1 for its neuroprotective role in drosophila melanogaster. *Neurobiol. Dis.* **2015**, *82*, 12–21. [[CrossRef](#)]
- Wen, J.; Scoles, D.R.; Facelli, J.C. Effects of the enlargement of polyglutamine segments on the structure and folding of ataxin-2 and ataxin-3 proteins. *J. Biomol. Struct. Dyn.* **2016**, *35*, 504–519. [[CrossRef](#)]
- Toonen, L.J.; Rigo, F.; van Attikum, H.; van Roon-Mom, W.M. Antisense oligonucleotide-mediated removal of the polyglutamine repeat in spinocerebellar ataxia type 3 mice. *Mol. Ther.-Nucleic Acids* **2017**, *8*, 232–242. [[CrossRef](#)]
- Evers, M.M.; Tran, H.-D.; Zalachoras, I.; Pepers, B.A.; Meijer, O.C.; den Dunnen, J.T.; van Ommen, G.-J.B.; Aartsma-Rus, A.; van Roon-Mom, W.M. Ataxin-3 protein modification as a treatment strategy for spinocerebellar ataxia type 3: Removal of the CAG containing exon. *Neurobiol. Dis.* **2013**, *58*, 49–56. [[CrossRef](#)]
- Evers, M.M.; Pepers, B.A.; van Deutekom, J.C.; Mulders, S.A.; den Dunnen, J.T.; Aartsma-Rus, A.; van Ommen, G.-J.B.; van Roon-Mom, W.M. Targeting several CAG expansion diseases by a single antisense oligonucleotide. *PLoS ONE* **2011**, *6*, e24308. [[CrossRef](#)]
- Shen, W.; De Hoyos, C.L.; Sun, H.; Vickers, T.A.; Liang, X.-h.; Crooke, S.T. Acute hepatotoxicity of 2' fluoro-modified 5–10–5 gapmer phosphorothioate oligonucleotides in mice correlates with intracellular protein binding and the loss of dbhs proteins. *Nucleic Acids Res.* **2018**, *46*, 2204–2217. [[CrossRef](#)] [[PubMed](#)]
- Shen, W.; Liang, X.-h.; Crooke, S.T. Phosphorothioate oligonucleotides can displace Neat1 RNA and form nuclear paraspeckle-like structures. *Nucleic Acids Res.* **2014**, *42*, 8648–8662. [[CrossRef](#)] [[PubMed](#)]
- Shen, W.; Liang, X.-h.; Sun, H.; Crooke, S.T. 2'-fluoro-modified phosphorothioate oligonucleotide can cause rapid degradation of p54nrb and psf. *Nucleic Acids Res.* **2015**, *43*, 4569–4578. [[CrossRef](#)] [[PubMed](#)]
- Crooke, S.T.; Baker, B.F.; Kwoh, T.J.; Cheng, W.; Schulz, D.J.; Xia, S.; Salgado, N.; Bui, H.-H.; Hart, C.E.; Burel, S.A. Integrated safety assessment of 2'-O-methoxyethyl chimeric antisense oligonucleotides in nonhuman primates and healthy human volunteers. *Mol. Ther.* **2016**, *24*, 1771–1782. [[CrossRef](#)]
- Toonen, L.J.; Casaca-Carreira, J.; Pellisé-Tintoré, M.; Mei, H.; Temel, Y.; Jahanshahi, A.; van Roon-Mom, W.M. Intracerebroventricular administration of a 2'-O-methyl phosphorothioate antisense oligonucleotide results in activation of the innate immune system in mouse brain. *Nucleic Acid Ther.* **2018**, *28*, 63–73. [[CrossRef](#)]
- Chi, X.; Gatti, P.; Papoian, T. Safety of antisense oligonucleotide and siRNA-based therapeutics. *Drug Discov. Today* **2017**, *22*, 823–833. [[CrossRef](#)]

17. Crooke, S.T.; Baker, B.F.; Witztum, J.L.; Kwok, T.J.; Pham, N.C.; Salgado, N.; McEvoy, B.W.; Cheng, W.; Hughes, S.G.; Bhanot, S. The effects of 2'-O-methoxyethyl containing antisense oligonucleotides on platelets in human clinical trials. *Nucleic Acid Ther.* **2017**, *27*, 121–129. [[CrossRef](#)]
18. Flynn, L.L.; Li, R.; Aung-Htut, M.T.; Pitout, I.L.; Cooper, J.; Hubbard, A.; Griffiths, L.; Bond, C.; Wilton, S.D.; Fox, A.H. Interaction of modified oligonucleotides with nuclear proteins, formation of novel nuclear structures and sequence-independent effects on RNA processing. *BioRxiv* **2018**, 446773. [[CrossRef](#)]
19. Havens, M.A.; Hastings, M.L. Splice-switching antisense oligonucleotides as therapeutic drugs. *Nucleic Acids Res.* **2016**, *44*, 6549–6563. [[CrossRef](#)]
20. Mendell, J.R.; Rodino-Klapac, L.R.; Sahenk, Z.; Roush, K.; Bird, L.; Lowes, L.P.; Alfano, L.; Gomez, A.M.; Lewis, S.; Kota, J. Eteplirsén for the treatment of Duchenne muscular dystrophy. *Ann. Neurol.* **2013**, *74*, 637–647. [[CrossRef](#)]
21. Cirak, S.; Arechavala-Gomez, V.; Guglieri, M.; Feng, L.; Torelli, S.; Anthony, K.; Abbs, S.; Garralda, M.E.; Bourke, J.; Wells, D.J. Exon skipping and dystrophin restoration in patients with Duchenne muscular dystrophy after systemic phosphorodiamidate morpholino oligomer treatment: An open-label, phase 2, dose-escalation study. *Lancet* **2011**, *378*, 595–605. [[CrossRef](#)]
22. Kinali, M.; Arechavala-Gomez, V.; Feng, L.; Cirak, S.; Hunt, D.; Adkin, C.; Guglieri, M.; Ashton, E.; Abbs, S.; Nihoyannopoulos, P. Local restoration of dystrophin expression with the morpholino oligomer avi-4658 in Duchenne muscular dystrophy: A single-blind, placebo-controlled, dose-escalation, proof-of-concept study. *Lancet Neurol.* **2009**, *8*, 918–928. [[CrossRef](#)]
23. Adams, A.M.; Harding, P.L.; Iversen, P.L.; Coleman, C.; Fletcher, S.; Wilton, S.D. Antisense oligonucleotide induced exon skipping and the dystrophin gene transcript: Cocktails and chemistries. *BMC Mol. Biol.* **2007**, *8*, 1. [[CrossRef](#)] [[PubMed](#)]
24. Mitropant, C.; Adams, A.M.; Meloni, P.L.; Muntoni, F.; Fletcher, S.; Wilton, S.D. Rational design of antisense oligomers to induce dystrophin exon skipping. *Mol. Ther.* **2009**, *17*, 1418–1426. [[CrossRef](#)]
25. Carver, M.P.; Charleston, J.S.; Shanks, C.; Zhang, J.; Mense, M.; Sharma, A.K.; Kaur, H.; Sazani, P. Toxicological characterization of exon skipping phosphorodiamidate morpholino oligomers (PMOs) in non-human primates. *J. Neuromuscul. Dis.* **2016**, *3*, 381–393. [[CrossRef](#)]
26. McClorey, G.; Moulton, H.; Iversen, P.; Fletcher, S.; Wilton, S. Antisense oligonucleotide-induced exon skipping restores dystrophin expression in vitro in a canine model of DMD. *Gene Ther.* **2006**, *13*, 1373. [[CrossRef](#)]
27. Saute, J.A.M.; Jardim, L.B. Machado-Joseph disease: Clinical and genetic aspects, and current treatment. *Expert Opin. Orphan Drugs* **2015**, *3*, 517–535. [[CrossRef](#)]
28. Matos, C.; Pereira de Almeida, L.; Nóbrega, C. Machado-Joseph disease/spinocerebellar ataxia type 3: Lessons from disease pathogenesis and clues into therapy. *J. Neurochem.* **2018**, *148*, 8–28. [[CrossRef](#)]
29. Weishäupl, D.; Schneider, J.; Pinheiro, B.P.; Ruess, C.; Dold, S.M.; von Zweyendorf, F.; Gloeckner, C.J.; Schmidt, J.; Riess, O.; Schmidt, T. Physiological and pathophysiological characteristics of ataxin-3 isoforms. *J. Biol. Chem.* **2018**, *294*, 644–661. [[CrossRef](#)]
30. Silverman, R.H. Viral encounters with 2', 5'-oligoadenylate synthetase and RNase I during the interferon antiviral response. *J. Virol.* **2007**, *81*, 12720–12729. [[CrossRef](#)]
31. Tokarev, A.; Skasko, M.; Fitzpatrick, K.; Guatelli, J. Antiviral activity of the interferon-induced cellular protein bst-2/tetherin. *Aids Res. Hum. Retrovir.* **2009**, *25*, 1197–1210. [[CrossRef](#)] [[PubMed](#)]
32. Zhao, P.; Zhao, L.; Zhang, T.; Qi, Y.; Wang, T.; Liu, K.; Wang, H.; Feng, H.; Jin, H.; Qin, C. Innate immune response gene expression profiles in central nervous system of mice infected with rabies virus. *Comp. Immunol. Microbiol. Infect. Dis.* **2011**, *34*, 503–512. [[CrossRef](#)] [[PubMed](#)]
33. Mendell, J.R.; Sahenk, Z.; Rodino-Klapac, L.R. Clinical trials of exon skipping in Duchenne muscular dystrophy. *Expert Opin. Orphan Drugs* **2017**, *5*, 683–690. [[CrossRef](#)]
34. Janas, M.M.; Jiang, Y.; Schlegel, M.K.; Waldron, S.; Kuchimanchi, S.; Barros, S.A. Impact of oligonucleotide structure, chemistry, and delivery method on in vitro cytotoxicity. *Nucleic Acid Ther.* **2017**, *27*, 11–22. [[CrossRef](#)] [[PubMed](#)]
35. Winkler, J.; Stessl, M.; Amartey, J.; Noe, C.R. Off-target effects related to the phosphorothioate modification of nucleic acids. *ChemMedChem* **2010**, *5*, 1344–1352. [[CrossRef](#)] [[PubMed](#)]

36. Mendell, J.R.; Goemans, N.; Lowes, L.P.; Alfano, L.N.; Berry, K.; Shao, J.; Kaye, E.M.; Mercuri, E.; Group, E.S.; Network, T.F.D.I.; et al. Longitudinal effect of *Eteplirsen* versus historical control on ambulation in Duchenne muscular dystrophy. *Ann. Neurol.* **2016**, *79*, 257–271. [[CrossRef](#)] [[PubMed](#)]
37. Pitout, I.; Flynn, L.L.; Wilton, S.D.; Fletcher, S. Antisense-mediated splice intervention to treat human disease: The odyssey continues. *F1000Research* **2019**, *8*. [[CrossRef](#)]
38. Summerton, J.; Stein, D.; Huang, S.B.; Matthews, P.; Weller, D.; Partridge, M. Morpholino and phosphorothioate antisense oligomers compared in cell-free and in-cell systems. *Antisense Nucleic Acid Drug Dev.* **1997**, *7*, 63–70. [[CrossRef](#)]
39. Summerton, J.; Weller, D. Morpholino antisense oligomers: Design, preparation, and properties. *Antisense Nucleic Acid Drug Dev.* **1997**, *7*, 187–195. [[CrossRef](#)]
40. Summerton, J.E. Morpholino, siRNA, and s-DNA compared: Impact of structure and mechanism of action on off-target effects and sequence specificity. *Curr. Top. Med. Chem.* **2007**, *7*, 651–660. [[CrossRef](#)]
41. Flynn, L.L.; Mitropant, C.; Pitout, I.L.; Fletcher, S.; Wilton, S.D. Antisense oligonucleotide-mediated terminal intron retention of the *SMN2* transcript. *Mol. Ther.-Nucleic Acids* **2018**, *11*, 91–102. [[CrossRef](#)] [[PubMed](#)]
42. Amantana, A.; Iversen, P.L. Pharmacokinetics and biodistribution of phosphorodiamidate morpholino antisense oligomers. *Curr. Opin. Pharmacol.* **2005**, *5*, 550–555. [[CrossRef](#)] [[PubMed](#)]
43. Arora, V.; Devi, G.R.; Iversen, P.L. Neutrally charged phosphorodiamidate morpholino antisense oligomers: Uptake, efficacy and pharmacokinetics. *Curr. Pharm. Biotechnol.* **2004**, *5*, 431–439. [[CrossRef](#)] [[PubMed](#)]
44. Miyatake, S.; Mizobe, Y.; Tsoumpra, M.K.; Lim, K.R.Q.; Hara, Y.; Shabanpoor, F.; Yokota, T.; Takeda, S.i.; Aoki, Y. Scavenger receptor class A1 mediates uptake of morpholino antisense oligonucleotide into dystrophic skeletal muscle. *Mol. Ther.-Nucleic Acids* **2019**, *14*, 520–535. [[CrossRef](#)] [[PubMed](#)]
45. Aoki, Y.; Nagata, T.; Yokota, T.; Nakamura, A.; Wood, M.J.; Partridge, T.; Takeda, S.i. Highly efficient in vivo delivery of PMO into regenerating myotubes and rescue in laminin- $\alpha$ 2 chain-null congenital muscular dystrophy mice. *Hum. Mol. Genet.* **2013**, *22*, 4914–4928. [[CrossRef](#)] [[PubMed](#)]
46. Miyatake, S.; Mizobe, Y.; Takizawa, H.; Hara, Y.; Yokota, T.; Takeda, S.i.; Aoki, Y. Exon skipping therapy using phosphorodiamidate morpholino oligomers in the *mdx52* mouse model of Duchenne muscular dystrophy. In *Duchenne Muscular Dystrophy*; Springer: Berlin/Heidelberg, Germany, 2018; pp. 1231–1241.
47. Toonen, L.J.; Schmidt, I.; Luijsterburg, M.S.; van Attikum, H.; van Roon-Mom, W.M. Antisense oligonucleotide-mediated exon skipping as a strategy to reduce proteolytic cleavage of ataxin-3. *Sci. Rep.* **2016**, *6*, 35200. [[CrossRef](#)]
48. Switonski, P.M.; Fiszer, A.; Kazmierska, K.; Kurpisz, M.; Krzyzosiak, W.J.; Figiel, M. Mouse ataxin-3 functional knock-out model. *Neuromol. Med.* **2011**, *13*, 54–65. [[CrossRef](#)]
49. Evers, M.M.; Toonen, L.J.; van Roon-Mom, W.M. Ataxin-3 protein and RNA toxicity in spinocerebellar ataxia type 3: Current insights and emerging therapeutic strategies. *Mol. Neurobiol.* **2014**, *49*, 1513–1531. [[CrossRef](#)]
50. Li, X.; Liu, H.; Fischhaber, P.L.; Tang, T.-S. Toward therapeutic targets for sca3: Insight into the role of Machado–Joseph disease protein ataxin-3 in misfolded proteins clearance. *Prog. Neurobiol.* **2015**, *132*, 34–58. [[CrossRef](#)]
51. Schmitt, I.; Linden, M.; Khazneh, H.; Evert, B.O.; Breuer, P.; Klockgether, T.; Wuellner, U. Inactivation of the mouse *atxn3* (ataxin-3) gene increases protein ubiquitination. *Biochem. Biophys. Res. Commun.* **2007**, *362*, 734–739. [[CrossRef](#)]
52. Moore, L.R.; Rajpal, G.; Dillingham, I.T.; Qutob, M.; Blumenstein, K.G.; Gattis, D.; Hung, G.; Kordasiewicz, H.B.; Paulson, H.L.; McLoughlin, H.S. Evaluation of antisense oligonucleotides targeting *Atxn3* in SCA3 mouse models. *Mol. Ther.-Nucleic Acids* **2017**, *7*, 200–210. [[CrossRef](#)] [[PubMed](#)]
53. Boy, J.; Schmidt, T.; Wolburg, H.; Mack, A.; Nuber, S.; Böttcher, M.; Schmitt, I.; Holzmann, C.; Zimmermann, F.; Servadio, A. Reversibility of symptoms in a conditional mouse model of spinocerebellar ataxia type 3. *Hum. Mol. Genet.* **2009**, *18*, 4282–4295. [[CrossRef](#)] [[PubMed](#)]
54. Zeng, L.; Zhang, D.; McLoughlin, H.S.; Zalon, A.J.; Aravind, L.; Paulson, H.L. Loss of the spinocerebellar ataxia type 3 disease protein *atxn3* alters transcription of multiple signal transduction pathways. *PLoS ONE* **2018**, *13*, e0204438. [[CrossRef](#)] [[PubMed](#)]
55. McLoughlin, H.S.; Moore, L.R.; Chopra, R.; Komlo, R.; McKenzie, M.; Blumenstein, K.G.; Zhao, H.; Kordasiewicz, H.B.; Shakkottai, V.G.; Paulson, H.L. Oligonucleotide therapy mitigates disease in spinocerebellar ataxia type 3 mice. *Ann. Neurol.* **2018**, *84*, 64–77. [[CrossRef](#)] [[PubMed](#)]



56. Desmet, F.-O.; Hamroun, D.; Lalande, M.; Collod-Bérout, G.; Claustres, M.; Bérout, C. Human splicing finder: An online bioinformatics tool to predict splicing signals. *Nucleic Acids Res.* **2009**, *37*, e67. [[CrossRef](#)] [[PubMed](#)]
57. Aung-Htut, M.T.; McIntosh, C.S.; Ham, K.A.; Pitout, I.L.; Flynn, L.L.; Greer, K.; Fletcher, S.; Wilton, S.D. Systematic approach to developing splice modulating antisense oligonucleotides. *Int. J. Mol. Sci.* **2019**, *20*, 5030. [[CrossRef](#)]
58. Aung-Htut, M.T.; McIntosh, C.S.; West, K.A.; Fletcher, S.; Wilton, S.D. In vitro validation of phosphorodiamidate morpholino oligomers. *Molecules* **2019**, *24*, 2922. [[CrossRef](#)]
59. Schneider, C.A.; Rasband, W.S.; Eliceiri, K.W. Nih image to imagej: 25 years of image analysis. *Nat. Methods* **2012**, *9*, 671. [[CrossRef](#)]



© 2019 by the authors. Licensee MDPI, Basel, Switzerland. This article is an open access article distributed under the terms and conditions of the Creative Commons Attribution (CC BY) license (<http://creativecommons.org/licenses/by/4.0/>).

# Chapter 6 – Published

## Research Article 2

Aung-Htut, M. T.\* , McIntosh, C. S\*., Ham, K. A., Pitout, I. L., Flynn, L. L., Greer, K., ... & Wilton, S. D. (2019). **Systematic approach to developing splice modulating antisense oligonucleotides**. *International Journal of Molecular Sciences*, 20(20), 5030.

### Co-First Authored

**Author Contributions:** Conceptualisation, C.S.M. and M.T.A-H.; Methodology, C.S.M., M.T.A-H., K.A.H., and S.D.W.; Formal Analysis: C.S.M., M.T.A-H., and K.A.H.; Investigation, C.S.M., M.T.A-H., and K.A.H.; Writing, C.S.M., M.T.A-H., K.A.H., S.F., and S.D.W.; Editing, C.S.M., M.T.A-H., K.A.H., I.L.P., L.L.F., K.G., S.F., and S.D.W.; Supervision, S.F. and S.D.W.; Resources, S.F. and S.D.W.; Funding Acquisition, S.F. and S.D.W.



Article

# Systematic Approach to Developing Splice Modulating Antisense Oligonucleotides

May T. Aung-Htut <sup>1,2,†</sup> , Craig S. McIntosh <sup>1,2,†</sup> , Kristin A. Ham <sup>1</sup>, Ianthe L. Pitout <sup>1,2</sup>, Loren L. Flynn <sup>1,2</sup>, Kane Greer <sup>1</sup>, Sue Fletcher <sup>1,2</sup> and Steve D. Wilton <sup>1,2,\*</sup>

<sup>1</sup> Centre for Molecular Medicine and Innovative Therapeutics, Murdoch University, Perth, WA 6150, Australia; M.Aung-Htut@murdoch.edu.au (M.T.A.-H.); C.McIntosh@murdoch.edu.au (C.S.M.);

Kristin.Ham@murdoch.edu.au (K.A.H.); I.pitout@murdoch.edu.au (I.L.P.);

Loren.Flynn@murdoch.edu.au (L.L.F.); k.greer@murdoch.edu.au (K.G.); s.fletcher@murdoch.edu.au (S.F.)

<sup>2</sup> Perron Institute for Neurological and Translational Science, Centre for Neuromuscular and Neurological Disorders, The University of Western Australia, Perth, WA 6009, Australia

\* Correspondence: s.wilton@murdoch.edu.au

† These authors contributed equally to this work.

Received: 27 September 2019; Accepted: 10 October 2019; Published: 11 October 2019



**Abstract:** The process of pre-mRNA splicing is a common and fundamental step in the expression of most human genes. Alternative splicing, whereby different splice motifs and sites are recognised in a developmental and/or tissue-specific manner, contributes to genetic plasticity and diversity of gene expression. Redirecting pre-mRNA processing of various genes has now been validated as a viable clinical therapeutic strategy, providing treatments for Duchenne muscular dystrophy (inducing specific exon skipping) and spinal muscular atrophy (promoting exon retention). We have designed and evaluated over 5000 different antisense oligonucleotides to alter splicing of a variety of pre-mRNAs, from the longest known human pre-mRNA to shorter, exon-dense primary gene transcripts. Here, we present our guidelines for designing, evaluating and optimising splice switching antisense oligomers in vitro. These systematic approaches assess several critical factors such as the selection of target splicing motifs, choice of cells, various delivery reagents and crucial aspects of validating assays for the screening of antisense oligonucleotides composed of 2'-O-methyl modified bases on a phosphorothioate backbone.

**Keywords:** antisense oligonucleotide; splice modulation; 2'-O-Methyl; transfection

## 1. Introduction

Splice switching antisense oligonucleotides (AOs) are gaining interest as therapeutics for a wide variety of inherited and acquired diseases, with the approvals of *Eteplirsen* and *Nusinersen* to treat Duchenne muscular dystrophy and spinal muscular atrophy, respectively [1–3]. Antisense oligonucleotides are short, synthetic nucleic acids or analogues, typically 18 to 30 nucleotides in length that can specifically anneal to a complementary DNA or RNA sequence via Watson–Crick base-pairing [4]. Depending upon the nature of the AO (modified bases and backbone chemistry), these compounds can be designed to alter gene expression through several distinct mechanisms; including, but not limited to, RNase H mediated mRNA degradation [5], induction of RNA silencing [6], translation blockade [7], suppression of miRNA action, and modulation of pre-mRNA splicing [8]. The specific mechanism induced is determined by the AO chemistry as well as the annealing location in the gene transcript. Here, we specifically focus on AO design and delivery to modulate pre-mRNA processing, by redirecting splice site/motif selection to promote either specific exon skipping or retention in a target pre-mRNA [9]. We also provide reference AOs optimised to modulate ubiquitously

expressed human gene transcripts that may be employed as controls to monitor the efficiency of transfection, RNA extraction, and RT-PCR amplification.

Splice modulating AOs are designed to anneal to elements within or flanking an exon and influence its recognition by the spliceosome so that the exon is preferentially retained or excised from the mature mRNA as required. Redirection of splicing is presumably a consequence of preventing positive (enhancer) or negative (silencer) splicing factors from recognising enhancer or silencer elements in the pre-mRNA transcript. Steric hindrance at these sites alters the recognition of normal splice sites by the splicing machinery and leads to alternative selection of exons or intronic sequences in the targeted transcript [10]. Web-based tools such as SpliceAid 2 [11], Human Splicing Finder [12], and RegRNA [13] have facilitated the prediction of potential splice factor motifs in any given sequence. Bioinformatics can contribute to the design of splice switching AOs [14,15]. While it is relatively straightforward to target AOs to predicted enhancer or silencer motifs, or to confirmed splice donor or acceptor sites [14–16], this approach does not consistently yield effective splice altering AO sequences. Although the original AO that induced specific dystrophin exon 23 skipping in *mdx* mouse muscle was directed to the donor splice site [17], AOs targeting the same coordinates of the human dystrophin transcript were completely ineffective [18]. Similarly, targeting the human dystrophin exon 51 donor splice site with AOs of different lengths and chemistries did not induce any exon skipping. Ultimately, identifying target domains within a pre-mRNA that influence splicing and then refining AO design through micro-walking must be done empirically.

To date, our laboratory has screened over 5,000 AOs directed at numerous gene transcripts, linked to genetic diseases that may be potentially amenable to a splice intervention therapy. In addition, we are also exploring non-productive splicing to downregulate expression of selected gene transcripts through inducing non-functional isoforms by either excising exons encoding crucial functional domains or disrupting the reading frame. Consequently, we have developed general guidelines that are efficient and effective in developing biologically active splice switching antisense oligomers.

1. The pre-mRNA sequence is interrogated by one or more in silico prediction programs to identify potential splice enhancer or silencer motifs.
2. Antisense oligonucleotides, typically 20 to 25 mers, are designed to anneal to the target motifs and synthesised as 2'-O-methyl (2-OMe) modified bases on a phosphorothioate (PS) backbone.
3. The test compounds are complexed with cationic liposome preparations and transfected into cells.
4. After incubation, total RNA is extracted and the target transcript is amplified using RT-PCR to assess differences in pre-mRNA processing, with and without AO treatment.
5. Oligomers shown to induce the desired changes in pre-mRNA processing are further refined by micro-walking around the annealing site and/or altering AO length.
6. Transfection studies over a range of concentrations are performed to identify compound(s) that modify splicing in a dose-dependent manner, and at the lowest concentration.

Oligomers composed of 2-OMe PS can be either sourced commercially from a variety of suppliers or, in our case, synthesised in-house on a nucleic acid synthesiser such as an Expedite 8909 or Akta OligoPilot plus 10. The 2-OMe PS AOs are excellent research tools as they are relatively easily transfected into many different cultured cells with the aid of cationic lipoplexes such as Lipofectamine™ 3000, Lipofectin™, and Lipofectamine™ 2000. However, when subsequent protein or functional studies are required, the optimised sequences are generally synthesised as phosphorodiamidate morpholino oligomers (PMOs), as this chemistry offers more efficient and sustained splicing modification and protein isoform expression without non-specific effects [19]. The PMO chemistry is well tolerated both in vitro and in vivo, even at relatively high dosages [20] and is our preferred oligomer chemistry for in vivo evaluation in animal studies and ultimately, for clinical application.

Unless directly coupled to a cell-penetrating agent, most AOs require a transfection reagent or protocol for efficient delivery into cultured cells, and in the case of splice switching compounds, be taken up into the nucleus where pre-mRNA processing occurs. Most commonly, a lipid-based solution is

complexed with the AO prior to transfection [21], as the creation of a cationic lipid-complex capable of entering the cell via endocytosis vastly increases the AO uptake into the cell, compared to a gymnotic AO uptake. For screening of 2-OMe PS AOs, we typically use commercially available lipid transfection reagents, depending on the cell type. We have previously described transfection methods for efficient delivery of PMOs into cultured cells [22]. In addition to the transfection reagent or protocol, other factors that affect AO transfection efficiency *in vitro* include cell type and hence expression of the target gene, cell passage number and growth stage in culture, differentiation status, cell density, media and cell morphology during transfection, and AO chemistry and sequence composition. Here, we describe *in vitro* methods for AO design and the factors to consider during an initial screen of the most effective splice modifying antisense sequences using 2-OMe PS.

## 2. Results

### Guidelines for Developing Splice Switching AOs

#### Step 1—Selection of Target Motifs

Once a target gene transcript and strategy is identified (e.g., exon skipping to remove a compromised exon from a disease causing gene, or disrupt expression of a target gene), open source web-based bioinformatics tools SpliceAid 2 [11] and Human Splicing Finder [12] may be used to identify predicted splice motifs, such as exon splice enhancers or exon splice silencers (Figure 1). Antisense oligomers complementary to the potential splice-associated motifs will then be synthesised as 2-OMe PS AOs. To induce exon skipping, the canonical acceptor and donor splice sites are obvious and well-defined targets, and since most exons are less than 200 bases in length, an additional three or four AOs, typically 20–25 nucleotides in length, provide reasonable coverage in the first pass.

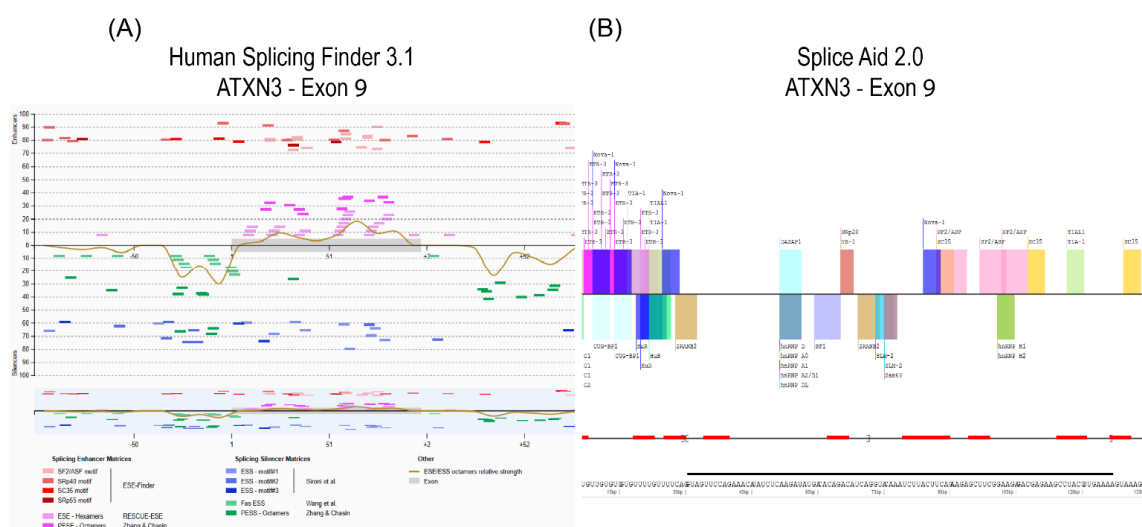


**Figure 1.** In silico prediction of splice motifs for exon 9 of the *ATXN3* transcript using Human Splicing Finder (A) and SpliceAid 2 (B). Exon position is identified by the black line above the sequence in SpliceAid 2.

We have reported a nomenclature system for the AOs according to gene, species, exon number, and annealing coordinates [23] (Figure 2). The nomenclature begins with the name of the transcript (e.g., survival of motor neuron 1; *SMN1*), then the species of the target mRNA (e.g., H: human or M: mouse), followed by the target exon number of the specified transcript and specification of an acceptor (A) or donor (D) site. The annealing coordinates are shown in brackets from the 5' to 3' position within the pre-mRNA transcript. The intronic bases are designated with a negative prefix (-) and the exonic position with a positive (+) symbol. The annealing coordinates are the positions of bases relative to the

acceptor or donor sites of the reference transcript as denoted by National Center for Biotechnology Information and *Ensembl genome browser* 96. It is important to describe the reference transcript ID, especially in the case of targeting gene transcript isoforms that are composed of different numbers of exons. This AO nomenclature provides researchers with a unique designation, conveying the precise annealing coordinates of the targeted transcript that is particularly relevant when refining AO design by micro-walking around a responsive annealing site. Subtle shifts in AO annealing coordinates or length are immediately apparent and facilitates optimal AO design.

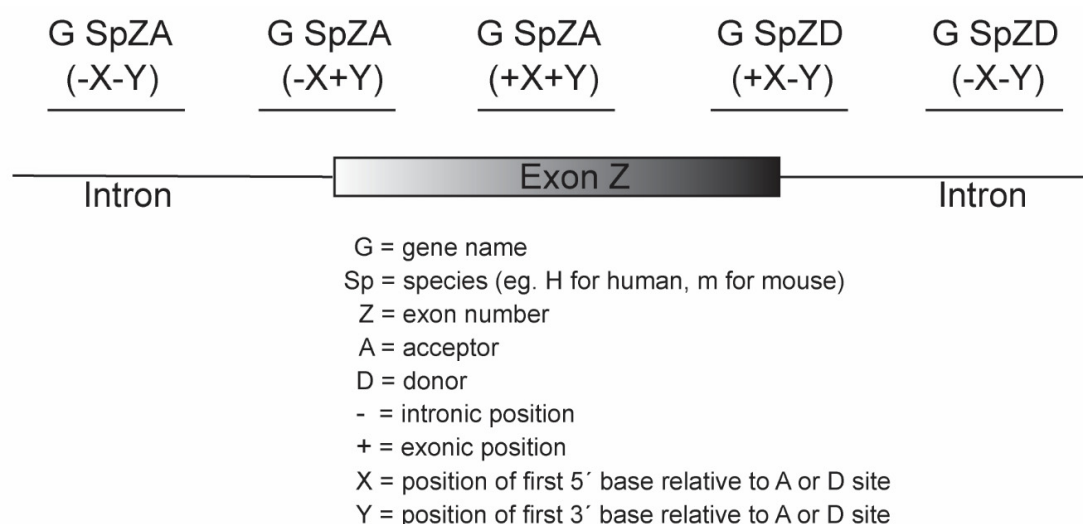


**Figure 2.** Nomenclature for antisense oligonucleotides.

## Step 2—Choice of Cell Type

When possible, screening and evaluation of splice switching AOs should be performed in cells expressing the target gene transcript and protein. GeneCards [24] offers a quick and convenient guide to cell and tissue-specific gene expression. However, certain disease-affected cell types—e.g., motor neurons or photoreceptors—may be difficult, impractical, or impossible to obtain and propagate from living patients. Consequently, it may be necessary to initiate AO design and evaluation in patient-derived lymphocytes or skin fibroblasts, and while not optimal, these cell types are relatively easy to obtain and culture. Although target gene expression may be relatively low in lymphocytes or fibroblasts, it may be sufficient for initial proof of concept studies at the RNA level.

When studying most muscle diseases, patient-derived myoblasts would be the preferred material for study. However, obtaining muscle biopsies for the propagation of myogenic cells requires more invasive procedures compared to collecting a skin punch or blood sample. Unless elective surgery has been scheduled, working with healthy or patient-derived myogenic cells should only be considered after careful deliberation and consultation. Dermal fibroblasts can be propagated and subsequently induced into the myogenic lineage using MyoD expressing vectors, a common method routinely used to differentiate fibroblasts into myogenic cells [25–27].

In some instances, it is not necessary to use patient cells for the design of potentially therapeutic AOs. For example, the most common type of Duchenne muscular dystrophy-causing mutation is the genomic deletion of one or more exons, with subsequent disruption of the open reading frame. Since a normal exon flanking the frame-shifting deletion must be excised to restore the reading frame, the current suite of dystrophin exon skipping oligomers were designed against the normal dystrophin sequence and first evaluated in cells derived from healthy individuals [1,2,8]. Furthermore, AO optimisation in healthy cells sets a high standard, since the full complement of splicing factors are present in the context of the normal transcript, and the transcript induced by skipping a frame-shifting exon will be out of frame and hence subject to nonsense-mediated decay. While developing AOs to

excise human dystrophin exon 8, compounds were first evaluated using healthy myoblasts, and clear differences in exon skipping efficiencies were readily evident. However, when these same compounds were tested in amenable patient-derived myogenic cells (e.g., missing exons 3-7 or 5-7), the distinction between poor and robust exon skipping AOs was much less evident [28]. For AOs designed to downregulate expression of a target protein by disrupting normal splicing, screening can again be undertaken initially in healthy cell lines. Once optimised, proof of concept studies can then be initiated in patient-derived cells for further validation and protein studies.

For gene transcripts not expressed in either fibroblasts, lymphocytes or myoblasts, other commercially available cell lines, such as HEK293 (human embryonic kidney epithelium) or SH-SY5Y (neuroblastoma) lines available from repositories (Coriell Institute for Medical Research or American Type Culture Collection), may suffice. However, for specific disease-causing mutations, patient-derived cells are required for testing and validation of the AO and assessing the mutation specific effect. The construction of mini-gene assays to study the consequences of a particular splice mutation and AO intervention can be helpful. However, the utility of mini-gene assays can be limited by the length and structure of the cloned exonic and intronic sequences, and the cell type or strain used.

### Step 3—Delivery Reagents

Once the AOs are designed and an appropriate cell type is chosen, we recommend exploring different transfection reagents for optimal AO delivery and uptake. Depending on the mechanism of action, AOs are required to be delivered to either the cytoplasm (for protein translation blockade and RNase H mediated mRNA degradation) or the nucleus (to alter pre-mRNA processing, including splicing or polyadenylation). Oligomers labelled with various fluorophores (e.g., FAM and TET) may be used to assess gross transfection efficiency, distribution, and uptake of each reagent; however, when exploring novel splice modification approaches, we recommend using a validated splice modulating AO as a control. As shown in Figure 3, one such control is an AO designed to induce skipping of exon 3 from the *ITGA4* transcript, a widely expressed gene in many different cell types. Not only will transfection of a control AO provide a guide to the transfection efficiencies, it can also be useful in assessing RNA quality and quantity in conjunction with the RT-PCR assays.

The *ITGA4* transcript in healthy human fibroblasts was analysed by end point RT-PCR. The cells were transfected with 100 nM ITGA4 H3A (+ 30 + 49), a 2-OMe PS AO that induces skipping of exons 3 and 4 from the *ITGA4* gene transcript, using three different lipid-based transfection reagents (Figure 3A). Although all transfection reagents tested did deliver the AO, the transfection using Lipofectamine™ 3000 reagent induced the highest level of exon skipping in these cells. Lipofectamine™ RNAiMax showed a similar exon skipping pattern as Lipofectamine™ 3000, however, higher levels of cell death were induced by the former. The recommended lipid-based transfection reagents for delivery of 2-OMe PS AOs into the cell lines tested in our laboratory are listed in Table 1. Once the optimal transfection reagent is identified for a particular cell type, evaluation of AO sequences can proceed.

**Table 1.** Recommended transfection reagents for different cell lines

Cell Lines	Transfection Reagents
Dermal fibroblasts	Lipofectin™, Lipofectamine™ 3000
Myoblasts and myotubes	Lipofectamine™ 2000
Lymphoblasts and lymphocytes	Nucleofection P3 Primary Cell Kit
Huh7	Lipofectamine™ 3000, Lipofectamine™ RNAiMax
HEK293	Lipofectamine™ 3000
H2k <i>mdx</i>	Lipofectin™
MO3.13	Lipofectamine™ 3000
iPSCs and neural stem cells	Lipofectamine™ Stem

Note: When evaluating AOs for splice modulation in primary cells, it is preferable to use cultures of lower passage number as we found that cultures with higher passage numbers tend to be transfected with lower efficiencies.

One important parameter to consider when designing primers for RT-PCR analysis of the full-length and AO-induced transcripts is to place the forward and reverse primers a few exons away from the targeted exon. We have now encountered several examples where targeting one exon for exclusion from the mature mRNA also influences recognition and retention of flanking exons and introns. As shown in Figure 3, amplification of the *ITGA4* transcript from exons 1 to 10 (Figure 3A) showed robust exon skipping, but not when amplified from exon 1 to 4 after transfection with the same AO designed to skip exon 3 (Figure 3B).

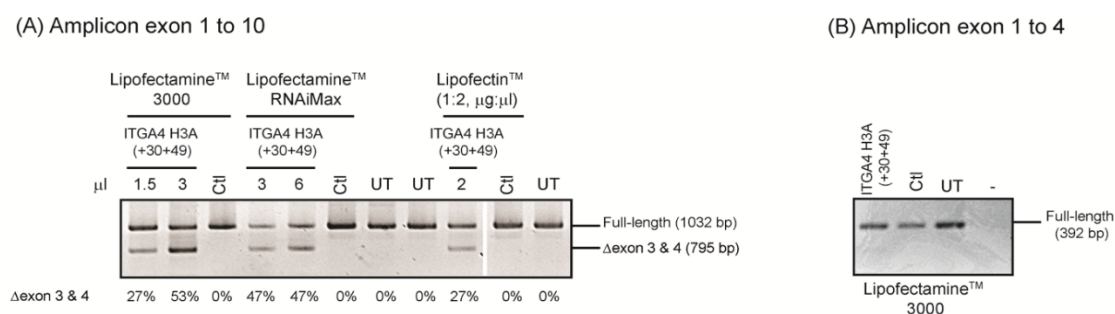


**Figure 3.** Modification of integrin alpha 4 (*ITGA4*) transcripts after healthy human fibroblasts were transfected with different lipid-based transfection reagents. (A) Three lipid-based reagents were used to transfect cells with *ITGA4* H3A (+30 + 39) at 100 nM for 24 hr. Total RNA was extracted and RT-PCR was undertaken across exons 1 to 10 of the *ITGA4* transcripts. Transfection reagent volumes are indicated above the gel. Ctl; control AO that does not anneal to any sequence, UT; untreated, -; no template control. Percentages of *ITGA4* exon 3 and 4 skipping are indicated below the gel. The control AO was transfected using the maximum volume of transfection reagents. (B) RT-PCR amplification of the *ITGA4* transcript across exons 1 to 4 from RNA extracted from sample transfected with Lipofectamine 3000 from (A).

#### Step 4—Initial AO Screen

In early AO splice switching studies, the use of negative AO control sequences—either random, scrambled, or unrelated sequences—was essential to confirm specific target modification. Establishing target specificity is particularly crucial in situations where gene downregulation is the desired outcome. However, in many cases of splice switching, either exon skipping, exon retention or intron retention, the presence of a novel transcript is proof of the anticipated antisense mechanism. When AOs designed to a specific target do not affect the processing of that specific gene transcript, it is likely (but not inconceivable) that imperfect annealing to another pre-mRNA would have a minimal, if any effect.

Depending upon the gene and targeted exon, it has been our experience that up to two out of three AOs designed in a first pass can induce some level of exon skipping. However, targeting certain motifs noticeably results in more efficient exon skipping than others, and when developing any AO for clinical use, it is obvious that the most appropriate compound will be one that induces robust splice switching at a low concentration. The use of a positive transfection control AO is recommended for each transfection experiment, as this can control for transfection efficiencies across different experiments. It is also important to note that cell confluency, passage number, and other culture conditions can substantially influence transfection efficiency in primary cells and may lead to variations in AO efficacy between biological replicates.

In some cases, individual AOs are ineffective at modifying exon selection, even after transfection at high concentrations. We have frequently found that selective AO cocktails, which include two or more AOs used in conjunction for a given exon target, mediate exon skipping in a synergistic manner, while each AO transfected alone is ineffective [18,29]. Conversely, we have also observed a marked decrease in exon skipping efficiency when two highly effective AOs are combined.

**Note:** It is recommended to confirm the identity of novel ‘exon skipped’ products by direct DNA sequencing, as nearby cryptic splice sites may be activated and generate amplicons of a similar



length to the expected product. A difference of only a few bases in length can be difficult to resolve on an agarose gel, and such differences would be impossible to detect in longer RT-PCR products representing multiple exons [30].

Upon identification of amenable sites in the pre-mRNA that induce the desired splice modulation, AOs can be further optimised by ‘micro-walking’ and shifting the AO annealing sites in either direction to ensure the most amenable splice motifs have been targeted. An example of micro-walking is illustrated in Figure 4. Generally, to find the most effective AO, the annealing sites are moved five nucleotides in either the 5’ or 3’ direction, while retaining the same AO length. As shown in Figure 4, secondary screening of the AOs, ITGA4 H3A (+ 41 + 65) and ITGA4 H3A (+ 51 + 75), marginally improved exon skipping efficiency, compared to ITGA4 H3A (+ 46 + 70) indicating this general region would be suitable as an AO target. Alternatively, shifting the annealing site targeted by ITGA4 H3D (+ 6 – 19) further into the intron with ITGA4 H3D (+ 1 – 24) improved exon skipping efficiency from 18% to 34%. If considered necessary and of particular relevance, further micro-walking could be undertaken via moving the lead AO candidate target sequence by a few nucleotides in either the 5’ or 3’ direction. As a final optimisation step, once the most responsive or amenable annealing site is defined, the AO length may be truncated from either end. Shorter AOs are not only more efficiently synthesized, but substantially less costly to produce, an important consideration that will influence eventual clinical implementation. In some cases, AOs longer than 25 bases may be justified and must be considered on a case-by-case basis. We showed that efficient dystrophin exon 16 could be induced by overlapping 25 mers but increasing the length to a 30 mer resulted in a four-fold increase in exon skipping efficiency [31]. Hence, a 20% increase in AO length (and cost) resulted in a 400% increase in potency as assessed in vitro, thus allowing cost: benefits to be assessed.

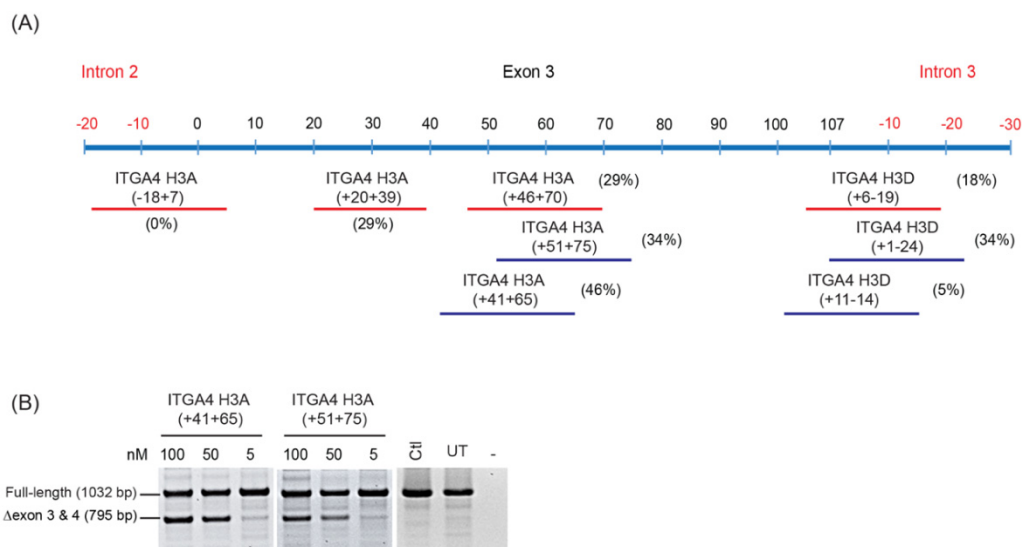


**Figure 4.** (A) RT-PCR analysis of *ITGA4* transcripts demonstrating refinement of splice switching AOs targeting *ITGA4* exon 3. Oligomers tested in the first screen are indicated by red lines and the micro-walked AOs tested in the second screen are represented by blue lines. Levels of exon skipping after transfection at 100 nM are indicated in brackets. (B) Comparison of two AOs that induce skipping of *ITGA4* exon 3 and 4 at various concentrations (100, 50, and 5 nM). Ctl; control AO that does not anneal to any sequence, UT; untreated, -; no template control.

As a final evaluation to demonstrate reproducibility and efficacy, AO titrations should be performed to discriminate between AOs that induce similar levels of exon skipping, as shown in Figure 4B. Both ITGA4 H3A (+ 41 + 65) and ITGA4 H3A (+ 51 + 75) resulted in efficient exon skipping at 100 nM. However, when both AOs were transfected at 50 nM, the lower efficiency of ITGA4 H3A (+ 51 + 75) compared to ITGA4 H3A (+ 41 + 65) was evident.

### 3. Discussion

Here we describe general guidelines for developing, screening, and refining splice modulating AO sequences. It has been our experience that within a given gene transcript, some exons are readily excised from the mature mRNA, albeit at variable efficiencies in vitro, whereas other exons in the same transcript are more resistant to exon skipping [22,29]. In some cases, there may be either only a single region found to mediate AO-induced exon skipping, or combinations of AOs are needed to induce exon skipping, with the combinations sometimes acting synergistically [29]. We are yet to determine parameters that predict the ideal exon or transcript target for the design of splice modulating AOs, and experimental optimisation is therefore critical to the development of AO therapeutics.

As with all forms of genetic therapies, AO delivery is a crucial aspect for splice switching efficacy. Relatively minor changes to the transfection protocol can dramatically improve or weaken apparent AO splice switching efficiency, and consequently, we suggest that before any AO is classified as ineffective in modulating splicing, various transfection methods should be evaluated. We describe an AO sequence that can be used as a positive control to modify the expression of the *ITGA4* transcript, widely expressed in most cell types. We suggest the use of this AO as a positive transfection control, an important inclusion during the initial stages of AO strategy design. A positive control AO allows one to monitor the experimental protocols (e.g., transfection, RNA extraction, RT-PCR).

Oligomer synthesis demands high coupling efficiencies and hence oligomer length can be an important and significant consideration in AO drug design, highlighting the need to keep the AO length as short as possible while still maintaining adequate exon skipping levels. Some sequences can be challenging to synthesise, for example AOs with a high GC content (>75%) and sequences that include stretches of four Gs have the ability to form G-quartets [32]; structures that stack on top of each other and form tetrad-helical structures, thus severely inhibiting the functionality and solubility of the oligomer [33].

One crucial aspect of developing splice modulating AOs is to enhance stability in biological systems without compromising efficiency and introducing toxicity. At present, 2-OMe PS AOs are cost-effective for initial screening. However, in several studies, the oligonucleotides on a PS backbone have shown toxicity, off-target effects, and injection site reactions [34–37]. Nevertheless, these negatively charged AOs are ideal as research tools as they can be readily transfected into cultured cells as cationic lipoplexes. The lead AO sequences identified by 2-OMe PS AO screens may prove more effective when synthesised as the clinically safe PMO chemistry. There are no reports of serious adverse events occurring after long-term treatment with *Exondys 51* [1,2], while the same cannot be said for the 2-OMe PS AO drug *Drisapersen*. PMOs escape the electrostatic repulsion from the negatively charged RNA or DNA due to their neutral backbone [20,38]. This enables much higher binding specificity and affinity when compared to 2-OMe PS AOs. Furthermore, PMOs exert little to no off-target effects or non-specific binding, which is largely attributed to their neutral charge [20].

In conclusion, we have described a robust approach for developing and designing splice modulating AOs that may eventually enter the clinic. Extensive refining of the AO sequences to achieve the shortest oligomer with high efficacy is crucial to reduce the cost and production issues of the candidate oligo sequences. Antisense oligomer-mediated modulation of gene transcripts involved in genetic diseases has great potential for therapeutic application. The systematic evaluation of AOs in the manner we describe here will ensure the selection of the most efficacious and safe AOs for clinical trials.

### 4. Materials and Methods

#### 4.1. Cell Culture

All cell culture reagents were purchased from Gibco, ThermoFisher Scientific, (Scoresby, Victoria, Australia) unless otherwise stated. Primary dermal fibroblasts obtained from a healthy volunteer, with informed consent (approved by the Murdoch University Human Research Ethics Committee,

approval number 2013/156, 25 October 2013) were propagated in Dulbecco's modified Eagle medium (DMEM) supplemented with L-Glutamine and 10% foetal bovine serum (FBS) (Scientifix, Cheltenham, Victoria, Australia).

#### 4.2. Antisense Oligonucleotides (AOs)

Antisense oligonucleotides comprising 2'-O-methyl modified bases on a phosphorothioate backbone (2-OMe PS) were synthesised in-house on an Expedite 8909 Nucleic Acid synthesiser (Applied Biosystems, Melbourne, Victoria, Australia) using the 1 µmol thioate synthesis protocol as described previously [39]. Briefly, phenyl acetyl disulphide was used in the sulphurisation of the oligonucleotide. The 2'-hydroxyl positions are protected with t-butyldimethylsilyl group. Specifically, benzoyl was used as the protection reagent for nucleotide A and C monomers, while isobutyryl was used for nucleotide G monomer and U monomer not requiring protection. After synthesis, the oligonucleotides were cleaved from the support following incubation in ammonium hydroxide for a minimum of 16 h at room temperature. The AOs were subsequently desalted under sterile conditions using the NAP-10 columns (GE Healthcare, Sydney, NSW, Australia) according to manufacturer's instructions. A list of 2-OMe PS AOs used in this study are summarised in Table 2.

#### 4.3. 2'-O-Methyl Phosphorothioate AO Transfection

Approximately 15,000 fibroblasts were seeded onto 24-well tissue culture plates and incubated overnight at 37 °C in fibroblast propagation media. When approximately 70–80% confluent, cells were transfected with 2-OMe PS AOs using Lipofectamine™ 3000, Lipofectamine™ RNAiMax, or Lipofectin™ transfection reagent according to the manufacturer protocols. Opti-MEM media was used for all transfections. Transfected cells were incubated at 37 °C for 24 h before RNA was extracted for transcript analysis.

#### 4.4. RT-PCR

Total RNA was extracted using Trizol (Life Technologies, Scoresby, Victoria, Australia) according to manufacturer's guidelines for transcript analysis. RT-PCR was performed using RNA (50 ng) from AO-treated and untreated cells and a Superscript III One-Step RT-PCR System (Life Technologies, Australia). Primer sequences for all RT-PCR primers used in this study can be found in Table 3. RT-PCR amplification was performed using the following thermocycling conditions: 55 °C for 30 min, 30 cycles of 94 °C for 30 s, 55 °C for 30 s, and 68 °C for 2 min. RT-PCR products were resolved on 2% agarose gels in Tris-acetate EDTA buffer and images were captured using a Fusion-FX gel documentation system (Vilber Lourmat, Eberhardzell, France). Product identity was confirmed by reamplification and purification of separated amplicons [40], followed by Sanger sequencing by the Australian Genome Research Facility (AGRF).

**Table 2.** List of AOs [41].

Name	Sequence (5' – 3')
ITGA4 H3A(+30+49)	UCUCUCUCUCCAAACAAGU
ITGA4 H3A(-18+7)	GGGCUACCUAUAGCAUGUGAAAAUA
ITGA4 H3A(+20+39)	CCAAACAAGUCUUCCACAA
ITGA4 H3A(+46+70)	GUGACCCCCAACCCACUGAUUGUCUC
ITGA4 H3A(+41+65)	CCCCAACCCACUGAUUGUCUCUCUCU
ITGA4 H3A(+51+75)	AAAGUGUGACCCCCAACCCACUGAUU
ITGA4 H3D(+6-19)	GACCAGUCCAAUACCUACCACGAU
ITGA4 H3D(+11-14)	GUUCCAAUACCUACCACGAUGGAUC
ITGA4 H3D(+1-24)	CUGUGGACCAGUCCAAUACCUACC
Ctl	GGAUGUCCUGAGUCUAGACCCUCCG

**Table 3.** List of primers used in this study.

Name	Sequence (5' – 3')	Amplification Performed after Treatment with the Following AOs
ITGA4 ex1_F ITGA4 ex10_R	gagagcgcgctgctttaccagg gccatcattgtcaatgtcgcca	All AOs
ITGA4 ex1_F ITGA4 ex4_R	gagagcgcgctgctttaccagg ggcactccatagcaaccacc	ITGA4 H3A(+30+49)

**Author Contributions:** Conceptualisation, M.T.A.-H. and C.S.M.; Methodology, M.T.A.-H., C.S.M., K.A.H., and S.D.W.; Formal Analysis: M.T.A.-H., C.S.M., and K.A.H.; Investigation, M.T.A.-H., C.S.M., and K.A.H.; Writing, M.T.A.-H., C.S.M., K.A.H., S.F., and S.D.W.; Editing, M.T.A.-H., C.S.M., K.A.H., I.L.P., L.L.F., K.G., S.F., and S.D.W.; Supervision, S.F. and S.D.W.; Resources, S.F. and S.D.W.; Funding Acquisition, S.F. and S.D.W.

**Funding:** Funding received from the NHMRC (AP1144791).

**Conflicts of Interest:** S.F. and S.D.W. are consultants for Sarepta Therapeutics, and M.T.A.-H.'s salary is partly supported by Sarepta Therapeutics. This association has not influenced this work in any fashion.

## References

- Mendell, J.R.; Goemans, N.; Lowes, L.P.; Alfano, L.N.; Berry, K.; Shao, J.; Kaye, E.M.; Mercuri, E.; Eteplirsen Study Group; Telethon Foundation DMD Italian Network; et al. Longitudinal effect of eteplirsen versus historical control on ambulation in Duchenne muscular dystrophy. *Ann. Neurol.* **2016**, *79*, 257–271. [[CrossRef](#)] [[PubMed](#)]
- Mendell, J.R.; Sahenk, Z.; Rodino-Klapac, L.R. Clinical trials of exon skipping in Duchenne muscular dystrophy. *Expert Opin. Orphan Drugs* **2017**, *5*, 683–690. [[CrossRef](#)]
- Finkel, R.S.; Chiriboga, C.A.; Vajsar, J.; Day, J.W.; Montes, J.; De Vivo, D.C.; Yamashita, M.; Rigo, F.; Hung, G.; Schneider, E. Treatment of infantile-onset spinal muscular atrophy with nusinersen: A phase 2, open-label, dose-escalation study. *Lancet* **2017**, *388*, 3017–3026. [[CrossRef](#)]
- Rinaldi, C.; Wood, M.J. Antisense oligonucleotides: The next frontier for treatment of neurological disorders. *Nat. Rev. Neurol.* **2018**, *14*, 9–21. [[CrossRef](#)] [[PubMed](#)]
- Scoles, D.R.; Meera, P.; Schneider, M.D.; Paul, S.; Dansithong, W.; Figueroa, K.P.; Hung, G.; Rigo, F.; Bennett, C.F.; Otis, T.S. Antisense oligonucleotide therapy for spinocerebellar ataxia type 2. *Nature* **2017**, *544*, 362–366. [[CrossRef](#)] [[PubMed](#)]
- Stein, C.; Hansen, J.B.; Lai, J.; Wu, S.; Voskresenskiy, A.; Høg, A.; Worm, J.; Hedtjärn, M.; Souleimanian, N.; Miller, P. Efficient gene silencing by delivery of locked nucleic acid antisense oligonucleotides, unassisted by transfection reagents. *Nucleic Acids Res.* **2009**, *38*, e3. [[CrossRef](#)] [[PubMed](#)]
- Julien, T.; Frankel, B.; Longo, S.; Kyle, M.; Gibson, S.; Shillitoe, E.; Ryken, T. Antisense-mediated inhibition of the bcl-2 gene induces apoptosis in human malignant glioma. *Surg. Neurol.* **2000**, *53*, 360–369. [[CrossRef](#)]
- Mendell, J.R.; Rodino-Klapac, L.R.; Sahenk, Z.; Roush, K.; Bird, L.; Lowes, L.P.; Alfano, L.; Gomez, A.M.; Lewis, S.; Kota, J. Eteplirsen for the treatment of Duchenne muscular dystrophy. *Ann. Neurol.* **2013**, *74*, 637–647. [[CrossRef](#)]
- Havens, M.A.; Hastings, M.L. Splice-switching antisense oligonucleotides as therapeutic drugs. *Nucleic Acids Res.* **2016**, *44*, 6549–6563. [[CrossRef](#)]
- Flynn, L.L.; Mitrpant, C.; Pitout, I.L.; Fletcher, S.; Wilton, S.D. Antisense oligonucleotide-mediated terminal intron retention of the smn2 transcript. *Mol. Ther. Nucleic Acids* **2018**, *11*, 91–102. [[CrossRef](#)]
- Piva, F.; Giulietti, M.; Burini, A.B.; Principato, G. Spliceaid 2: A database of human splicing factors expression data and rna target motifs. *Hum. Mutat.* **2012**, *33*, 81–85. [[CrossRef](#)] [[PubMed](#)]
- Desmet, F.-O.; Hamroun, D.; Lalande, M.; Collod-Bérout, G.; Claustres, M.; Bérout, C. Human splicing finder: An online bioinformatics tool to predict splicing signals. *Nucleic Acids Res.* **2009**, *37*, e67. [[CrossRef](#)] [[PubMed](#)]
- Huang, H.-Y.; Chien, C.-H.; Jen, K.-H.; Huang, H.-D. RegRNA: An integrated web server for identifying regulatory rna motifs and elements. *Nucleic Acids Res.* **2006**, *34*, W429–W434. [[CrossRef](#)] [[PubMed](#)]
- Aartsma-Rus, A. Overview on aon design. In *Exon Skipping*; Springer: Heidelberg, Germany, 2012; pp. 117–129.

15. Pramono, Z.A.D.; Wee, K.B.; Wang, J.L.; Chen, Y.J.; Xiong, Q.B.; Lai, P.S.; Yee, W.C. A prospective study in the rational design of efficient antisense oligonucleotides for exon skipping in the *dmd* gene. *Hum. Gene Ther.* **2012**, *23*, 781–790. [CrossRef] [PubMed]
16. Aartsma-Rus, A.; Van Vliet, L.; Hirschi, M.; Janson, A.A.; Heemskerk, H.; De Winter, C.L.; De Kimpe, S.; Van Deutekom, J.C.; Ac't Hoen, P.; van Ommen, G.-J.B. Guidelines for antisense oligonucleotide design and insight into splice-modulating mechanisms. *Mol. Ther.* **2009**, *17*, 548–553. [CrossRef] [PubMed]
17. Gebiski, B.L.; Mann, C.J.; Fletcher, S.; Wilton, S.D. Morpholino antisense oligonucleotide induced dystrophin exon 23 skipping in *mdx* mouse muscle. *Hum. Mol. Genet.* **2003**, *12*, 1801–1811. [CrossRef]
18. Mitrpant, C.; Adams, A.M.; Meloni, P.L.; Muntoni, F.; Fletcher, S.; Wilton, S.D. Rational design of antisense oligomers to induce dystrophin exon skipping. *Mol. Ther.* **2009**, *17*, 1418–1426. [CrossRef]
19. Greer, K.L.; Lochmüller, H.; Flanigan, K.; Fletcher, S.; Wilton, S.D. Targeted exon skipping to correct exon duplications in the dystrophin gene. *Mol. Ther. Nucleic Acids* **2014**, *3*, e155. [CrossRef]
20. Summerton, J.E. Morpholino, sirna, and s-DNA compared: Impact of structure and mechanism of action on off-target effects and sequence specificity. *Curr. Top. Med. Chem.* **2007**, *7*, 651–660. [CrossRef]
21. Zuhorn, I.S.; Engberts, J.B.; Hoekstra, D. Gene delivery by cationic lipid vectors: Overcoming cellular barriers. *Eur. Biophys. J.* **2007**, *36*, 349–362. [CrossRef]
22. Aung-Htut, M.T.; McIntosh, C.S.; West, K.A.; Fletcher, S.; Wilton, S.D. In vitro validation of phosphorodiamidate morpholino oligomers. *Molecules* **2019**, *24*, 2922. [CrossRef] [PubMed]
23. Mann, C.J.; Honeyman, K.; McClorey, G.; Fletcher, S.; Wilton, S.D. Improved antisense oligonucleotide induced exon skipping in the *mdx* mouse model of muscular dystrophy. *J. Gene Med. Cross-Discip. J. Res. Sci. Gene Transf. Clin. Appl.* **2002**, *4*, 644–654.
24. Weizmann-Insitite. Gene Cards Human Gene Database. Available online: <https://www.genecards.org/> (accessed on 14 March 2019).
25. Murry, C.E.; Kay, M.A.; Bartosek, T.; Hauschka, S.D.; Schwartz, S.M. Muscle differentiation during repair of myocardial necrosis in rats via gene transfer with myod. *J. Clin. Investig.* **1996**, *98*, 2209–2217. [CrossRef] [PubMed]
26. Lattanzi, L.; Salvatori, G.; Coletta, M.; Sonnino, C.; De Angelis, M.C.; Gioglio, L.; Murry, C.E.; Kelly, R.; Ferrari, G.; Molinaro, M. High efficiency myogenic conversion of human fibroblasts by adenoviral vector-mediated myod gene transfer. An alternative strategy for ex vivo gene therapy of primary myopathies. *J. Clin. Investig.* **1998**, *101*, 2119–2128. [CrossRef] [PubMed]
27. Choi, J.; Costa, M.; Mermelstein, C.; Chagas, C.; Holtzer, S.; Holtzer, H. Myod converts primary dermal fibroblasts, chondroblasts, smooth muscle, and retinal pigmented epithelial cells into striated mononucleated myoblasts and multinucleated myotubes. *Proc. Natl. Acad. Sci. USA* **1990**, *87*, 7988–7992. [CrossRef] [PubMed]
28. Fletcher, S.; Adkin, C.F.; Meloni, P.; Wong, B.; Muntoni, F.; Kole, R.; Fragall, C.; Greer, K.; Johnsen, R.; Wilton, S.D. Targeted exon skipping to address “leaky” mutations in the dystrophin gene. *Mol. Ther. Nucleic Acids* **2012**, *1*, e48. [CrossRef] [PubMed]
29. Adams, A.M.; Harding, P.L.; Iversen, P.L.; Coleman, C.; Fletcher, S.; Wilton, S.D. Antisense oligonucleotide induced exon skipping and the dystrophin gene transcript: Cocktails and chemistries. *BMC Mol. Biol.* **2007**, *8*, 57. [CrossRef] [PubMed]
30. Fletcher, S.; Ly, T.; Duff, R.; Howell, J.M.; Wilton, S. Cryptic splicing involving the splice site mutation in the canine model of duchenne muscular dystrophy. *Neuromuscul. Disord.* **2001**, *11*, 239–243. [CrossRef]
31. Harding, P.; Fall, A.; Honeyman, K.; Fletcher, S.; Wilton, S. The influence of antisense oligonucleotide length on dystrophin exon skipping. *Mol. Ther.* **2007**, *15*, 157–166. [CrossRef]
32. Jing, N.; Li, Y.; Xiong, W.; Sha, W.; Jing, L.; Tweardy, D.J. G-quartet oligonucleotides: A new class of signal transducer and activator of transcription 3 inhibitors that suppresses growth of prostate and breast tumors through induction of apoptosis. *Cancer Res.* **2004**, *64*, 6603–6609. [CrossRef]
33. Williamson, J.R. G-quartet structures in telomeric DNA. *Annu. Rev. Biophys. Biomol. Struct.* **1994**, *23*, 703–730. [CrossRef] [PubMed]
34. Flanigan, K.M.; Voit, T.; Rosales, X.Q.; Servais, L.; Kraus, J.E.; Wardell, C.; Morgan, A.; Dorricott, S.; Nakielnny, J.; Quarcoo, N. Pharmacokinetics and safety of single doses of drisapersen in non-ambulant subjects with duchenne muscular dystrophy: Results of a double-blind randomized clinical trial. *Neuromuscul. Disord.* **2014**, *24*, 16–24. [CrossRef] [PubMed]

35. Dias, N.; Stein, C. Antisense oligonucleotides: Basic concepts and mechanisms. *Mol. Cancer Ther.* **2002**, *1*, 347–355. [[PubMed](#)]
36. Wong, E.; Goldberg, T. Mipomersen (kynamro): A novel antisense oligonucleotide inhibitor for the management of homozygous familial hypercholesterolemia. *Pharm. Ther.* **2014**, *39*, 119–122.
37. Chi, X.; Gatti, P.; Papoian, T. Safety of antisense oligonucleotide and sirna-based therapeutics. *Drug Discov. Today* **2017**, *22*, 823–833. [[CrossRef](#)]
38. Summerton, J.; Weller, D. Morpholino antisense oligomers: Design, preparation, and properties. *Antisense Nucleic Acid Drug Dev.* **1997**, *7*, 187–195. [[CrossRef](#)]
39. Wilton, S.D.; Fall, A.M.; Harding, P.L.; McClorey, G.; Coleman, C.; Fletcher, S. Antisense oligonucleotide-induced exon skipping across the human dystrophin gene transcript. *Mol. Ther.* **2007**, *15*, 1288–1296. [[CrossRef](#)]
40. Bjourson, A.J.; Cooper, J.E. Band-stab pcr: A simple technique for the purification of individual pcr products. *Nucleic Acids Res.* **1992**, *20*, 4675. [[CrossRef](#)]
41. Aung-Htut, M.T.; Comerford, I.; Johnsen, R.; Foyle, K.; Fletcher, S.; Wilton, S.D. Reduction of integrin alpha 4 activity through splice modulating antisense oligonucleotides. *Sci. Rep.* **2019**, *9*, 12994. [[CrossRef](#)]



© 2019 by the authors. Licensee MDPI, Basel, Switzerland. This article is an open access article distributed under the terms and conditions of the Creative Commons Attribution (CC BY) license (<http://creativecommons.org/licenses/by/4.0/>).

# Chapter 7 – Published

## Research Article 3


Aung-Htut, M. T.\* , McIntosh, C. S.\* , West, K. A., Fletcher, S., & Wilton, S. D. (2019). *In vitro validation of phosphorodiamidate morpholino oligomers*. *Molecules*, 24(16), 2922.

### Co-First Authored

**Author Contributions:** Conceptualisation, C.S.M. and M.T.A-H.; Methodology, C.S.M., M.T.A-H., K.A.W., and S.D.W.; Formal Analysis: C.S.M., M.T.A-H., and K.A.W.; Investigation, C.S.M., M.T.A-H., and K.A.W.; Writing, C.S.M., M.T.A-H., K.A.W., S.F., and S.D.W.; Editing, C.S.M., M.T.A-H., K.A.W., S.F., and S.D.W.; Supervision, S.F. and S.D.W.; Resources, S.F. and S.D.W.; Funding Acquisition, S.F. and S.D.W.

Article

# In Vitro Validation of Phosphorodiamidate Morpholino Oligomers

May T. Aung-Htut <sup>1,2,†</sup> , Craig S. McIntosh <sup>1,2,\*</sup>, Kristin A. West <sup>1</sup>, Sue Fletcher <sup>1,2</sup> and Steve D. Wilton <sup>1,2</sup>

<sup>1</sup> Centre for Molecular Medicine and Innovative Therapeutics, Murdoch University, Perth, WA 6150, Australia

<sup>2</sup> Perron Institute for Neurological and Translational Science, the University of Western Australia, Perth, WA 6009, Australia

\* Correspondence: c.mcintosh@murdoch.edu.au

† These authors contributed equally to this work.

Academic Editor: Rakesh N. Veedu

Received: 19 June 2019; Accepted: 8 August 2019; Published: 12 August 2019



**Abstract:** One of the crucial aspects of screening antisense oligonucleotides destined for therapeutic application is confidence that the antisense oligomer is delivered efficiently into cultured cells. Efficient delivery is particularly vital for antisense phosphorodiamidate morpholino oligomers, which have a neutral backbone, and are known to show poor gymnotic uptake. Here, we report several methods to deliver these oligomers into cultured cells. Although 4D-Nucleofector™ or Neon™ electroporation systems provide efficient delivery and use lower amounts of phosphorodiamidate morpholino oligomer, both systems are costly. We show that some readily available transfection reagents can be used to deliver phosphorodiamidate morpholino oligomers as efficiently as the electroporation systems. Among the transfection reagents tested, we recommend Lipofectamine 3000™ for delivering phosphorodiamidate morpholino oligomers into fibroblasts and Lipofectamine 3000™ or Lipofectamine 2000™ for myoblasts/myotubes. We also provide optimal programs for nucleofection into various cell lines using the P3 Primary Cell 4D-Nucleofector™ X Kit (Lonza), as well as antisense oligomers that redirect expression of ubiquitously expressed genes that may be used as positive treatments for human and murine cell transfections.

**Keywords:** antisense oligonucleotide; morpholino; PMO; transfection; electroporation; exon skipping

## 1. Introduction

Antisense oligonucleotides (ASOs) are short, single-stranded molecules that can be designed to specifically bind to DNA or RNA via Watson-Crick base pairing, with the aim of modifying specific gene expression. Although ASOs have been used as laboratory tools since these agents were first reported, it took more than three decades for their arrival in the clinic as therapeutics. An extensive amount of time and effort can often be spent on in vitro development, assessment, and validation of antisense oligomer efficacy, to ensure that the optimal ASOs progress to clinical trials. In 1978, Zamecnik and Stephenson were the first to report blocking Rous sarcoma viral replication in chick embryo fibroblast cell cultures after transfection with a 13-nucleotide oligomer and, despite not knowing the mode of action, proposed the use of ASOs as antiviral agents [1,2]. As natural DNA oligonucleotides with the phosphodiester backbone are susceptible to enzymatic degradation, chemical modifications to bases and backbones were developed to enhance binding affinity, increase resistance to nuclease digestion and allow different modes of action that include specific degradation through RNase H induction or siRNA action, blocking protein translation or redirecting pre-mRNA processing [3–6]. Since these modifications and mechanisms were introduced, research into ASO compounds as therapeutics for many diseases, including those caused by genetic mutations, has grown immensely.



The U.S. Food and Drug Administration has now approved several ASO drugs involving various chemistries in different stages of clinical development [7–10]. The success of all approved therapeutic ASOs was based upon careful design and screening of the optimal sequences, first in an *in vitro* system and then *in vivo*. Therefore, it is imperative to have confidence in a consistent and reliable delivery protocol to ensure cellular or nuclear uptake of the ASOs [11].

Unlike many other synthetic nucleic acid analogues in clinical development, phosphorodiamidate morpholino oligomers (PMOs) have a neutral charge and delivering these compounds into cultured cells can be problematic [5,12,13]. Although gymnotic delivery for some PMOs has been reported in human myotube cultures when applied at high concentrations [14], this process is largely inefficient. The inefficiency is generally attributed to the PMO's inability to translocate through cell membranes as an uncharged molecule and may be overcome by the addition of a peptide-conjugated tag, which provides a significant charge to the PMO allowing for easier delivery. Thus, uncharged PMOs generally require delivery agents or protocols to enhance intracellular uptake, although recently Miyatake et al. (2019) demonstrated that scavenger Receptor Class A1 mediated uptake of PMOs both *in vitro* and *in vivo* [15]. This study may provide further insight into the gymnotic uptake of these compounds and lead towards an improved drug delivery system.

One must be confident that any transfection protocol used efficiently delivers the PMO into the cell. As learnt from previous reports, *in vitro* analysis of DMD exon 46 skipping using a morpholino oligomer was ineffective compared to the same sequence composed of 2'-O-methyl-modified bases on a phosphorothioate backbone (2'-OMe ASOs) [16]. Conversely, *in vivo* assessment of PMOs showed efficient exon 46 skipping of the DMD transcript in humanised DMD mice [17]. Therefore, the discrepancy between these results arose from an issue of delivery rather than an ineffective ASO, highlighting the need for confidence in efficient delivery *in vitro* during ASO development.

The importance of PMO chemistry for protein studies was revealed during the development of ASOs to correct the defect in the canine model of DMD [18]. Antisense oligomer optimisation to skip dystrophin exons 6 and 8 used the 2'-OMe ASOs, and while this chemistry was suitable for RNA studies, detecting dystrophin restoration was not possible [18]. However, when the equivalent ASOs were prepared as PMOs or PMOs conjugated to a peptide-conjugated tag (PPMO), dystrophin protein of near full-length was readily detected [18]. When the uncomplexed PMO cocktail was added to cell media, uptake was poor and dystrophin expression modest. In contrast, the PPMO-treated canine DMD cells showed robust multi-exon skipping and unequivocal dystrophin restoration [18].

One simple and relatively effective means of delivering PMOs into cultured cells is "scrape-loading", where adherent cells are gently scraped to create small transient holes in the plasma membrane, thus allowing for better uptake of the PMO [19]. Alternatively, Gebiski et al. reported annealing sense-strand DNA "leashes" to antisense PMOs, thereby allowing the negatively charged PMO: DNA duplex to form complexes with commercially available cationic lipid transfection reagents [20]. In this approach, the PMO delivery is more comparable to that used to transfect the commonly used ASOs composed of 2'-OMe or locked nucleic acid (LNA) oligomers. Gene Tools has developed a novel peptide-mediated delivery reagent, Endo-Porter, that allows PMO delivery via endocytosis to adhered cells without the use of a leash [21]. Electroporation-mediated transfection using a 4D-Nucleofector™ or Neon™ system also offers efficient delivery of PMOs to different cell types, including both adherent and suspension cells [22,23].

The first compound to be granted accelerated approval for the treatment of Duchenne muscular dystrophy, *Exondys 51*, was developed in our laboratory [24–26], and we are currently researching nucleic acid therapeutics for numerous diseases amenable to RNA splicing intervention [24,25,27–29]. Consequently, we have experience in the design, delivery and evaluation of hundreds of PMOs in different cell lines to address various mutations. We found that PMOs can be delivered into adherent cells, without a leash, using commercially available cationic lipid-mediated transfection reagents, with an efficiency similar to that observed with nucleofection. Cationic lipid transfection reagents were chosen due to the ease of accessibility to most laboratories throughout the world. In addition, little

literature exists regarding alternative transfection methods. Of the transfection reagents evaluated, we found that Lipofectamine 3000™ had the least impact on cell morphology and viability but offered relatively effective PMO delivery into fibroblasts. In addition to Lipofectamine 3000™, Lipofectamine 2000™ also offered effective PMO delivery into cultured myoblasts/myotubes. Nucleofector or Neon electroporator instruments and their consumables are relatively costly; however, the advantage of these delivery systems is that the PMO can be delivered to as many as 20 or 6 million cells, respectively, using substantially lower amounts of PMO. Consequently, we routinely use nucleofection for PMO delivery, and we report optimised PMO delivery programs using the P3 Primary Cell 4D-Nucleofector™ X Kit (Lonza) that can be used for various cell lines.

## 2. Results

### 2.1. PMO Delivery into Human Dermal Fibroblasts

We have chosen previously optimised exon skipping PMOs targeting the *ITGA4* and *SMN* transcripts expressed in most cell types and cell lines (Figure S1). To determine whether the nominated widely used cationic lipid transfection reagents available in the laboratory offer an economical and reliable method to deliver PMOs into human dermal fibroblasts, we selected two commonly used cationic lipid transfection reagents; Lipofectamine 3000™ and Lipofectin™, for complex formation with ASO 1, optimised to induce skipping of exons 3 and 4 from the *ITGA4* pre mRNA transcript [30]. In addition to the lipoplex: PMO transfection, alternative transfection strategies including nucleofection, Endo-Porter and gymnotic uptake of uncomplexed PMO were evaluated in a direct comparison. The same experiments were repeated using human myoblasts, except Lipofectin™ was replaced with Lipofectamine 2000™ for comparison, as the latter shows better transfection efficiency in myoblasts in our laboratory.

The morphology and viability of fibroblasts and myoblasts treated with PMOs complexed with the Lipofectamine 3000™ reagent were similar to that of cells treated with the uncomplexed PMO and untreated fibroblasts or myoblasts (Figure 1A,B). In contrast, substantial cell death was observed after fibroblasts were treated with PMO complexed with Lipofectin™ (10 µl/mL) and myoblasts treated with PMO: Lipofectamine 2000™ complex (Figure 1C,D). Nucleofection did not visibly affect the morphology or viability of the fibroblasts or myoblasts (Figure 1A–D). The morphology of fibroblast cultures after Endo-Porter-mediated PMO delivery was atypical when compared to other reagents (Figure 1A). Aggregates, possibly complexes of PMO and peptide, bordered the cells, and small cell bodies with slender cell extensions were prominent in Endo-porter treated cells, but not observed in untreated fibroblasts.

The uptake of ASO 1 and subsequent ability to redirect pre-mRNA processing was demonstrated by RT-PCR analysis of the *ITGA4* transcripts (Figure 1E,F). All treatments, except for the uncomplexed PMO, induced exon 3 and 4 skipping with similar efficiencies, although higher levels of exon skipping were observed in the fibroblasts treated with PMO: Lipofectin. Increased levels of exon skipping may have been a consequence of the extensive cell death observed after the Lipofectin™ transfection, compared to the other treatments. Similarly, myoblasts treated with PMO: Lipofectamine 2000™ caused more than 50% cell death. The average percentages of exon skipping from three biological replicates are shown in Figure 1E,F and the original gel images are shown in Supplementary Figure S3.

Although evidence of cell death appeared minimal after Endo-Porter-mediated PMO delivery (Figure 1C,D), the fibroblasts nevertheless showed signs of cell stress. Therefore, we analysed the expression profile of the cell stress-related proteins using the proteome profiler human cell stress array kit (Figure S2), which consists of an analysis of relative expression levels of 26 cell stress-related proteins. Although the levels of some of the stress-related proteins were altered, the most compelling changes were observed in two proteins, Cited 2 and p21, which were decreased by more than 50% in Endo-Porter treated fibroblasts, compared to the untreated cells.

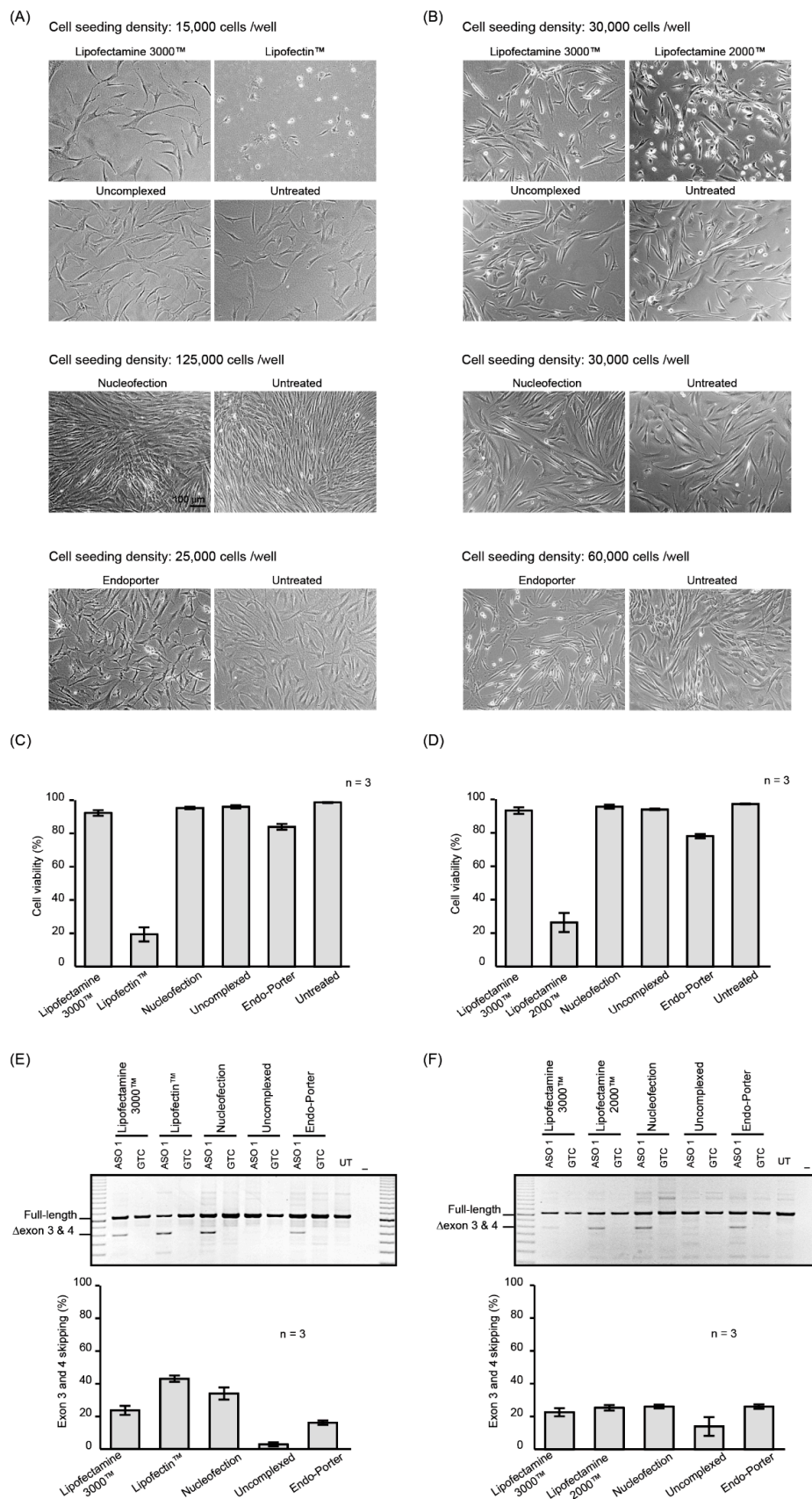


**Figure 1.** Micrographs of fibroblasts (A) and myoblasts (B) treated with 10 μM of ASO 1 for 24 h using the delivery methods indicated above each panel. Cell viability of (C) fibroblasts and (D) myoblasts

treated with PMO complexed with indicated reagent, uncomplexed and untreated. RT-PCR products of the *ITGA4* transcript amplified from (E) fibroblasts and (F) myoblasts treated as in (A) and (B) respectively. Shown are the average percentages of exon skipping from three biological replicates represented as a bar graph below the gel image. GTC: Gene Tools Control PMO. Error bar; SEM.

## 2.2. Nucleofection Programs for PMO Delivery into Different Cell Lines

Nucleofection is one of the commonly used methods to efficiently deliver nucleic acids, including PMOs, into cultured cells. Nucleofection is our preferred method for PMO delivery as the test compounds can be delivered into a million cells (using the 4D-Nucleofector X Kit S) without compromising the efficiency (Figure 2A) or using excessive amounts of PMO, as well as being highly reproducible (Figure 2A). We have optimised nucleofection programs using the P3 kit (Table 1) for multiple, extensively used cell lines that are commercially available, and achieved 70% or more exon skipping of the target transcript with less than 10% cell death as shown in Figure 2B. We selected two PMOs, ASO 2 targeting exon 3 of the *ITGA4* transcript (Figure 2A), and ASO 3 targeting exon 7 of the murine *Smn* transcript [31] for standardised evaluation (Figure 2B). Although ASO 3 was designed to target the murine *Smn* transcript, it is also capable of inducing exon 7 skipping from the human *SMN* transcript despite 2 mismatches at the 8th and 21st position. From these experiments, it can be seen that nucleofection is an efficient and reproducible method of transfection.

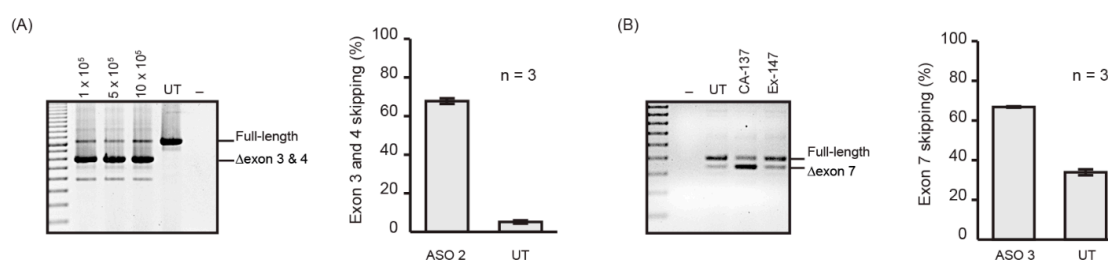


**Figure 2.** (A) RT-PCR products of *ITGA4* transcript amplified from human fibroblasts nucleofected with ASO 2 at 50 μM concentration in the cuvette using the P3 nucleofection kit and CA-137 program and various cell densities. The number of cells nucleofected is shown above the gel. Shown are the average percentages of exon skipping from three biological replicates represented as a bar graph next to the gel image. UT: Untreated. Error bar; SEM. (B) RT-PCR products of *SMN* transcript from Huh7 cells nucleofected with ASO 3 at 50 μM concentration in the cuvette using P3 kit, and CA-137 or Ex-147 program. Shown are the average percentages of exon skipping using CA-137 program from three biological replicates represented as a bar graph next to the gel image. UT: Untreated. Error bar; SEM.

**Table 1.** Optimal nucleofection programs for the P3 kit and the cell numbers tested in specified cell lines.

Cell Type	Name	P3 Program	Cell Number
Human dermal fibroblasts	HDF	CA-137	2.5–10 × 10 <sup>5</sup>
Human skeletal muscle myoblasts	HSkM	CM-138	2.5 × 10 <sup>5</sup>
Human T lymphocytes	Jurkat	CL-120	2–5 × 10 <sup>5</sup>
Human Glial (Oligodendrocytic) Hybrid Cell Line	MO3.13	CA-138	2.5 × 10 <sup>5</sup>
		DR-114	2.5 × 10 <sup>5</sup>
		EM-110	2.5 × 10 <sup>5</sup>
Human neuroblastoma	SH-SY5Y	CA-137	2.5–10 × 10 <sup>5</sup>
Human hepatocarcinoma	Huh7	CA-137	2.5 × 10 <sup>5</sup>
Human hepatocarcinoma	HepG2	EH-100	2.5 × 10 <sup>5</sup>
Murine primary splenocytes		DN-100	10 × 10 <sup>5</sup>
Murine myoblast	H2Kmdx	CM-138	2.5 × 10 <sup>5</sup>

### 3. Discussion

It is often stated that there are three great challenges to genetic therapies: delivery, delivery and delivery. While the design of the therapeutic vector, plasmid or antisense oligomer is a fundamentally crucial aspect, without efficient and effective delivery to the target tissue or cells, the most therapeutically active compound may appear inert. We have extensive experience in designing and assessing the potential of splice modulating antisense oligomers, initially as research-grade 2'-OMe phosphorothioate oligonucleotides that can be readily synthesised in-house, and perhaps more importantly, easily and efficiently transfected into cultured cells as cationic lipoplexes.

Apart from the considerable cost, PMOs have other limitations, including poor cellular/nuclear uptake unless particular strategies are employed. Indeed, PMOs were discounted as possible splice switching agents for dystrophin exon skipping after researchers compared PMOs, 2'-OMe, LNA and peptide nucleic acids (PNA) [16]. The PNA was ineffective while the PMOs induced only weak exon skipping compared to the 2'-OMe ASOs and LNAs. It is of interest to note that the transfection conditions to compare these different oligonucleotides were not equivalent in this study, with polyethylenimine complexed with the 2'-OMe and LNA oligomers, ethoxylated polyethylenimine mixed with PMO and a DNA sense strand, and no transfection agent for the PNA. We had earlier shown that an optimised PMO, when annealed to a variety of sense strand DNA/RNA-like leashes and complexed with Lipofectin™, was found to induce robust exon skipping after transfection at concentrations as low as 30 nM, whereas the uncomplexed PMO showed no activity at 30-fold higher transfection concentrations [20].

Conscious of the importance of PMO delivery, we evaluated various protocols to introduce PMOs into cultured cells. The most common cell types studied in our laboratory are human dermal fibroblasts and myoblasts, as these cells could be readily obtained from individuals after Human Ethics Committee approval and informed consent through our collaborating clinicians. Depending upon commercial availability and tissue-specific gene expression, other cell lines may also be studied, and we provide nucleofection programs for the P3 kit to deliver PMO into various cell lines, in addition to liposome transfection.

Convention dictates that when delivering uncharged PMOs into cells with cationic liposome transfection reagents, annealing the PMO to a complementary strand DNA or RNA-like "leash" would provide the necessary negative charge for PMO: lipoplex formation. Counter-intuitively, we found that a leash was not necessary for PMO: lipoplex formation with either Lipofectamine 3000™/2000™ or Lipofectin™. Significantly, these reagents can deliver PMOs into cells with efficiencies similar to that achieved by nucleofection. Transfection with ASO 1 showed consistent but modest levels of exon skipping and was therefore chosen for study so it would be possible to discern between the efficiencies of different delivery protocols confidently [31]. When assessing a PMO that induces efficient skipping (>80%), it can become more difficult to reliably discern subtle differences in transfection efficiency and densitometric analysis with titration experiments. Uncomplexed ASO 1 was not taken up by fibroblasts after 24 h incubation, and therefore, any exon skipping detected in the fibroblasts transfected with ASO 1 complexed with transfection reagent must be attributed to enhanced delivery through these transfection reagents. In our experience, Lipofectamine 3000™ is versatile and shows little or no toxicity in most cell types. It is possible that the cell death observed in fibroblasts treated with Lipofectin™ may be limited by lowering the concentration of Lipofectin™ utilised for PMO delivery. However, the 10 µL/mL Lipofectin™ we applied is lower than the recommended DNA: transfection reagent ratio of 1:1. Lipofectamine 2000™ consistently outperformed Lipofectamine 3000™ in myoblasts regarding the exon skipping efficiency, although it caused higher levels of cell death. Among the biological replicates performed in myoblasts, we noticed that there was a positive correlation between the extent of myotube formation and uncomplexed PMO uptake. However, once the PMO was complexed with a delivery agent, uptake improved in all cultures, regardless of myotube formation.

The fibroblasts treated with Endo-Porter and PMOs showed anomalies around the cell membrane, and this may be due to the novel peptide promoting endocytosis and thus stressing the membrane.

Although endocytosis is a natural biological process in most cells, we speculate that Endo-Porter may induce a degree of endocytosis that exceeds the capacity of the pathway during normal endogenous function, compromising the cell membrane and thus inducing cell stress. Analysis of cell stress-related protein levels in Endo-Porter-treated cells suggested that cells may be under considerable stress, as indicated by the reduced expression of Cited 2, one of the proteins downregulated under ER stress [32]. Although the level of p21 in Endo-Porter-treated fibroblasts was lower than that in untreated fibroblasts, we speculate that the untreated fibroblasts were more confluent at collection than the Endo-Porter treated fibroblasts, accounting for the relatively higher p21 level.

In summary, this study provides various PMOs to modify the expression of broadly expressed genes that may be used as positive treatments for assessment of PMO delivery in a range of cultured cell types. We recommend the use of an electroporation system, particularly nucleofection that, over the years, has provided efficient and reproducible PMO delivery into many different cell types in our laboratory, with very little evidence of stress on the cells. We have provided optimised programs for various cell lines using a single P3 kit, but if this system is not available, Lipofectamine 3000™ can be used for reliably delivering PMO to most cell types, including fibroblasts, and Lipofectamine 2000™ for myoblasts. The PMOs described here target genes widely expressed in many different cell types and could be used as controls to monitor and confirm efficient delivery into most cell lines under investigation.

#### 4. Materials and Methods

##### 4.1. PMO Nomenclature

The nomenclature of all PMOs outlined in this study is as described by Mann et al. 2002 [33], as it indicates annealing coordinates and allows a sharp distinction between overlapping ASOs targeting a common region. Briefly, the first letter designates the species (H: human) followed by the targeted exon number with the specification of an acceptor (A) or donor (D) site and the annealing coordinates in brackets from 5' to 3' position of the mRNA transcript. The intronic bases are represented by negative (−) and the exonic position by positive (+). The annealing coordinates were based on the reference transcript as denoted by NCBI and *Ensembl genome browser 96*.

##### 4.2. PMOs

The PMOs used in this study, optimised after microwalking and designed to redirect *ITGA4* or *Smn* pre-mRNA processing [30,31] (Table 2), were purchased from Gene Tools, LLC (Philomath, OR, USA). These oligomers target ubiquitously expressed genes (*ITGA4* and *Smn*) and may be useful as positive transfection controls in other studies. These gene targets were chosen as they are widely expressed throughout common commercial cell lines. Expression patterns of both genes (adapted from GeneCards.org) can be found in Supplementary Figure S1.

**Table 2.** Information for ASOs.

Name	ASO Nomenclature	Sequence (5' to 3')	Target Protein
ASO 1	ITGA4 H3A (+ 30 + 49)	TCTCTCTCTCCAAACAAGT	Integrin alpha 4
ASO 2	ITGA4 H3A (+ 41 + 65)	CCCCAACCACTGATTGTCTCTCTCT	Integrin alpha 4
ASO 3	Smn M7A (+ 7 + 36)	TGAGCACTTTCCTTCTTTTTTATTGCT	Survival motor neuron
GTC	GTC-Gene Tools Control	CCTCTTACCTCAGTTACAATTTATA	Beta-globin chain

##### 4.3. Cell Culture

All cell culture reagents were purchased from Thermo Fisher Scientific Australia Pty. Ltd. (Scoresby, VIC, Australia) and cultures were maintained at 37 °C under a 5% CO<sub>2</sub>/95% air atmosphere, unless otherwise stated. The use of human cells was approved by the Murdoch University Human Research Ethics Committee (approval 2013/156). Human dermal fibroblasts were propagated in DMEM

supplemented with L-Glutamine and 10% foetal bovine serum (FBS). Human myogenic cells were prepared from biopsies taken from healthy individuals undergoing elective surgery at Royal Perth Hospital, Perth Western Australia, as described by Rando and Blau [34] with minor modifications [35]. Primary human myogenic cells were propagated in Hams F-10 Medium supplemented with 20% FBS and 0.5% chick embryo extract (Jomar Life Research, Scoresby, VIC, Australia) on flasks coated with 100 µg/mL Matrigel (BD Biosciences, Sydney, NSW, Australia). Jurkat cells were supplied by the European Collection of Cell Cultures (ECACC; Salisbury UK) and purchased from CellBank Australia (Westmead, NSW, Australia) and maintained in RPMI-1640 supplemented with 10% FBS. Human glial (oligodendrocytic) hybrid cell line MO3.13 was purchased from BioScientific Pty. Ltd. (Kirrawee, NSW, Australia) and maintained in DMEM supplemented with 10% FBS. The human bone marrow neuroblastoma cell line, SH-SY5Y, was purchased from ATCC (In Vitro Technologies Pty. Ltd., Noble Park North, VIC, Australia) and maintained in a 1:1 mixture of MEM and F-12 Medium supplemented with 10% FBS. The human hepatocarcinoma cell lines, Huh7 and HepG2, were supplied by the JCRB Cell Bank (Osaka, Japan) and purchased from CellBank Australia (Westmead, NSW, Australia). These cells were maintained in DMEM supplemented with 10% FBS. Murine H2k *mdx* myoblasts were cultured in poly D-lysine (50 µg/mL) and Matrigel (100 µg/mL) coated flasks at 33 °C under a 10% CO<sub>2</sub>/90% air atmosphere in high-glucose DMEM supplemented with 20% FBS and 10% horse serum, 0.5% chicken embryo extract and 20 units/mL γ-interferon (Roche Products Pty. Ltd., Sydney, NSW, Australia).

#### 4.4. Isolation of Splenocytes

Splenocytes were freshly isolated from the spleens taken from two *mdx* mice (Murdoch University approval number R2829/16). All steps were performed on ice and in RPMI-1640 supplemented with 10% FBS. Both spleens were sliced into small pieces (approximately 4 mm<sup>2</sup>) and mashed using the frosted side of pre-sterilised glass slide. The undissociated pieces of spleen were removed by centrifugation at 100× *g* for 8 min before the supernatant was centrifuged for a further 8 min at 200× *g*. The pellet of splenocytes was resuspended in 10% FBS, RPMI-1640 and the number of cells was determined using a haemocytometer (Sigma-Aldrich, Sydney, NSW, Australia).

#### 4.5. Transfection

Approximately 70% confluency/15,000 fibroblasts per well were plated in a 24-well plate one day prior to transfection [31]. Human myoblasts were plated in a 24-well plate that had been previously coated for 1 h with 50 µg/mL poly D-lysine (Sigma-Aldrich, Sydney, NSW, Australia) and 100 µg/mL Matrigel at 70% confluency/30,000 cells per well in Low Glucose DMEM supplemented with 5% horse serum, and cultured for 24 h [36]. Transfection complexes were formed according to the manufacturer's recommendations. PMO was transfected at a final concentration of 10 µM using 3 µL/mL Lipofectamine 3000™, 10 µL/mL Lipofectin™ or 10 µL/mL Lipofectamine 2000™. Briefly, the PMO and transfection reagents were separately diluted into 50 µL OptiMEM before mixing. PMO/lipid complexes were formed by incubating for the recommended time (10–15 min Lipofectamine 3000™; 30–45 min Lipofectin™; 5 min Lipofectamine 2000™) at room temperature before topping up to 300 µL with OptiMEM and adding to the cells. For Endo-Porter (Gene Tools) transfection, 80% confluency/25,000 cells were plated per well (as per the manufacturer's recommendations) one day before transfection, replaced with fresh media, and PMO was added to the media before adding the Endo-Porter (3 µL/mL).

#### 4.6. Nucleofection

All nucleofections were performed using the 4D-Nucleofector™ X Unit and P3 kit (Lonza, Mt Waverley, VIC, Australia) with the concentration of PMO set at 50 µM in the cuvette (volume of 1 µL 1 mM PMO in 20 µL cuvette volume), unless otherwise stated. The cell type, number of cells, and the program used for nucleofection is shown in Table 1, in accordance with the manufacturer's

recommendations. After the nucleofection pulse with the PMO, the cells were allowed to recover for 10 min at room temperature before being resuspended in the appropriate growth medium. Total RNA was extracted after 24 h using Direct-zol™ RNA Kit (Zymo Research, Tustin, CA, USA) according to the manufacturer's instructions.

#### 4.7. Microscopy

The images of transfected cells were captured using a Nikon® TS100 (Nikon, Sydney, NSW, Australia) prior to extracting total RNA using the Direct-zol™ RNA Kit.

#### 4.8. RT-PCR

RT-PCR was performed using a Superscript III One-Step RT-PCR System (Life Technologies, Scoresby, VIC, Australia). Total RNA (50 ng) from PMO-treated and untreated cells was used as a template for all reactions. RT-PCR amplification across the *ITGA4* transcript was performed using exon 1F (5' gagagcgcgctgctttaccagg 3') and 10R (5' gccatcattgtcaatgtcgcca 3') primers with the cycling conditions of 55 °C for 30 min for the reverse transcription step, followed by 28 cycles of 94 °C for 30 s, 55 °C for 30 s and 68 °C for 2 min. The RT-PCR products were fractionated on 2% agarose gels in Tris-acetate EDTA buffer and images of RedSafe™ (iNtRON Biotechnology, Inc., Burlington, MA, USA) stained gels were captured using a Fusion-FX gel documentation system (Vilber Lourmat, Marne la Vallée, France). Densitometric analysis was performed using ImageJ (NIH).

#### 4.9. Protein Stress Array

The GTC PMO was delivered to fibroblasts using Endo-Porter as described above and analysis of stress proteins performed using the proteome profiler human cell stress array kit (R&D Systems, Minneapolis, MN, USA) according to the manufacturer's protocol. Protein concentrations were determined using Pierce BCA protein assay kit (Thermo Fisher Scientific, Scoresby, VIC, Australia) and 200 µg protein was used for each assay. The pixel density was analysed using Image J (NIH).

**Supplementary Materials:** The following are available online, Figure S1: Genecards.org gene expression profile of human *ITGA4* and *SMN2* transcripts in major tissues. Figure S2: Normal human dermal fibroblasts were either untreated or treated with Endo-Porter complexed with GTC for 48 hours, and 200 µg of cell lysates were analysed on human stress arrays. Figure S3: Experimental biological replicates for Figure 1.

**Author Contributions:** Conceptualisation, M.T.A.-H. and C.S.M.; Methodology, M.T.A.-H., C.S.M., K.A.W. and S.D.W.; Formal Analysis: M.T.A.-H., C.S.M. and K.A.W.; Investigation, M.T.A.-H., C.S.M. and K.A.W.; Writing, M.T.A.-H., C.S.M., K.A.W., S.F. and S.D.W.; Supervision, S.F. and S.D.W.; Resources, S.F. and S.D.W.; Funding Acquisition, S.F. and S.D.W.

**Funding:** Funding received from the NHMRC and Multiple sclerosis research Australia incubator and project grants.

**Conflicts of Interest:** There is no conflict of interest reported. SF and SDW are named inventors on patents on modifying expression of *ITGA4* and the dystrophin gene. As such they are entitled to milestone and royalty payments should they arise.

## References

1. Stephenson, M.L.; Zamecnik, P.C. Inhibition of rous sarcoma viral rna translation by a specific oligodeoxyribonucleotide. *Proc. Natl. Acad. Sci. USA* **1978**, *75*, 285–288. [[CrossRef](#)] [[PubMed](#)]
2. Zamecnik, P.C.; Stephenson, M.L. Inhibition of rous sarcoma virus replication and cell transformation by a specific oligodeoxynucleotide. *Proc. Natl. Acad. Sci. USA* **1978**, *75*, 280–284. [[CrossRef](#)] [[PubMed](#)]
3. Dias, N.; Stein, C. Antisense oligonucleotides: Basic concepts and mechanisms. *Mol. Cancer Ther.* **2002**, *1*, 347–355. [[PubMed](#)]
4. Chery, J.; Näär, A. Rna therapeutics: Rnai and antisense mechanisms and clinical applications. *Postdoc J.* **2016**, *4*, 35. [[CrossRef](#)] [[PubMed](#)]
5. Summerton, J.; Weller, D. Morpholino antisense oligomers: Design, preparation, and properties. *Antisense Nucleic Acid Drug Dev.* **1997**, *7*, 187–195. [[CrossRef](#)] [[PubMed](#)]



6. Bauman, J.; Jearawiriyapaisarn, N.; Kole, R. Therapeutic potential of splice-switching oligonucleotides. *Oligonucleotides* **2009**, *19*, 1–13. [[CrossRef](#)] [[PubMed](#)]
7. Craig, K.; Abrams, M.; Amiji, M. Recent preclinical and clinical advances in oligonucleotide conjugates. *Expert Opin. Drug Deliv.* **2018**, *15*, 629–640. [[CrossRef](#)]
8. Aartsma-Rus, A. Fda approval of nusinersen for spinal muscular atrophy makes 2016 the year of splice modulating oligonucleotides. *Nucleic Acid Ther.* **2017**, *27*, 67–69. [[CrossRef](#)]
9. Mendell, J.R.; Sahenk, Z.; Rodino-Klapac, L.R. Clinical trials of exon skipping in duchenne muscular dystrophy. *Expert Opin. Orphan Drugs* **2017**, *5*, 683–690. [[CrossRef](#)]
10. Rinaldi, C.; Wood, M.J. Antisense oligonucleotides: The next frontier for treatment of neurological disorders. *Nat. Rev. Neurol.* **2018**, *14*, 9. [[CrossRef](#)]
11. Godfrey, C.; Desviat, L.R.; Smedsrød, B.; Piétri-Rouxel, F.; Denti, M.A.; Disterer, P.; Lorain, S.; Nogales-Gadea, G.; Sardone, V.; Anwar, R. Delivery is key: Lessons learnt from developing splice-switching antisense therapies. *EMBO Mol. Med.* **2017**, *9*, 545–557. [[CrossRef](#)]
12. Summerton, J.; Stein, D.; Huang, S.B.; Matthews, P.; Weller, D.; Partridge, M. Morpholino and phosphorothioate antisense oligomers compared in cell-free and in-cell systems. *Antisense Nucleic Acid Drug Dev.* **1997**, *7*, 63–70. [[CrossRef](#)]
13. Summerton, J.E. Morpholino, sirna, and s-DNA compared: Impact of structure and mechanism of action on off-target effects and sequence specificity. *Curr. Top. Med. Chem.* **2007**, *7*, 651–660. [[CrossRef](#)]
14. Adams, A.M.; Harding, P.L.; Iversen, P.L.; Coleman, C.; Fletcher, S.; Wilton, S.D. Antisense oligonucleotide induced exon skipping and the dystrophin gene transcript: Cocktails and chemistries. *BMC Mol. Biol.* **2007**, *8*, 57. [[CrossRef](#)]
15. Miyatake, S.; Mizobe, Y.; Tsoumpra, M.K.; Lim, K.R.Q.; Hara, Y.; Shabanpoor, F.; Yokota, T.; Takeda, S.I.; Aoki, Y. Scavenger receptor class a1 mediates uptake of morpholino antisense oligonucleotide into dystrophic skeletal muscle. *Mol. Ther. Nucleic Acids* **2019**, *14*, 520–535. [[CrossRef](#)]
16. Aartsma-Rus, A.; Kaman, W.; Bremmer-Bout, M.; Janson, A.; Den Dunnen, J.; van Ommen, G.B.; Van Deutekom, J. Comparative analysis of antisense oligonucleotide analogs for targeted dmd exon 46 skipping in muscle cells. *Gene Ther.* **2004**, *11*, 1391. [[CrossRef](#)]
17. Heemskerk, H.A.; de Winter, C.L.; de Kimpe, S.J.; van Kuik-Romeijn, P.; Heuvelmans, N.; Platenburg, G.J.; van Ommen, G.J.B.; van Deutekom, J.C.; Aartsma-Rus, A. In Vivo comparison of 2'-o-methyl phosphorothioate and morpholino antisense oligonucleotides for duchenne muscular dystrophy exon skipping. *J. Gene Med.* **2009**, *11*, 257–266. [[CrossRef](#)]
18. McClorey, G.; Moulton, H.; Iversen, P.; Fletcher, S.; Wilton, S. Antisense oligonucleotide-induced exon skipping restores dystrophin expression in vitro in a canine model of dmd. *Gene Ther.* **2006**, *13*, 1373–1381. [[CrossRef](#)]
19. Partridge, M.; Vincent, A.; Matthews, P.; Puma, J.; Stein, D.; Summerton, J. A simple method for delivering morpholino antisense oligos into the cytoplasm of cells. *Antisense Nucleic Acid Drug Dev.* **1996**, *6*, 169–175. [[CrossRef](#)]
20. Gebiski, B.L.; Mann, C.J.; Fletcher, S.; Wilton, S.D. Morpholino antisense oligonucleotide induced dystrophin exon 23 skipping in mdx mouse muscle. *Hum. Mol. Genet.* **2003**, *12*, 1801–1811. [[CrossRef](#)]
21. Summerton, J.E. Endo-porter: A novel reagent for safe, effective delivery of substances into cells. *Ann. N. Y. Acad. Sci.* **2005**, *1058*, 62–75. [[CrossRef](#)]
22. Brees, C.; Fransen, M. A cost-effective approach to microporate mammalian cells with the neon transfection system. *Anal. Biochem.* **2014**, *466*, 49–50. [[CrossRef](#)]
23. Singh, N.N.; Luo, D.; Singh, R.N. Pre-mrna splicing modulation by antisense oligonucleotides. In *Exon Skipping and Inclusion Therapies*; Springer: New York, NY, USA, 2018; pp. 415–437.
24. Wilton, S.D.; Fletcher, S.; McClorey, G. Antisense oligonucleotides for inducing exon skipping and methods of use thereof. Patent Number 1766010, 28 March 2007.
25. Fletcher, S.; Bellgard, M.; Price, L.; Akkari, A.; Wilton, S. Translational development of splice-modifying antisense oligomers. *Expert Opin. Biol. Ther.* **2017**, *17*, 15–30. [[CrossRef](#)]
26. Arechavala-Gomez, V.; Graham, I.; Popplewell, L.; Adams, A.; Aartsma-Rus, A.; Kinali, M.; Morgan, J.; Van Deutekom, J.; Wilton, S.; Dickson, G. Comparative analysis of antisense oligonucleotide sequences for targeted skipping of exon 51 during dystrophin pre-mrna splicing in human muscle. *Hum. Gene Ther.* **2007**, *18*, 798–810. [[CrossRef](#)]

27. Charleston, J.; Schnell, F.; Dworzak, J.; Donoghue, C.; Lewis, S.; Rodino-Klapac, L.; Sahenk, Z.; Shanks, C.; Voss, J.; DeAlwis, U. Long-term treatment with eteplirsen promotes exon 51 skipping and novel dystrophin protein production in duchenne muscular dystrophy patients. *Neuromuscul. Disord.* **2016**, *26*, S153. [[CrossRef](#)]
28. Mendell, J.R.; Goemans, N.; Lowes, L.P.; Alfano, L.N.; Berry, K.; Shao, J.; Kaye, E.M.; Mercuri, E.; Group, E.S.; Network, T.F.D.I.; et al. Longitudinal effect of eteplirsen versus historical control on ambulation in d uchenne muscular dystrophy. *Ann. Neurol.* **2016**, *79*, 257–271. [[CrossRef](#)]
29. Mendell, J.R.; Rodino-Klapac, L.R.; Sahenk, Z.; Roush, K.; Bird, L.; Lowes, L.P.; Alfano, L.; Gomez, A.M.; Lewis, S.; Kota, J. Eteplirsen for the treatment of duchenne muscular dystrophy. *Ann. Neurol.* **2013**, *74*, 637–647. [[CrossRef](#)]
30. Wilton, S.D.; Fletcher, S.; Aung-Htut, M. Multiple sclerosis treatment. Patent Number 20180104273, 19 April 2018.
31. Flynn, L.L.; Mitrpant, C.; Pitout, I.L.; Fletcher, S.; Wilton, S.D. Antisense oligonucleotide-mediated terminal intron retention of the smn2 transcript. *Mol. Ther. Nucleic Acids* **2018**, *11*, 91–102. [[CrossRef](#)]
32. Collett, G.P.; Redman, C.W.; Sargent, I.L.; Vatish, M. Endoplasmic reticulum stress stimulates the release of extracellular vesicles carrying danger-associated molecular pattern (damp) molecules. *Oncotarget* **2018**, *9*, 6707–6717. [[CrossRef](#)]
33. Mann, C.J.; Honeyman, K.; McClorey, G.; Fletcher, S.; Wilton, S.D. Improved antisense oligonucleotide induced exon skipping in the mdx mouse model of muscular dystrophy. *J. Gene Med.* **2002**, *4*, 644–654. [[CrossRef](#)]
34. Rando, T.A.; Blau, H.M. Primary mouse myoblast purification, characterization, and transplantation for cell-mediated gene therapy. *J. Cell Biol.* **1994**, *125*, 1275–1287. [[CrossRef](#)]
35. Harding, P.; Fall, A.; Honeyman, K.; Fletcher, S.; Wilton, S. The influence of antisense oligonucleotide length on dystrophin exon skipping. *Mol. Ther.* **2007**, *15*, 157–166. [[CrossRef](#)]
36. Greer, K.L.; Lochmüller, H.; Flanigan, K.; Fletcher, S.; Wilton, S.D. Targeted exon skipping to correct exon duplications in the dystrophin gene. *Mol. Ther. Nucleic Acids* **2014**, *3*, e155. [[CrossRef](#)]

**Sample Availability:** Samples of 2'-OMe ASOs are available on request from the authors. However, PMOs can be purchased from Gene Tools.



© 2019 by the authors. Licensee MDPI, Basel, Switzerland. This article is an open access article distributed under the terms and conditions of the Creative Commons Attribution (CC BY) license (<http://creativecommons.org/licenses/by/4.0/>).

# **Chapter 8 – Final**

## **Discussion and**

## **Conclusion**

## 8.1 The Current Therapeutic Landscape for Expansion Diseases

Microsatellites are classified as repetitive tracts of single bases (e.g. A) or blocks up to 10 bases repeated typically 5 – 100 times, although as many as 1000s of repeats may occur, without being disease causing. Sequence repeats occur at thousands of locations throughout the genome, and differences in repeat length are often used in a forensic setting for genotyping individuals [199]. However, in 1991 an unexpected discovery occurred; “expansions” of a specific microsatellite having the ability to cause genetic disease [10,200].

Two independent groups identified the causative genetic mutations for two distinct X-linked diseases: fragile X syndrome and spinal and bulbar muscular atrophy. Fragile X syndrome and spinal and bulbar muscular atrophy were initially reported to produce disease phenotypes by encoding proteins with expanded poly-amino acid tracts in the *FMR1* and *AR* genes, respectively [200,201]. Although it was initially thought that fragile X syndrome was caused by an expanded polyarginine tract, subsequent studies revealed that the predicted translation initiation codon for the FMRP was incorrect. Instead, the CGG repeat expansion in *FMR1* is actually located in the 5' UTR of the gene [201,202], so that the expansion significantly reduced *FMR1* expression through hypermethylation of *FMR1*'s CpG-rich promoter [203,204]. Spinal and bulbar muscular atrophy is recognised as the first member of a sub-category of expansion diseases, known as the polyglutamine (polyQ) diseases [7,150]. As polyQ disease expansions are always located in the coding regions, these diseases often contain “small and defined expansions”, typically 30 – 180 repeats, while the ‘explosions’ as seen in the 3'-UTR of *DMPK* (causative gene of myotonic dystrophy type 1) where up to 30 repeats are seen in healthy individuals, with the potential for affected individuals to have expansions up to 2000 repeats [7].

Since 1991, over 40 diseases have been linked to expansions of microsatellites at various intragenic regions, leading to at least four known mechanisms of repeat expansion disease; loss-of-function of the gene containing the repeat; toxic gain-of-function due to production of a protein containing an expanded

polyQ tract (protein misfolding and aggregation); toxic gain-of-function due to production of RNA containing an expanded CUG tract (toxic RNA); and gain-of-function due to production of a protein containing an expanded polyalanine tract (protein misfolding and aggregation) [7,10,158,194]. Of these mechanisms the most common in neurodegenerative expansion diseases, is the toxic gain-of-function leading to protein misfolding and insoluble protein aggregation, a hallmark of neurodegenerative disease [205].

Currently, there are no effective therapies for any of the expansion diseases, with symptomatic management the only available option [8]. As there is a large number of expansion diseases, only the most common diseases and potential therapeutics will be discussed. Due to the variety in pathogenic pathways of mutant repeat expansion proteins or mRNA, therapeutic strategies targeting a wide range of disease mechanisms exist, with three general approaches emerging [206].

- 1) Modulation of critical pathways in cognitive aging
- 2) Modulating endogenous mechanisms to increase misfolded protein clearance
- 3) Genetic therapies to suppress disease-causing protein and RNA expression and/or mutation correction mediated by antisense oligonucleotides (AOs) or genome editing

### **8.1.1 Modulation of Cognitive Aging Pathways**

The average age of onset differs for the different expansion diseases; however, disease progression and manifestation are age related and directly linked to the size of the expansion. A common theme exists: as the expansion increases in size, disease severity increases and age of onset decreases [9]. Therefore, any modulation of the pathways that are linked to cognitive aging could have enormous therapeutic consequences. Although addressing cognitive aging does not tackle the mutant proteins or mRNAs directly, it has gained traction as a potential blanket approach in treating expansion diseases and many other neurodegenerative diseases for that matter.

Over the past decade, the link between diet, cognition and mental well-being has been established, albeit with sometimes equivocal data [207-210]. Many studies have applied various methods of calorie restriction, such as a ketogenic diet, intermittent fasting or a diet rich in phenols, in multiple different murine models of human Huntington's disease (HD) and Alzheimer's disease, in an effort to delay or slow neurodegeneration [206,208,209]. Some studies show that an intermittent caloric fasting intervention slows cognitive aging and delays aspects of neurodegeneration onset and/or progression in various models of neurodegeneration, such as HD and Alzheimer's disease [207-209]. However, the inconsistencies in reports of therapeutic benefit leaves this approach flawed in many ways, attributed to imperfect murine models and experimental design shortcomings [206]. The issues surrounding transgenic mouse models of human disease arise when trying to recapitulate human disease progression. Some models show acute phenotypes for diseases such as HD, where progression in humans is slow and gradual, thus short term benefit of calorie restriction may not provide an accurate outcome regarding delaying neurodegeneration [207]. Thus, a conundrum exists when assessing cognitive aging in transgenic models; aggressive disease models are most likely not an appropriate vehicle to examine anti-aging interventions.

While there is some scientific backing for calorie restriction being linked to positive cognitive outcome in healthy individuals; the underlying complex, multifaceted disease pathogenesis associated with neurodegenerative disorders is too powerful to be overcome by diet and calorie restrictions alone, emphasising the urgent need for drug interventions to address pathogenic pathways.

### **8.1.2 Increasing Mutant Protein Clearance**

The presence of misfolded and aggregated mutant proteins are hallmark features of neurodegenerative diseases, including most protein coding expansion diseases. In expansion diseases where the mutation is located in the coding region of the gene, the additional amino acids leads to conformational changes that confer a toxic gain-of-function and result in misfolding and eventually insoluble and currently

irreversible protein aggregation [211]. The exact role of misfolded proteins in neurodegeneration disease progression is still not well understood, however what is known is that the presence of these proteins is widespread in a variety of diseases [212]. Thus, targeting mechanisms that are responsible for the homeostatic maintenance of endogenous protein misfolding, such as autophagy, is an obvious and logical pathway of interest [213]. Efforts have focused on activating and increasing either autophagy or chaperone-dependent pathways to enhance mechanisms that clear misfolded proteins.

Chaperone-targeted therapies have focused on heat shock proteins Hsp70 and Hsp90 that act together to regulate the proteostasis of targeted proteins, and interestingly regulate both HTT and the androgen receptor, proteins implicated in Huntington's disease and spinal-bulbar muscular atrophy, respectively [214]. Various small molecule inhibitors of Hsp90 promote expanded polyglutamine (polyQ) HTT and androgen receptor degradation to ameliorate phenotypes in disease models [215]. However, targeting the chaperone-dependent machinery as a therapeutic strategy is not without significant challenges. The Hsp90 chaperone machinery targets hundreds of proteins, including critical regulators of signal transduction and gene expression. Inhibition of Hsp90 not only affects aggregates and mis-folded proteins, but also dozens of other critical proteins [215]. A potential alternative to targeted clearance of misfolded proteins is to activate or upregulate Hsp70-dependent ubiquitination, a strategy that has been demonstrated to rescue the phenotype in mouse models of repeat expansion disease [215]. Moreover, due to overexpression of Hsp70 being beneficial in several disease models, efforts to target the Hsp70 transcriptional regulator (heat shock factor protein 1) have recently garnered attention [216]. Although targeting the chaperone machinery may be a difficult and challenging therapeutic strategy to achieve without off-target effects, it could provide insights into disease mechanisms and pathology.

There is strong evidence that the autophagy pathway clears cytosolic protein aggregates and has a critical role in maintaining neuronal homeostasis [217-222], with dysregulation implicated in the pathogenesis of expansion diseases [213]. The induction of autophagy was first reported in models of

Huntington's disease, demonstrating degradation of aggregate-prone polyQ proteins by autophagy [223,224]. Several pre-clinical and clinical trials are underway, using small molecules to upregulate the autophagic process [213,225,226]. These include rapamycin, a known inhibitor of mTOR, administered to Huntington's disease patients, however, the downfalls of rapamycin are that it also exerts an immunosuppressive and sometimes toxic effect, as well as showing little benefit in ALS patients [225]. Nearly 20 pharmacological agents have been assessed for therapeutic effect in mouse models of various expansion diseases, and showed some benefit [148]. However, most compounds entering clinical trials fall short of demonstrating a clinical improvement, and only a handful of the compounds provide some symptomatic relief. A clinical trial assessed the effect of lithium in 20 SCA2 patients and a significant effect was observed for only the Beck Depression Inventory, while no benefit was evident on the Scale for the Assessment and Rating of Ataxia score [227]. Although small molecules have failed to provide a therapeutic benefit to date, stimulation of autophagy still remains a promising area of investigation. Other methods, including genetic therapies that stimulate autophagy have the potential to ameliorate the consequences of repeat expansion disorders.

### **8.1.3 Genetic Therapies to treat repeat expansion disorders**

Over the past 15 years, genetic therapies targeting the causative mutations in a wide assortment of genetic diseases have been implemented [228]. Genetic therapies provide the greatest hope for expansion diseases by directly targeting the cause of the disease, rather than the associated symptoms. Three approaches gene and genetic therapies are being investigated in pre-clinical and early-phase clinical studies of expansion diseases, mostly for HD; adeno-associated viral vector delivery of small-interfering RNAs (AAV-siRNAs); CRISPR-Cas9 and single stranded antisense oligonucleotides (AOs).



### 8.1.3.1 Gene silencing in repeat expansion disorders

siRNAs induce a process known as RNA interference that is a mechanism for sequence-specific, post-transcriptional gene silencing, initiated by double stranded RNA that is homologous to a target gene [99]. A 2013 study in a humanised SCA3 mouse model demonstrated that intracerebellar injection of synthetic siRNA or AAV-mediated delivery of siRNAs targeting the 3' UTR of the *ATXN3* transcript induced silencing of the human disease-causing ataxin-3 [229]. Interestingly, acute treatment with siRNA cleared the nuclear accumulation of ataxin-3 throughout the cerebellum, however there was no long-term rescue of motor impairment or increased survival [229]. Keiser and colleagues conducted multiple studies using siRNA to knockdown ataxin-1 in various SCA1 mouse models [230-232]. Upon bilateral injection into the dorsal cochlear nucleus, SCA1 mice showed improvements in behavioural and neuronal phenotypes [230]. In 2018, the FDA approved the first-ever RNAi therapeutic, *Patisiran*, for the treatment of polyneuropathy of hereditary transthyretin-mediated amyloidosis, and a year later a second approval was granted for treatment of acute hepatic porphyrinemia with *Givosiran* [138,167]. Although siRNAs are known for off-target silencing, approval for this type of intervention, and on-going investigations into nontoxic chemical modifications and delivery methods will support further advances in the field and promote broader application of the technology.

The CRISPR-Cas9 system has been adapted from a naturally occurring genome editing and antiviral defence system in bacteria for use as a unique technology that enables editing of parts of the genome [233,234]. By delivering the Cas9 nuclease, together with a synthetic guide RNA targeting the region of interest, the genome of a cell can be cut, allowing a gene to be inactivated and/or new genes or sequences to be added, *in vitro* and *in vivo* [233]. This process of genome editing fundamentally requires two steps [235] :

- 1) The successful and specific recognition by a "DNA-binding domain" and
- 2) An "effector domain" to cleave the DNA or regulate transcription

Therefore, inducing a double-strand break in the DNA demonstrates a higher degree of gene modification than if one was not induced. This occurs mainly through the activation of the two DNA repair mechanisms: homology directed repair or non-homologous end joining. Non-homologous joining introduces deletions or insertions within a given sequence, while homology directed repair requires a donor sequence, that allows recombination with the target sequence ultimately leading to a point insertion of the given donor sequence [235]. When related to repeat expansion diseases one would ideally aim to excise the expanded repeat region in a given expansion diseased gene, followed by HDR-mediated repair and introduction of a normal, non-expanded sequence. However, it has been shown that large expansions as seen in the *DMPK* gene may be too difficult to delete and the subsequent HDR is likely to have a low efficacy [233,235,236]. Therefore, the more discrete expansions seen in the polyQ diseases may be more applicable to CRISPR-Cas9 technology.

Studies in mice suggest that non-selective CRISPR/Cas9-mediated deletion of the *HTT* repeats from both alleles could be used to permanently eliminate polyglutamine expansion-induced neuronal toxicity in the adult mouse brain [237,238]. Lastly, genome editing has been successfully tested in various repeat expansion disease cell lines, including SCA2, SCA3 and fragile X syndrome [236,239,240]. However, due to the high incidence of permanent off-target gene edits, the field requires further careful scrutiny, with rigorous testing and validation, prior to commencement of first-in-human studies [235]. In saying that, with careful guide selection and the development of targeted nucleases with improved safety profiles. Given the potential of this technology for the treatment of repeat expansion disorders and other targets where AO technology is not applicable the field could provide a revolutionary treatment for several neurological diseases.

#### 8.1.3.2 *Single stranded oligonucleotide therapies*

Single stranded antisense oligonucleotide intervention (AOs from here on) is currently one of the most promising therapies for expansion diseases. With several approvals over the past 15 years, AOs are now

showing commercial success as genetic therapies for rare diseases. Rather than reviewing all strategies and current studies, a broad overview is presented.

The first AO approach targeting expansion diseases was conducted in 1997, using an 18-mer DNA PS AO targeting the *HTT* gene transcript for RNaseH degradation, however, this *in vivo* study did not show any reduction in the mutant protein [241]. RNaseH degradation of a target transcript has since become the most widely reported application of AOs for therapeutic development.

IONIS Pharmaceuticals are currently conducting the only Phase III clinical trial for AO-mediated downregulation of an expansion disease, with the aim to downregulate the *HTT* mRNA and hence protein as a therapeutic strategy for Huntington's Disease. Other RNaseH-mediated downregulation studies by a number of groups target several CAG polyglutamine disorders, including SCA1, SCA2, SCA3, spinal and bulbar muscular atrophy and myotonic dystrophy type 1 [229,242-247]. These studies all show promise, with each reporting some degree of phenotypic rescue. To date, SCA3 is the only polyQ disease for which successful removal of the exon encoding the polyQ repeat, mediated by a splice switching AO, has been published [169,248-250]. The Van Roon-Mom laboratory was the first to describe the removal of the polyQ repeat in ataxin-3 *in vitro* [248,249], and have further validated the outcomes *in vivo*, showing modest phenotypic rescue in a humanised *ATXN3* transgenic mouse model of SCA3 [248]. With the current therapeutic landscape of repeat expansion diseases looking promising, on-going efforts to reduce phenotype and/or delay onset of disease via various AO-mediated interventions should only increase.

## **8.2 AO Strategies to Treat Expansion Diseases and the Major Findings**

The main focus of this thesis was to develop splice-switching AO strategies that are safe and effective for the treatment of diseases caused by repeat expansions, as risk/benefit considerations will always be important when assessing if a treatment is acceptable and cost effective. Two separate approaches were investigated:

- 1) Targeted exon 10 removal from the *ATXN3* transcript as a therapy for spinocerebellar ataxia type 3 (SCA3).
- 2) Targeted knockdown of transcription elongation factor SUPT4H1 through AO-induced exon skipping.

### **8.2.1 Antisense Oligonucleotide-mediated removal of the polyglutamine repeat in *ATXN3***

Initial *in vitro* data derived from transfection of 2'-O-Methyl AOs on a phosphorothioate backbone (2'-Me PS AOs) into SCA3 patient cells show that it is possible to create an internally truncated protein, missing the toxic polyQ repeat contained in ataxin-3 while maintaining normal function of the protein [169,248]. Toonen *et al.* (2017) were able to show that the truncated ataxin-3 has the ability to bind ubiquitin at a similar level to that of the wild-type protein [248]. This indicates that the protein retains the critical deubiquitinating properties in SCA3 patient cells, confirmed that skipping of the target exon can generate an internally truncated ataxin-3 protein missing the toxic polyQ repeat. These studies used 2'-O-Methyl AOs on a phosphorothioate backbone (2'-Me PS AOs), and the outcomes were greatly improved when the patient cells were transfected with the same sequences synthesised as PMOs. Furthermore, we also noted significant downregulation of both the mutant and non-expanded protein. Clinically, this may be important as downregulation of the mutant protein, in addition to removing the toxic repeat in the expressed protein, would provide a combination of benefits. While the impact of global and sustained ataxin-3 knockdown is under debate, the role of ataxin-3 in the ubiquitin-proteasome machinery is well-established, and there are currently conflicting viewpoints as to whether ataxin-3 is vital in maintaining normal cellular homeostasis [251-253]. In saying that, the Figiel group (2011) created a functional *Atxn3* knockout mouse that showed no obvious phenotype, with a life span comparable to that of the wildtype mouse [252]. Moreover, the average onset of SCA3 is in the fourth decade, it takes decades for misfolded *ATXN3* to accumulate, aggregate and eventually cause disease. Consequently, reducing expression of

ataxin-3 via long term PMO administration could result in a significant delay in SCA3 disease onset if successfully applied *in vivo* [148]. Based upon our experiences with the 2'-Me PS AO and PMO chemistries, we consider the latter to be superior for *in vivo* and clinical application, as these compounds are chemically stable and have an excellent safety profile to date [97,99,108,117,168,175,176,189].

Widely reported off-target effects of the PS backbone also suggest that PMOs are a safer and more efficacious chemistry for RNA interventions to treat human disease, including SCA3 [85,169,175]. The off-target effects observed in the current study are sequence-independent and complemented by several *in vitro* studies that show sequestration of paraspeckle proteins by AOs on a PS backbone [85,175]. Several additional studies show other non-specific off-target effects of PS chemistries *in vitro* [84,86]. Taken together, there is mounting evidence that PMOs are a safer chemistry than PS AOs for long-term RNA therapeutics, with data presented in this thesis supporting these findings.

## **8.2.2 AO-Mediated Knockdown of SUPT4H1 as a Modifier to Ameliorate Repeat Expansion Diseases**

The transcription elongation factor SUPT4H1 is reported to be selectively required for transcription through expanded repeats, signifying a potential therapeutic target in repeat expansion diseases. Both *in vitro* and *in vivo* studies in mouse models showed that targeted knockdown of SUPT4H1, mostly siRNA-mediated, reduces toxic protein and RNA foci, leading to improvements in disease phenotype [151-153]. The concept is that downregulation of SUPT4H1 may reduce efficiency of transcription through large repeats by tapping into regulatory transcription elongation mechanisms. Currently, it is theorised that SUPT4H1 is only activated when RNA Pol II encounters large, repeated regions (i.e. disease expansions). However, the exact threshold of the repeat and/or other regulatory mechanisms, such as the surrounding RNA sequence, is still unknown and can only be assessed through empirical observation [152,153]. We aimed to downregulate SUPT4H1 through an AO-mediated exon skipping strategy that disrupts the open reading frame, thereby reducing translation of the full length, functional protein.

We induced significant downregulation of SUPT4H1 expression in SCA3 patient-derived fibroblasts (71Q) and SHY-SY5Y (neuroblastoma) cells transfected with splice modulating peptide-conjugated PMOs (PPMOs) designed to skip *SUPT4H1* exon 2. Most encouragingly, RNA-sequencing data from PPMO transfected SH-SY5Y cells show only mild to moderate changes in the transcriptome, as only a small number of genes were differentially expressed. The lead candidate sequence 1083 did not induce an overall reduction in RNA output. However, transcripts that are differentially expressed, relative to the GeneTools Control transfected samples show minor changes to a few biological pathways, including 'gene expression', 'RNA metabolism', 'RNA splicing' and 'mRNA processivity'. We were unable to demonstrate a reduction in mutant ATXN3 protein and mRNA levels in transfected patient-derived SCA3 fibroblasts, despite inducing nearly 80% knockdown of SUPT4H1. This result was very surprising considering when reviewing reports from SUPT4H1 knockdown studies that suggested a 50% knockdown of SUPT4H1 was sufficient to indirectly reduce expression of expansion proteins/RNA [153,173]. Although disappointed, we speculate that SUPT4H1 knockdown may be more effective in modulating expression of larger expansions, certainly larger than the expansions explored in this thesis. We suggest this hypothesis because evidence relating to the threshold repeat size requiring SUPT4H1 'support' for RNA Pol II transcription is currently lacking [153]. Thus, we believe that the lack of evidence for ataxin-3 knockdown may be due to the relatively modest expansion (71Q) in these cells. Future work will assess SUPT4H1 knockdown in cell lines that carry massive expansions, such as a 180Q repeat expansion causing Huntington's disease, and cells carrying ~1000 triplet repeats in *DMPK*, derived from a myotonic dystrophy type 1 patient.

In conclusion, direct targeting of the causative mutation could address a single expansion disease (SCA3), the SUPT4H1 downregulation approach may provide a 'pan-genetic' therapy for several expansion diseases caused by the larger repeat expansions. A cautious approach is advised, as modulating pathways critical to overall transcriptome homeostasis may prove to be catastrophic where long term administration in patients is needed. With that being said, further pre-clinical data *in vitro* and

*in vivo* systems would potentially provide insight as to why no follow-on knockdown of expanded ATXN3 was observed.

### **8.2.3 Systematic Development of 2'-Me PS AO and Delivery Optimisation of PMOs**

In addition to the design and appraisal of AO therapeutic strategies described in this thesis, a significant goal herein was to create a systematic approach (or approaches) to developing and evaluating splice switching AOs. We provide a step-by-step description of AO development, from AO design to functional assays [156]. This provides the basis for a comprehensive design protocol and screening method to ensure that the optimal AO sequences enter the clinical development pipeline [143,254]. After 25 years' experience designing AOs, our laboratory has found that within a given gene transcript, some exons are readily excised from the mature mRNA, albeit at variable proficiencies *in vitro*, whereas other exons in the same transcript are much more recalcitrant to AO mediated exon skipping [93,156,174,176]. We have yet to determine why this selective exon skipping occurs, however, the purpose of this section of the thesis was to eliminate the potential to overlook sequences that induce efficient exon skipping through poor experimental design. We show that relatively minor changes, such as transfection reagents, cell type or even cell density or passage number, can dramatically improve or weaken apparent AO splice switching efficiencies [156]. Thus, it is imperative to follow robust guidelines to ensure selection of the most effective and safe AOs for clinical trials.

In another independent study, we also identified uptake by cells *in vitro* as a major limitation when assessing efficiency of splice modulation by PMO sequences, and recognise the importance of methods to enhance PMO delivery [113,114,177]. The PMOs are neutrally charged and do not readily traverse the cell membrane [97,99], prompting numerous programs by several research groups and industry partners to develop cell-penetrating peptides, aptamers and other novel entities to enhance cellular and nuclear uptake [255]. A section of this thesis was dedicated to developing a validation method for efficiently delivering PMOs into cultured cells. Our study provides sequences of PMOs that can be used as positive

transfection controls that may be particularly useful in studies using cells for which delivery is an impediment. Additionally, we show that by changing specific nucleofection electroporation protocols we can greatly increase or decrease the efficiencies of PMOs *in vitro*. The gene target we use, *ITGA4*, is ubiquitously expressed in most cell types, and can be used as a control to monitor and confirm efficient AO delivery into most cell lines under investigation.

### 8.3 Final Thoughts and Conclusion

This thesis aimed to investigate the potential of AOs as agents to treat expansion diseases, with a particular focus on polyQ diseases and SCA3 in particular. We showed that it was possible to generate an internally truncated ataxin-3 protein, missing the toxic polyQ repeat, while retaining the function of the protein. Although we did not directly conduct the ATXN3 functional assay, Toonen *et al.* (2017) induced the exact same isoform and demonstrated that the truncated ATXN3 isoform bound ubiquitin at similar rates to that of the full-length, non-expanded ATXN3 isoform [248]. Due to intellectual property constraints on using *ATXN3* exon 10 skipping AOs, our research could not be taken further, however, we demonstrated that PMOs may be a safer and more effective chemistry, compared to AOs composed of the 2'-Me PS chemistry. With that being said, the research presented here offers industry partners additional data on the efficacy of PMOs as a potential therapeutic strategy for SCA3, prior to drug translation. We are firmly of the belief that cooperation and collaboration between academic researchers and industry could provide a better drug development pipeline, safer chemistries, and expedited development for future AO therapeutics.

We also investigated the potential application of targeted knockdown of SUPT4H1, a transcription elongation factor reported to selectively assist RNA polymerase II in transcribing though pathological repeat expansions. We showed highly reproducible targeted knockdown of SUPT4H1 with our lead candidate, while only inducing minor disturbance of the transcriptome. Further work will be required in patient derived organoids and in animal models, e.g. humanised rodent models of expansion diseases



to ascertain any clinical benefit. Although no modification to mutant ATXN3 was observed *in vitro*, we believe that the AO has therapeutic potential and may show a discernible effect in diseases with non-discrete expansions of 1000s of repeats, such as myotonic dystrophies. In saying that, assuming off-target effects are minimal, a dose escalation study in diseases with discrete expansions such as the polyQ diseases could be worthwhile, perhaps on small patient numbers, using an adaptive trial design.

Lastly, we provide detailed and systematic approaches to designing, developing, and evaluating splice-switching AOs, while also providing validation of methods to enhance PMO delivery *in vitro*. This thesis provides the scientific community with detailed and published protocols, while also addressing the need for therapeutics for expansion diseases. Whether applied to exon skipping to truncate a protein or as a means to downregulate protein production, this thesis demonstrates the power and versatility of splice switching antisense oligonucleotides as potential therapeutics for rare genetic diseases.

# **Chapter 9 – Appendices**

## 9.1 Appendix 1: Supplementary Figures

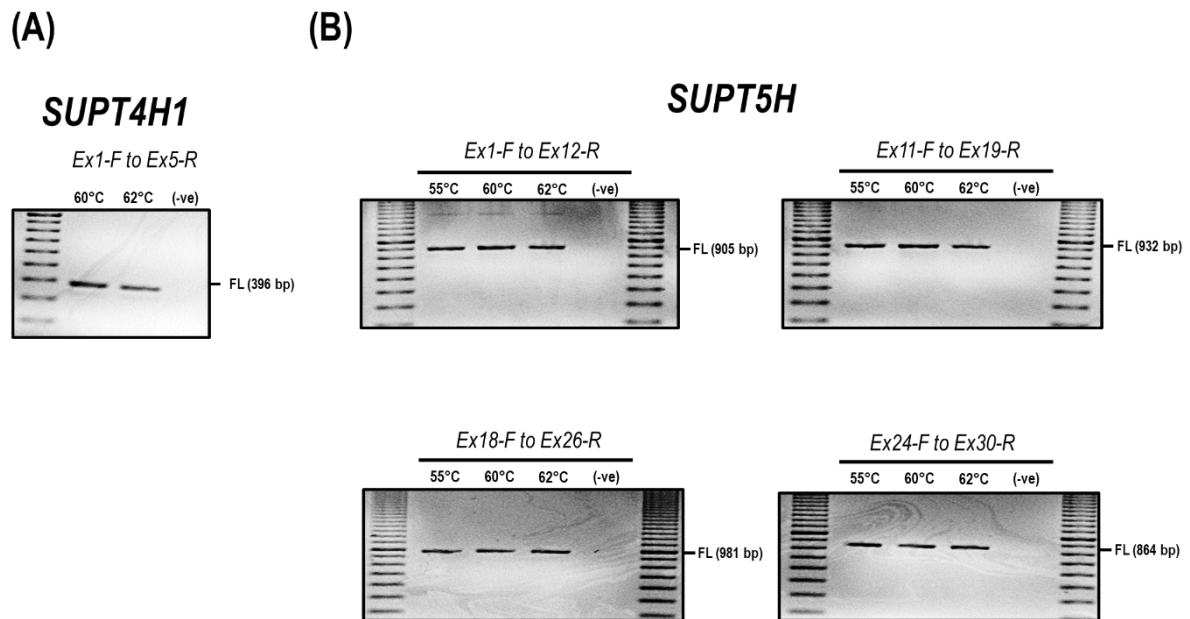
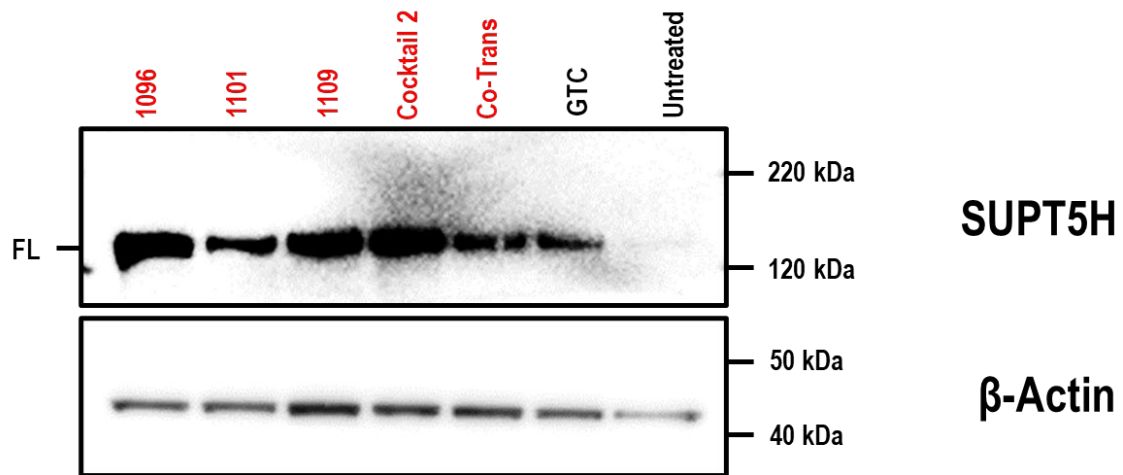


**Figure S3.1:** RT-PCR analysis of PCR primers conducted in normal human fibroblasts at three various annealing temperatures 55, 60 and 62°C (A) RT-PCR optimisation of SUPT4H1 transcript from exon 1 to exon 5. (B) Top left - RT-PCR optimisation of SUPT5H transcript from exon 1 to exon 12, top right - exon 11 to exon 19, bottom left - exon 18 to exon 26, bottom right - exon 24 to exon 30



**Supplementary Figure S3.2:** Evaluation of SUPT5H exon skipping in SH-SY5Y cells, transfected with peptide conjugated-PMOs (PPMOs). Cells were harvested 4 days following transfection for protein analysis. SUPT5H protein was analysed by Western blotting following transfection at a concentration of 5  $\mu$ M and it shows full-length SUPT5H at approximately 150 kDa. Beta-Actin was used as a loading control

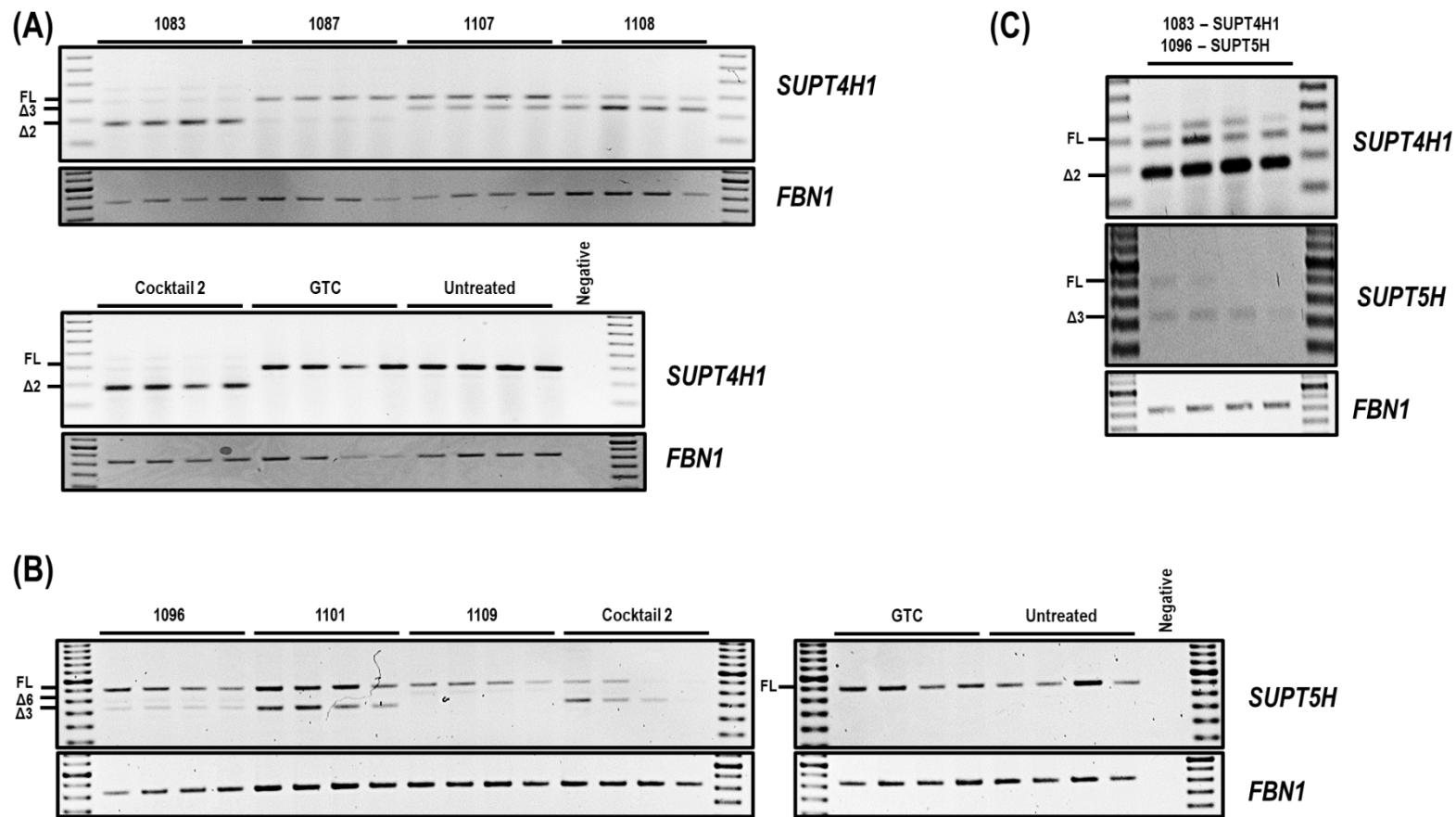


**Figure S3.2:** RT-PCR analysis of free uptake of peptide conjugated-PMOs (PPMOs) in SH-SY5Y cells at a concentration of 5  $\mu$ M for 72 hours. (A) Screening of PPMOs targeting exon 2 or exon 3 of the SUPT4H1 transcript for removal. After RT-PCR and gel fractionation, products representing the full-length (FL) and exon 2/3-skipped ( $\Delta$ 2/3) transcripts were identified. (B) Screening of PPMOs targeting exon 3 or exon 6 of the SUPT5H transcript for removal. After RT-PCR and gel fractionation, products representing the full-length (FL) and exon 3/6-skipped ( $\Delta$ 3/6) transcripts were identified. (C) Analysis of PPMOs targeting exon 2 of the SUPT4H1 transcript and exon 6 of the SUPT5H transcript transfected simultaneously for exon removal. After RT-PCR and gel fractionation, products representing the full-length (FL) and exon 2 and exon 3-skipped ( $\Delta$ 2/3) of the SUPT4H1 and SUPT5H transcripts, respectively

## **9.2 Appendix 2: List of Awards and Achievements Received during PhD Candidature**

### **2017**

- Best Student Oral – Australasian Gene and Cell Therapy Society Conference 2017
- Best Student Oral (Genetics) – Combined Biological Sciences Meeting 2017
- 2<sup>nd</sup> Place Fast-forward Oral Presentation – Murdoch Annual Research Symposium
- Murdoch Annual Research Symposium Organising Committee (2017 – Present)

### **2018**

- Invited Speaker - International Society for Cell and Gene Therapy of Cancer (ISCGT) 2018 China Conference.

### **2019**

- Best Student Oral - 3-minute thesis – Symposium of Western Australian Neuroscience 2019
- Best Student Oral - Australasian Gene and Cell Therapy Society Conference 2019
- Appointed Higher Degree Research Representative for The Centre of Molecular Medicine and Innovative Therapeutics (2019 – Present)

### **2020**

- Murdoch University Women in STEM Organising Committee (2020 – Present)
- Internal Perron 2020 grant – Chief Investigator (\$22 560) – with M. T. Aung-Htut; T. Fairchild; L. Gray Whiley & N. Gray Whiley.
- City of Perth 2020 Aspire Award Winner

## REFERENCES

---

1. Leal, N.A.; Kim, H.-J.; Hoshika, S.; Kim, M.-J.; Carrigan, M.A.; Benner, S.A. Transcription, reverse transcription, and analysis of rna containing artificial genetic components. *ACS synthetic biology* **2014**, *4*, 407-413.
2. He, Y.; Vogelstein, B.; Velculescu, V.E.; Papadopoulos, N.; Kinzler, K.W. The antisense transcriptomes of human cells. *Science* **2008**, *322*, 1855-1857.
3. Romero, I.G.; Ruvinsky, I.; Gilad, Y. Comparative studies of gene expression and the evolution of gene regulation. *Nature Reviews Genetics* **2012**, *13*, 505.
4. Jacob, F.; Monod, J. In *On the regulation of gene activity*, Cold Spring Harbor Symposia on Quantitative Biology, 1961; Cold Spring Harbor Laboratory Press: pp 193-211.
5. Keren, H.; Lev-Maor, G.; Ast, G. Alternative splicing and evolution: Diversification, exon definition and function. *Nature Reviews Genetics* **2010**, *11*, 345-355.
6. Yoon, J.-H.; Abdelmohsen, K.; Gorospe, M. Posttranscriptional gene regulation by long noncoding rna. *Journal of molecular biology* **2013**, *425*, 3723-3730.
7. Paulson, H. Repeat expansion diseases. In *Handbook of clinical neurology*, Elsevier: 2018; Vol. 147, pp 105-123.
8. Ellerby, L.M. Repeat expansion disorders: Mechanisms and therapeutics. Springer: 2020.
9. McIntosh, C.; Aung-Htut, M.; Fletcher, S.; Wilton, S. Polyglutamine ataxias: From clinical and molecular features to current therapeutic strategies. *J Genet Syndr Gene Ther* **2017**, *8*, 2.
10. La Spada, A.R.; Taylor, J.P. Repeat expansion disease: Progress and puzzles in disease pathogenesis. *Nature Reviews Genetics* **2010**, *11*, 247-258.
11. Cramer, P. Organization and regulation of gene transcription. *Nature* **2019**, *573*, 45-54.

12. Sainsbury, S.; Bernecky, C.; Cramer, P. Structural basis of transcription initiation by rna polymerase ii. *Nature reviews Molecular cell biology* **2015**, *16*, 129-143.
13. Fuda, N.J.; Ardehali, M.B.; Lis, J.T. Defining mechanisms that regulate rna polymerase ii transcription in vivo. *Nature* **2009**, *461*, 186.
14. Deaton, A.M.; Bird, A. CpG islands and the regulation of transcription. *Genes & development* **2011**, *25*, 1010-1022.
15. White, R.J.; Jackson, S.P. The tata-binding protein: A central role in transcription by rna polymerases i, ii and iii. *Trends in Genetics* **1992**, *8*, 284-288.
16. Martianov, I.; Viville, S.; Davidson, I. Rna polymerase ii transcription in murine cells lacking the tata binding protein. *Science* **2002**, *298*, 1036-1039.
17. Furlong, E.E.; Levine, M. Developmental enhancers and chromosome topology. *Science* **2018**, *361*, 1341-1345.
18. Reiter, F.; Wienerroither, S.; Stark, A. Combinatorial function of transcription factors and cofactors. *Current Opinion in Genetics & Development* **2017**, *43*, 73-81.
19. Nora, E.P.; Lajoie, B.R.; Schulz, E.G.; Giorgetti, L.; Okamoto, I.; Servant, N.; Piolot, T.; van Berkum, N.L.; Meisig, J.; Sedat, J. Spatial partitioning of the regulatory landscape of the x-inactivation centre. *Nature* **2012**, *485*, 381.
20. Lescure, A.; Lutz, Y.; Eberhard, D.; Jacq, X.; Krol, A.; Grummt, I.; Davidson, I.; Chambon, P.; Tora, L. The n-terminal domain of the human tata-binding protein plays a role in transcription from tata-containing rna polymerase ii and iii promoters. *The EMBO journal* **1994**, *13*, 1166.
21. Lambert, S.A.; Jolma, A.; Campitelli, L.F.; Das, P.K.; Yin, Y.; Albu, M.; Chen, X.; Taipale, J.; Hughes, T.R.; Weirauch, M.T. The human transcription factors. *Cell* **2018**, *172*, 650-665.
22. Young, B.A.; Gruber, T.M.; Gross, C.A. Views of transcription initiation. *Cell* **2002**, *109*, 417-420.



23. Abascal-Palacios, G.; Ramsay, E.P.; Beuron, F.; Morris, E.; Vannini, A. Structural basis of rna polymerase iii transcription initiation. *Nature* **2018**, *553*, 301.
24. Dvir, A.; Conaway, J.W.; Conaway, R.C. Mechanism of transcription initiation and promoter escape by rna polymerase ii. *Current opinion in genetics & development* **2001**, *11*, 209-214.
25. Engel, C.; Neyer, S.; Cramer, P. Distinct mechanisms of transcription initiation by ma polymerases i and ii. *Annual review of biophysics* **2018**, *47*, 425-446.
26. Roeder, R.G. The complexities of eukaryotic transcription initiation: Regulation of preinitiation complex assembly. *Trends in biochemical sciences* **1991**, *16*, 402-408.
27. Nikolov, D.B.; Hu, S.-H.; Lin, J.; Gasch, A.; Hoffmann, A.; Horikoshi, M.; Chua, N.-H.; Roeder, R.G.; Burley, S.K. Crystal structure of tffid tata-box binding protein. *Nature* **1992**, *360*, 40-46.
28. Nikolov, D.B.; Chen, H.; Halay, E.D.; Hoffman, A.; Roeder, R.G.; Burley, S.K. Crystal structure of a human tata box-binding protein/tata element complex. *Proceedings of the National Academy of Sciences* **1996**, *93*, 4862-4867.
29. Tsai, F.T.; Sigler, P.B. Structural basis of preinitiation complex assembly on human pol ii promoters. *The EMBO journal* **2000**, *19*, 25-36.
30. Fishburn, J.; Tomko, E.; Galburt, E.; Hahn, S. Double-stranded DNA translocase activity of transcription factor tfiih and the mechanism of rna polymerase ii open complex formation. *Proceedings of the National Academy of Sciences* **2015**, *112*, 3961-3966.
31. Yamaguchi, Y.; Wada, T.; Watanabe, D.; Takagi, T.; Hasegawa, J.; Handa, H. Structure and function of the human transcription elongation factor dsif. *Journal of Biological Chemistry* **1999**, *274*, 8085-8092.
32. Hartzog, G.A.; Fu, J. The spt4–spt5 complex: A multi-faceted regulator of transcription elongation. *Biochimica et Biophysica Acta (BBA)-Gene Regulatory Mechanisms* **2013**, *1829*, 105-115.

33. Jonkers, I.; Lis, J.T. Getting up to speed with transcription elongation by rna polymerase ii. *Nature reviews Molecular cell biology* **2015**, *16*, 167-177.
34. Kwak, H.; Lis, J.T. Control of transcriptional elongation. *Annual review of genetics* **2013**, *47*, 483-508.
35. Crickard, J.B.; Lee, J.; Lee, T.-H.; Reese, J.C. The elongation factor spt4/5 regulates rna polymerase ii transcription through the nucleosome. *Nucleic acids research* **2017**, *45*, 6362-6374.
36. Wada, T.; Takagi, T.; Yamaguchi, Y.; Ferdous, A.; Imai, T.; Hirose, S.; Sugimoto, S.; Yano, K.; Hartzog, G.A.; Winston, F. Dsif, a novel transcription elongation factor that regulates rna polymerase ii processivity, is composed of human spt4 and spt5 homologs. *Genes & development* **1998**, *12*, 343-356.
37. Chen, F.X.; Smith, E.R.; Shilatifard, A. Born to run: Control of transcription elongation by rna polymerase ii. *Nature reviews Molecular cell biology* **2018**, *19*, 464-478.
38. Westover, K.D.; Bushnell, D.A.; Kornberg, R.D. Structural basis of transcription: Nucleotide selection by rotation in the rna polymerase ii active center. *Cell* **2004**, *119*, 481-489.
39. Wang, D.; Bushnell, D.A.; Westover, K.D.; Kaplan, C.D.; Kornberg, R.D. Structural basis of transcription: Role of the trigger loop in substrate specificity and catalysis. *Cell* **2006**, *127*, 941-954.
40. Kuehner, J.N.; Pearson, E.L.; Moore, C. Unravelling the means to an end: Rna polymerase ii transcription termination. *Nature reviews Molecular cell biology* **2011**, *12*, 283.
41. Nechaev, S.; Adelman, K. Pol ii waiting in the starting gates: Regulating the transition from transcription initiation into productive elongation. *Biochimica et Biophysica Acta (BBA)-Gene Regulatory Mechanisms* **2011**, *1809*, 34-45.
42. Richard, P.; Manley, J.L. Transcription termination by nuclear rna polymerases. *Genes & development* **2009**, *23*, 1247-1269.

43. Proudfoot, N.J. Transcriptional termination in mammals: Stopping the rna polymerase ii juggernaut. *Science* **2016**, 352, aad9926.
44. Proudfoot, N.J. Ending the message: Poly (a) signals then and now. *Genes & development* **2011**, 25, 1770-1782.
45. Porrua, O.; Libri, D. Transcription termination and the control of the transcriptome: Why, where and how to stop. *Nature reviews Molecular cell biology* **2015**, 16, 190-202.
46. Rosonina, E.; Kaneko, S.; Manley, J.L. Terminating the transcript: Breaking up is hard to do. *Genes & development* **2006**, 20, 1050-1056.
47. Douglas, A.G.; Wood, M.J. Rna splicing: Disease and therapy. *Briefings in functional genomics* **2011**, 10, 151-164.
48. Ward, A.J.; Cooper, T.A. The pathobiology of splicing. *The Journal of Pathology: A Journal of the Pathological Society of Great Britain and Ireland* **2010**, 220, 152-163.
49. Lim, K.H.; Ferraris, L.; Filloux, M.E.; Raphael, B.J.; Fairbrother, W.G. Using positional distribution to identify splicing elements and predict pre-mrna processing defects in human genes. *Proceedings of the National Academy of Sciences* **2011**, 108, 11093-11098.
50. Will, C.L.; Lührmann, R. Spliceosome structure and function. *Cold Spring Harbor perspectives in biology* **2011**, 3, a003707.
51. Krämer, A. The structure and function of proteins involved in mammalian pre-mrna splicing. *Annual review of biochemistry* **1996**, 65, 367-409.
52. Singh, R.; Valcarcel, J.; Green, M.R. Distinct binding specificities and functions of higher eukaryotic polypyrimidine tract-binding proteins. *Science* **1995**, 268, 1173-1176.
53. Turunen, J.J.; Niemelä, E.H.; Verma, B.; Frilander, M.J. The significant other: Splicing by the minor spliceosome. *Wiley Interdisciplinary Reviews: RNA* **2013**, 4, 61-76.

54. Patel, A.A.; Steitz, J.A. Splicing double: Insights from the second spliceosome. *Nature reviews Molecular cell biology* **2003**, *4*, 960.
55. Wu, Q.; Krainer, A.R. Splicing of a divergent subclass of at-ac introns requires the major spliceosomal snrnas. *RNA-CAMBRIDGE-* **1997**, *3*, 586-601.
56. Sperling, R. The nuts and bolts of the endogenous spliceosome. *Wiley Interdisciplinary Reviews: RNA* **2017**, *8*, e1377.
57. Staley, J.P.; Woolford Jr, J.L. Assembly of ribosomes and spliceosomes: Complex ribonucleoprotein machines. *Current opinion in cell biology* **2009**, *21*, 109-118.
58. Reed, R. Mechanisms of fidelity in pre-mrna splicing. *Current opinion in cell biology* **2000**, *12*, 340-345.
59. Kędzierska, H.; Piekiełko-Witkowska, A. Splicing factors of sr and hnrnp families as regulators of apoptosis in cancer. *Cancer letters* **2017**, *396*, 53-65.
60. Busch, A.; Hertel, K.J. Evolution of sr protein and hnrnp splicing regulatory factors. *Wiley Interdisciplinary Reviews: RNA* **2012**, *3*, 1-12.
61. Lee, Y.; Rio, D.C. Mechanisms and regulation of alternative pre-mrna splicing. *Annual review of biochemistry* **2015**, *84*, 291.
62. Baralle, F.E.; Giudice, J. Alternative splicing as a regulator of development and tissue identity. *Nature Reviews Molecular Cell Biology* **2017**, *18*, 437.
63. Kelemen, O.; Convertini, P.; Zhang, Z.; Wen, Y.; Shen, M.; Falaleeva, M.; Stamm, S. Function of alternative splicing. *Gene* **2013**, *514*, 1-30.
64. De Conti, L.; Baralle, M.; Buratti, E. Exon and intron definition in pre-mrna splicing. *Wiley Interdisciplinary Reviews: RNA* **2013**, *4*, 49-60.
65. Sumanasekera, C.; Kelemen, O.; Beullens, M.; Aubol, B.E.; Adams, J.A.; Sunkara, M.; Morris, A.; Bollen, M.; Andreadis, A.; Stamm, S. C6 pyridinium ceramide influences alternative pre-mrna splicing by inhibiting protein phosphatase-1. *Nucleic acids research* **2011**, *40*, 4025-4039.

66. Kondo, S.; Yamamoto, N.; Murakami, T.; Okumura, M.; Mayeda, A.; Imaizumi, K. Tra2 $\beta$ , sf2/asf and srp30c modulate the function of an exonic splicing enhancer in exon 10 of tau pre-mrna. *Genes to Cells* **2004**, *9*, 121-130.
67. Tazi, J.; Bakkour, N.; Stamm, S. Alternative splicing and disease. *Biochimica et Biophysica Acta (BBA)-Molecular Basis of Disease* **2009**, *1792*, 14-26.
68. Hammond, S.M.; Wood, M.J. Genetic therapies for rna mis-splicing diseases. *Trends in genetics* **2011**, *27*, 196-205.
69. Scotti, M.M.; Swanson, M.S. Rna mis-splicing in disease. *Nature Reviews Genetics* **2016**, *17*, 19-32.
70. Cartegni, L.; Chew, S.L.; Krainer, A.R. Listening to silence and understanding nonsense: Exonic mutations that affect splicing. *Nature Reviews Genetics* **2002**, *3*, 285-298.
71. Cartegni, L.; Hastings, M.L.; Calarco, J.A.; De Stanchina, E.; Krainer, A.R. Determinants of exon 7 splicing in the spinal muscular atrophy genes, smn1 and smn2. *The American Journal of Human Genetics* **2006**, *78*, 63-77.
72. Liu, M.M.; Zack, D.J. Alternative splicing and retinal degeneration. *Clinical genetics* **2013**, *84*, 142-149.
73. Tanackovic, G.; Ransijn, A.; Thibault, P.; Abou Elela, S.; Klinck, R.; Berson, E.L.; Chabot, B.; Rivolta, C. Prpf mutations are associated with generalized defects in spliceosome formation and pre-mrna splicing in patients with retinitis pigmentosa. *Human molecular genetics* **2011**, *20*, 2116-2130.
74. Stephenson, M.L.; Zamecnik, P.C. Inhibition of rous sarcoma viral rna translation by a specific oligodeoxyribonucleotide. *Proceedings of the National Academy of Sciences* **1978**, *75*, 285-288.
75. Furdon, P.J.; Dominski, Z.; Kole, R. Rnase h cleavage of rna hybridized to oligonucleotides containing methylphosphonate, phosphorothioate and phosphodiester bonds. *Nucleic acids research* **1989**, *17*, 9193-9204.

76. Bennett, C.F. Therapeutic antisense oligonucleotides are coming of age. *Annual review of medicine* **2019**, *70*, 307-321.
77. Singh, N.N.; Luo, D.; Singh, R.N. Pre-mrna splicing modulation by antisense oligonucleotides. In *Exon skipping and inclusion therapies*, Springer: 2018; pp 415-437.
78. Chan, J.H.; Lim, S.; Wong, W.F. Antisense oligonucleotides: From design to therapeutic application. *Clinical and experimental pharmacology and physiology* **2006**, *33*, 533-540.
79. Pitout, I.; Flynn, L.L.; Wilton, S.D.; Fletcher, S. Antisense-mediated splice intervention to treat human disease: The odyssey continues. *F1000Research* **2019**, *8*.
80. Zamecnik, P.C.; Stephenson, M.L. Inhibition of rous sarcoma virus replication and cell transformation by a specific oligodeoxynucleotide. *Proceedings of the National Academy of Sciences* **1978**, *75*, 280-284.
81. Aartsma-Rus, A. Overview on aon design. In *Exon skipping*, Springer: 2012; pp 117-129.
82. Zhao, Q.; MATSON, S.; HERRERA, C.J.; FISHER, E.; YU, H.; KRIEG, A.M. Comparison of cellular binding and uptake of antisense phosphodiester, phosphorothioate, and mixed phosphorothioate and methylphosphonate oligonucleotides. *Antisense research and development* **1993**, *3*, 53-66.
83. Goyal, N.; Narayanaswami, P. Making sense of antisense oligonucleotides: A narrative review. *Muscle & nerve* **2018**, *57*, 356-370.
84. Toonen, L.J.; Casaca-Carreira, J.; Pellisé-Tintoré, M.; Mei, H.; Temel, Y.; Jahanshahi, A.; van Roon-Mom, W.M. Intracerebroventricular administration of a 2'-o-methyl phosphorothioate antisense oligonucleotide results in activation of the innate immune system in mouse brain. *nucleic acid therapeutics* **2018**, *28*, 63-73.
85. Shen, W.; Liang, X.-h.; Crooke, S.T. Phosphorothioate oligonucleotides can displace neat1 rna and form nuclear paraspeckle-like structures. *Nucleic acids research* **2014**, *42*, 8648-8662.

86. Shen, W.; De Hoyos, C.L.; Sun, H.; Vickers, T.A.; Liang, X.-h.; Crooke, S.T. Acute hepatotoxicity of 2'-fluoro-modified 5'-10'-5' gapmer phosphorothioate oligonucleotides in mice correlates with intracellular protein binding and the loss of dbhs proteins. *Nucleic acids research* **2018**, *46*, 2204-2217.
87. Shen, W.; Liang, X.-h.; Sun, H.; Crooke, S.T. 2'-fluoro-modified phosphorothioate oligonucleotide can cause rapid degradation of p54nrb and psf. *Nucleic acids research* **2015**, *43*, 4569-4578.
88. Inoue, H.; Hayase, Y.; Imura, A.; Iwai, S.; Miura, K.; Ohtsuka, E. Synthesis and hybridization studies on two complementary nona (2'-o-methyl) ribonucleotides. *Nucleic acids research* **1987**, *15*, 6131-6148.
89. Ravikumar, V.T.; Cole, D.L. Development of 2'-o-methoxyethyl phosphorothioate oligonucleotides as antisense drugs under stereochemical control. *Organic process research & development* **2002**, *6*, 798-806.
90. Kumar, R.; Singh, S.K.; Koshkin, A.A.; Rajwanshi, V.K.; Meldgaard, M.; Wengel, J. The first analogues of lna (locked nucleic acids): Phosphorothioate-lna and 2'-thio-lna. *Bioorganic & medicinal chemistry letters* **1998**, *8*, 2219-2222.
91. Koshkin, A.A.; Singh, S.K.; Nielsen, P.; Rajwanshi, V.K.; Kumar, R.; Meldgaard, M.; Olsen, C.E.; Wengel, J. Lna (locked nucleic acids): Synthesis of the adenine, cytosine, guanine, 5-methylcytosine, thymine and uracil bicyclonucleoside monomers, oligomerisation, and unprecedented nucleic acid recognition. *Tetrahedron* **1998**, *54*, 3607-3630.
92. Geary, R.S.; Norris, D.; Yu, R.; Bennett, C.F. Pharmacokinetics, biodistribution and cell uptake of antisense oligonucleotides. *Advanced drug delivery reviews* **2015**, *87*, 46-51.
93. Zaw, K.; Greer, K.; Aung-Htut, M.T.; Veedu, R.N.; Fletcher, S.; Wilton, S.D. Making the inactive active through changes in antisense oligonucleotide chemistries. *Frontiers in Genetics* **2019**, *10*, 1249.

94. Stanton, R.; Sciabola, S.; Salatto, C.; Weng, Y.; Moshinsky, D.; Little, J.; Walters, E.; Kreeger, J.; DiMattia, D.; Chen, T. Chemical modification study of antisense gapmers. *Nucleic acid therapeutics* **2012**, *22*, 344-359.
95. Kurreck, J. Antisense technologies: Improvement through novel chemical modifications. *European Journal of Biochemistry* **2003**, *270*, 1628-1644.
96. Nielsen, P.E.; Egholm, M.; Berg, R.H.; Buchardt, O. Sequence-selective recognition of DNA by strand displacement with a thymine-substituted polyamide. *Science* **1991**, *254*, 1497-1500.
97. Summerton, J.; Weller, D. Morpholino antisense oligomers: Design, preparation, and properties. *Antisense and Nucleic Acid Drug Development* **1997**, *7*, 187-195.
98. Summerton, J.; Stein, D.; Huang, S.B.; Matthews, P.; Weller, D.; Partridge, M. Morpholino and phosphorothioate antisense oligomers compared in cell-free and in-cell systems. *Antisense and Nucleic Acid Drug Development* **1997**, *7*, 63-70.
99. Summerton, J.E. Morpholino, sirna, and s-DNA compared: Impact of structure and mechanism of action on off-target effects and sequence specificity. *Current topics in medicinal chemistry* **2007**, *7*, 651-660.
100. Arora, V.; Devi, G.R.; Iversen, P.L. Neutrally charged phosphorodiamidate morpholino antisense oligomers: Uptake, efficacy and pharmacokinetics. *Current pharmaceutical biotechnology* **2004**, *5*, 431-439.
101. Cerritelli, S.M.; Crouch, R.J. Ribonuclease h: The enzymes in eukaryotes. *The FEBS journal* **2009**, *276*, 1494-1505.
102. Group, V.S. Safety of intravitreal fomivirsen for treatment of cytomegalovirus retinitis in patients with aids. *American journal of ophthalmology* **2002**, *133*, 484-498.
103. Roehr, B. Fomivirsen approved for cmv retinitis. *Journal of the International Association of Physicians in AIDS Care* **1998**, *4*, 14.
104. Stessl, M.; Noe, C.R.; Winkler, J. Off-target effects and safety aspects of phosphorothioate oligonucleotides. In *From nucleic acids sequences to molecular medicine*, Springer: 2012; pp 67-83.



105. Geary, R.S.; Baker, B.F.; Crooke, S.T. Clinical and preclinical pharmacokinetics and pharmacodynamics of mipomersen (kynamro®): A second-generation antisense oligonucleotide inhibitor of apolipoprotein b. *Clinical pharmacokinetics* **2015**, *54*, 133-146.
106. Havens, M.A.; Hastings, M.L. Splice-switching antisense oligonucleotides as therapeutic drugs. *Nucleic acids research* **2016**, gkw533.
107. Bauman, J.; Jearawiriyapaisarn, N.; Kole, R. Therapeutic potential of splice-switching oligonucleotides. *Oligonucleotides* **2009**, *19*, 1-13.
108. Mendell, J.R.; Goemans, N.; Lowes, L.P.; Alfano, L.N.; Berry, K.; Shao, J.; Kaye, E.M.; Mercuri, E.; Group, E.S.; Network, T.F.D.I., *et al.* Longitudinal effect of eteplirsen versus historical control on ambulation in duchenne muscular dystrophy. *Annals of neurology* **2016**, *79*, 257-271.
109. Mendell, J.R.; Rodino-Klapac, L.R.; Sahenk, Z.; Roush, K.; Bird, L.; Lowes, L.P.; Alfano, L.; Gomez, A.M.; Lewis, S.; Kota, J. Eteplirsen for the treatment of duchenne muscular dystrophy. *Annals of neurology* **2013**, *74*, 637-647.
110. Mendell, J.R.; Sahenk, Z.; Rodino-Klapac, L.R. Clinical trials of exon skipping in duchenne muscular dystrophy. *Expert Opinion on Orphan Drugs* **2017**, *5*, 683-690.
111. Fletcher, S.; Ly, T.; Duff, R.; Howell, J.M.; Wilton, S. Cryptic splicing involving the splice site mutation in the canine model of duchenne muscular dystrophy. *Neuromuscular Disorders* **2001**, *11*, 239-243.
112. Mann, C.J.; Honeyman, K.; McClorey, G.; Fletcher, S.; Wilton, S.D. Improved antisense oligonucleotide induced exon skipping in the mdx mouse model of muscular dystrophy. *The Journal of Gene Medicine: A cross-disciplinary journal for research on the science of gene transfer and its clinical applications* **2002**, *4*, 644-654.
113. Errington, S.J.; Mann, C.J.; Fletcher, S.; Wilton, S.D. Target selection for antisense oligonucleotide induced exon skipping in the dystrophin gene. *The journal of gene medicine* **2003**, *5*, 518-527.

114. Gebiski, B.L.; Mann, C.J.; Fletcher, S.; Wilton, S.D. Morpholino antisense oligonucleotide induced dystrophin exon 23 skipping in mdx mouse muscle. *Human molecular genetics* **2003**, *12*, 1801-1811.
115. Aartsma-Rus, A.; Bremmer-Bout, M.; Janson, A.A.; den Dunnen, J.T.; van Ommen, G.-J.B.; van Deutekom, J.C. Targeted exon skipping as a potential gene correction therapy for duchenne muscular dystrophy. *Neuromuscular Disorders* **2002**, *12*, S71-S77.
116. Negishi, Y.; Ishii, Y.; Nirasawa, K.; Sasaki, E.; Endo-Takahashi, Y.; Suzuki, R.; Maruyama, K. Pmo delivery system using bubble liposomes and ultrasound exposure for duchenne muscular dystrophy treatment. In *Duchenne muscular dystrophy*, Springer: 2018; pp 185-192.
117. Alfano, L.N.; Charleston, J.S.; Connolly, A.M.; Cripe, L.; Donoghue, C.; Dracker, R.; Dworzak, J.; Eliopoulos, H.; Frank, D.E.; Lewis, S. Long-term treatment with eteplirsen in nonambulatory patients with duchenne muscular dystrophy. *Medicine* **2019**, *98*.
118. Kinali, M.; Arechavala-Gomez, V.; Feng, L.; Cirak, S.; Hunt, D.; Adkin, C.; Guglieri, M.; Ashton, E.; Abbs, S.; Nihoyannopoulos, P. Local restoration of dystrophin expression with the morpholino oligomer avi-4658 in duchenne muscular dystrophy: A single-blind, placebo-controlled, dose-escalation, proof-of-concept study. *The Lancet Neurology* **2009**, *8*, 918-928.
119. Heemskerk, H.A.; de Winter, C.L.; de Kimpe, S.J.; van Kuik-Romeijn, P.; Heuvelmans, N.; Platenburg, G.J.; van Ommen, G.J.B.; van Deutekom, J.C.; Aartsma-Rus, A. In vivo comparison of 2'-o-methyl phosphorothioate and morpholino antisense oligonucleotides for duchenne muscular dystrophy exon skipping. *The Journal of Gene Medicine: A cross-disciplinary journal for research on the science of gene transfer and its clinical applications* **2009**, *11*, 257-266.
120. Cirak, S.; Arechavala-Gomez, V.; Guglieri, M.; Feng, L.; Torelli, S.; Anthony, K.; Abbs, S.; Garralda, M.E.; Bourke, J.; Wells, D.J. Exon skipping and dystrophin restoration in patients with duchenne muscular dystrophy after systemic

- phosphorodiamidate morpholino oligomer treatment: An open-label, phase 2, dose-escalation study. *The Lancet* **2011**, *378*, 595-605.
121. Novack, G.D. Eyes on new product development. *Journal of Ocular Pharmacology and Therapeutics* **2020**, *36*, 1-2.
  122. Ahmad, S.; Bhatia, K.; Kannan, A.; Gangwani, L. Molecular mechanisms of neurodegeneration in spinal muscular atrophy. *Journal of experimental neuroscience* **2016**, *10*, JEN. S33122.
  123. Ottesen, E.W. Iss-n1 makes the first fda-approved drug for spinal muscular atrophy. *Translational neuroscience* **2017**, *8*, 1-6.
  124. Singh, N.K.; Singh, N.N.; Androphy, E.J.; Singh, R.N. Splicing of a critical exon of human survival motor neuron is regulated by a unique silencer element located in the last intron. *Molecular and cellular biology* **2006**, *26*, 1333-1346.
  125. Finkel, R.S.; Chiriboga, C.A.; Vajsar, J.; Day, J.W.; Montes, J.; De Vivo, D.C.; Yamashita, M.; Rigo, F.; Hung, G.; Schneider, E. Treatment of infantile-onset spinal muscular atrophy with nusinersen: A phase 2, open-label, dose-escalation study. *The Lancet* **2017**, *388*, 3017-3026.
  126. Arechavala-Gomez, V.; Graham, I.; Popplewell, L.; Adams, A.; Aartsma-Rus, A.; Kinali, M.; Morgan, J.; Van Deutekom, J.; Wilton, S.; Dickson, G. Comparative analysis of antisense oligonucleotide sequences for targeted skipping of exon 51 during dystrophin pre-mrna splicing in human muscle. *Human gene therapy* **2007**, *18*, 798-810.
  127. Iversen, P.; Newbry, S. Manipulation of zebrafish embryogenesis by phosphorodiamidate morpholino oligomers indicates minimal non-specific teratogenesis. *Current opinion in molecular therapeutics* **2005**, *7*, 104-108.
  128. Kim, J.; Clark, K.; Barton, C.; Tanguay, R.; Moulton, H. A novel zebrafish model for assessing in vivo delivery of morpholino oligomers. In *Exon skipping and inclusion therapies*, Springer: 2018; pp 293-306.

129. Hanvey, J.C.; Peffer, N.J.; Bisi, J.E.; Thomson, S.A.; Cadilla, R.; Josey, J.A.; Ricca, D.J.; Hassman, C.F.; Bonham, M.A.; Au, K.G. Antisense and antigene properties of peptide nucleic acids. *Science* **1992**, *258*, 1481-1485.
130. Dias, N.; Stein, C. Antisense oligonucleotides: Basic concepts and mechanisms. *Molecular cancer therapeutics* **2002**, *1*, 347-355.
131. Vickers, i.A.; Griffith, M.C.; Ramasamy, K.; Risen, L.M.; Freier, S.M. Inhibition of nf- $\kappa$ b specific transcriptional activation by pna strand invasion. *Nucleic acids research* **1995**, *23*, 3003-3008.
132. Whitfield, J.R.; Beaulieu, M.-E.; Soucek, L. Strategies to inhibit myc and their clinical applicability. *Frontiers in cell and developmental biology* **2017**, *5*, 10.
133. Philipp, S.; Sack, S.; Kordish, I.; Brachmann, J.; Hardt, S.; Horn, J. The appraisal-trial: Evaluating resten-mptm in patients with bare metal stent de novo native coronary artery lesions. *J. Clin. Exp. Cardiol* **2012**, *3*, 10.4172.
134. Kipshidze, N.; Iversen, P.; Overlie, P.; Dunlap, T.; Titus, B.; Lee, D.; Moses, J.; O'Hanley, P.; Lauer, M.; Leon, M.B. First human experience with local delivery of novel antisense avi-4126 with infiltrator catheter in de novo native and restenotic coronary arteries: 6-month clinical and angiographic follow-up from avail study. *Cardiovascular Revascularization Medicine* **2007**, *8*, 230-235.
135. Vickers, T.A.; Wyatt, J.R.; Burckin, T.; Bennett, C.F.; Freier, S.M. Fully modified 2' moe oligonucleotides redirect polyadenylation. *Nucleic acids research* **2001**, *29*, 1293-1299.
136. Li, R.; Harvey, A.R.; Hodgetts, S.I.; Fox, A.H. Functional dissection of neat1 using genome editing reveals substantial localization of the neat1\_1 isoform outside paraspeckles. *Rna* **2017**, *23*, 872-881.
137. Chi, X.; Gatti, P.; Papoian, T. Safety of antisense oligonucleotide and sirna-based therapeutics. *Drug discovery today* **2017**, *22*, 823-833.
138. Adams, D.; Gonzalez-Duarte, A.; O'Riordan, W.D.; Yang, C.-C.; Ueda, M.; Kristen, A.V.; Tournev, I.; Schmidt, H.H.; Coelho, T.; Berk, J.L. Patisiran, an rnai therapeutic,

- for hereditary transthyretin amyloidosis. *New England Journal of Medicine* **2018**, *379*, 11-21.
139. Wood, H. Fda approves patisiran to treat hereditary transthyretin amyloidosis. Nature Publishing Group: 2018.
140. Wong, E.; Goldberg, T. Mipomersen (kynamro): A novel antisense oligonucleotide inhibitor for the management of homozygous familial hypercholesterolemia. *Pharmacy and Therapeutics* **2014**, *39*, 119.
141. Crooke, S.T.; Baker, B.F.; Kwoh, T.J.; Cheng, W.; Schulz, D.J.; Xia, S.; Salgado, N.; Bui, H.-H.; Hart, C.E.; Burel, S.A. Integrated safety assessment of 2'-o-methoxyethyl chimeric antisense oligonucleotides in nonhuman primates and healthy human volunteers. *Molecular Therapy* **2016**, *24*, 1771-1782.
142. Harding, P.; Fall, A.; Honeyman, K.; Fletcher, S.; Wilton, S. The influence of antisense oligonucleotide length on dystrophin exon skipping. *Molecular Therapy* **2007**, *15*, 157-166.
143. Aartsma-Rus, A.; Van Vliet, L.; Hirschi, M.; Janson, A.A.; Heemskerk, H.; De Winter, C.L.; De Kimpe, S.; Van Deutekom, J.C.; Ac't Hoen, P.; van Ommen, G.-J.B. Guidelines for antisense oligonucleotide design and insight into splice-modulating mechanisms. *Molecular Therapy* **2009**, *17*, 548-553.
144. Kim, J.; Hu, C.; Moufawad El Achkar, C.; Black, L.E.; Douville, J.; Larson, A.; Pendergast, M.K.; Goldkind, S.F.; Lee, E.A.; Kuniholm, A. Patient-customized oligonucleotide therapy for a rare genetic disease. *New England Journal of Medicine* **2019**, *381*, 1644-1652.
145. Crooke, S.T.; Baker, B.F.; Witztum, J.L.; Kwoh, T.J.; Pham, N.C.; Salgado, N.; McEvoy, B.W.; Cheng, W.; Hughes, S.G.; Bhanot, S. The effects of 2'-o-methoxyethyl containing antisense oligonucleotides on platelets in human clinical trials. *nucleic acid therapeutics* **2017**, *27*, 121-129.
146. Thomas, K. Costly drug for fatal muscular disease wins fda approval. *The New York Times* **2016**.

147. Paulson, H.L.; Shakkottai, V.G.; Clark, H.B.; Orr, H.T. Polyglutamine spinocerebellar ataxias—from genes to potential treatments. *Nature Reviews Neuroscience* **2017**, *18*, 613.
148. Buijsen, R.A.; Toonen, L.J.; Gardiner, S.L.; van Roon-Mom, W.M. Genetics, mechanisms, and therapeutic progress in polyglutamine spinocerebellar ataxias. *Neurotherapeutics* **2019**, 1-24.
149. Ashley, C.T.; Warren, S.T. Trinucleotide repeat expansion and human disease. *Annual review of genetics* **1995**, *29*, 703-728.
150. Lee, D.-Y.; McMurray, C.T. Trinucleotide expansion in disease: Why is there a length threshold? *Current opinion in genetics & development* **2014**, *26*, 131-140.
151. Furuta, N.; Tsukagoshi, S.; Hirayanagi, K.; Ikeda, Y. Suppression of the yeast elongation factor spt4 ortholog reduces expanded sca36 ggccug repeat aggregation and cytotoxicity. *Brain research* **2019**, *1711*, 29-40.
152. Kramer, N.J.; Carlomagno, Y.; Zhang, Y.-J.; Almeida, S.; Cook, C.N.; Gendron, T.F.; Prudencio, M.; Van Blitterswijk, M.; Belzil, V.; Couthouis, J. Spt4 selectively regulates the expression of c9orf72 sense and antisense mutant transcripts. *Science* **2016**, *353*, 708-712.
153. Liu, C.-R.; Chang, C.-R.; Chern, Y.; Wang, T.-H.; Hsieh, W.-C.; Shen, W.-C.; Chang, C.-Y.; Chu, I.-C.; Deng, N.; Cohen, S.N. Spt4 is selectively required for transcription of extended trinucleotide repeats. *Cell* **2012**, *148*, 690-701.
154. Desmet, F.-O.; Hamroun, D.; Lalande, M.; Collod-Bérout, G.; Claustres, M.; Bérout, C. Human splicing finder: An online bioinformatics tool to predict splicing signals. *Nucleic acids research* **2009**, *37*, e67-e67.
155. Piva, F.; Giulietti, M.; Burini, A.B.; Principato, G. Spliceaid 2: A database of human splicing factors expression data and rna target motifs. *Human mutation* **2012**, *33*, 81-85.
156. Aung-Htut, M.T.; McIntosh, C.S.; Ham, K.A.; Pitout, I.L.; Flynn, L.L.; Greer, K.; Fletcher, S.; Wilton, S.D. Systematic approach to developing splice modulating

- antisense oligonucleotides. *International Journal of Molecular Sciences* **2019**, *20*, 5030.
157. Summerton, J.E. Endo-porter: A novel reagent for safe, effective delivery of substances into cells. *Annals of the New York Academy of Sciences* **2005**, *1058*, 62-75.
158. Gatchel, J.R.; Zoghbi, H.Y. Diseases of unstable repeat expansion: Mechanisms and common principles. *Nature Reviews Genetics* **2005**, *6*, 743-755.
159. Usdin, K. The biological effects of simple tandem repeats: Lessons from the repeat expansion diseases. *Genome research* **2008**, *18*, 1011-1019.
160. Zoghbi, H.Y.; Orr, H.T. Pathogenic mechanisms of a polyglutamine-mediated neurodegenerative disease, spinocerebellar ataxia type 1. *Journal of Biological Chemistry* **2009**, *284*, 7425-7429.
161. DeJesus-Hernandez, M.; Mackenzie, I.R.; Boeve, B.F.; Boxer, A.L.; Baker, M.; Rutherford, N.J.; Nicholson, A.M.; Finch, N.A.; Flynn, H.; Adamson, J. Expanded ggggcc hexanucleotide repeat in noncoding region of c9orf72 causes chromosome 9p-linked ftd and als. *Neuron* **2011**, *72*, 245-256.
162. Zhang, K.; Donnelly, C.J.; Haeusler, A.R.; Grima, J.C.; Machamer, J.B.; Steinwald, P.; Daley, E.L.; Miller, S.J.; Cunningham, K.M.; Vidensky, S. The c9orf72 repeat expansion disrupts nucleocytoplasmic transport. *Nature* **2015**, *525*, 56.
163. Shi, Y.; Lin, S.; Staats, K.A.; Li, Y.; Chang, W.-H.; Hung, S.-T.; Hendricks, E.; Linares, G.R.; Wang, Y.; Son, E.Y. Haploinsufficiency leads to neurodegeneration in c9orf72 als/ftd human induced motor neurons. *Nature medicine* **2018**, *24*, 313.
164. Kumar, V.; Hasan, G.M.; Hassan, M. Unraveling the role of rna mediated toxicity of c9orf72 repeats in c9-ftd/als. *Frontiers in neuroscience* **2017**, *11*, 711.
165. Wenzel, S.; Schweimer, K.; Rösch, P.; Wöhrl, B.M. The small hsp4 subunit of the human transcription elongation factor dsif is a zn-finger protein with  $\alpha/\beta$  type topology. *Biochemical and biophysical research communications* **2008**, *370*, 414-418.

166. Aartsma-Rus, A. Fda approval of nusinersen for spinal muscular atrophy makes 2016 the year of splice modulating oligonucleotides. *Nucleic acid therapeutics* **2017**, *27*, 67-69.
167. Aartsma-Rus, A.; Corey, D.R. The 10th oligonucleotide therapy approved: Golodirsen for duchenne muscular dystrophy. *nucleic acid therapeutics* **2020**.
168. Adams, A.M.; Harding, P.L.; Iversen, P.L.; Coleman, C.; Fletcher, S.; Wilton, S.D. Antisense oligonucleotide induced exon skipping and the dystrophin gene transcript: Cocktails and chemistries. *BMC molecular biology* **2007**, *8*, 1.
169. McIntosh, C.S.; Aung-Htut, M.T.; Fletcher, S.; Wilton, S.D. Removal of the polyglutamine repeat of ataxin-3 by redirecting pre-mrna processing. *International Journal of Molecular Sciences* **2019**, *20*, 5434.
170. David Powell; Michael Milton; Andrew Perry; Santos, K. *Drpowell/degust 4.1.1 (version 4.1.1)*. *Zenodo.*, Version 4.1.1; Monash University, 2019.
171. Pomaznoy, M.; Ha, B.; Peters, B. Gonet: A tool for interactive gene ontology analysis. *BMC bioinformatics* **2018**, *19*, 470.
172. Schneider, C.A.; Rasband, W.S.; Eliceiri, K.W. Nih image to imagej: 25 years of image analysis. *Nature methods* **2012**, *9*, 671.
173. Cheng, H.-M.; Chern, Y.; Chen, I.-H.; Liu, C.-R.; Li, S.-H.; Chun, S.J.; Rigo, F.; Bennett, C.F.; Deng, N.; Feng, Y. Effects on murine behavior and lifespan of selectively decreasing expression of mutant huntingtin allele by supt4h knockdown. *PLoS genetics* **2015**, *11*, e1005043.
174. Aung-Htut, M.T.; Comerford, I.; Johnsen, R.; Foyle, K.; Fletcher, S.; Wilton, S.D. Reduction of integrin alpha 4 activity through splice modulating antisense oligonucleotides. *Scientific reports* **2019**, *9*, 1-12.
175. Flynn, L.L.; Li, R.; Aung-Htut, M.T.; Pitout, I.L.; Cooper, J.; Hubbard, A.; Griffiths, L.; Bond, C.; Wilton, S.D.; Fox, A.H. Interaction of modified oligonucleotides with nuclear proteins, formation of novel nuclear structures and sequence-independent effects on rna processing. *bioRxiv* **2018**, 446773.



176. Flynn, L.L.; Mitrpant, C.; Pitout, I.L.; Fletcher, S.; Wilton, S.D. Antisense oligonucleotide-mediated terminal intron retention of the *smn2* transcript. *Molecular Therapy-Nucleic Acids* **2018**, *11*, 91-102.
177. Aung-Htut, M.T.; McIntosh, C.S.; West, K.A.; Fletcher, S.; Wilton, S.D. In vitro validation of phosphorodiamidate morpholino oligomers. *Molecules* **2019**, *24*, 2922.
178. Pei, Y.; Shuman, S. Characterization of the schizosaccharomyces pombe cdk9/pchl protein kinase spt5 phosphorylation, autophosphorylation, and mutational analysis. *Journal of Biological Chemistry* **2003**, *278*, 43346-43356.
179. Shetty, A.; Kallgren, S.P.; Demel, C.; Maier, K.C.; Spatt, D.; Alver, B.H.; Cramer, P.; Park, P.J.; Winston, F. Spt5 plays vital roles in the control of sense and antisense transcription elongation. *Molecular cell* **2017**, *66*, 77-88. e75.
180. Ivanov, D.; Kwak, Y.T.; Guo, J.; Gaynor, R.B. Domains in the spt5 protein that modulate its transcriptional regulatory properties. *Molecular and cellular biology* **2000**, *20*, 2970-2983.
181. Naguib, A.; Sandmann, T.; Yi, F.; Watts, R.J.; Lewcock, J.W.; Dowdle, W.E. Supt4h1 depletion leads to a global reduction in rna. *Cell reports* **2019**, *26*, 45-53. e44.
182. Lovén, J.; Orlando, D.A.; Sigova, A.A.; Lin, C.Y.; Rahl, P.B.; Burge, C.B.; Levens, D.L.; Lee, T.I.; Young, R.A. Revisiting global gene expression analysis. *Cell* **2012**, *151*, 476-482.
183. Suter, S.R.; Sheu-Gruttadauria, J.; Schirle, N.T.; Valenzuela, R.; Ball-Jones, A.A.; Onizuka, K.; MacRae, I.J.; Beal, P.A. Structure-guided control of sirna off-target effects. *Journal of the American Chemical Society* **2016**, *138*, 8667-8669.
184. Fedorov, Y.; Anderson, E.M.; Birmingham, A.; Reynolds, A.; Karpilow, J.; Robinson, K.; Leake, D.; Marshall, W.S.; Khvorova, A. Off-target effects by sirna can induce toxic phenotype. *Rna* **2006**, *12*, 1188-1196.
185. Lin, X.; Ruan, X.; Anderson, M.G.; McDowell, J.A.; Kroeger, P.E.; Fesik, S.W.; Shen, Y. Sirna-mediated off-target gene silencing triggered by a 7 nt complementation. *Nucleic acids research* **2005**, *33*, 4527-4535.

186. Birmingham, A.; Anderson, E.M.; Reynolds, A.; Ilsley-Tyree, D.; Leake, D.; Fedorov, Y.; Baskerville, S.; Maksimova, E.; Robinson, K.; Karpilow, J. 3' utr seed matches, but not overall identity, are associated with rnaï off-targets. *Nature methods* **2006**, *3*, 199-204.
187. Jackson, A.L.; Bartz, S.R.; Schelter, J.; Kobayashi, S.V.; Burchard, J.; Mao, M.; Li, B.; Cavet, G.; Linsley, P.S. Expression profiling reveals off-target gene regulation by rnaï. *Nature biotechnology* **2003**, *21*, 635-637.
188. Haley, B.; Zamore, P.D. Kinetic analysis of the rnaï enzyme complex. *Nature structural & molecular biology* **2004**, *11*, 599-606.
189. Charleston, J.; Schnell, F.; Dworzak, J.; Donoghue, C.; Lewis, S.; Rodino-Klapac, L.; Sahenk, Z.; Shanks, C.; Voss, J.; DeAlwis, U. Long-term treatment with eteplirsen promotes exon 51 skipping and novel dystrophin protein production in duchenne muscular dystrophy patients. *Neuromuscular Disorders* **2016**, *26*, S153.
190. Flanigan, K.M.; Voit, T.; Rosales, X.Q.; Servais, L.; Kraus, J.E.; Wardell, C.; Morgan, A.; Dorricott, S.; Nakielny, J.; Quarcoo, N. Pharmacokinetics and safety of single doses of drisapersen in non-ambulant subjects with duchenne muscular dystrophy: Results of a double-blind randomized clinical trial. *Neuromuscular Disorders* **2014**, *24*, 16-24.
191. Janas, M.M.; Jiang, Y.; Schlegel, M.K.; Waldron, S.; Kuchimanchi, S.; Barros, S.A. Impact of oligonucleotide structure, chemistry, and delivery method on in vitro cytotoxicity. *nucleic acid therapeutics* **2017**, *27*, 11-22.
192. Winkler, J.; Stessl, M.; Amartey, J.; Noe, C.R. Off-target effects related to the phosphorothioate modification of nucleic acids. *ChemMedChem* **2010**, *5*, 1344-1352.
193. Sathasivam, K.; Woodman, B.; Mahal, A.; Bertaux, F.; Wanker, E.E.; Shima, D.T.; Bates, G.P. Centrosome disorganization in fibroblast cultures derived from r6/2 huntington's disease (hd) transgenic mice and hd patients. *Human molecular genetics* **2001**, *10*, 2425-2435.
194. Zhang, N.; Ashizawa, T. Rna toxicity and foci formation in microsatellite expansion diseases. *Current Opinion in Genetics & Development* **2017**, *44*, 17-29.

195. Wojciechowska, M.; Krzyzosiak, W.J. Cellular toxicity of expanded rna repeats: Focus on rna foci. *Human molecular genetics* **2011**, *20*, 3811-3821.
196. Wheeler, V.C.; White, J.K.; Gutekunst, C.-A.; Vrbanac, V.; Weaver, M.; Li, X.-J.; Li, S.-H.; Yi, H.; Vonsattel, J.-P.; Gusella, J.F. Long glutamine tracts cause nuclear localization of a novel form of huntingtin in medium spiny striatal neurons in hdh q92 and hdh q111 knock-in mice. *Human molecular genetics* **2000**, *9*, 503-513.
197. Trettel, F.; Rigamonti, D.; Hilditch-Maguire, P.; Wheeler, V.C.; Sharp, A.H.; Persichetti, F.; Cattaneo, E.; MacDonald, M.E. Dominant phenotypes produced by the hd mutation in st hdh q111 striatal cells. *Human molecular genetics* **2000**, *9*, 2799-2809.
198. Cohen, A.; Ross, L.; Nachman, I.; Bar-Nun, S. Aggregation of polyq proteins is increased upon yeast aging and affected by sir2 and hsf1: Novel quantitative biochemical and microscopic assays. *PloS one* **2012**, *7*.
199. Butler, J.M. Short tandem repeat typing technologies used in human identity testing. *Biotechniques* **2007**, *43*, Sii-Sv.
200. La Spada, A.R.; Wilson, E.M. Androgen receptor gene mutations in x-linked spinal and bulbar muscular atrophy. *Nature* **1991**, *352*, 77.
201. Verkerk, A.J.; Pieretti, M.; Sutcliffe, J.S.; Fu, Y.-H.; Kuhl, D.P.; Pizzuti, A.; Reiner, O.; Richards, S.; Victoria, M.F.; Zhang, F. Identification of a gene (fmr-1) containing a cgg repeat coincident with a breakpoint cluster region exhibiting length variation in fragile x syndrome. *Cell* **1991**, *65*, 905-914.
202. Ashley, C.T.; Sutcliffe, J.S.; Kunst, C.B.; Leiner, H.A.; Eichler, E.E.; Nelson, D.L.; Warren, S.T. Human and murine fmr-1: Alternative splicing and translational initiation downstream of the cgg-repeat. *Nature genetics* **1993**, *4*, 244-251.
203. Bell, M.; Hirst, M.; Nakahori, Y.; MacKinnon, R.; Roche, A.; Flint, T.; Jacobs, P.; Tommerup, N.; Tranebjaerg, L.; Froster-Iskenius, U. Physical mapping across the fragile x: Hypermethylation and clinical expression of the fragile x syndrome. *Cell* **1991**, *64*, 861-866.

204. Heitz, D.; Rousseau, F.; Devys, D.; Saccone, S.; Abderrahim, H.; Le Paslier, D.; Cohen, D.; Vincent, A.; Toniolo, D.; Della Valle, G. Isolation of sequences that span the fragile x and identification of a fragile x-related cpg island. *Science* **1991**, *251*, 1236-1239.
205. Sweeney, P.; Park, H.; Baumann, M.; Dunlop, J.; Frydman, J.; Kopito, R.; McCampbell, A.; Leblanc, G.; Venkateswaran, A.; Nurmi, A. Protein misfolding in neurodegenerative diseases: Implications and strategies. *Translational Neurodegeneration* **2017**, *6*, 6.
206. Lieberman, A.P.; Shakkottai, V.G.; Albin, R.L. Polyglutamine repeats in neurodegenerative diseases. *Annual Review of Pathology: Mechanisms of Disease* **2019**, *14*, 1-27.
207. Albin, R.L.; Miller, R.A. Mini-review: Retarding aging in murine genetic models of neurodegeneration. *Neurobiology of disease* **2016**, *85*, 73-80.
208. Rossi, L.; Mazzitelli, S.; Arciello, M.; Capo, C.; Rotilio, G. Benefits from dietary polyphenols for brain aging and alzheimer's disease. *Neurochemical research* **2008**, *33*, 2390-2400.
209. Paoli, A.; Bianco, A.; Damiani, E.; Bosco, G. Ketogenic diet in neuromuscular and neurodegenerative diseases. *BioMed research international* **2014**, *2014*.
210. Esposito, E.; Rotilio, D.; Di Matteo, V.; Di Giulio, C.; Cacchio, M.; Algeri, S. A review of specific dietary antioxidants and the effects on biochemical mechanisms related to neurodegenerative processes. *Neurobiology of aging* **2002**, *23*, 719-735.
211. Takeuchi, T.; Nagai, Y. Protein misfolding and aggregation as a therapeutic target for polyglutamine diseases. *Brain sciences* **2017**, *7*, 128.
212. Ross, C.A.; Poirier, M.A. Protein aggregation and neurodegenerative disease. **2004**.
213. Jimenez-Sanchez, M.; Thomson, F.; Zavodszky, E.; Rubinsztein, D.C. Autophagy and polyglutamine diseases. *Progress in neurobiology* **2012**, *97*, 67-82.
214. Chai, Y.; Koppenhafer, S.L.; Bonini, N.M.; Paulson, H.L. Analysis of the role of heat shock protein (hsp) molecular chaperones in polyglutamine disease. *The Journal of neuroscience* **1999**, *19*, 10338-10347.

215. Pratt, W.B.; Gestwicki, J.E.; Osawa, Y.; Lieberman, A.P. Targeting hsp90/hsp70-based protein quality control for treatment of adult onset neurodegenerative diseases. *Annual review of pharmacology and toxicology* **2015**, *55*, 353-371.
216. Neef, D.W.; Jaeger, A.M.; Thiele, D.J. Heat shock transcription factor 1 as a therapeutic target in neurodegenerative diseases. *Nature reviews Drug discovery* **2011**, *10*, 930-944.
217. Saha, S.; Panigrahi, D.P.; Patil, S.; Bhutia, S.K. Autophagy in health and disease: A comprehensive review. *Biomedicine & Pharmacotherapy* **2018**, *104*, 485-495.
218. Puorro, G.; Marsili, A.; Sapone, F.; Pane, C.; De Rosa, A.; Peluso, S.; De Michele, G.; Filla, A.; Saccà, F. Peripheral markers of autophagy in polyglutamine diseases. *Neurological Sciences* **2018**, *39*, 149-152.
219. Ashkenazi, A.; Bento, C.F.; Ricketts, T.; Vicinanza, M.; Siddiqi, F.; Pavel, M.; Squitieri, F.; Hardenberg, M.C.; Imarisio, S.; Menzies, F.M. Polyglutamine tracts regulate autophagy. *Autophagy* **2017**, *13*, 1613-1614.
220. Cortes, C.J.; La Spada, A.R. Autophagy in polyglutamine disease: Imposing order on disorder or contributing to the chaos? *Molecular and Cellular Neuroscience* **2015**, *66*, 53-61.
221. Levine, B.; Kroemer, G. Autophagy in the pathogenesis of disease. *Cell* **2008**, *132*, 27-42.
222. Mizushima, N. Autophagy: Process and function. *Genes & development* **2007**, *21*, 2861-2873.
223. Kegel, K.B.; Kim, M.; Sapp, E.; McIntyre, C.; Castano, J.G.; Aronin, N.; DiFiglia, M. Huntingtin expression stimulates endosomal-lysosomal activity, endosome tubulation, and autophagy. *Journal of Neuroscience* **2000**, *20*, 7268-7278.
224. Ravikumar, B.; Duden, R.; Rubinsztein, D.C. Aggregate-prone proteins with polyglutamine and polyalanine expansions are degraded by autophagy. *Human molecular genetics* **2002**, *11*, 1107-1117.

225. Ha, J.; Kim, J. Novel pharmacological modulators of autophagy: An updated patent review (2012-2015). *Expert opinion on therapeutic patents* **2016**, *26*, 1273-1289.
226. Duarte-Silva, S.; Silva-Fernandes, A.; Neves-Carvalho, A.; Soares-Cunha, C.; Teixeira-Castro, A.; Maciel, P. Combined therapy with m-tor-dependent and-independent autophagy inducers causes neurotoxicity in a mouse model of machado–joseph disease. *Neuroscience* **2016**, *313*, 162-173.
227. Sacca, F.; Puorro, G.; Brunetti, A.; Capasso, G.; Cervo, A.; Coccozza, S.; de Leva, M.; Marsili, A.; Pane, C.; Quarantelli, M. A randomized controlled pilot trial of lithium in spinocerebellar ataxia type 2. *Journal of neurology* **2015**, *262*, 149-153.
228. Ginn, S.L.; Amaya, A.K.; Alexander, I.E.; Edelstein, M.; Abedi, M.R. Gene therapy clinical trials worldwide to 2017: An update. *The journal of gene medicine* **2018**, *20*, e3015.
229. Rodríguez-Lebrón, E.; doCarmo Costa, M.; Luna-Cancelon, K.; Peron, T.M.; Fischer, S.; Boudreau, R.L.; Davidson, B.L.; Paulson, H.L. Silencing mutant atxn3 expression resolves molecular phenotypes in sca3 transgenic mice. *Molecular Therapy* **2013**, *21*, 1909-1918.
230. Keiser, M.S.; Monteys, A.M.; Corbau, R.; Gonzalez-Alegre, P.; Davidson, B.L. Rnai prevents and reverses phenotypes induced by mutant human ataxin-1. *Annals of neurology* **2016**, *80*, 754-765.
231. Keiser, M.S.; Boudreau, R.L.; Davidson, B.L. Broad therapeutic benefit after rnai expression vector delivery to deep cerebellar nuclei: Implications for spinocerebellar ataxia type 1 therapy. *Molecular Therapy* **2014**, *22*, 588-595.
232. Keiser, M.S.; Geoghegan, J.C.; Boudreau, R.L.; Lennox, K.A.; Davidson, B.L. Rnai or overexpression: Alternative therapies for spinocerebellar ataxia type 1. *Neurobiology of disease* **2013**, *56*, 6-13.
233. Doudna, J.A.; Charpentier, E. The new frontier of genome engineering with crispr-cas9. *Science* **2014**, *346*, 1258096.

234. Sander, J.D.; Joung, J.K. Crispr-cas systems for editing, regulating and targeting genomes. *Nature biotechnology* **2014**, *32*, 347-355.
235. Babačić, H.; Mehta, A.; Merkel, O.; Schoser, B. Crispr-cas gene-editing as plausible treatment of neuromuscular and nucleotide-repeat-expansion diseases: A systematic review. *PloS one* **2019**, *14*.
236. Ouyang, S.; Xie, Y.; Xiong, Z.; Yang, Y.; Xian, Y.; Ou, Z.; Song, B.; Chen, Y.; Xie, Y.; Li, H. Crispr/cas9-targeted deletion of polyglutamine in spinocerebellar ataxia type 3-derived induced pluripotent stem cells. *Stem cells and development* **2018**, *27*, 756-770.
237. Shin, J.W.; Kim, K.-H.; Chao, M.J.; Atwal, R.S.; Gillis, T.; MacDonald, M.E.; Gusella, J.F.; Lee, J.-M. Permanent inactivation of huntington's disease mutation by personalized allele-specific crispr/cas9. *Human molecular genetics* **2016**, *25*, 4566-4576.
238. Yang, S.; Chang, R.; Yang, H.; Zhao, T.; Hong, Y.; Kong, H.E.; Sun, X.; Qin, Z.; Jin, P.; Li, S. Crispr/cas9-mediated gene editing ameliorates neurotoxicity in mouse model of huntington's disease. *The Journal of clinical investigation* **2017**, *127*, 2719-2724.
239. Park, C.-Y.; Halevy, T.; Lee, D.R.; Sung, J.J.; Lee, J.S.; Yanuka, O.; Benvenisty, N.; Kim, D.-W. Reversion of fmr1 methylation and silencing by editing the triplet repeats in fragile x ipsc-derived neurons. *Cell reports* **2015**, *13*, 234-241.
240. Marthaler, A.G.; Schmid, B.; Tubsuwan, A.; Poulsen, U.B.; Engelbrecht, A.F.; Mau-Holzmann, U.A.; Hyttel, P.; Nielsen, J.E.; Nielsen, T.T.; Holst, B. Generation of an isogenic, gene-corrected control cell line of the spinocerebellar ataxia type 2 patient-derived ipsc line h196. *Stem cell research* **2016**, *16*, 162-165.
241. Haque, N.; Isacson, O. Antisense gene therapy for neurodegenerative disease? *Experimental neurology* **1997**, *144*, 139-146.
242. McLoughlin, H.S.; Moore, L.R.; Chopra, R.; Komlo, R.; McKenzie, M.; Blumenstein, K.G.; Zhao, H.; Kordasiewicz, H.B.; Shakkottai, V.G.; Paulson, H.L. Oligonucleotide therapy mitigates disease in spinocerebellar ataxia type 3 mice. *Annals of neurology* **2018**, *84*, 64-77.

243. Zain, R.; Smith, C.E. Targeted oligonucleotides for treating neurodegenerative tandem repeat diseases. *Neurotherapeutics* **2019**, 1-15.
244. Scoles, D.R.; Pulst, S.M. Oligonucleotide therapeutics in neurodegenerative diseases. *RNA biology* **2018**, 1-23.
245. Scoles, D.R.; Meera, P.; Schneider, M.D.; Paul, S.; Dansithong, W.; Figueroa, K.P.; Hung, G.; Rigo, F.; Bennett, C.F.; Otis, T.S. Antisense oligonucleotide therapy for spinocerebellar ataxia type 2. *Nature* **2017**, *544*, 362-366.
246. Mulders, S.A.; van den Broek, W.J.; Wheeler, T.M.; Croes, H.J.; van Kuik-Romeijn, P.; de Kimpe, S.J.; Furling, D.; Platenburg, G.J.; Gourdon, G.; Thornton, C.A. Triplet-repeat oligonucleotide-mediated reversal of rna toxicity in myotonic dystrophy. *Proceedings of the National Academy of Sciences* **2009**, *106*, 13915-13920.
247. Sahashi, K.; Katsuno, M.; Hung, G.; Adachi, H.; Kondo, N.; Nakatsuji, H.; Tohnai, G.; Iida, M.; Bennett, C.F.; Sobue, G. Silencing neuronal mutant androgen receptor in a mouse model of spinal and bulbar muscular atrophy. *Human molecular genetics* **2015**, *24*, 5985-5994.
248. Toonen, L.J.; Rigo, F.; van Attikum, H.; van Roon-Mom, W.M. Antisense oligonucleotide-mediated removal of the polyglutamine repeat in spinocerebellar ataxia type 3 mice. *Molecular Therapy-Nucleic Acids* **2017**.
249. Evers, M.M.; Tran, H.-D.; Zalachoras, I.; Pepers, B.A.; Meijer, O.C.; den Dunnen, J.T.; van Ommen, G.-J.B.; Aartsma-Rus, A.; van Roon-Mom, W.M. Ataxin-3 protein modification as a treatment strategy for spinocerebellar ataxia type 3: Removal of the cag containing exon. *Neurobiology of disease* **2013**, *58*, 49-56.
250. Evers, M.M.; Pepers, B.A.; van Deutekom, J.C.; Mulders, S.A.; den Dunnen, J.T.; Aartsma-Rus, A.; van Ommen, G.-J.B.; van Roon-Mom, W.M. Targeting several cag expansion diseases by a single antisense oligonucleotide. *PLoS One* **2011**, *6*, e24308.
251. Evers, M.M.; Toonen, L.J.; van Roon-Mom, W.M. Ataxin-3 protein and rna toxicity in spinocerebellar ataxia type 3: Current insights and emerging therapeutic strategies. *Molecular neurobiology* **2014**, *49*, 1513-1531.



252. Switonski, P.M.; Fiszer, A.; Kazmierska, K.; Kurpisz, M.; Krzyzosiak, W.J.; Figiel, M. Mouse ataxin-3 functional knock-out model. *Neuromolecular medicine* **2011**, *13*, 54-65.
253. Rodrigues, A.J.; Neves-Carvalho, A.; Teixeira-Castro, A.; Rokka, A.; Corthals, G.; Logarinho, E.; Maciel, P. Absence of ataxin-3 leads to enhanced stress response in *c. Elegans*. *PLoS One* **2011**, *6*, e18512.
254. Aartsma-Rus, A.; van Ommen, G.-J.B. Progress in therapeutic antisense applications for neuromuscular disorders. *European Journal of Human Genetics* **2010**, *18*, 146-153.
255. Godfrey, C.; Desviat, L.R.; Smedsrød, B.; Piétri-Rouxel, F.; Denti, M.A.; Disterer, P.; Lorain, S.; Nogales-Gadea, G.; Sardone, V.; Anwar, R. Delivery is key: Lessons learnt from developing splice-switching antisense therapies. *EMBO molecular medicine* **2017**, *9*, 545-557.